To the Graduate Council:

I am submitting herewith a dissertation written by Steven Mack Trotter entitled "Characterization of the Relationship of Mixing Height Development and Collapse to Surface-Level Ozone Concentrations." I have examined the final copy of this dissertation for form and content and recommend that it be accepted in partial fulfilment of the requirements for the degree Doctor of Philosophy, with a major in Civil Engineering.

Wayne T. Davis, Major Professor

We have read this dissertation
and recommend its acceptance:

Accepted for the Council:

Associate Vice Chancellor and
Dean of The Graduate School

CHARACTERIZATION OF THE RELATIONSHIP OF MIXING HEIGHT DEVELOPMENT AND COLLAPSE TO SURFACE-LEVEL OZONE CONCENTRATIONS

A Dissertation
Presented for the
Doctor of Philosophy
Degree
The University of Tennessee, Knoxville

Steven Mack Trotter
August, 1998

DEDICATION

This dissertation is dedicated to my parents, Troy C. Trotter and Marion G. Trotter, and to my wife, Kimberly D. Gwinn. I would also like to dedicate this dissertation to my son, Jackson Lucas (Luke) Trotter, and nieces, Abbey Lauren Atchley and Emily Elise Atchley; the future of science and engineering depends upon their generation.

ACKNOWLEDGMENTS

There are many people to whom I am extremely grateful for their encouragement and support during the research for and preparation of this dissertation. I am grateful to my Dissertation Committee, Wayne T. Davis, Terry L. Miller, Gregory D. Reed, and Mary Sue Younger for their constructive suggestions regarding design of the research project and subsequent preparation of the dissertation. I am also extremely appreciative of the kindness, generosity, and support provided by William R. Pendergrass, NOAA, who not only made this research possible but constantly guided my efforts. In addition, I wish to thank Ray P. Hosker, Director, NOAA Atmospheric Turbulence and Diffusion Division (ATDD), Oak Ridge, Tennessee and his staff for their willingness to share information and resources during the past five years. I also thank Roland B. Stull, University of British Columbia, for his assistance with atmospheric thermodynamics and Dennis J. Beal for his assistance with statistical analyses. I am grateful to Carroll J. Southards and Charles D. Pless, Department of Entomology and Plant Pathology, for use of resources.

I also wish to thank David M. Bonner, Larry C. Masters, and Logan B. Pendergrass for their assistance with sampling. Ann H. Pendergrass deserves special recognition for her patience and support.

In addition, the field research and preparation of the dissertation would have been impossible without the assistance and support of two people whom I greatly love, my father, Troy C. Trotter, and my wife, Kimberly D. Gwinn. Foremost, appreciation is also given to our Lord Jesus Christ through whom all things are possible.

ABSTRACT

The eastern Tennessee ridge-and-valley region has recently experienced tropospheric ozone levels that approach the national ambient air quality standards. The objective of this research was to characterize the atmospheric mixing height and vertical structure of ozone during morning and evening at a site within the ridge-and-valley. Historically, high ozone concentrations in eastern Tennessee occurred in summer months during hot, stagnant days. Thus, this study focused on periods when the region was under the influence of high pressure systems and elevated temperatures during July and August, 1995. Meteorological and ozone measurements were made during daytime and nighttime to provide information on the development and subsequent collapse of the mixing height during morning and evening, respectively; measurements were obtained using a tethered balloon sounding system. Morning profiles were characterized by growth of the mixing height and entrainment of upper ozone reservoirs. Evening profiles depicted reduction of the mixing height and growth of the nocturnal, stable boundary layer. Ground-level ozone concentrations decreased whereas ozone concentrations at greater heights (100-300 m) remained comparatively high. This study demonstrated that the entrainment of ozone reservoirs aloft played a significant, if not dominant, role in increased ozone concentrations at the surface. Experimental data were used to construct an alternative model for mixing heights in regions under meteorological conditions of elevated temperatures and high pressure systems.

TABLE OF CONTENTS

1. INTRODUCTION 1
2. LITERATURE REVIEW 5
2.1. Air Pollution Meteorology 5
2.1.1. Boundary layer structure 5
2.1.2. Temperature structure 8
2.1.3. The diurnal cycle of vertical temperature structure 9
2.1.4. Atmospheric stability and vertical temperature structure 12
2.1.5. Meteorological wind patterns associated with topographic features 14
2.2. Tropospheric Ozone Photochemistry 17
2.3. Health Effects of Ozone 22
2.4. Environmental Effects of Ozone 23
2.5. Ozone Pollution in the Southeastern United States 24
2.6. Case Studies 25
2.6.1. South Dakota, Louisiana, and Virginia 25
2.6.2. Kentucky and North Dakota 26
2.6.3. Great Smoky Mountain National Park 29
2.6.4. Virginia and West Virginia 32
2.6.5. West Virginia 32
2.6.6. Vertical profiles of ozone concentrations 34
3. MATERIALS AND METHODS 38
3.1. Objective 1: Comparison/Assessment of Ozone Monitoring Station Data 38
3.1.1. Description of the study area 38
3.1.2. Ozone monitoring stations 39
3.1.3. Construction of data set 42
3.1.4. Examination of data 43
3.1.5. Assessment of compliance with EPA standards 44
3.2. Objective 2: Characterization of Mixing Heights and Ozone Concentrations 45
3.2.1. Description of experimental site 45
3.2.2. Experimental design 46
3.2.3. Ozone/meteorological measurement 46
3.2.4. Ozone/meteorological sampling 48
3.2.5. Measurement period 49
3.2.6. Examination of data 50

3.3. Objective 3: Mixing Height Profiles/Thermophysical Relationships 50
3.3.1. Estimation of mixing heights 50
3.3.2. Mixing height profiles 51
3.3.3. Thermophysical relationship between added heat and mixing height 51
3.4. Objective 4: Comparison of Observed Mixing Height Profiles to Modeled Mixing Height Profiles 51
3.4.1. PCRAMMET mixing height profiles 51
3.4.2. Mixing height profiles comparison 52
3.5. Objective 5: Predictive Model for Mixing Heights 52
4. RESULTS AND DISCUSSION
4.1. Objective 1: Comparison/Assessment of Ozone Monitoring Station Data . 55
4.1.1. Graphical comparison of daily mean and maximum ozone concentrations 55
4.1.2. Assessment of compliance with EPA standards 67
4.2. Objective 2: Characterization of Mixing Heights and Ozone Profiles 67
4.2.1. Tethersonde measurements 67
4.2.2. Summary of Tethersonde measurements 146
4.3. Objective 3: Mixing Height Profiles/Thermophysical Relationships 157
4.3.1. Mixing height profiles 157
4.3.2. Thermophysical relationships 158
4.4. Objective 4: Comparison of Observed Mixing Height Profiles to PCRAMMET Modeled Mixing Height Profiles 164
4.5. Objective 5: Alternative Predictive Model for Mixing Heights 172
5. CONCLUSIONS 180
REFERENCES 182
VITA 192

LIST OF TABLES

3.1. Ozone Monitoring Stations and NOAA Laboratory 41

4.1. Number of Days Hourly Averaged Ozone Concentration (ppb) Exceeded Respective Concentration by Station 63

4.2. Frequency of Hours Exceeding Hourly Averaged Ozone Concentrations ≥ 80 ppb 64

4.3. Frequency of Hours Exceeding Hourly Averaged Ozone Concentrations ≥ 100 ppb 65

4.4. Frequency of Hours Exceeding Hourly Averaged Ozone Concentrations ≥ 120 ppb 66

4.5. Number of Days at Eastern Tennessee Monitoring Stations in July and August, 1995 that Would Have Exceeded the Current 8-Hour NAAQS Ozone Standards . . . 68

4.6. Frequency of Hours Exceeding 8-Hour Averaged Ozone Concentrations ≥ 80 ppb 69

4.7. Changes in Near-Surface and Aloft Ozone Concentrations 152

4.8. Comparison of Ozone Concentrations Monitored at Freels Bend, TN and at the NOAA Laboratory (Oak Ridge, TN) 153

LIST OF FIGURES

2.1. Boundary Layer Structure in Regions of High Pressure 6

2.2. Examples of Boundary Layer Vertical Temperature Structure 10

2.3. Average Diurnal Variation of the Vertical Temperature Structure at Oak Ridge National Laboratory During the Period September-October 1950 11

2.4. Adiabatic and Environmental Temperature Profiles 13

2.5. Anabatic and Katabatic Winds 15

2.6. Conceptual Representation of Circulation Patterns in a Valley on a Clear Night .. 16

2.7. Mean Diurnal Ozone Patterns for Three Rural Sites in Virginia, Louisiana, and South Dakota 27

2.8. Ozone Diurnal Profiles for a Rural Site in Louisiana During Episodic and Nonepisodic Conditions 27

2.9. Average Pattern for Mixing Height from 0500 to 1130 LDT 28

2.10. Average Diurnal Patterns for Ozone Monitoring Sites in Jefferson County, Kentucky and Oliver County, North Dakota 30

2.11. Comparison of Diurnal Patterns for Ozone Monitoring Stations at Giles County, Look Rock, and Cove Mountain, Tennessee 31

2.12. Comparison of Seasonally Averaged Diurnal Patterns for Ozone Concentrations at Bearden Knob and Parsons, West Virginia 33

2.13. Diurnal Patterns of Mean Ozone Concentrations for Monitoring Stations in Wood County and Greenbrier Country, West Virginia for June and July, 1988 . 35

2.14. Ozone Vertical Profiles at Oak Ridge, Tennessee on July 29, 1987 37

3.1. Topographical Map of Eastern Tennessee 40

3.2. Schematic Illustration of Urban and Rural Mixing Height Interpolation Procedures 53

4.1. Daily Mean One-Hour Averaged Ozone Concentrations for Regional Monitoring Stations (July 1995) 56

4.2. Daily Mean One-Hour Averaged Ozone Concentrations for Regional Monitoring Stations (August 1995) 57

4.3. Box Plots of Daily One-Hour Averaged Ozone Concentration Mean Recorded at Regional Monitoring Stations During July and August 1995 58

4.4. Daily One-Hour Averaged Ozone Concentration Maxima Recorded at Regional Monitoring Stations (July 1995) 60

4.5. Daily One-Hour Averaged Ozone Concentration Maxima for Regional Monitoring Stations (August 1995) 61

4.6. Box Plot of Daily One-Hour Averaged Ozone Concentration Maxima Recorded at Regional Monitoring Stations During July and August 1995 62

4.7. Profiles of Potential Temperature, Ozone Concentration, Wind Speed and Wind Direction Developed from Tethersonde Data Obtained on the Morning of July 8, 1995 71

4.8. Profiles of Potential Temperature, Ozone Concentration, Wind Speed and Wind Direction Developed from Tethersonde Data Obtained During the Afternoon-evening of July 8, 1995 76

4.9. Comparison of Hourly Mean Ozone Concentrations on July 8, 1995 Obtained from Look Rock and Freels Bend Regional Monitoring Stations with Reading Obtained at Oak Ridge with Tethersonde Instrumentation 80

4.10. Hourly Mean Ozone Concentrations Obtained from Regional Monitoring Stations on July 8, 1995 81

4.11. Profiles of Potential Temperature, Ozone Concentration, Wind Speed and Wind Direction Developed from Tethersonde Data Obtained During the Morning of July 14, 1995 83

4.12. Profiles of Potential Temperature, Ozone Concentration, Wind Speed and Wind Direction Developed from Tethersonde Data Obtained During the Afternoon-evening of July 14, 1995 87

4.13. Comparison of Hourly Mean Ozone Concentrations on July 14, 1995 Obtained from Look Rock and Freels Bend Regional Monitoring Stations with Reading Obtained at Oak Ridge with Tethersonde Instrumentation 89

4.14. Hourly Mean Ozone Concentrations Obtained from Regional Monitoring Stations on July 14, 1995 91

4.15. Profiles of Potential Temperature, Ozone Concentration, Wind Speed and Wind Direction Developed from Tethersonde Data Obtained During the Morning of July 17, 1995 93

4.16. Comparison of Hourly Mean Ozone Concentrations on July 17, 1995 Obtained from Look Rock and Freels Bend Regional Monitoring Stations with Reading Obtained at Oak Ridge with Tethersonde Instrumentation 95

4.17. Hourly Mean Ozone Concentrations Obtained from Regional Monitoring Stations on July 17, 1995 97

4.18. Profiles of Potential Temperature, Ozone Concentration, Wind Speed and Wind Direction Developed from Tethersonde Data Obtained During the Morning of July 20, 1995 99

4.19. Profiles of Potential Temperature, Ozone Concentration, Wind Speed and Wind Direction Developed from Tethersonde Data Obtained During the Afternoon-evening of July 20, 1995 101

4.20. Comparison of Hourly Mean Ozone Concentrations on July 20, 1995 Obtained from Look Rock and Freels Bend Regional Monitoring Stations with Reading Obtained at Oak Ridge with Tethersonde Instrumentation 103

4.21. Hourly Mean Ozone Concentrations Obtained from Regional Monitoring Stations on July 20, 1995 104

4.22. Profiles of Potential Temperature, Ozone Concentration, Wind Speed and Wind Direction Developed from Tethersonde Data Obtained During the Morning of July 30, 1995 107

4.23. Profiles of Potential Temperature, Ozone Concentration, Wind Speed and Wind Direction Developed from Tethersonde Data Obtained During the Afternoon-evening of July 30, 1995 108

4.24. Comparison of Hourly Mean Ozone Concentrations on July 30, 1995 Obtained from Look Rock and Freels Bend Regional Monitoring Stations with Reading Obtained at Oak Ridge with Tethersonde Instrumentation 110

4.25. Hourly Mean Ozone Concentrations Obtained from Regional Monitoring Stations on July 30, 1995 110

4.26. Profiles of Potential Temperature, Ozone Concentration, Wind Speed and Wind Direction Developed from Tethersonde Data Obtained During the Morning of July 31, 1995 113

4.27. Comparison of Hourly Mean Ozone Concentrations on July 31, 1995 Obtained from Look Rock and Freels Bend Regional Monitoring Stations with Reading Obtained at Oak Ridge with Tethersonde Instrumentation 114

4.28. Hourly Mean Ozone Concentrations Obtained from Regional Monitoring Stations on July 31, 1995 115

4.29. Profiles of Potential Temperature, Ozone Concentration, Wind Speed and Wind Direction Developed from Tethersonde Data Obtained During the Morning of August 1, 1995 118

4.30. Comparison of Hourly Mean Ozone Concentrations on August 1, 1995 Obtained from Look Rock and Freels Bend Regional Monitoring Stations with Reading Obtained at Oak Ridge with Tethersonde Instrumentation 119

4.31. Hourly Mean Ozone Concentrations Obtained from Regional Monitoring Stations on August 1, 1995 120

4.32. Profiles of Potential Temperature, Ozone Concentration, Wind Speed and Wind Direction Developed from Tethersonde Data Obtained During the Afternoon-evening of August 23, 1995 122

4.33. Comparison of Hourly Mean Ozone Concentrations on August 23, 1995 Obtained from Look Rock and Freels Bend Regional Monitoring Stations with Reading Obtained at Oak Ridge with Tethersonde Instrumentation 124

4.34. Hourly Mean Ozone Concentrations Obtained from Regional Monitoring Stations on August 23, 1995 125

4.35. Profiles of Potential Temperature, Ozone Concentration, Wind Speed and Wind Direction Developed from Tethersonde Data Obtained During the Afternoon-evening of August 24, 1995 127

4.36. Comparison of Hourly Mean Ozone Concentrations on August 24, 1995 Obtained from Look Rock and Freels Bend Regional Monitoring Stations with Reading Obtained at Oak Ridge with Tethersonde Instrumentation 129

4.37. Hourly Mean Ozone Concentrations Obtained from Regional Monitoring Stations on August 24, 1995 130

4.38. Profiles of Potential Temperature, Ozone Concentration, Wind Speed and Wind Direction Developed from Tethersonde Data Obtained During the Afternoon-evening of August 29, 1995 132

4.39. Comparison of Hourly Mean Ozone Concentrations on August 29, 1995 Obtained from Look Rock and Freels Bend Regional Monitoring Stations with Reading Obtained at Oak Ridge with Tethersonde Instrumentation 133

4.40. Hourly Mean Ozone Concentrations Obtained from Regional Monitoring Stations on August 29, 1995 135

4.41. Profiles of Potential Temperature, Ozone Concentration, Wind Speed and Wind Direction Developed from Tethersonde Data Obtained During the Morning of August 30, 1995 136

4.42. Profiles of Potential Temperature, Ozone Concentration, Wind Speed and Wind Direction Developed from Tethersonde Data Obtained During the Afternoon-evening of August 30, 1995 138

4.43. Comparison of Hourly Mean Ozone Concentrations on August 30, 1995 Obtained from Look Rock and Freels Bend Regional Monitoring Stations with Reading Obtained at Oak Ridge with Tethersonde Instrumentation 139

4.44. Hourly Mean Ozone Concentrations Obtained from Regional Monitoring Stations on August 30, 1995 141

4.45. Profiles of Potential Temperature, Ozone Concentration, Wind Speed and Wind Direction Developed from Tethersonde Data Obtained During the Morning of August 31, 1995 143

4.46. Comparison of Hourly Mean Ozone Concentrations on August 31, 1995 Obtained from Look Rock and Freels Bend Regional Monitoring Stations with Reading Obtained at Oak Ridge with Tethersonde Instrumentation 144

4.47. Hourly Mean Ozone Concentrations Obtained from Regional Monitoring Stations on August 31, 1995 145

4.48. Stable Boundary Layer (Nocturnal Inversion) Height as a Function of Time ... 148

4.49. Profiles of Ozone Concentrations Developed from Tethersonde Data Obtained on July 8, 1995 and Used to Define Near-Surface and Aloft Ozone Concentrations 150

4.50. Mean Ozone Concentrations Measured in the Residual and Stable Boundary Layers and Predicted in the Mixed Layer 154

4.51. A Comparison of Predicted Ozone Concentrations Versus Observed Ozone Concentrations at Freels Bend 156

4.52. Mixing Height Profile for July 8, 1995 159

4.53. Mixing Height Profile for July 14, 1995 160

4.54. Mixing Height Profile for July 20, 1995 161

4.55. Thermophysical Relationship Between Heat Input and Mixing Height 163

4.56. Experimentally- Determined And PCRAMMET-modeled Mixing Height Profiles For July 8, 1995 168

4.57. Experimentally- Determined And PCRAMMET-modeled Mixing Height Profiles For July 14, 1995 169

4.58. Experimentally- Determined and PCRAMMET-modeled Mixing Height Profiles for July 20, 1995 170

4.59. Schematic Illustration of The Predictive Model For Mixing Heights 173

4.60. Exponential Model For Mixing Height (M) as a Function of Time of Day 175

4.61. Reduction and Reestablishment of Mixing Heights near the Surface with Respect to Sunset 177

CHAPTER 1

INTRODUCTION

A number of urban areas throughout the United States are nonattainment for one or more national ambient air quality standards. Approximately 60 to 100 U.S. metropolitan areas (representing populations of 80 to 130 million people, respectively) do not meet current ambient air quality standards for ozone as specified in the Clean Air Act (Sperling, 1990). Recently, the Environmental Protection Agency (EPA) revised national ambient air quality standards (NAAQS) for ozone based on review of evidence linking ambient ozone exposures (at levels allowed by current standards) to adverse health and welfare effects. The previous one hour primary standard (0.12 ppm) was replaced by an eight-hour standard (0.08 ppm). The new standard is based on a the three-year average of the annual fourth-highest daily maximum eight-hour average ozone concentration measured at each monitor within a region. The one-hour secondary standard was replaced by an eight-hour standard identical to the new primary standard. The new secondary standard will provide enhanced protection to the public welfare against ozone-induced effects on vegetation, such as agricultural crop loss and forest/ecosystem damage. The standards became effective September 16, 1997. Following promulgation of the new standards, the Clean Air Act (CAA) provides up to three years for designation of areas according to their most recent air quality. After designation, an additional three years is provided to develop and submit State Implementation Plans (SIPs) for attainment. Under this approach, areas would be designated as nonattainment for the eight-hour standard by the year 2000 and would submit SIPs by 2003 (FR, July 18, 1997).

In 1990, Knoxville, Tennessee was classified as nonattainment (marginal) based on noncompliance with the one-hour primary standard (0.12 ppm). Although re-attainment status was granted by 1993, it remains highly questionable whether Knoxville and other regional metropolitan areas will remain compliant under the new standards. Air quality in the Knoxville-Oak Ridge region is of particular interest because of the central location in the eastern Tennessee ridge-and-valley and proximity to the Great Smoky Mountain National Park (GSMNP). The GSMNP has documented damage to vegetation in the park due to concentrations of ozone which are in the 70-120 ppb range (Renfro, 1995).

Daily ozone concentrations are heavily dependent on variations in meteorological conditions. Of particular importance to air pollution modelers is the mixing height (MH), the height above the surface through which relatively vigorous vertical mixing occurs (Holzworth, 1972). Accurate representation of the mixing height plays an essential role in the ability of photochemical and dispersion models to accurately predict pollutant concentrations. In addition to the mixing height determining the atmospheric volume in which chemical reactions occur, many other model parameters are calculated using mixing height values (EPA, 1996; Marsik et al., 1995, Stull, 1988). Concentration of ozone depends upon the degree of mixing in the times between emission of ozone precursors, photochemical formation and transport to the receptor. Inversion layers are prominent determinants of vertical mixing in the atmosphere and therefore influence the degree to which ozone will be dispersed or accumulated. Ozone remaining in a layer aloft, as the result of reduced turbulence and mixing at day's end, may be transported

through the night, often to regions far removed from metropolitan areas. On the subsequent day, developing mixing heights may entrain ozone from reservoirs aloft. The downward mixing of ozone-rich reservoirs can result in significant increases in local concentrations from transported ozone (EPA, 1996). Preliminary research in eastern Tennessee has shown that ozone concentrations increase in the presence of high pressure air masses, and that concentrations exceeding the air quality standards required periods of stagnant air (Hutton, 1993; Mueller, 1994).

Based on prior studies (Nappo et al., 1989; Hutton, 1993; Mueller, 1994; Lefohn et al., 1994; Gilliam and Turrill, 1995) which reported the presence of high ozone concentrations throughout the night at high elevation monitoring stations in the Appalachians, it was hypothesized that high ozone concentrations recorded at low-elevation monitoring stations in eastern Tennessee result from formation of ozone during the day as well as the entrainment of ozone aloft. The presence of ozone reservoirs aloft may result from regional transport or previous days of local high ozone. Regardless of origin, entrainment of ozone-enriched reservoirs may play a significant (and sometime dominant) role in high ozone concentrations at low-elevation monitoring stations. This process also plays a major role in creating relatively constant concentrations at high elevation stations in the mountainous areas such as the GSMNP, particularly in those areas that are typically higher in elevation than the nighttime inversion. These areas do not experience the significant ozone scavenging (removal) and deposition which occur at night in low elevation areas. Reaction of ozone may overshadow local anthropogenic sources. The net result is that ozone at the low level stations is reduced to nearly zero (0-

30 ppb) at night, whereas concentrations in the air above the monitoring stations remain high throughout the night. The purpose of this study was to characterize development and decay of mixing heights and investigate relationships between mixing heights and ozone concentrations aloft.

In support of this purpose, the following objectives were identified:

1. To compare ozone concentration data from selected high and low elevation monitoring stations in eastern Tennessee for a two-month period (July and August, 1995) and to assess compliance with new EPA standards.

2. To characterize mixing height and ozone concentration using instrumentation attached to a tethered balloon and to document the development and reduction and reestablishment of mixing heights in relationship to vertical ozone structure.

3. To construct regional mixing height profiles using data from tethered balloon instruments and to determine thermophysical relationships between mixing height development and added atomospheric heat.

4. To compare the mixing height profiles constructed to mixing height profiles generated by PCRAMMET, the primary EPA mixing height model.

5. To design an algorithm which is better predictive of mixing heights during periods when regions are under the influence of both high-pressure systems and high temperatures.

CHAPTER 2

LITERATURE REVIEW

2.1 Air Pollution Meteorology

2.1.1. Boundary Layer Structure

The atmospheric boundary layer has been defined as the component of the troposphere which is directly influenced by the earth's surface and which responds to surface forces which have timescales of an hour or less (Pielke, 1984; Stull, 1988). Effluents generated by man's activities are released directly into this layer and are subsequently transported, dispersed, and transformed there until they are finally removed (Randerson, 1984; Stull, 1988).

In the presence of high pressure systems, the boundary layer above land surfaces produces a characteristic morphological structure which unfolds with the diurnal cycle (Figure 2.1). The layer comprises three sublayers: the mixed layer, ML; the stable (nocturnal) boundary layer, SBL; and the residual layer, RL (Stull, 1988). During early morning hours, prior to sunrise, stratification of the boundary layer is stable because the earth is cooler than the air masses overhead. As the sun rises on clear days, the earth is heated by solar radiation. The ground transfers heat to atmospheric air near the surface, and initiates the formation of a shallow mixed layer. As warm air rises and is replaced by more dense, cool air from above; a continual, cyclical mixing process is established which grows throughout the day until midafternoon. The initial early morning growth is slow because of the inhibitory presence of the nocturnal stable layer. However, by late morning, continued warming of the nighttime air has resulted in dissipation (often

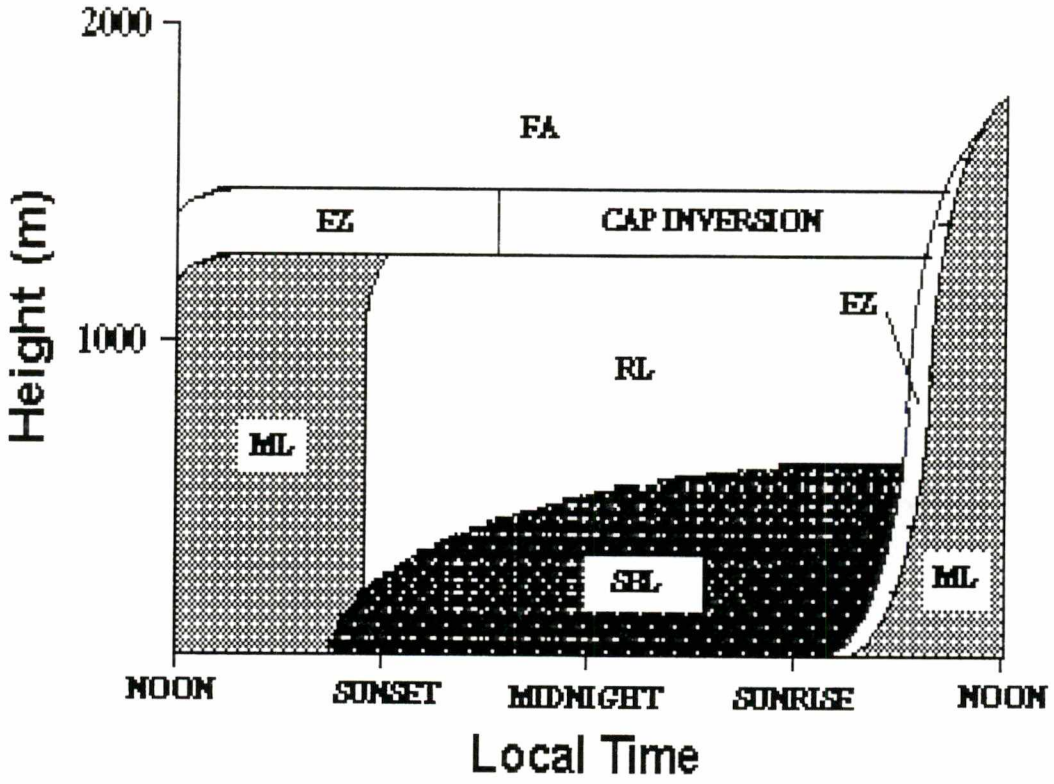

FIGURE 2.1. BOUNDARY LAYER STRUCTURE IN REGIONS OF HIGH PRESSURE. The structure is comprised of three major parts: the mixed layer (ML), the residual layer (RL), and the nocturnal stable boundary layer (SBL). Also depicted are the free atmosphere (FA), and entrainment zone (EZ). Adapted from Stull, 1988.

referred to as breakup) of the nocturnal inversion (Slade, 1968; Randerson, 1984; Stull, 1988). As the lower air temperature approximates that of air in the RL, the top of the ML rises to the RL-base elevation. Since the capping effect of the nocturnal stable layer is no longer present, the ML grows rapidly upward (Stull, 1988). Exponential growth of the ML may result in mixing heights of 1000 to 2000 m (Holzworth, 1972). As the sun sets, the ground cools rapidly and an intense, shallow inversion forms. As surface temperature continues to decrease throughout the night, the SBL becomes more pronounced. By morning, the SBL typically extends up to 100 m to 500 m above the earth's surface, but heights of 1000 m have been observed. The layer which lies between the SBL and the prior day's entrainment zone is the RL. This warmer, less dense air will not sink into the SBL during the night. The next day this cycle repeats (Slade, 1968; Randerson, 1984; Stull, 1988).

According to boundary-layer theory, most pollutants emitted into the mixed layer during the day are uniformly diffused. As surface cooling begins, stable layers develop and vertical diffusion of pollutants between layers ceases. More important, layers are released from physical constraints of adjacent layers, and surface-layer exchange processes significantly slow or stop. In this decoupled state, pollutants aloft may be transported downstream without appreciable dilution. On the following day, if sufficient surface heating occurs, pollutants will be entrained into the ML of the rising boundary layer. If surface heating is weaker, the maximum boundary layer height may remain below some polluted layers thereby allowing them to remain intact (Sisterson and Shannon, 1979; Eagleman, 1979; Wesely and Hicks, 1977). The effect of the

atmospheric stability of these layers on pollutant dispersion is well documented (Anonymous, 1955; Slade, 1968; Plate, 1971; Byers, 1974; Hess, 1979; Wark and Warner, 1981; Randerson, 1984; Ahrens, 1985; Lyons and Scott, 1990). Dispersion of pollutants in the boundary layer is influenced by the convective and turbulent mixing associated with stability conditions. In turn, stability conditions are created by vertical temperature profiles. The ML depth provides important information on the ability of the atmosphere to disperse pollutants and is of considerable importance in estimating the concentration of pollutants downwind from a source (Eagleman, 1991). Evaluation of these diurnal patterns is useful for distinguishing between possible influence of changes in emission levels and possible influence of meteorological transport of pollutants (Lefohn et al., 1993).

2.1.2. Temperature Structure

Atmospheric temperature structure is closely related to boundary layer structure. The vertical temperature gradient serves as an index for determining the magnitude of atmospheric turbulence. Typically, decrease of temperature is associated with an increase of elevation. This inverse relationship results from the earth's surface serving as the primary source of heat energy for heating the atmosphere (Slade, 1968; Randerson, 1984).

The negative of the temperature gradient in the atmosphere is referred to as a lapse rate. Of special significance are the adiabatic and normal or standard lapse rates. The adiabatic lapse rate is the unique atmospheric lapse rate where an element of air is displaced from one level to another while maintaining the same temperature or density as the surrounding air. The adiabatic lapse rate is equal to approximately 1 °C/100 m

(5.4°F/1000 ft). The troposphere is characterized by the normal or standard lapse rate which is 0.66°C/100m (3.6°F/1000 ft). If there is no change of temperature with height, the atmospheric layer is described as isothermal. If temperature increases with elevation, the layer is referred to as an inversion. If the temperature decreases at a rate greater than the adiabatic rate, the lapse rate is termed superadiabatic and the atmosphere is unstable. Under superadiabatic conditions, vertical motions are accelerated because warmer masses of air are forced to rise whereas cooler air is forced downward. Conversely, if the atmospheric temperature decreases at a rate less than the adiabatic rate, the lapse rate is called subadiabatic and the atmosphere is stable. Figure 2.2 illustrates examples of low-level vertical temperature structure (Slade, 1968; Wark and Warner, 1971; Randerson, 1984; Stull, 1988).

2.1.3. The Diurnal Cycle of Vertical Temperature Structure

The typical diurnal cycle of a vertical temperature pattern is shown in Figure 2.3. The plots were constructed from data obtained during late summer and early fall at Oak Ridge, Tennessee. During the early morning, 0600 to 0700 EST, a surface-based temperature inversion is present. By 0800 EST, the heating effect of the rising sun has resulted in the initial destruction of the lowest section of the inversion. By 1000 EST, the inversion layer has completely dissipated. Throughout the day, an unstable layer is present near the ground and continued heating of the entire air column is displayed. The nocturnal inversion begins to return at 1800 EST. As the earth progressively cools throughout the night, the inversion becomes far more pronounced (Holland, 1953).

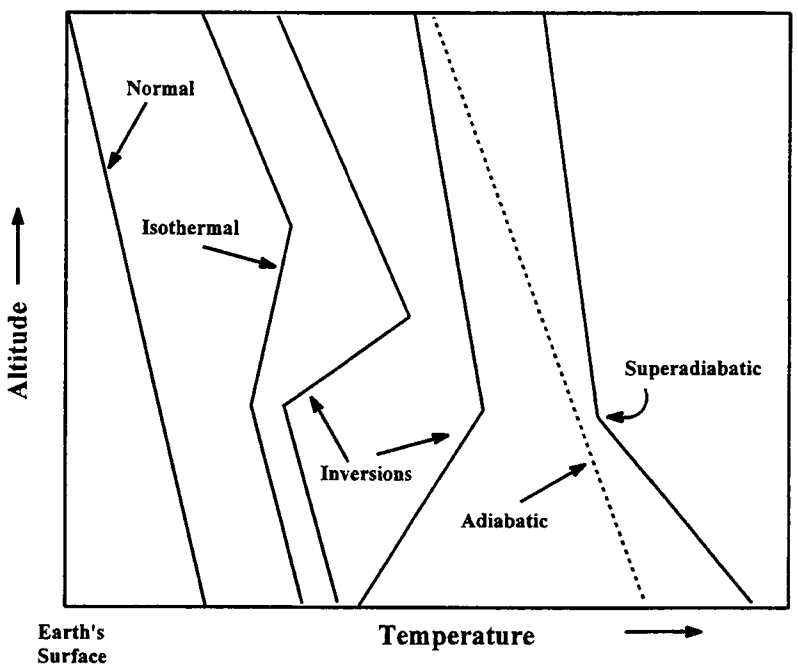

FIGURE 2.2. EXAMPLES OF BOUNDARY LAYER VERTICAL TEMPERATURE STRUCTURE. Adapted from Slade, 1968.

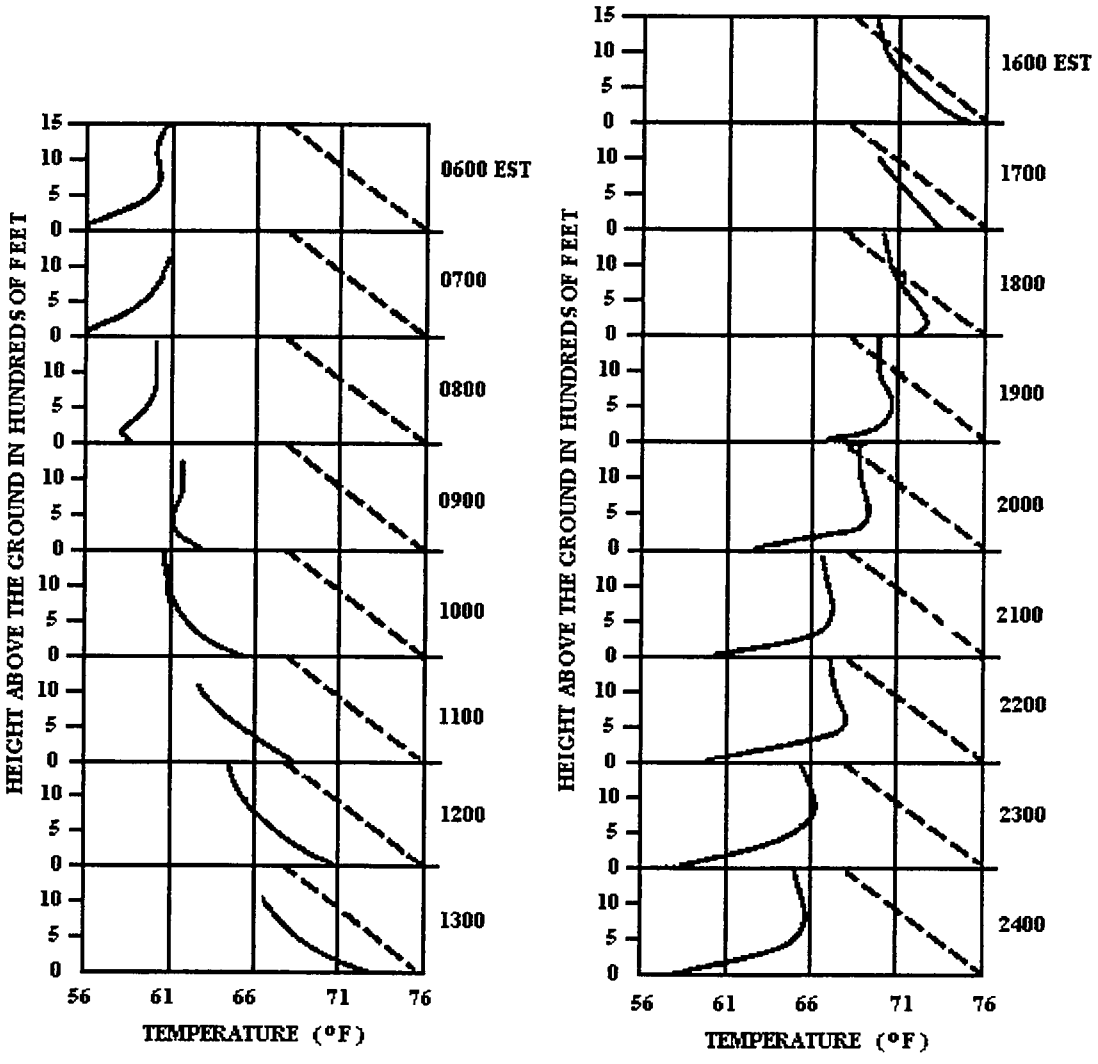

FIGURE 2.3. AVERAGE DIURNAL VARIATION OF THE VERTICAL TEMPERATURE STRUCTURE AT OAK RIDGE NATIONAL LABORATORY DURING THE PERIOD SEPTEMBER-OCTOBER, 1950. Data were obtained from tethered-balloon soundings. The dashed lines represent the adiabatic lapse rate. Adapted from Holland, 1953.

2.1.4. Atmospheric Stability and Vertical Temperature Structure

The degree of atmospheric stability must be known to understand dispersion, transport, transformation, and deposition of air pollutants. Atmospheric stability classes are typically categorized into three states: unstable, neutral, and stable. The states refer to the reaction of an air parcel displaced adiabatically in the vertical direction. Figure 2.4 illustrates environmental lapse rates associated with the three stability classes. An air parcel originates at an elevation represented by the small circle in the figure. The temperature of the air parcel is the same as that of the surrounding environment. If the density of the air parcel is less than that of the environment ($\rho_p < \rho_e$ or $T_p > T_e$), the parcel accelerates upward; the atmosphere is classified as unstable. If the density of the air parcel is greater than that of the environment ($\rho_p > \rho_e$ or $T_p < T_e$), the parcel accelerates downward and the atmosphere is viewed as stable. If the density of the air parcel is the same as that of the environment ($\rho_p = \rho_e$ or $T_p = T_e$), there is no force applied and the parcel continues at its original speed. Under these conditions, the atmosphere is said to be neutral. The stability criteria are formalized in the following manner (Hanna et al., 1982):

$$Unstable: \frac{\partial T}{\partial z} < -0.98\,^{\circ}C/100m$$

$$Stable: \frac{\partial T}{\partial z} > -0.98\,^{\circ}C/100m$$

$$Neutral: \frac{\partial T}{\partial z} = -0.98\,^{\circ}C/100m$$

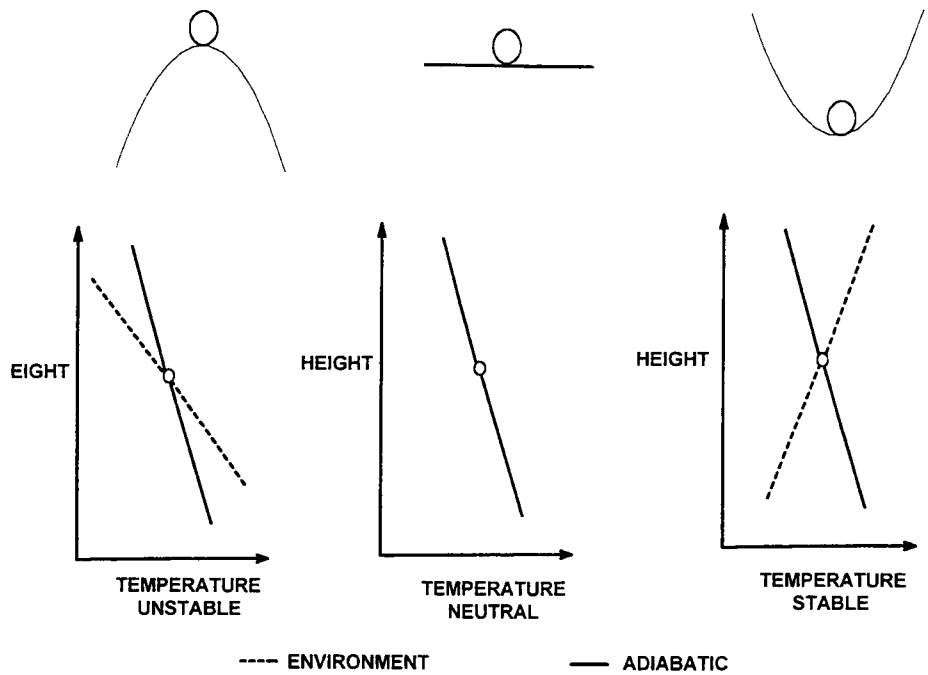

FIGURE 2.4. ADIABATIC AND ENVIRONMENTAL TEMPERATURE PROFILES. Unstable, neutral, and stable environmental temperature profiles are represented by dashed lines. Adapted from Hanna et al., 1982.

2.1.5. Meteorological Wind Patterns Associated with Topographic Features

Meteorological systems associated with topographic features result from influences on airflow produced by differing, juxtaposed topographic features such as mountains and valleys. Of special interest are the airflows typically present in regions of complex terrain. These airflow patterns consist of cross-valley axis and along-valley axis circulations. Cross-valley-axis circulations result when a sloping surface is heated or cooled. Rising or sinking air parcels follow the terrain as depicted in Figure 2.5. Figure 2.5(A) illustrates rising motions called anabatic winds. These winds result from heating of mountain-valley slopes by the rising sun. When the rising air reaches ridge top, it separates and continues to rise until reaching the capping stable layer or entrainment zone. Figure 2.5(B) depicts the nighttime situation where cool air drains down mountain-valley slopes and pools in the valley floor. In areas with comparatively steep slopes, these descending flows are referred to as katabatic winds (Slade, 1968; Randerson, 1984; Stull, 1988).

Along-axis circulations are generally referred to as mountain-valley or slope-valley winds. On clear nights with light prevailing winds, the wind in a valley frequently assumes a configuration similar to that depicted in Figure 2.6. As the valley slopes cool by radiation, air adjacent to the slopes cools and becomes more dense than air over the center of the valley floor. This dense air flows down the mountain-valley slopes toward the valley floor. However, since drainage flow occurs at locations throughout the valley, descending air will combine into a general flow toward the valley mouth. After the slope-valley circulation is established, it will normally extend to ridge top height. This wind

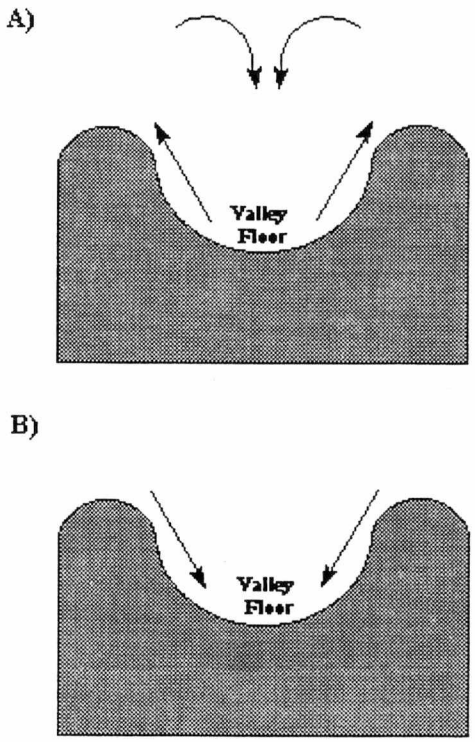

Figure 2.5. ANABATIC (A) AND KATABATIC (B) WINDS.

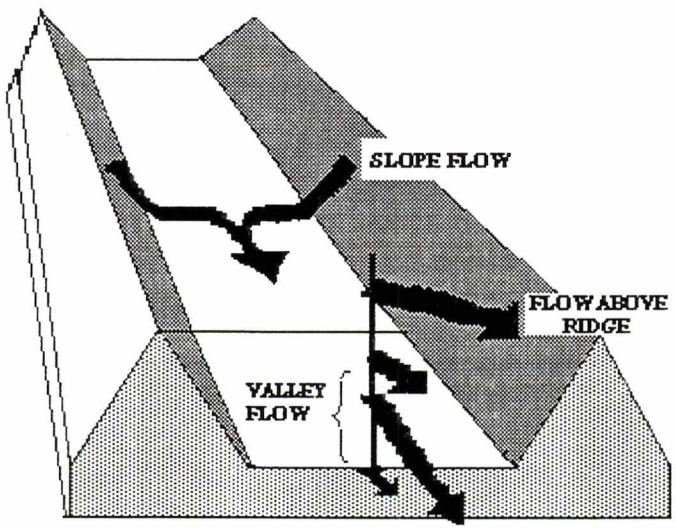

FIGURE 2.6. CONCEPTUAL REPRESENTATION OF CIRCULATION PATTERNS IN A VALLEY ON A CLEAR NIGHT. Adapted from Slade, 1968.

pattern is destroyed after sunrise by heating of the valley floor and slopes. On clear days with light winds, an opposite effect, an up valley, up slope wind may develop. This flow results from heating of air adjacent to the sun-warmed valley floor and slopes. However, this condition is not as pronounced as the nighttime flow. At night, turbulence in the valley is suppressed by the nocturnal boundary layer. Thus, airflow patterns in the valley floor remain relatively undisturbed. During the day, heated land surfaces warm adjacent air and create atmospheric turbulence. As turbulence increases, air within the valley mixes with free air flow above the ridge tops. The development of daytime turbulent mixing constitutes a disruptive mechanism which hinders establishment of the up slope, up valley wind patterns. Although such patterns are known to exist, they are neither as common nor pronounced as the nighttime down-valley flows (Slade, 1968; Randerson, 1984; Stull, 1988).

2.2 Tropospheric Ozone Photochemistry

Ozone is an elemental allotrope of oxygen which consists of three oxygen atoms. Ozone has a characteristic odor and is derived from the Greek word for "I smell" (Lange and Forker, 1961). Although most atmospheric ozone is located in the stratosphere where it prevents ultraviolet solar radiation from penetrating to the earth's surface, the increasing presence of ozone in the troposphere has caused it to become the most significant air pollutant in many parts of the world.

Ozone may be photochemically generated in both polluted and unpolluted tropospheres. In both regions, ozone results from anthropogenic and biogenic emissions of nitrogen oxides (NO_x) and volatile organic carbons (VOCs), from transport of those

emissions and their respective reaction products, and from chemical reactions occurring in the atmosphere concurrent with transport and dispersion of emissions (EPA, 1996).

Specific chemical reactions which lead to the production of ozone, often referred to as the "photochemical smog" reactions, involve oxidation of hydrocarbons and carbon monoxide in the presence of nitrogen oxides (NO_x) and sunlight (Calvert et al., 1972; Seinfeld, 1989; Lefohn, 1992). Ozone concentration is controlled by the following four reactions:

$$NO_2 + h\nu \rightarrow NO + O \qquad \text{(Equation 2.1)}$$

$$O + O_2 \rightarrow O_3 \qquad \text{(Equation 2.2)}$$

$$NO + O_3 \rightarrow NO_2 + O_2 \qquad \text{(Equation 2.3)}$$

$$NO_2 + O_3 \rightarrow NO_3 + O_2 \qquad \text{(Equation 2.4)}$$

In the presence of sunlight, nitrogen dioxide dissociates according to equation 2.1. The highly active monatomic oxygen, O, combines with O_2 to form O_3 via equation 2.2. Equation 2.3 shows the process whereby ozone subsequently oxidizes nitric oxide to nitrogen dioxide. Equation 2.4 is comparatively slow and is of less importance during the day. The first three chemical reactions are rapid, and should form a photostationary state whereby ozone levels would remain low. Although the cyclical reactions result in no net production of ozone, other photochemical reactions which lead to oxidation of NO to NO_2 occur. These reactions prevent NO from reducing ozone by equation 2.3 and result in rising ozone concentrations (Wark and Warner, 1981; Randerson, 1984; Lefohn, 1992).

The OH radical is the key reactive species in the troposphere associated with other chemical oxidation reactions. In the presence of NO, OH radical reactions with VOCs lead to formation of ozone and increased ozone concentrations (EPA, 1996). Specifically, the OH radical, and to a smaller extent O and O_3, reacts with hydrocarbons, carbon monoxide (CO), aldehydes, and other hydrocarbon oxidation products to begin degradation reactions for most VOCs. These reactions produce free peroxy radical chains [hyperoxy (HO_2), alkylperoxy (RO_2), and acylperoxy ($RCOO_2$)] which subsequently oxidize NO to NO_2 (Randerson, 1984; Lefohn, 1992). In the remote troposphere, OH radical production occurs from the near-UV photolysis of O_3 itself (Levy, 1971). In polluted atmospheres, radical production results from the photolysis of aldehyde and nitrous acid emissions (Calvert, 1976; Rodgers and Davis, 1989).

In the remote, pristine troposphere, O_3 photochemistry is primarily driven by the oxidation of CH_4 and CO. However, in forested areas such as the GSMNP and its surrounding area, the oxidation of biogenic hydrocarbons plays a dominant role in the production of atmospheric O_3 (Rasmussen, 1972; Zimmerman, 1979, 1980; Lamb et al., 1987; Trainer et al., 1987, 1991; Stull, 1992; Grosjean et al., 1993). In polluted regions of the boundary layer, photochemical processes cause the vast majority of summertime air pollution episodes to have high levels of O_3. Using atmospheric smog chambers, numerous studies have demonstrated that irradiation of air mixtures containing hydrocarbons and nitrogen oxides at concentrations typical of urban anthropogenic emissions can yield O_3 concentrations well above the 120 ppb NAAQS for O_3 (Jefferies et al., 1976; Carter, et al., 1979; Leone, et al., 1985; Lefohn, 1992).

Although hydrocarbons and nitrogen oxides have documented roles as precursors for ozone episodes in both rural and urban areas, the exact relationship between precursor levels and ozone generation is extremely complex and not yet fully understood (McKeen et al., 1991; Trainer et al., 1991; Lefohn, 1992; Grosjean et al., 1993). While there are numerous ground-based ozone monitoring stations, very little data have been collected to show the vertical extent of ozone. Limited understanding of these relationships may be partially responsible for the limited success of efforts in the United States to develop and implement an effective program to control O_3 through reductions in anthropogenic emissions in specific geographical locations (Chang et al., 1992; Lefohn, 1992).

Complexities inherent in the development of an O_3 control strategy based on precursor relationships are threefold. First, calculated impacts on O_3 concentrations as a result of reductions in volatile organic compounds (VOCs) and nitrogen oxides (NO_x) vary considerably with changes in ambient concentrations of VOCs and nitrogen oxides. Thus, one must accurately define ambient precursor levels and their reactivity in the region of interest in order to implement a pragmatic control program. In the case of hydrocarbons, this is not a simple task. The polluted troposphere contains hundreds of organic compounds (alkanes, alkenes, carbonyls, alcohols, carboxylic acids, and aromatics) whose reactivity toward OH radicals varies widely (Calvert et al., 1972; Seinfeld, 1989; Trainer et al., 1991; Lefohn, 1992; Grosjean et al., 1993). In order to calculate peak O_3 concentrations as a functional result of initial organic and nitrogen oxide levels, one must know the accurate concentration of each organic species at the respective site (Lefohn, 1992). Second, air quality models simulating urban or regional

air quality use approximate chemical mechanisms in which organic compounds are grouped according to class or bonding, or small numbers of specific organic compounds are selected as representative of the entire class of atmospheric volatile organic compounds (Stockwell, 1986; Gery et al., 1988; Stull, 1992; EPA, 1996). Specifically, both the Urban Airshed Model-IV (UAM-IV) and the Regional Oxidant Model (ROM) utilize the carbon-bond mechanism (CBM-IV) which is considered to represent the state of the science. The mechanism combines kinetic, mechanistic, and photolytic information associated with more than eighty reactions involving more than thirty species to simulate urban and regional photochemistry. Chemical representations of aromatics, biogenic hydrocarbons, peroxyacetyl nitrates, and formaldehyde performed well when compared with smog chamber studies. However, fundamental kinetic data are needed on the photooxidation of aromatics, higher alkanes, and higher alkenes to address areas of uncertainty in existing mechanisms. In addition, many of the smog chamber studies are somewhat dated and require validation based on more current understandings (EPA, 1990; EPA, 1996). Third, a major complication in the control of O_3 centers on the significant role which natural hydrocarbons emitted from trees may play in the generation of high O_3 concentrations in both rural and urban settings (Trainer et al., 1987; Chameides et al., 1988). In the U.S., emissions of biogenic hydrocarbons from trees are equivalent or greater than anthropogenic hydrocarbon emissions (Lamb et al., 1987, 1993). Biogenic emission rates are also relatively high in the southeastern United States, even in large metropolitan areas, where high temperatures and large tracts of forested land combine to favor natural emissions (Westberg and Lamb, 1985; Chameides et al., 1988;

Lefohn, 1992; Lamb et al., 1993; EPA, 1996). Forest emissions are larger in this region than any other region in the United States. In summer, average regional volatile organic carbon emissions from forests exceed those of anthropogenic sources (Fehsenfeld et al., 1993; Lamb et al., 1993; EPA, 1996). Thus, effective control of urban O_3 might be obtained by moving toward a strategy which is based on nitrogen oxides and hydrocarbons rather than concentrating on reductions of hydrocarbon emissions (Lefohn, 1992).

2.3 Health Effects of Ozone

Ozone is a pulmonary irritant which affects mucous membranes, other lung tissues, and respiratory function (Lyons and Scott, 1990). Pulmonary responses to ozone include decreased inspiratory capacity (Kulle et al., 1985), mild bronchoconstriction (Beckett et al., 1985; Hazucha et al., 1989), rapid shallow breathing during exercise (Adams et al., 1981, Folinsbee et al., 1978, McDonnell et al., 1983, Kulle et al., 1985), and coughing or pain during deep inhalation (Hazucha et al., 1973; Seal et al., 1993). In addition to pulmonary irritation, several recent studies have suggested ozone may have statistically significant effects on mortality for urban areas which experience one-hour maximum concentrations above 150 ppb (Kinney and Ozkaynak, 1991).

Of particular concern are recent studies which evaluate responses of subjects exposed to low ozone concentrations (80 to 160 ppb) for times of four to eight hours. Both during and after exposure to ozone, adult subjects had adverse changes in measures of pulmonary function (e.g. airway spirometry, resistance, and responsiveness) (Hortsman et al., 1990; Larsen et al., 1991; Kehrl et al., 1991; McDonnell et al., 1991; Horvath et al.,

1991, Folinsbee et al., 1988, Hazucha et al., 1992; Folinsbee et al., 1993). When ozone levels equaled or exceeded 110 ppb, children in Atlanta received treatment for asthma more often (White et al., 1994). Based on data from these studies, it is not unreasonable to assume that chronic exposure to ozone at levels at or below 120 ppb may cause health risks.

2.4 Environmental Effects of Ozone

Of gaseous pollutants, ozone is the most injurious to agricultural crops, trees and vegetation. Effects of O_3 on plants may be observed at the cell, organ, whole plant, and population levels. Ozone is able to react with a diverse array of biological compounds and metabolites found in plants (Mudd, 1982; Heath, 1984; Pryor et al., 1984; EPA, 1996). Chemical reactive effects include ultrastructural changes to internal membranes (Thomson et al., 1974; Miyake et al., 1984), inhibition of photosynthetic gas exchange (Miller, 1987, 1988; Darrall, 1989), and reduction in the reproductive yield of crops (Kress and Miller, 1983). Ozone alters partitioning of carbon in tree seedlings (Adams et al., 1990; Spence et al., 1990) and in mature trees (Wilkinson and Barnes, 1973; McLaughlin et al., 1982). The disruption of photosynthesis and carbon allocation can suppress the growth of crops, trees, shrubs, and other vegetation. In addition, loss of vigor impairs the ability of trees and crops to reproduce and increases their susceptibility to insects and pathogens (Peterson et al., 1995; EPA, 1996).

In Tennessee, ambient ozone may have reduced radial growth of eastern white pine on the Cumberland Plateau as much as fifty per cent annually during a fifteen to twenty year period (Mann et al., 1980). Similarly, Appalachian mountain studies reported

reductions in overall growth (Benoit et al., 1983) and foliar damage (Anderson et al., 1988). In the GSMNP, recent field surveys identified 90 species with ozone-like damage. Fumigation studies have confirmed visible ozone injury on 30 of 46 species. Intensive field investigations on black cherry, yellow-poplar, sassafras and tall milkweed have documented significant visible injury in both the overstory of hardwood trees and the understory of seedlings and saplings. Eight to twenty-nine percent of black cherry leaves studied in GSMNP were injured by ozone (Chappelka et al., 1992; Renfro, 1996).

2.5 Ozone Pollution in the Southeastern United States

During the summer, the rural southern environment is characterized by stagnant conditions with small horizontal transport during the day. However, at night, winds are stronger in the remnant boundary layer. This pattern is important in evaluation of regional dispersion of pollutants from source areas (Fehsenfeld et al., 1993). Although ozone pollution was once considered an urban pollutant with high concentrations associated with large urban centers, it is now recognized as a regional problem. Ozone distribution is determined by precursor sources, chemical formation and destruction, transport and mixing. Of these atmospheric mixing is the most important factor with respect to vertical distribution of ozone.

Atmospheric mixing determines the height to which precursors are carried and the downward transport of ozone to the surface. Of particular interest is that ozone may be transported aloft, isolated from the surface by the stationary boundary layer, until daytime surface heating increases the ML depth and the ozone becomes entrained into the regional atmosphere (Nappo et al., 1989).

Annual ozone concentrations in the southeast United States are highest from April to October. Between 1978 and 1983, the highest O_3 concentrations were in the peidmont/mountain/ridge and valley sub-area of the South. Highest O_3 concentrations were observed at monitoring sites near Birmingham, Atlanta, Charlotte, and Richmond. Although the density of monitoring stations was insufficient to develop a detailed spatial distribution of ozone throughout this sub-area, it is apparent that forests adjacent to the larger metropolitan areas are exposed to somewhat higher concentrations than forests further away from larger cities (Pinkerton and Lefohn, 1987).

At rural and remote sites, the annual cycle in daily average ozone concentration was found to peak during the spring months. A similar spring maximum has been observed at other rural and remote sites and is often attributed to downward mixing of ozone from the stratosphere (Anonymous, 1980), but studies in the Tennessee Valley region found that the spring peak results from annual variation in night-time ozone and suggests the annual cycle in nocturnal mixing causes this peak (Meagher et al., 1987). In addition, background levels of natural O_3 may contribute 20-50 percent of the observed concentrations (Altshuller, 1987).

2.6 Case Studies

2.6.1. South Dakota, Louisiana, and Virginia (Kelly et. al., 1984)

During the summers of 1978-1980, the authors collected ozone and precursor data at rural sites in South Dakota, Louisiana, and Virginia. The patterns display a period of ozone in-crease from sunrise until mid-afternoon. A period of ozone decrease occurs from late afternoon until sunrise. The mean diurnal ozone patterns at all three sites are

shown in Figure 2.7. Figure 2.8 contains ozone profiles during episode and non-episode periods at the Louisiana site. Diurnal patterns are similar with periods of significant ozone increase occurring from 0700 to 1100, and periods of significant ozone decrease occurring from late afternoon until sunrise. However, episode ozone concentrations throughout the night and early morning are 10-15 ppb higher than non-episode concentrations. During the daytime, peak ozone concentrations for episodes are approximately 30 ppb higher than non-episodes. It is also interesting to note average patterns for mixing heights in Louisiana and Virginia as shown in Figure 2.9. The authors estimated the height of the nocturnal inversion at 50 ± 30 m. The inversion dissipated by approximately 0700. By 1000, the mixing height exceeded 1500 m at both the sites more than 95% of the time. The authors attempted to separate the effects of mixing from those of photochemistry by breaking the period of increasing ozone into smaller time segments whereby one mechanism should predominate over the other. Using this framework, the ambient data at the three sites suggested vertical mixing accounted for approximately half of the overall increase in ozone from morning to afternoon.

2.6.2. Kentucky and North Dakota (Lefohn et al., 1993)

Evaluation of diurnal pattern may be useful for investigation of possible influences of change in emission levels. In this study, diurnal pattern, pollutant concentrations, and the possible influence of meteorological variation are examined. Composite ozone diurnal patterns for Jefferson Co., KY were compared with those of

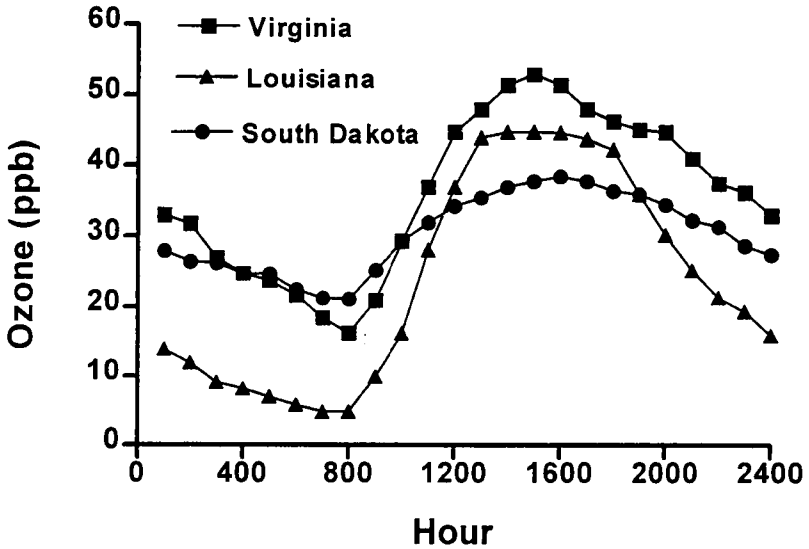

FIGURE 2.7. MEAN DIURNAL OZONE PATTERNS FOR THREE RURAL SITES IN VIRGINIA, LOUISIANA, AND SOUTH DAKOTA. Hour of the day refers to local daylight time (LDT) for each site. Adapted from Kelly et al., 1984.

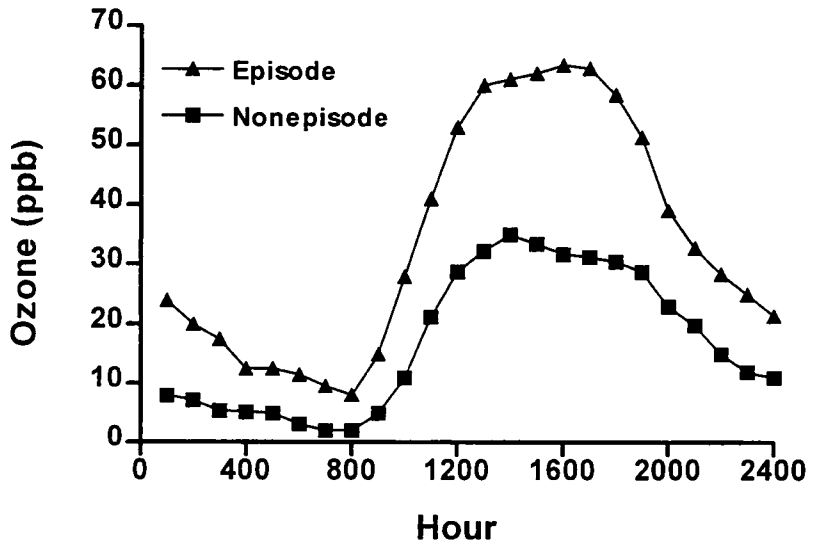

FIGURE 2.8. OZONE DIURNAL PROFILES FOR A RURAL SITE IN LOUISIANA DURING EPISODIC AND NON-EPISODIC CONDITIONS. Episodic conditions were described as periods of high pollution based on maximum ozone concentrations. Hour of the day is LDT. Adapted from Kelly et al., 1984.

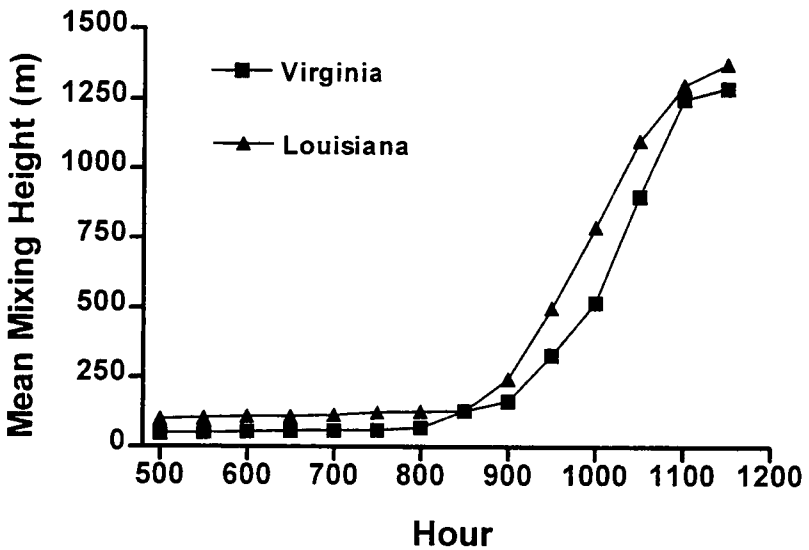

FIGURE 2.9. AVERAGE PATTERN FOR MIXING HEIGHT FROM 0500 TO 1130 LDT. The mixing height was determined using an Aerovironment Model 310 monostatic acoustic sounder. Adapted from Kelly et al., 1984.

Oliver Co., ND (Figure 2.10). The KY site experienced elevated levels of O_3 and NO_x as the result of urban influences. In contrast, the ND site is isolated from anthropogenic sources and O_3 concentrations usually remain below 90 ppb. Varying diurnal pattern observed in KY may be interpreted to indicate efficient scavenging of O_3 and/or presence of photochemical pre-cursors; whereas, the pattern observed in ND may be interpreted as the opposite.

2.6.3. Great Smoky Mountain National Park (Mueller, 1994)

In the GSMNP, concern over the impact of ambient ozone on sensitive vegetation has prompted more detailed studies on the cause and extent of this pollutant. Of specific interest is the report by Mueller (1994) which examines average diurnal patterns at two sites in the park, Look Rock and Cove Mountain, and contrasts them with a low elevation site in Tennessee, Giles County.

Giles County, located 120 km (75 miles) south-southwest of Nashville is representative of a remote low elevation site. Most topographic elevations within the GSMNP range from 600-2000 m. Look Rock (LRK) with an elevation of 792 m is representative of a medium elevation for the park. Cove Mountain at 1220 m is representative of a high elevation site. Diurnal patterns for these three sites are compared in Figure 2.11. Diurnal ozone variation is greatest for the low elevation site and diminishes as site elevation increases. Mueller attributes the slight dip at 9:00 EST in ozone at LRK to vertical expansion of the early morning surface-based mixing layer containing ozone-depleted air until its height exceeds monitoring station elevation and free tropospheric ozone enters the expanding mixing layer from draft.

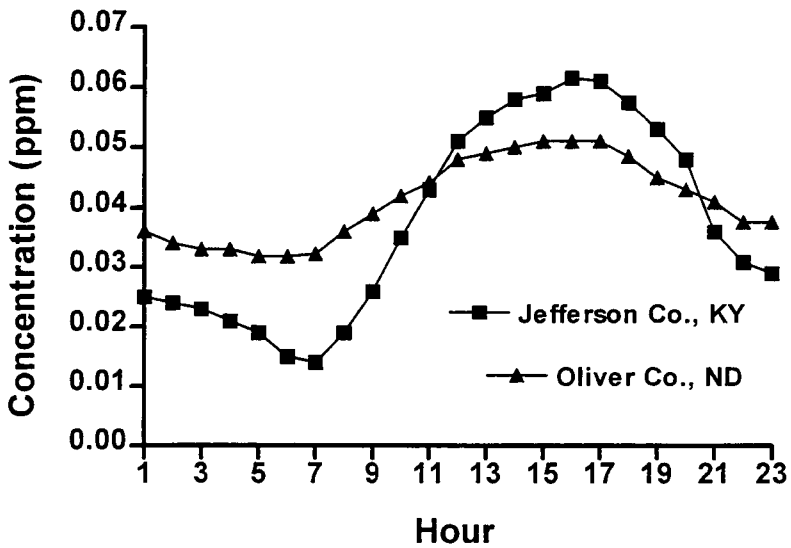

FIGURE 2.10. AVERAGE DIURNAL PATTERNS FOR OZONE MONITORING SITES IN JEFFERSON COUNTY, KENTUCKY AND OLIVER COUNTY, NORTH DAKOTA. Hour of the day is local standard time (LST). Adapted from Lefohn et al., 1993.

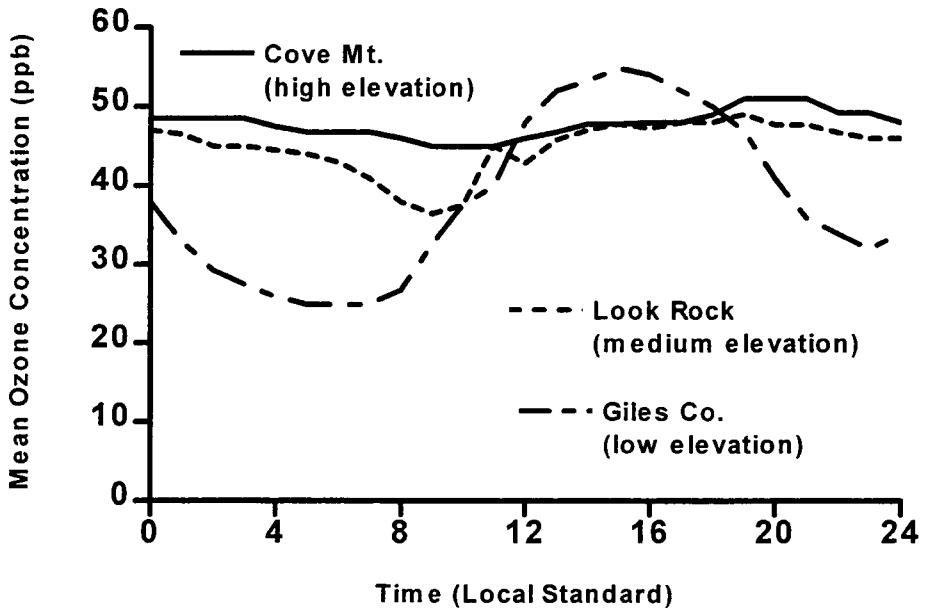

FIGURE 2.11. COMPARISON OF DIURNAL PATTERNS FOR OZONE MONITORING STATIONS AT GILES COUNTY, LOOK ROCK, AND COVE MOUNTAIN, TENNESSEE. Hour of the day is LST. Adapted from Mueller, 1993.

2.6.4. Virginia and West Virginia (Lefohn et al., 1994)

Concern that O_3 concentrations may be injuring trees in the central Appalachian mountains prompted studies in Virginia and West Virginia to assess relative exposures of vegetation. Although ozone levels were monitored at several sites, comparisons of the seasonal diurnal patterns for Parsons and Bearden Knob, West Virginia sites are particularly illustrative (Figure 2.12). Parsons is a remote site positioned more than 50 km (30 miles) from any town of significant size and 510 m above sea level. In 1992, Bearden Knob was established in close proximity to Parsons as a high elevation (1175 m) monitoring site. Similar to Mueller's observations, the authors found diurnal ozone variation to be greater for the low elevation site. Bearden Knob experienced a comparatively flat diurnal pattern while the nearby Parsons displayed a varying diurnal pattern, the latter indicative of scavenging. Interestingly, Parsons experiences the highest concentrations during the afternoon when the mixing layer achieves its greatest height.

2.6.5. West Virginia (Gilliam and Turrill, 1995)

In attempting to evaluate ozone pollution implications for high-elevation hardwood forests, the authors analyzed hourly ozone data from one rural and four urban the result of urban influences. In contrast, the ND site is isolated from anthropogenic sources and O_3 concentrations usually remain below 90 ppb. Varying diurnal pattern observed in KY may be interpreted to indicate efficient scavenging of O_3 and/or presence of photochemical pre-cursors; whereas, the pattern observed in ND may be interpreted as the opposite. Diurnal patterns for these three sites are compared sites throughout

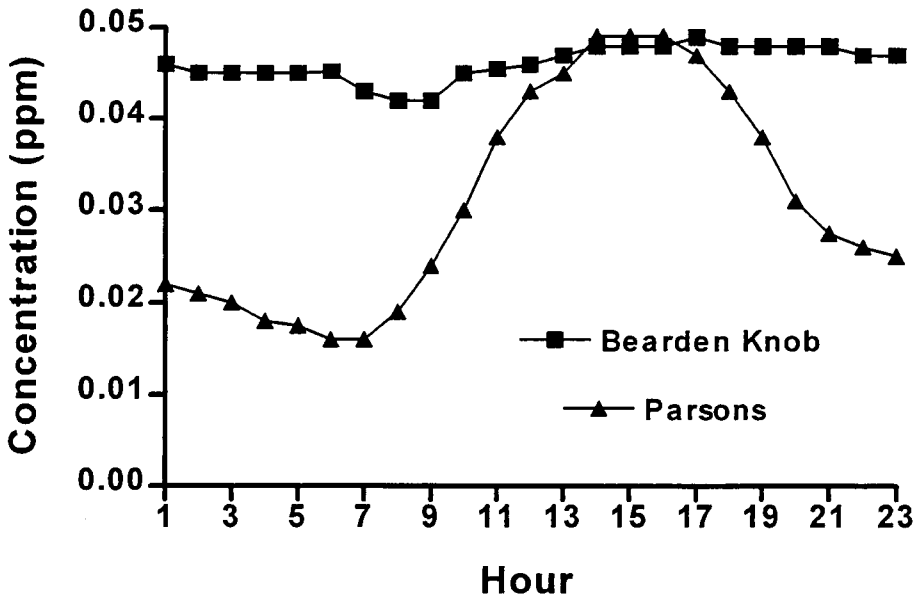

FIGURE 2.12. COMPARISON OF SEASONALLY AVERAGED (APRIL TO OCTOBER) DIURNAL PATTERNS FOR OZONE CONCENTRATIONS AT BEARDEN KNOB AND PARSONS, WEST VIRGINIA. Hour of the day is LST. Adapted from Lefohn et al., 1994.

West Virginia for a three-year period (1987-1989). Of special interest are the diurnal ozone patterns determined from data collected in Greenbrier and Wood counties during June and July, 1988. The Greenbrier site is a rural, high-elevation (829 m) site whereas the Wood site is a typical urban, low-elevation (190 m) site. The hourly ozone values shown in Figure 2.13 represent the 24-hour mean of daily concentrations for the respective month. The two sites are similar in that ozone concentrations in June were generally higher than in July, and maximum mean hourly ozone concentrations exceeded 0.100 ppm. The two sites contrasted significantly with respect to diurnal fluctuation. The Greenbrier site had a minimum-maximum ozone range of approximately 0.030 ppm whereas the Wood site had a range near 0.060 ppm. Although high-levels of ozone were attained at both sites, the Greenbrier site experienced higher concentrations for greater duration during typical 24-hour periods. The authors attributed the differences between sites to differences in elevation and site-specific processes of ozone production and scavenging.

2.6.6. Vertical Profiles of Ozone Concentrations (Nappo et al., 1989)

In order to demonstrate the importance of vertical transport of ozone into the boundary layer by entrainment from above, Nappo et al (1989) determined simultaneous profiles of meteorological variables and ozone concentrations (obtained using a tethered-balloon sounding system). Of particular interest is the study performed in Oak Ridge, Tennessee on July 29, 1987. The day began with a light fog which dissipated by 08:00 EDT. Clear skies subsequently prevailed throughout the remaining morning. Utilizing

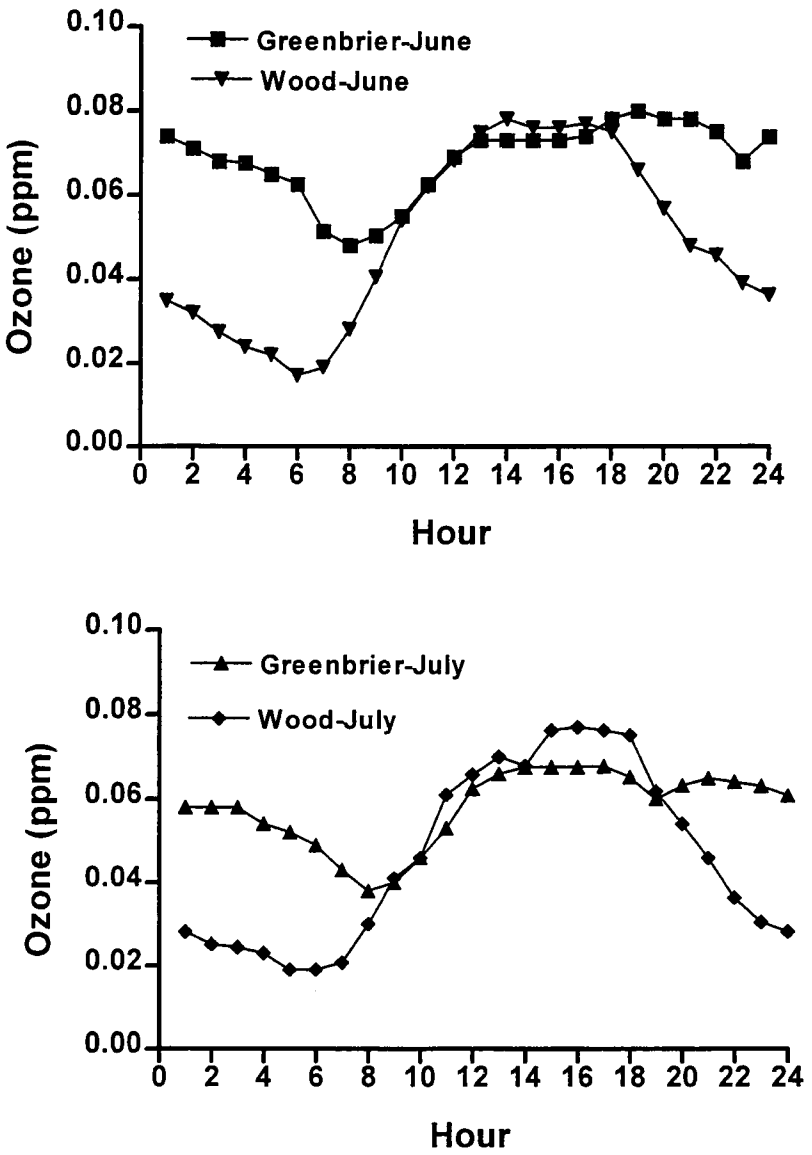

FIGURE 2.13. DIURNAL PATTERNS OF MEAN OZONE CONCENTRATIONS FOR MONITORING STATIONS IN WOOD COUNTY AND GREENBRIER COUNTY, WEST VIRGINIA FOR JUNE AND JULY, 1988. Hour of the day is LST. Adapted from Gilliam and Turrill, 1995.

vertical profiles of wind speed, wind direction, and potential temperature obtained at three separate times (08:37-09:08, 10:07-10:41, and 11:39-12:13 EDT), they characterized meteorological conditions. A strong, ground-based inversion extended upward to an approximate height of 400 m. By 10:00 EDT, this inversion was destroyed by convection thereby resulting in a near-thermal structure. A jet located at an approximate height of 300 m which was observed at 08:37 EDT was no longer evident by 10:00 EDT. Wind speeds were variable at 3 m/s throughout the boundary layer. Ozone concentrations decreased from 70 ppb at 500 m above ground to 5 ppb at ground level at 8:37 EDT, a time which corresponds with inversion (Figure 2.14). By 10:07 EDT, ozone concentrations remain vertically uniform below 480 m. The 11:39 EDT soundings reveal no trace of ozone depletion.

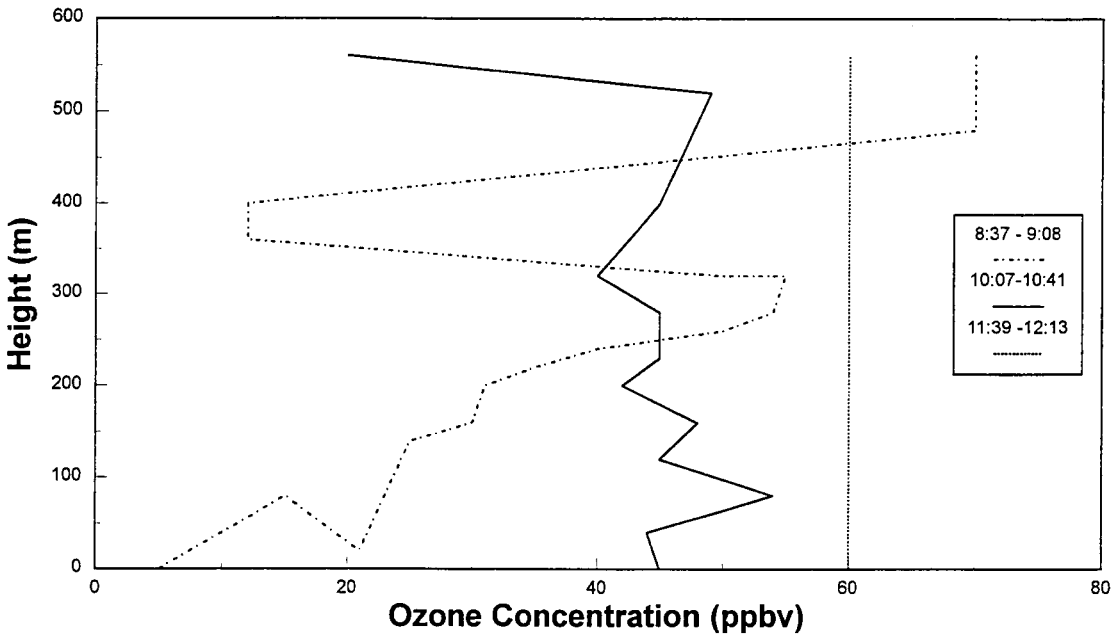

FIGURE 2.14. OZONE VERTICAL PROFILES AT OAK RIDGE, TENNESSEE ON JULY 29, 1987. Times are eastern daylight time (EDT). Adapted from Nappo et al., 1989.

CHAPTER 3

MATERIALS AND METHODS

3.1 Objective 1: Comparison/Assessment of Ozone Monitoring Station Data

3.1.1 Description of the Study Area

The eastern Tennessee ridge-and-valley region splits the southern Appalachian Range into the Great Smoky Mountains on the southeast and the Cumberland Plateau on the northwest. Oriented ENE-WSW north of the Tennessee-Virginia line, where it is narrow and indistinct, the valley turns southwestward in the Knoxville-Oak Ridge area, where it is about 64km (40 miles) wide and enclosed by steep walls, then south-southwestward to Chattanooga and southward to Rome, Georgia, becoming gradually wider and less clearly defined. The valley floor is a region of complex terrain consisting mostly of parallel ridges and valleys running from the southwest to the northeast and slopes from more than 458 m Mean Sea Level (MSL) at Bristol, Tennessee to below 213 m MSL at Chattanooga. It is highly corrugated with broken ridges that are typically 30 to 75 m high and 1000 m wide; the valleys between the ridges are typically 1-2 km wide. The regional surface cover is mostly deciduous forest. The winds are generally from the SW, up-valley during the day and from the NE, down-valley, during the night. The Great Smoky Mountains and Blue Ridge east and southeast of Knoxville exceeds 1982 m MSL at several points; this highland about 112 km (70 miles) wide is largely drained by the Tennessee River, and falls off abruptly to the Piedmont of North and South Carolina. The Cumberland Mountains extend to 16 to 24 km (10-15 miles) north and northwest of Oak Ridge and rise to heights of 1067 m MSL. The Cumberland Mountains are drained

by the Cumberland River and gradually give way to the hilly country of middle Tennessee and Kentucky (Holland, 1953).

3.1.2 Ozone Monitoring Stations

Hourly-averaged ozone concentration data for July and August 1995 were obtained from the Knox County Department of Air Pollution Control (KCAPC), the Tennessee Department of Environment and Conservation (TDEC), and the National Park Service (NPS) for monitoring stations in the eastern Tennessee ridge-and-valley near Knoxville and Oak Ridge. Locations for the seven monitoring stations [Clingmans Dome (CD), Cove Mountain (CM), East Knox (EK), Freels Bend (FB), Look Rock (LR), Nances Grove (NG), and Spring Hill (SH)] are shown (Figure 3.1); additional information for each station is also provided (Table 3.1).

The EK and SH monitors are in Knox County, Tennessee. These stations are operated by KCAPC. The SH location was chosen as representative of urban Knoxville. The EK site is 19 km (12 miles) northeast of Knoxville. Considering the daytime, southwesterly wind patterns, the EK station is positioned to monitor plume effects northeast of the city. The FB and NG monitors are in Anderson and Jefferson Counties, respectively. The monitors are operated by TDEC. During the summer, the dominant daytime wind direction is generally from the southwest. Therefore, FB located 27 km (17 miles) west of Knoxville, was assumed to be an upwind station and was chosen to assess pollutant concentrations prior to their reaching the city. Conversely, the NG site, located 40 km (25 miles) northeast of Knoxville, is typically downwind of Knoxville during the

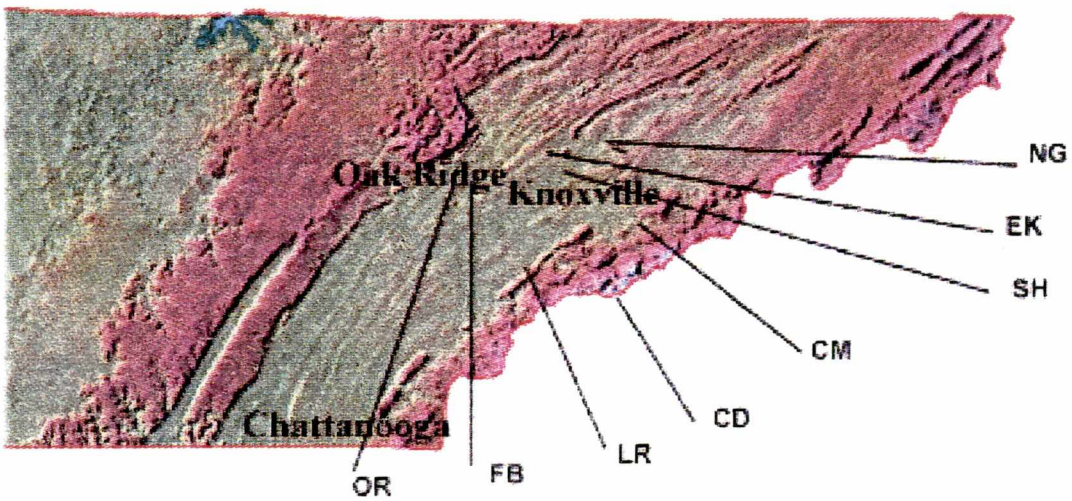

FIGURE 3.1 TOPOGRAPHICAL MAP OF EASTERN TENNESSEE (http://fermi.jhuapl.edu/states/map1/tn_east.gif). Locations of Tethersonde measurements (OR, Oak Ridge) and regional ozone monitoring stations [Clingmans Dome (CD); Cove Mountain (CM); East Knox (EK); Freels Bend (FB); Look Rock (LR); Nances Grove (NG) and Spring Hill (SH)] are indicated.

Table 3.1. OZONE MONITORING STATIONS AND NOAA LABORATORY. [a] Elevation is defined as height relative to sea level. [b] Relative height is defined as the height relative to the NOAA laboratory at Oak Ridge, TN. (0) = relative heights below 100 m were assumed to be zero in subsequent evaluations.

Station	Agency	Geographical Position		Elevation[a] (m)	Relative Height[b] (m)
		Latitude (°)	Longitude (°)		
CD	NPS	35.5628	83.4981	2021	1754
CM	NPS	35.6967	83.6097	1243	976
EK	KCAPC	36.0859	89.7621	303	36 (0)
FB	TDEC	35.9648	84.2232	247	-20 (0)
LR	NPS	35.6272	83.9422	793	526
NG	TDEC	36.1229	89.6003	343	76 (0)
SH	KCAPC	36.0183	89.8762	306	39 (0)
OR	NOAA	36.0000	84.1500	267	0

day and strategically positioned to monitor emissions resulting from metropolitan, anthropogenic sources (Hutton, 1993).

3.1.3 Construction of Data Set

In order to characterize and compare ozone concentrations in eastern Tennessee, hourly ozone data from the seven stations were used. Parameters examined were station, sampling time, and ozone concentration. Stations and respective elevations were used as parameters in the data set. This information is contained in Table 3.1.

In constructing the data set, standardization of time period and respective ozone concentration was necessary. Hourly-averaged ozone concentration data for July and August 1995 were obtained from the Knox County Department of Air Pollution Control (KCAPC), the Tennessee Department of Environment and Conservation (TDEC), and the National Park Service (NPS). Although all agencies report ozone concentrations using a format based on month, day, and hour, the method is inconsistent. The KCAPC reported ozone concentrations by month, day, and hour with twenty-four hours recorded as hour 00 through hour 23. Hour 00 was the time associated with the hourly ozone concentration between 00:00:00 and 00:59:59, inclusive. Reporting times were based on Eastern Daylight Time (EDT). Similarly, TDEC used the same framework, hour 00 through hour 23, but reporting times were based on Eastern Standard Time (EST). The NPS reported hourly ozone concentrations based on hour 01:00 through hour 00:00. Hour 01:00 was the time for the ozone concentration between 00:00:00 and 00:59:59, inclusive. In constructing the data set, daily twenty-four hour periods were designated as hours

00:00:00 through 23:00:00. Eastern Standard Time (EST), also referred to as Local Standard Time (LST), served as the reference. After establishing the time structure, ozone concentration data were entered for the respective periods. Furthermore, for the purposes of this dissertation, all referenced times are based on Eastern Standard Time (EST) or Local Standard Time (LST) unless otherwise noted.

The KCAPC and the TDEC report ozone concentrations in parts per billion (ppb) units. This convention has been retained for the purposes of this dissertation. The NPS reports ozone concentration in parts per million (ppm) units and these concentrations were converted to units of ppb.

3.1.4 Examination of Data

Ozone concentration data from the seven regional stations were compared graphically. Stations were classified as either high-elevation or low-elevation depending on geographical location and relative height. Stations located in the ridge-and-valley (EK, FB, NG, and SH) were classified as low-elevation stations; elevations ranged from a maximum 343 m (NG) to a minimum 247 m (FB). Relative heights of low-elevation stations were assumed to be zero. Stations located in the GSMNP (CD, CM, and LR) were classified as high-elevation stations; elevations ranged from a maximum 2021 m (CD) to a minimum 793 m (LR). Relative heights were calculated by subtracting the elevation of the NOAA laboratory (267 m) from the elevation of the station. Summary statistics were generated by SAS® PROC MEANS (Statistical Analysis Systems, SAS Institute, Cary, NC). Specifically, the mean and maximum hourly averaged concentrations were found for each day by station. Subsequently, daily average and daily

maximum concentrations for each station were plotted for July and August 1995. In addition, box plots of daily mean and daily maximum ozone concentrations by station for July-August 1995 were constructed (SAS PROC INSIGHT). Frequency tables were also produced for times when hourly averaged concentrations equaled or exceeded 80, 100, and 120 ppb (SAS PROC FREQ) In this manner, the number of days at each station which equaled or exceeded the respective concentrations was determined.

3.1.5 Assessment of Compliance with EPA Standards

Ozone concentration data from the seven regional stations were assessed with respect to the 8-hour primary and secondary NAAQS which became effective on September 16, 1997 (FR, 1997). The running 8-hour averages were computed (constructed SAS code) from the hourly ozone concentration data for each hour of the month and the result was stored in the first hour of the 8-hour period (FR, 1997; Brawner, 1997). For example, on July 1, the hourly averaged ozone concentration for the hour between 0000 and 0100 was recorded. The next seven hourly averaged concentrations for the same station were added to the first hourly averaged concentration. The sum of the eight hourly averaged concentrations was subsequently divided by eight to obtain an 8-hour average. This result was logged as the 8-hour average for the first hour. The results of the calculations were compared with the primary and secondary ozone standards. The primary and secondary ozone ambient air quality standards were met when the 3-year average of the annual fourth-highest daily maximum 8-hour average ozone concentration was less than or equal to 0.08 ppm. An 8-hour average was considered valid if at least 75% of the hourly averages for the 8-hour period were available. Since data units were

ppb, a concentration of 85 ppb was the smallest value greater than 0.08 ppm (FR, 1997). Frequency tables were also produced for times when the 8-hour averaged concentrations equaled or exceeded 85 ppb (SAS PROC FREQ). In this manner, the number of days at each station which equaled or exceeded the respective regulatory standard was determined.

3.2 Objective 2: Characterization of Mixing Heights and Ozone Concentrations.

3.2.1 Description of Experimental Site

This study was conducted at the National Oceanic and Atmospheric Administration (NOAA) Air Resources Laboratory (ARL) in Oak Ridge. The laboratory is located within the ridge-and-valley at latitude 36°00' N, longitude 84°15' W at an elevation of 267 m MSL. It is approximately 10 km southeast of the Cumberland Mountains, 30 km west of Knoxville, and 60 km northwest of the GSMNP. The locale surrounding Oak Ridge is typical of complex terrain throughout the ridge-and-valley. The study site is characterized by a valley with an 80 m ridge located 500 m to the southeast (Birdwell, 1995).

Oak Ridge was selected as the study site based on four factors. First, the site's terrain is typical of that found throughout the ridge-and-valley. Second, the city's geographical location generally places it outside effects of pollutants from Knoxville. Third, meteorological information collected by permanent monitoring equipment located at the laboratory was used during the investigation. Fourth, the laboratory is located near a permanent low-elevation ozone monitoring station (Freels Bend) operated by the State of Tennessee.

3.2.2 Experimental Design

Weather conditions were monitored in July and August 1995 to identify periods when the region was both under the influence of high pressure systems and had daily temperatures equal to or greater than 32.2°C (90°F). Measurements for ozone, pressure, potential temperature, wind direction, and wind speed were collected on nine mornings and eight evenings which met sampling criteria. Morning sampling typically began at sunrise and ended near noon. Evening sampling commenced at approximately 1600 and ended after sunset. By following these procedures, measurements were obtained throughout the diurnal boundary layer changes. For the purposes of this study, mixing height (MH) was defined as the height below which the slope of the potential temperature profile between the surface and respective height was less than or equaled zero. Development and decay of daily mixing heights (MH) were estimated from potential temperature profiles. MH estimates were corroborated by examination of simultaneous profile measurements for ozone concentration, wind speed and wind direction.

3.2.3 Ozone/Meteorological Measurement

A Tethersonde Ozone Sounding System (Model OZ-3A-T, Atmospheric Instrumentation Research, Inc., Boulder, Colorado) supplied by NOAA was used for all vertical profile measurements. This Tethersonde system combines an ozone sonde with a meteorological sonde to provide accurate (±5%) ozone concentration measurements in a range of 1 to 1,000 ppb in conjunction with pressure, temperature, wind direction, and wind speed. As air was bubbled through a solution of potassium iodide at a known rate, the chemical reaction created an electrical current between the two electrodes. The

current was proportional to the oxidant content in the air. The ozone sensor package contained a bubbler, pump, and circuit board which measured current from the bubbler and converted it to a voltage. The sensor was operated by placing reagent (2.52 $Na_2HPO_4.12\ H_2O$ mg/ml, 1.15 mg/ml NaH_2PO_4 and 1.1 mg/ml KI in distilled H_2O) in the bubbler. Air was subsequently bubbled at a known rate through the reagent which reacted with ozone in the air to produce an electrical current proportional to the partial pressure of ozone in the air.

The partial pressure of ozone in the air flowing through the bubbler was

$$P_o = \quad 4.31 \times 10^{-3}\ iTt$$

and ozone concentration X_o in parts per million (ppm) was

$$X_o = \frac{4.31 \times 10^{-3} iTt}{P_a}$$

where P_o is the partial pressure of ozone (micromillibars), i is the electrical current flow in the bubbler (microamperes), T is the temperature (degrees Kelvin) of the air being sampled, t is time (seconds) required to pump 100 ml of air through the bubble, and P_a is the pressure (millibars) of the air being sampled. The constant 4.31×10^{-3} is a theoretical value derived on the assumptions that 1) all ozone in the air reacts with the reagent in the bubbler, 2) no ozone is lost in the system prior to reaching the bubbler, and 3) no other molecules present in the air interfere with the process.

The reagent was prepared by dissolving 0.252 grams $Na_2HPO_4.12\ H_2O$ in a small amount of distilled, deionized water. Subsequently, 0.115 grams NaH_2PO_4 followed by 0.100 grams KI were added. The mixture was stirred, diluted to 100 ml, and then poured

into brown bottles with polyseal caps. After being aged for one day at room temperature, the reagent was kept refrigerated except during sampling periods. Solutions were used or discarded within one week of preparation.

According to The American Society for Testing and Materials Method ANSI/ASTM D2912-76, many oxidizing substances will liberate iodine in this reagent. Among them are nitrogen dioxide, chlorine, peroxy acids, hydroperoxides, and peroxacetyl nitrates. Also, the reducing gases, sulfur dioxide and hydrogen sulfide, act as interferences in the reaction. Of these, the reaction of sulfur dioxide is often the most serious. Interference caused by sulfur dioxide was eliminated by placing a chromic acid paper absorber in the airstream upstream of the impinger.

The meteorological sonde contained sensors which provided information on pressure, potential temperature, wind direction, and wind speed. Pressure was measured by an electronic aneroid capacitance sensor with precision of ± 1 mb. A thermistor was attached to the pressure senor to provide temperature data for compensation. Temperature was measured using a thermistor with precision of ± 0.5 °C. Wind direction was measured with precision of ± 5 ° using a small electronically controlled magnetic compass. Wind direction detection was dependent upon the balloon serving as a wind vane. Wind speed was measured with precision of ± 5 ° using a three-cup anemometer and light-chopper tachometer.

3.2.4 Ozone/Meteorological Sampling

The Tethersonde sensor package was suspended from the tethered balloon, and ascent and descent controlled by a winch. The ascent rate was between 0.25 and 0.50

meters per second, and observations were taken approximately every ten seconds during the ascent. Although the balloon may be operated at heights up to 1000 meters, in this study balloon operation was generally limited to 600-700 m since operating at higher elevations or during periods when wind speed exceeds ten meters per second greatly increases the probability of losing the balloon and sounding system. Data were telemetered to the ground station, changed from analog to digital form, displayed by the ground station and presented to various output ports. Since sensor package height was calculated from Tethersonde data, ozone and meteorological parameters were determined as a function of elevation.

3.2.5 Measurement Period

Measurements were conducted during July and August 1995. During July, the upper-air westerly flow, mid-latitude cyclones, and associated surface fronts shifted northward as part of the seasonal atmospheric circulation cycle. The "Bermuda subtropical high" was the dominant meteorological phenomenon (Muller, 1995). In August, the polar-front jet remained over southern to central Canada. Simultaneously, an upper-air ridge extending from the Atlantic to the Pacific was positioned across the southern United States. This presence of this upper air-ridge prevented frontal, rainy weather from entering very far into the southern region (Anonymous, 1995). In general, July and August weather in eastern Tennessee was drier and hotter than usual. The region experienced high pressure systems and daily temperatures equaling or exceeding 32.2°C (90°F) on approximately 36 days (Birdwell, 1995a; Birdwell, 1995b) Of these, thirteen

days (nine mornings and eight evenings) were selected for meteorological and ozone measurements.

3.2.6 Examination of Data

Tethersonde data for potential temperature, ozone concentration, wind speed, and wind direction were plotted against height. In this study, height was used to indicate relative height, the height above the ground at the NOAA laboratory. In addition to graphical inspections of Tethersonde data, graphs were also constructed for comparison of Tethersonde measured ozone concentrations at ground-level with hourly-averaged concentrations at Freels Bend (same relative height). Similarly, Tethersonde measured concentrations at 526 m were compared with hourly-averaged concentrations at Look Rock (same relative height). The last comparisons were those made between the high and low elevation monitoring stations on the respective days. The FB station served as the reference between the two graphs.

3.3 Objective 3: Mixing Height Profiles/Thermophysical Relationships

3.3.1 Estimation of Mixing Heights

Mixing heights were estimated using potential temperature data from Tethersonde measurements in Oak Ridge, Tennessee. Data were used to assess initial development and subsequent growth of the MH between the surface and approximately 600-700 m during the morning, and reduction and reestablishment of the MH near the surface in the afternoon-evening.

3.3.2 Mixing Height Profiles

Mixing height profiles were determined for three days: July 8, July 14, and July 20. Tethersonde measurements were conducted on thirteen days (nine mornings and eight afternoon-evenings), but only five days were measured throughout the day (morning and afternoon-evening). Of the five days, July 30 was excluded because measurements were stopped at 1917, 25 minutes prior to sunset, because of severe thunderstorms. August 30 was excluded because afternoon-evening clouds blocked the sun for approximately two hours and caused premature reduction of the MH.

3.3.3 Thermophysical Relationship Between Added Heat and Mixing Height

For each set of profile measurements, areas between potential temperature soundings (which were directly related to heat input both from the surface and from warm air entrained from aloft) were calculated. Mixing heights were then plotted as a function of heat input to the atmosphere (Stull, 1988; Stull, 1998).

3.4 Objective 4: Comparison of Observed Mixing Height Profiles to Modeled Mixing Height Profiles.

3.4.1 PCRAMMET Mixing Height Profiles

In order to generate MH profiles, two external files containing hourly surface data and twice daily MH values were input to the PCRAMMET program. The surface and upper air measurements selected for input were those from National Weather Service (NWS) stations in Knoxville and Nashville, Tennessee, respectively (Nashville is the closest station which conducts upper air measurements representative of eastern

Tennessee). The two files were obtained from the National Climatic Data Center (NCDC) in Asheville, North Carolina.

The hourly surface data provided by NCDC consisted of four quarterly files of surface observations which were combined to produce one annual file for 1995. From the hourly surface data, PCRAMMET selects data for station number, year, month, day, hour, cloud ceiling height, wind direction, wind speed, dry bulb temperature, and opaque cloud cover.

Twice-daily, morning and afternoon, MH data were obtained from the National Climatic Data Center (NCDC) in Asheville, North Carolina. The MH data were produced by NCDC personnel using a MH estimation program, MIXHGT, which utilized hourly surface data from Knoxville, Tennessee and upper air data from Nashville, Tennessee. The morning and afternoon MH estimates were based on the method of Holzworth (1972). PCRAMMET utilizes the surface and MH data to produce MH profiles for both rural and urban locations (Figure 3.2).

3.4.2 Mixing Height Profiles Comparison

Mixing heights for July 8, July 14, and July 20 were constructed from Tethersonde data and were generated by PCRAMMET (both rural and urban mixing height profiles). Data for each day were placed on separate graphs.

3.5 Objective 5: Predictive Model for Mixing Heights

The nocturnal surface-layer MH was estimated by examining temperature and ozone concentration data collected by the Tethersonde on July 14, August 30, and August 31 prior to sunrise (data collection for all other days began after sunrise).

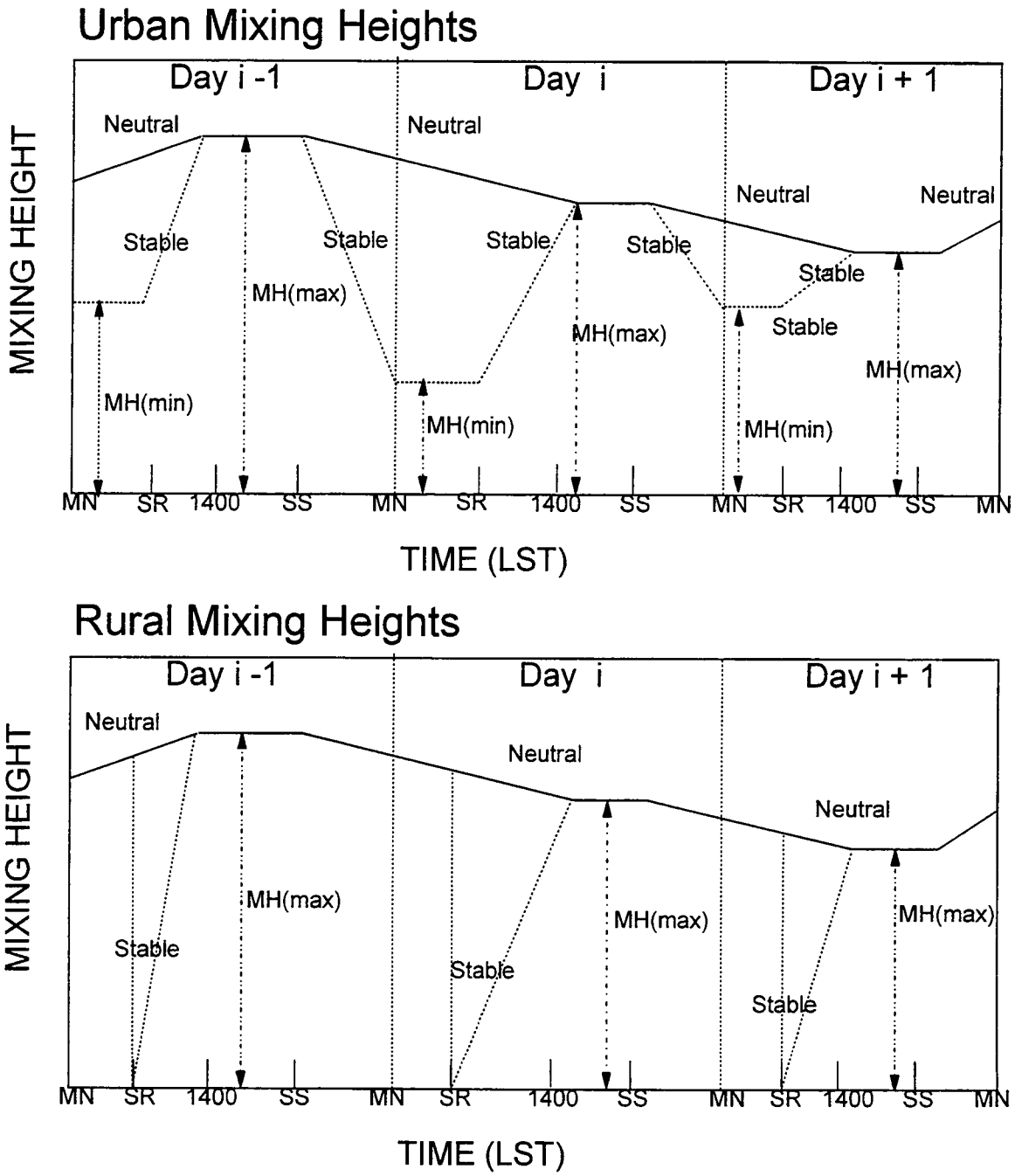

FIGURE 3.2 SCHEMATIC ILLUSTRATION OF (a) URBAN AND (b) RURAL MIXING HEIGHT INTERPOLATION PROCEDURES (EPA PCRAMMET User's Guide, 1995)

Development of the mixing height during the morning and early afternoon was determined by plotting morning mixing heights (ascertained from potential temperature profiles) as function of time (SAS PROC GPLOT). Data consisted of morning measurements from all nine mornings and were standardized by setting the time of sunrise as time zero hour.

Reduction of the afternoon-evening mixing height and reestablishment of the nocturnal surface layer mixing height was assumed to be instantaneous near sunset. Specifically, "near sunset" was determined to be an average of 27-31 minutes prior to sunset based on potential temperature profiles for six afternoon-evenings (July 30 and August 30 measurements were excluded because of storms and clouds, respectively).

CHAPTER 4

RESULTS AND DISCUSSION

4.1 Objective 1: Comparison/Assessment of Ozone Monitoring Station Data

4.1.1 Graphical Comparison of Daily Mean and Maximum Ozone Concentrations

Daily mean ozone concentrations at regional ozone monitoring stations, were examined. In July 1995, there appeared to be few differences between CM and LR (Figure 4.1). When data were available, daily mean concentrations at CD were lower than those at CM and LR. Daily mean concentrations at FB, the reference monitoring station, were generally below those for high elevation stations. Since low elevation monitoring stations experience greater diurnal variation than high elevation monitoring stations, this observation was not surprising. For the four low elevation monitoring stations, there were few differences among three stations (EK, FB, and SH). Typically, daily mean concentrations at NG were higher than those at the remaining three stations. In August 1995 (Figure 4.2), daily mean concentrations at CD were more similar to those at CM and LR when compared to July. Daily mean concentrations at low elevation stations were comparable. Similar to July, daily mean concentrations at NG in August were somewhat higher than those at EK, FB, and SH. A box plot diagram of daily mean ozone concentrations for each station was constructed (Figure 4.3). Daily mean ozone concentrations at CM and LR were similar and higher than all other stations. Daily mean ozone concentrations at CD were typically below concentrations at CM and LR, but higher than concentrations at the low elevation monitoring stations. Of the low elevation monitoring stations, EK and SH were very similar. Daily mean concentrations at FB

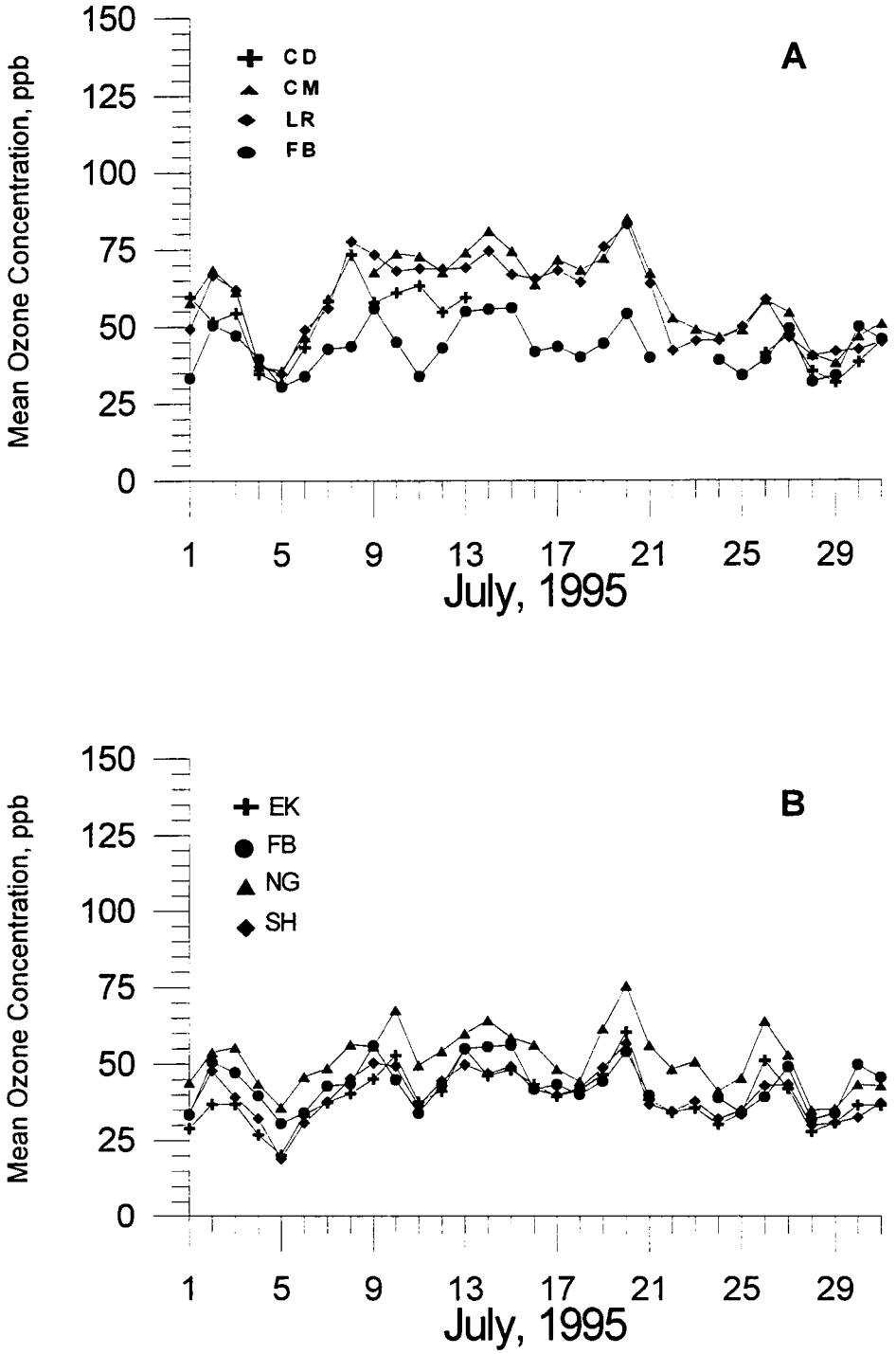

FIGURE 4.1. DAILY MEAN ONE-HOUR AVERAGED OZONE CONCENTRATIONS FOR REGIONAL MONITORING STATIONS (JULY 1995). A. High elevation stations (located above 793m MSL) [Clingmans Dome (CD), Cove Mountain (CM), and Look Rock (LR)] and Freels Bend (elevation 247m MSL). B. Low elevation stations (below 343 m MSL)[East Knox (EK), Freels Bend (FB), Nance's Grove (NG) and Spring Hill (SH)].

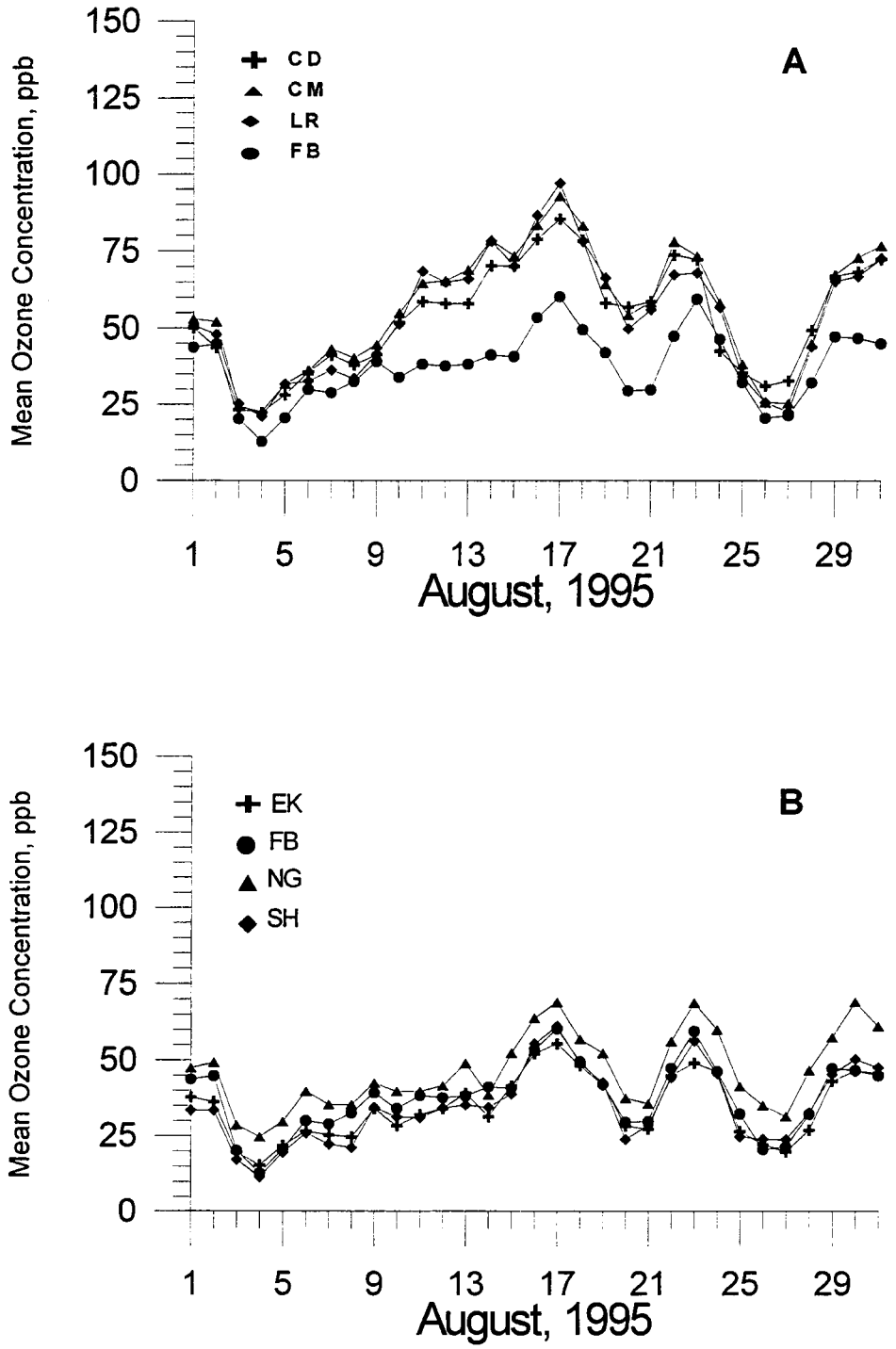

FIGURE 4.2. DAILY MEAN ONE-HOUR AVERAGED OZONE CONCENTRATIONS FOR REGIONAL MONITORING STATIONS (AUGUST 1995). A. High elevation stations (located above 793 m MSL) [Clingmans Dome (CD), Cove Mountain (CM), and Look Rock (LR)] and Freels Bend (elevation 247 m MSL). B. Low elevation stations (below 343) [East Knox (EK), Freels Bend (FB), Nance's Grove (NG) and Spring Hill (SH)].

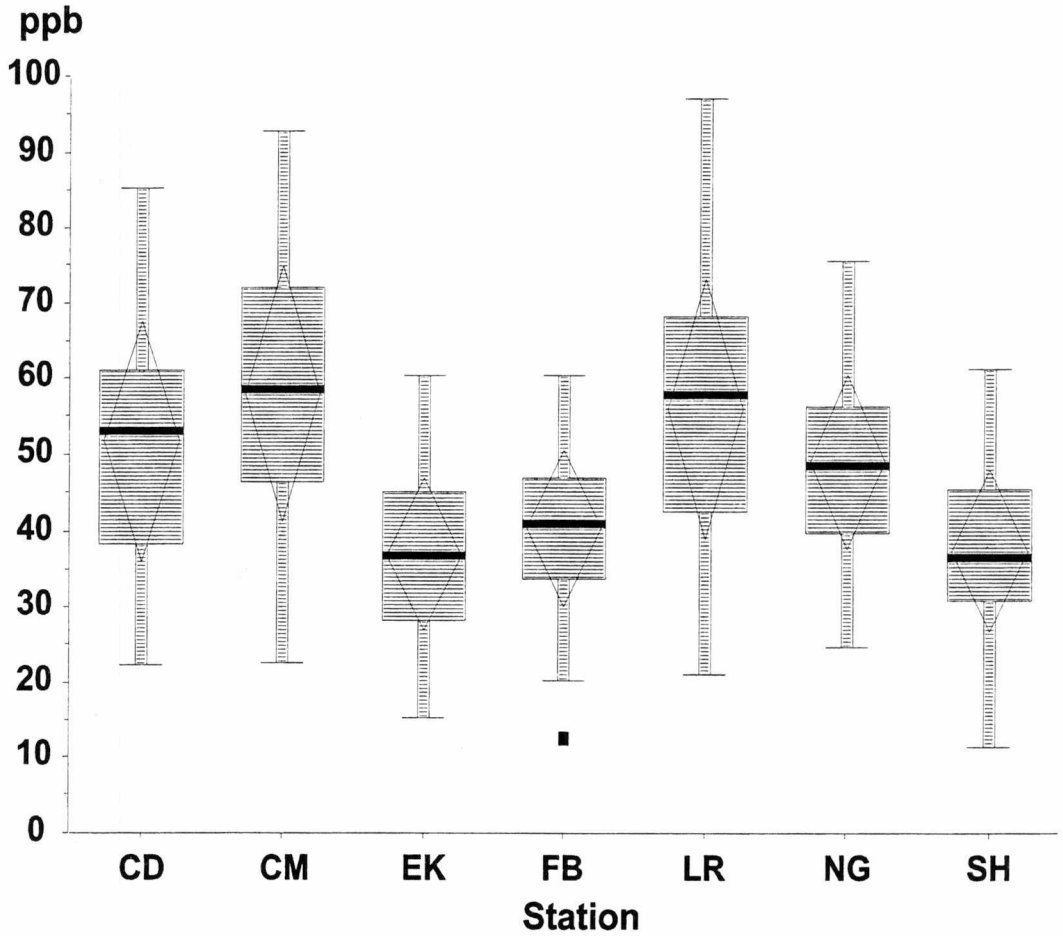

FIGURE 4.3. BOX PLOTS OF DAILY ONE-HOUR AVERAGED OZONE CONCENTRATION MEAN RECORDED AT REGIONAL MONITORING STATIONS DURING JULY AND AUGUST 1995. [Clingmans Dome (CD), Cove Mountain (CM), Look Rock (LR), East Knox (EK), Freels Bend (FB), Nance's Grove (NG) and Spring Hill (SH)].

were somewhat higher than EK and SH. Daily mean concentrations at NG exceeded those of all other low elevation stations.

Daily maximum ozone concentrations at the monitoring stations were also examined. In July 1995, there was little difference between CM and LR (Figure 4.4). Daily concentration maxima at CD were generally lower than those at CM and LR. Daily concentration maxima at FB often exceeded those at the high elevation stations. For low elevation monitoring stations, there were few differences among the four stations (EK, FB, NG, and SH). Typically, daily concentration maxima at NG were higher than those at the remaining three stations. In August 1995, daily concentration maxima at all stations were similar (Figure 4.5). The highest concentration of the month (123 ppb) occurred at LR on August 17 at 1800. A box plot diagram of daily ozone concentration maxima for each station was constructed (Figure 4.6). Daily ozone concentration maxima at CM, FB, LR, and NG were similar. In addition, they exceeded the daily concentration maxima at CD, EK, and SH. The highest concentrations at EK and NG exceeded the 1.5 inter-quartile range.

Table 4.1 provides information regarding the number of days which equaled or exceeded the respective hourly-averaged ozone concentration by station. In addition, Tables 4.2, 4.3. and 4.4 provide information regarding the hour in which the respective concentration was equaled or exceeded, the frequency of occurrence, and the percent of occurrence. For hourly-averaged ozone concentrations of 80, 100, and 120 ppb; approximately one-half of these observations occurred before 1500. The maximum occurrences by hour for equaling or exceeding 80 ppb occurred at 1400-1500. The

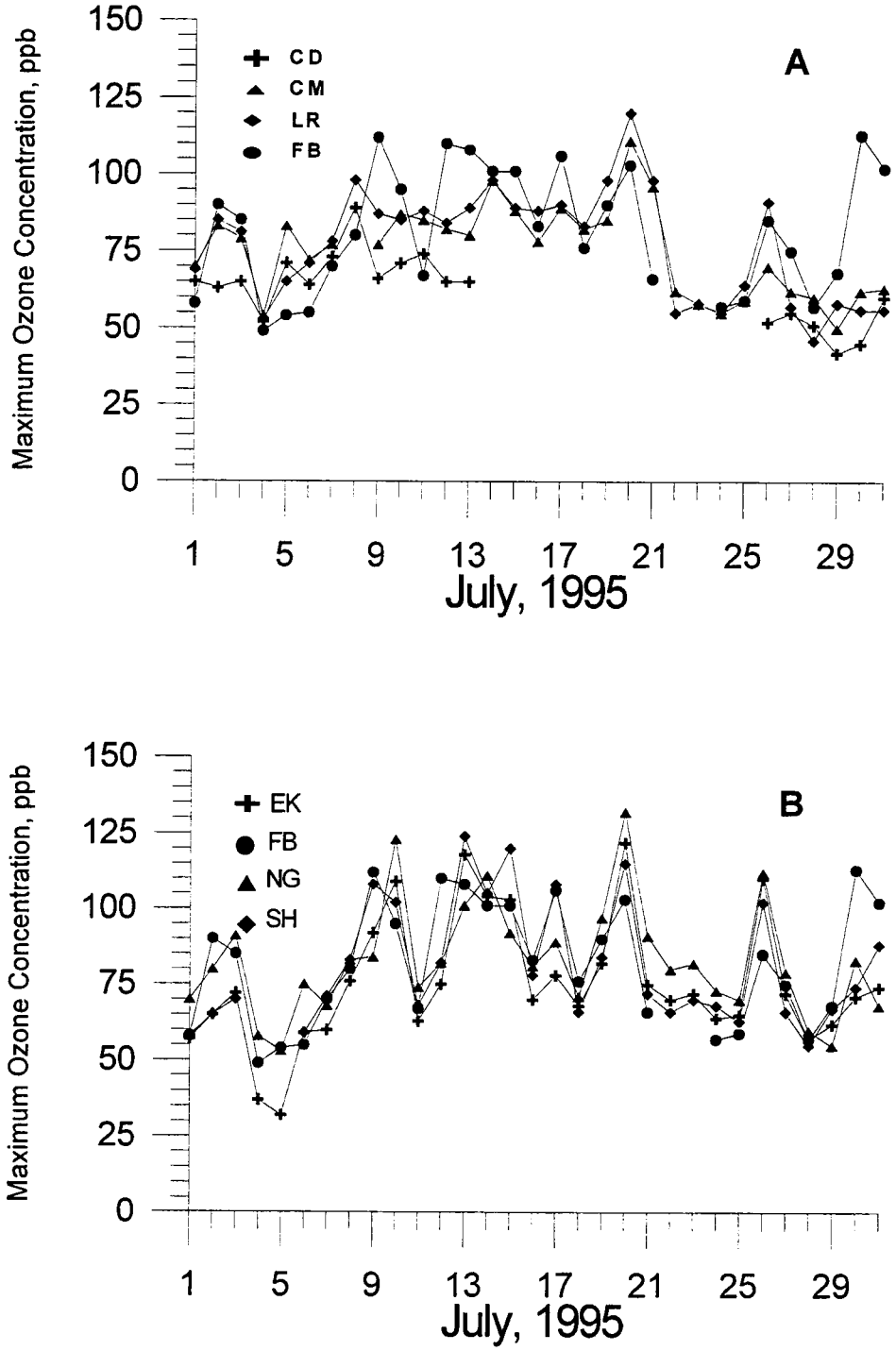

FIGURE 4.4. DAILY ONE-HOUR AVERAGED OZONE CONCENTRATION MAXIMA RECORDED AT REGIONAL MONITORING STATIONS (JULY 1995). A. High elevation stations (located above 793 m MSL) [Clingmans Dome (CD), Cove Mountain (CM), and Look Rock (LR)] and Freels Bend (elevation 247 m). B. Low elevation stations (below 343 m MSL)[East Knox (EK), Freels Bend (FB), Nance's Grove (NG) and Spring Hill (SH)].

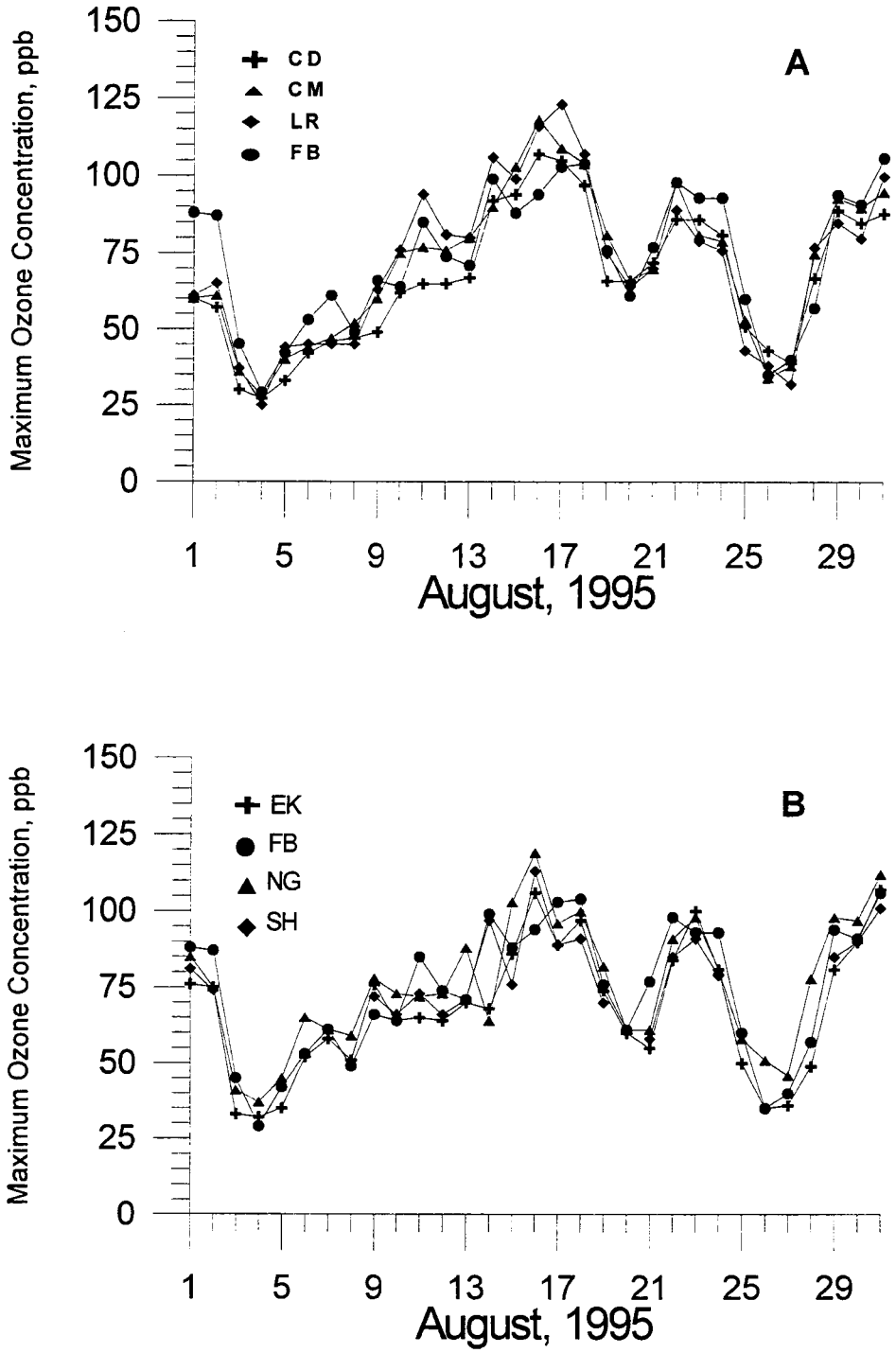

FIGURE 4.5. DAILY ONE-HOUR AVERAGED OZONE CONCENTRATION MAXIMA FOR REGIONAL MONITORING STATIONS (AUGUST 1995). A. High elevation stations (located above 793 m MSL) [Clingmans Dome (CD), Cove Mountain (CM), and Look Rock (LR)] and Freels Bend (elevation 247 m MSL). B. Low elevation stations (below 343 m MSL)[East Knox (EK), Freels Bend (FB), Nance's Grove (NG) and Spring Hill (SH)].

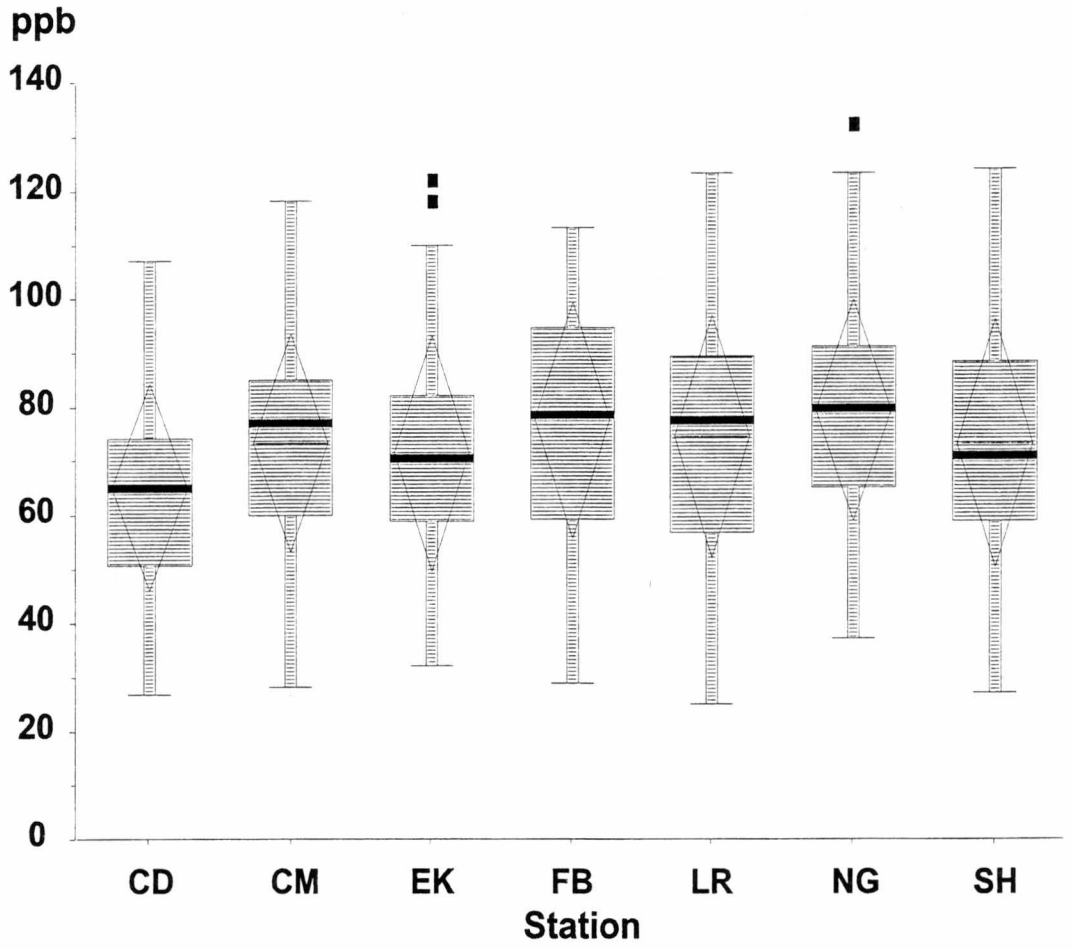

FIGURE 4.6. BOX PLOT OF DAILY ONE-HOUR AVERAGED OZONE CONCENTRATION MAXIMA RECORDED AT REGIONAL MONITORING STATIONS DURING JULY AND AUGUST 1995. [Clingmans Dome (CD), Cove Mountain (CM), East Knox (EK), Freels Bend (FB), Look Rock (LR), Nance's Grove (NG) and Spring Hill (SH)].

TABLE 4.1. NUMBER OF DAYS HOURLY AVERAGED OZONE CONCENTRATION (ppb) EXCEEDED RESPECTIVE CONCENTRATION BY STATION.

Station	Hourly Averaged Ozone Concentrations, ppb		
	≥ 80 ppb	≥ 100 ppb	≥120 ppb
CD	12	2	0
CM	25	5	0
EK	18	9	1
FB	30	12	0
LR	29	6	2
NG	31	9	2
SH	22	10	2

TABLE 4.2. FREQUENCY OF HOURS EXCEEDING HOURLY AVERAGED OZONE CONCENTRATIONS $\geq$ 80 ppb.

Hour	Frequency	Percent	Cumulative	
			Frequency	Percent
0	18	2.0	18	2.0
1	18	2.0	36	4.0
2	17	1.9	53	5.9
3	13	1.4	66	7.3
4	7	0.8	73	8.1
5	5	0.6	78	8.7
6	10	1.1	88	9.8
7	8	0.9	96	10.7
8	3	0.3	99	11.0
9	3	0.3	102	11.3
10	16	1.8	118	13.1
11	61	6.8	179	19.9
12	87	9.7	266	29.5
13	88	9.8	354	39.3
14	92	10.2	446	49.5
15	91	10.1	537	59.6
16	87	9.7	624	69.3
17	66	7.3	690	76.6
18	48	5.3	738	81.9
19	43	4.8	781	86.7
20	41	4.6	822	91.2
21	34	3.8	856	95.0
22	24	2.7	880	97.7
23	21	2.3	901	100.0

TABLE 4.3. FREQUENCY OF HOURS EXCEEDING HOURLY AVERAGED OZONE CONCENTRATIONS ≥100 ppb.

Hour	Frequency	Percent	Cumulative	
			Frequency	Percent
0	2	1.3	2	1.3
1	2	1.3	4	2.5
2	2	1.3	6	3.8
3	2	1.3	8	5.1
5	1	0.6	9	5.7
6	1	0.6	10	6.3
7	0	0	10	6.3
8	0	0	10	6.3
9	0	0	10	6.3
10	1	0.6	10	6.3
11	8	5.1	18	11.4
12	17	10.8	35	22.2
13	25	15.8	60	38.0
14	20	12.7	80	50.6
15	16	10.1	96	60.8
16	13	8.2	109	69.0
17	14	8.9	123	77.8
18	10	6.3	133	84.2
19	7	4.4	140	88.6
20	7	4.4	147	93.0
21	5	3.2	152	96.2
22	3	1.9	155	98.1
23	3	1.9	158	100.0

TABLE 4.4. FREQUENCY OF HOURS EXCEEDING HOURLY AVERAGED OZONE CONCENTRATIONS ≥ 120 ppb.

Hour	Frequency	Percent	Cumulative	
			Frequency	Percent
12	1	7.7	1	7.7
13	2	15.4	3	23.1
14	3	23.1	6	46.2
15	1	7.7	7	53.8
16	1	7.7	8	61.5
17	3	23.1	11	84.6
18	1	7.7	12	92.3
19	1	7.7	13	100.0

maximum occurrences by hour for equaling or exceeding 100 ppb occurred at 1300-1400. The maximum occurrences by hour for equaling or exceeding 120 ppb occurred at 1400-1700.

4.1.2 Assessment of Compliance with EPA Standards

Table 4.5 provides information regarding the number of days which would have exceeded the 8-hour primary and secondary NAAQS if they had been in place in 1995. In addition, Table 4.6 provides information regarding the hour in which the standards were exceeded, the frequency of occurrence, and the percent of occurrence. Approximately one-half of the daily maximum 8-hour averaged ozone concentrations exceeding 0.080 ppm occurred before 1300.

4.2 Objective 2: Characterization of Mixing Heights and Ozone Profiles

4.2.1 Tethersonde Measurements

JULY 8, 1995 Saturday

On July 8, the minimum and maximum temperatures at ground-level were 14.2°C and 31.7°C, respectively. The minimum temperature occurred at 0546 and the maximum temperature at 1506. Wind speeds averaged 0.2 m/s in the early morning, increased to 1.9 m/s at 1500, and diminished to 0.2 m/s at 2100. Maximum wind speed, 5.8 m/s, occurred at approximately 1600. The skies were clear throughout the day; there was no precipitation. Although the maximum temperature was below the sampling criterion of 32.2°C, measurements were performed because forecasted peak temperature exceeded criterion. Sunrise occurred at 0527 and sunset at 1955. Measurements were conducted during morning and afternoon-evening.

TABLE 4.5. NUMBER OF DAYS AT EASTERN TENNESSEE MONITORING STATIONS IN JULY AND AUGUST,1995 THAT WOULD HAVE EXCEEDED THE CURRENT 8-HOUR NAAQS OZONE STANDARDS (IF THOSE STANDARDS HAD BEEN IN PLACE IN 1995).

Station	Number of Days
CD	4
CM	9
EK	7
FB	10
LR	9
NG	15
SH	8

TABLE 4.6. FREQUENCY OF HOURS EXCEEDING 8-HOUR AVERAGED OZONE CONCENTRATIONS $\geq$ 80 ppb.

Hour	Frequency	Percent	Cumulative Frequency	Cumulative Percent
0	10	1.5	10	1.5
1	7	1.1	17	2.6
2	7	1.1	24	3.7
3	5	0.8	29	4.4
4	4	0.6	33	5.1
5	4	0.6	37	5.7
6	4	0.6	41	6.3
7	9	1.4	50	7.7
8	31	4.8	81	12.4
9	54	8.3	135	20.7
10	66	10.1	201	30.8
11	74	11.3	275	42.2
12	65	10.0	340	52.1
13	55	8.4	395	60.6
14	46	7.1	441	67.6
15	39	6.0	480	73.6
16	35	5.4	515	79.0
17	30	4.6	545	83.6
18	25	3.8	570	87.4
19	22	3.4	592	90.8
20	18	2.8	610	93.6
21	16	2.5	626	96.0
22	14	2.1	640	98.2
23	12	1.8	652	100.0

Morning measurements began at 0619 (52 minutes after sunrise) and concluded at 1119 after reaching 400 m. Profiles of potential temperature, ozone concentration, wind speed and wind direction are presented in Figure 4.7. Measurements for the first set of profiles were conducted from 0619 to 0631. Potential temperatures at ground-level were 289°K and increased to 296°K at 170 m. Surface ozone concentrations were approximately 12 ppb and increased with height until reaching 70-75 ppb at 170 m. Surface wind speeds were 0.2 m/s and increased uniformly until peaking at 3 m/s at 170 m. Surface wind directions were SSE and S. At 7 m, wind directions shifted to the NNE and NE. At 30 m, wind directions shifted NNW and oscillated between NNW and W between 30 m and 220 m. Based on profile measurements, the height of the stable boundary layer (nocturnal inversion) was estimated to be 170 m.

Measurements for the second set of profiles were conducted from 0646 to 0716. Whereas measurements for the first set were stopped when reaching 220 m, measurements for the second set continued to 600 m. Although the strong surface-based inversion remained, initial erosion of the inversion was noted based on increased air temperatures near the surface (14.4 °C at 0600 and 15.7 °C at 0700) and near vertical potential temperature profile below 35 m. The potential temperature was 290°K from the surface up to 35-40 m. At the beginning of these measurements, surface ozone concentrations had dropped to 2-3 ppb probably due to scavenging by early morning traffic from nearby Illinois Avenue. At 8 m, ozone concentrations increased to 12 ppb and the profile was similar to the earlier (0619-0631) profile. Ozone concentrations were comparatively uniform above the stable boundary layer and gradually increased from 70-

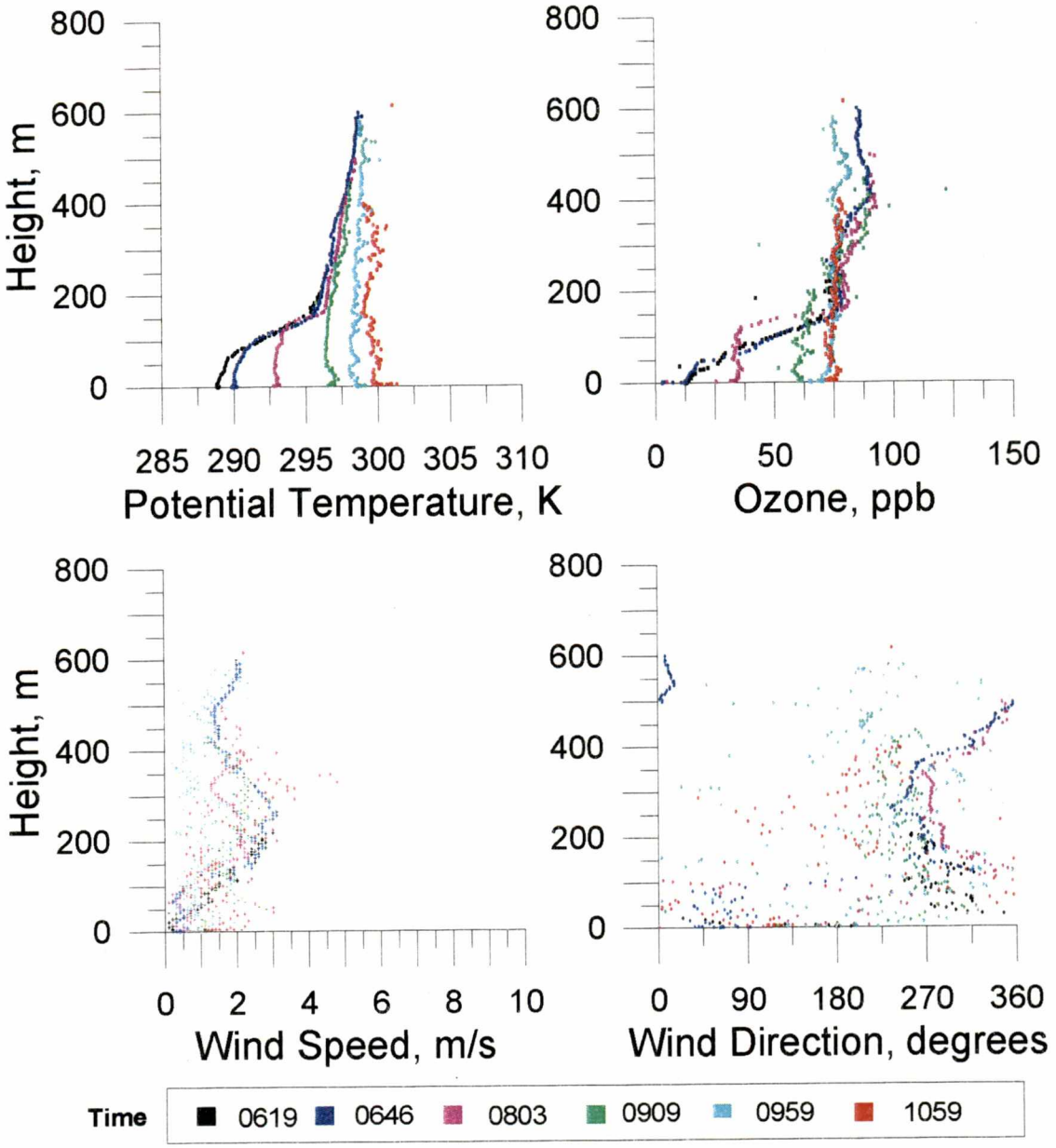

FIGURE 4.7. PROFILES OF POTENTIAL TEMPERATURE, OZONE CONCENTRATION, WIND SPEED AND WIND DIRECTION DEVELOPED FROM TETHERSONDE DATA OBTAINED ON THE MORNING OF JULY 8, 1995. Tethersonde readings were initiated at 0619, and the final balloon ascent began at 1059.

80 ppb at 170 m to 80-90 ppb from 340-600 m. Surface wind speeds increased slightly (0.4 m/s) during the timespan between this and the first profile (0.2 m/s). This increase was evident until the Tethersonde reached the bottom of the stable boundary layer (35-40 m) when wind speeds slowed. Above the stable boundary layer, wind speeds increased to 3.1 m/s at 260 m prior to decreasing at higher elevations. A directional shift of the wind occurred at ridge-top height. The shift from 45-90° to 270° provided additional evidence for identification of separate layers. Oscillations in wind directions between the surface and 35-40 m were associated with mixing. The heights of the stable boundary layer and mixing regime were 170 m and 35-40 m, respectively.

Measurements for the third set of profiles began at 0803 and terminated at 0828 after reaching a height of 498 m. The potential temperature at the surface increased 3°, from 290°K at the time of the second profile to 293°K during these measurements. The profile was vertical between the surface and 135 m. Above 135 m, remnants of the stable boundary layer were encountered based on the pronounced temperature inversion between 135 m and 170 m. From 170 m to 500 m, potential temperatures increased from 293°K to 298°K. Ozone concentrations were uniform at 30-35 ppb between the surface and the stable boundary layer. Between 135 m and 160 m, ozone concentrations increased from 30-35 ppb to 80 ppb. Above the stable boundary layer, the ozone profile was near vertical with concentrations of 80-90 ppb. Wind speeds and directions were highly variable between the surface and the stable boundary layer. They varied between 0.1 and 1.2 m/s and 0-356°, respectively. Above the stable boundary layer, wind speeds and directions became more uniform. Wind speeds averaged 1.7 m/s and wind directions

were from 270-355°. The height of the stable boundary layer remained at 170 m, but the mixing height increased to 135 m.

Measurements for the fourth set of profiles began at 0909 and terminated at 0933 after reaching 445 m. Potential temperatures at the surface increased to 297 °K, a 4°K increase compared to measurements the previous hour. The pronounced potential temperature inversion visible in the 0803-0828 profile dissipated and the profile was near vertical. Potential temperatures increased from 297°K at the surface to 298°K at 445 m. As the result of entrainment, ozone concentrations at the surface rapidly increased from 30-35 to 60 ppb. Concentrations between 294-445 m remained at 80-90 ppb. Surface wind speeds doubled to 1.1-2.1 m/s resulting in a rather uniform profile between the surface and 445 m. Variable wind directions displayed in the 0803-0828 profile increased in height to 400 m with winds from 180-315°. The stable boundary layer was destroyed, and the mixing height exceeded 445 m.

Measurements for the fifth set of profiles began at 0959 and terminated at 1032 after reaching 581 m. The potential temperature profile was vertical at 298-299 °K. The entrainment of ozone from elevated sources resulted in a twofold increase of ground-level ozone concentrations within 45 minutes. Ozone concentrations at the surface and throughout the profile were 65-80 ppb. Surface wind speeds were variable between 0.2 and 2.7 m/s. Wind directions were highly variable throughout the profile. The mixing height exceeded 581 m.

Measurements for the sixth set of profiles were conducted from 1059 to 1119 and reached 400 m. Potential temperatures increased and the profile remained near vertical at

299-300 °K. The ozone concentration profile was vertical with concentrations equaling 70-80 ppb . Wind speeds increased at all elevations with the most significant increase occurring at approximately 330 m when speeds ranged from 3.2 to 4.8 m/s. Wind directions remained variable throughout the profile ranging from 0-360°.

Afternoon-evening measurements began at 1659 and concluded at 2148. Profiles of potential temperature, ozone concentrations, wind speed and wind directions are presented in Figure 4.8. Measurements for the first set of profiles were conducted from 1659 to 1727 and were obtained up to a height of 604 m. Potential temperatures were 301-302°K and ozone concentrations were 55-65 ppb. Wind speeds were highly variable between the surface and 350 m with minimum speeds of 0.2 m/s at 2 m and maximum speeds of 4.9 m/s at 271 m. Above 350 m, variability decreased and speeds remained between 1.0 and 2.5 m/s. Wind directions throughout the profile were primarily north. Consistent potential temperatures and ozone concentrations throughout the profiles indicated complete mixing.

Measurements for the second set of profiles were taken from 1757 to 1837 and the balloon attained a height of 539 m. The potential temperature profile was similar to the preceding profile with temperatures ranging from 301-302°K. However, one exception to the similarity occurred at the surface where a slight temperature decrease was noted. The ozone profile was near vertical with concentrations ranging between 60-65 ppb above 30 m, but there was a noticeable decrease in concentrations at the surface. Surface concentrations decreased from 60 to 55 ppb when compared to the 1659-1727 profile. Although variability decreased, the wind speed profile from the surface to 250-350 m was

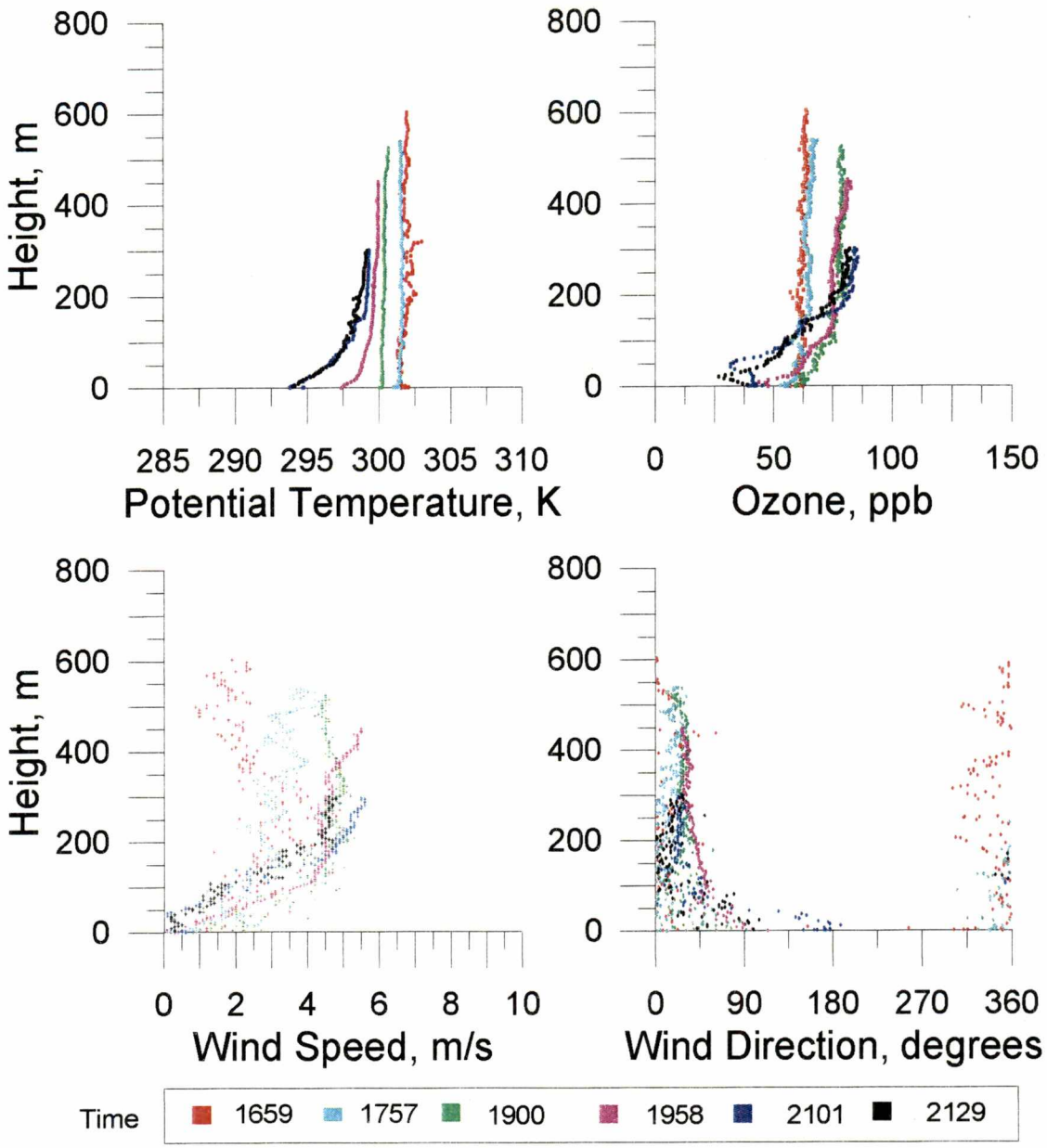

FIGURE 4.8. PROFILES OF POTENTIAL TEMPERATURE, OZONE CONCENTRATION, WIND SPEED AND WIND DIRECTION DEVELOPED FROM TETHERSONDE DATA OBTAINED DURING THE AFTERNOON-EVENING OF JULY 8, 1995. Tethersonde readings were initiated at 1659, and the final balloon ascent began at 2129.

similar to the preceding profile. Above 350 m, wind speeds increased with maximum speeds equaling 4.6 m/s. Wind direction variability decreased and shifted toward the N-NNE, particularly above 200 m. Based on the profiles, the earth's surface had begun to cool.

Measurements for the third set of profiles were conducted from 1900 to 1941 to a maximum height of 525 m. Although potential temperatures decreased 1-1.5 °K throughout the atmosphere, the potential temperature profile remained vertical. Potential temperatures at the surface were 300 °K. The ozone profile contained two distinct components. Between the surface and 200 m, concentrations increased with height from 55-60 ppb at the surface to 80 ppb at 200 m. Between 200-525 m, the profile was near vertical with concentrations of 77-79 ppb. Wind speeds below 50 m ranged from 0.5-2.5 m/s. Above 200 m, the wind speed profile was vertical with speeds between 4.5-5.1 m/s. Between 50-200 m, wind speeds quickly shifted from comparatively calm winds below 50 m to faster winds above 200 m. Winds below 200 m remained variable from the N-NE. Above 200 m, winds were from NNE. Examination of the profiles suggested continued cooling of the earth's surface and increased differences between ozone concentrations at the surface and aloft.

Measurements for the fourth set of profiles began at 1958 (3 minutes after sunset) and concluded at 2028 when balloon height attained was 451 m. Interpretation of these profiles focused on formation of the nocturnal stable boundary layer. Potential temperatures at ground-level decreased to 297°K. Potential temperatures increased with height until reaching approximately 250 m. Above 250 m, temperatures were constant at

299-300°K. Though the inversion existed between the surface and 250 m, the inversion between the surface and 25 m was far more pronounced and more accurately represented the height of the stable boundary layer. Surface ozone concentrations were 45-50 ppb and increased in a profile similar to that of potential temperature. At 100 m, concentrations were about 70 ppb. Between 100 m and 451 m, the profile was near vertical with concentrations ranging 70-82 ppb. Interestingly, ozone concentrations were higher at the surface than at 10 m. This phenomenon became more prominent probably as a result of drainage winds from nearby ridges that transported air parcels containing higher ozone concentrations from ridge-top altitudes to the valley-floor. Surface wind speeds remained less than 1 m/s. Speeds increased uniformly until reaching 4 m/s at 107 m. The wind speed profile was essentially vertical between 107 and 380 m with speeds ranging from 4-5 m/s. Above 380 m, speeds exceeded 5 m/s. Although surface winds remained variable from N-NE-E, variability significantly decreased above 70 m. Above 70 m, winds were from NNE-NE. Potential temperature data signified formation of the stable boundary layer height of the stable boundary layer was estimated to be 25 m. Atmospheric mixing between the surface and upper atmosphere ceased and preliminary formation of the stable boundary layer (nocturnal inversion) commenced.

Measurements for the fifth set of profiles started at 2101, finished at 2116, and terminated at 302 m. Interpretation of these profiles portrayed continuing development of the nocturnal stable boundary layer. Potential temperatures at ground-level further decreased to 294°K. With increasing altitudes, potential temperatures increased to 299°K at 160 m. Between 160-302 m, potential temperatures remained constant.

Surface ozone concentrations were 40-45 ppb. However, ozone concentrations increased markedly at the surface when compared to concentrations of 30-35 ppb at 40 m. Drainage winds maintained surface concentrations while concentrations at slightly higher altitudes decreased. Above 190 m, ozone concentrations were 80-85 ppb. Wind speeds between the surface and 60 m remained less than 1 m/s. From 60 m to 302 m, speeds increased uniformly attaining 4.4-5.5 m/s. In the stable boundary layer, wind directions were variable with surface winds from the S and higher elevation winds shifting more from the NNE. Above the stable boundary layer (160 m), winds were from the NNE. Based on the pronounced potential temperature inversion and supporting data from the wind speed-directional profiles, stable boundary layer height was estimated to be 160 m.

Measurements for the sixth set of profiles began at 2129 and finished at 2147 at 300 m. Potential temperatures at ground-level remained approximately 294 °K, but the inversion between the surface and 80 m became more pronounced. In addition, the profile between 160-300 m was no longer vertical when compared with data from the previous measurements. Temperatures were 298°K at 160 m and 299°K at 300 m. Based on these complimentary events, depth of the stable boundary layer was estimated to be 220 m. Surface ozone concentrations were 35-40 ppb, higher than concentrations of 25-30 ppb at 20 m as the result of drainage winds. Above 20 m, concentrations consistently increased to 80 ppb at 220 m where they remained constant. Surface wind speeds remained less than 1 m/s. At 60-70 m, speeds uniformly increased until reaching 4.5 m/s at 200 m. Above 200 m, speeds remained constant. In the stable boundary layer, directional variability decreased as surface winds originated in the NE-E; higher

elevation winds continued transition toward the NNE. Inspection of the profiles revealed further development of the nocturnal stable boundary layer.

In attempting to extrapolate measurement data toward enhanced understanding of regional tropospheric ozone concentrations, Tethersonde measurements were compared with hourly averaged ozone concentrations recorded at the high-elevation Look Rock station and the low-elevation Freels Bend station (Figure 4.9). Heights of Look Rock and Freels Bend are 526 m and 0 m relative to Tethersonde, respectively. Thus, profile measurements at 526 m and 0 m were compared with hourly-averaged measurements at Look Rock and Freels Bend, respectively. In the morning and afternoon-evening, Tethersonde measurements at 526 m were consistent with concentrations at the Look Rock station (Figure 4.9A). Measurements obtained at the surface in Oak Ridge corresponded closely with concentrations recorded at Freels Bend (Figure 4.9B).

In comparing the regional ozone monitoring stations (Figure 4.10), ozone concentrations at the high-elevation stations showed little diurnal variation. The peak concentrations for Clingmans Dome and Look Rock were 89 and 98 ppb, respectively. Those concentrations were recorded at 1500 and 1700-1800. Cove Mountain was not operational on July 8. Ozone concentrations for the low-elevation stations were remarkably similar. The peak concentrations for East Knox, Freels Bend, Nances Grove and Spring Hill were 76, 80, 83, and 83 ppb, respectively. Those concentrations were recorded at 1200, 1100, 1100, and 1300. Of special note were the higher concentrations at Nances Grove throughout the morning. At midnight, concentrations at Nances Grove were 56 ppb, approximately 20-25 ppb higher than other low-elevation stations. They

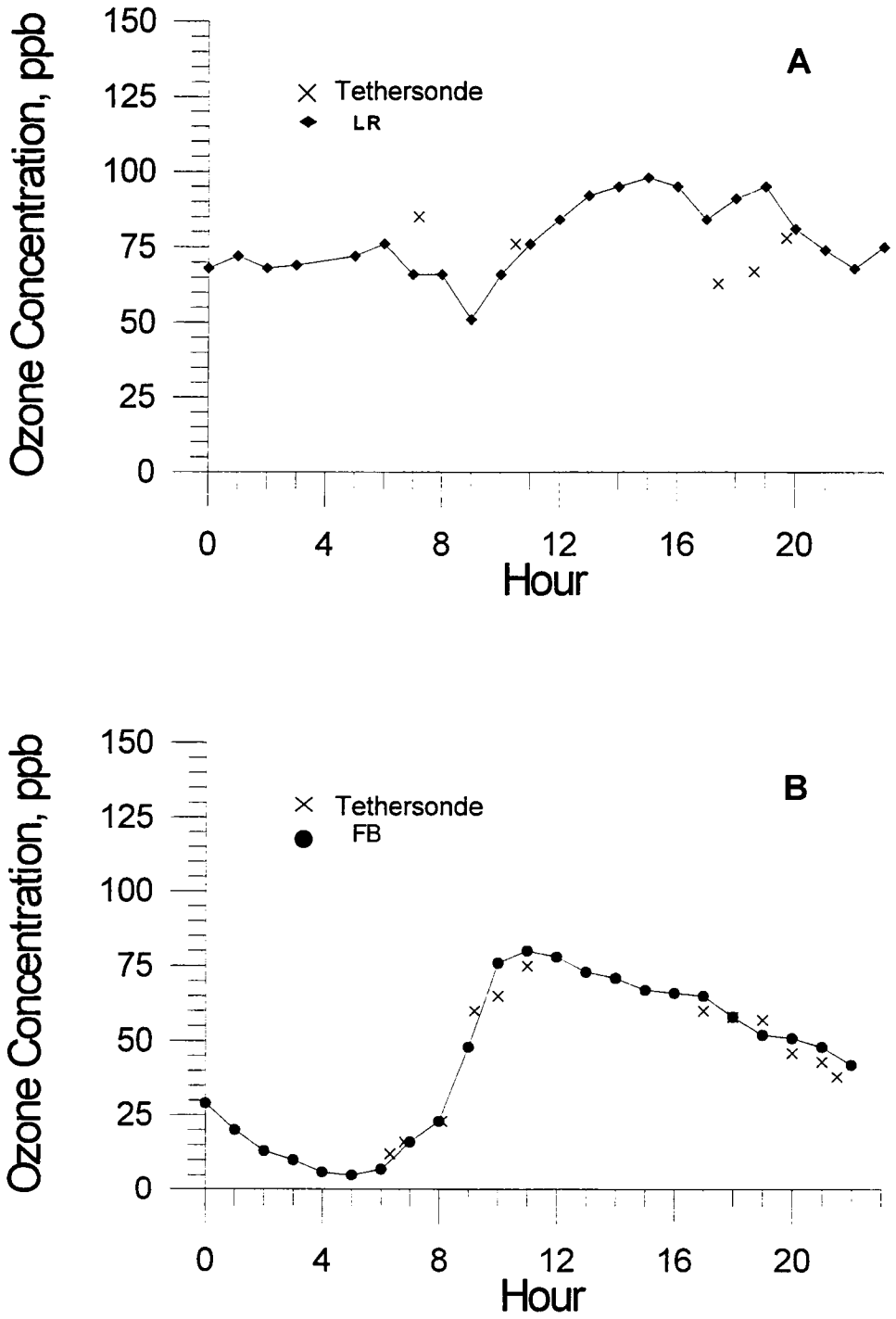

FIGURE 4.9. COMPARISON OF HOURLY MEAN OZONE CONCENTRATIONS ON JULY 8, 1995 OBTAINED FROM LOOK ROCK AND FREELS BEND REGIONAL MONITORING STATIONS WITH READING OBTAINED AT OAK RIDGE WITH TETHERSONDE INSTRUMENTATION. A) Look Rock and B) Freels Bend.

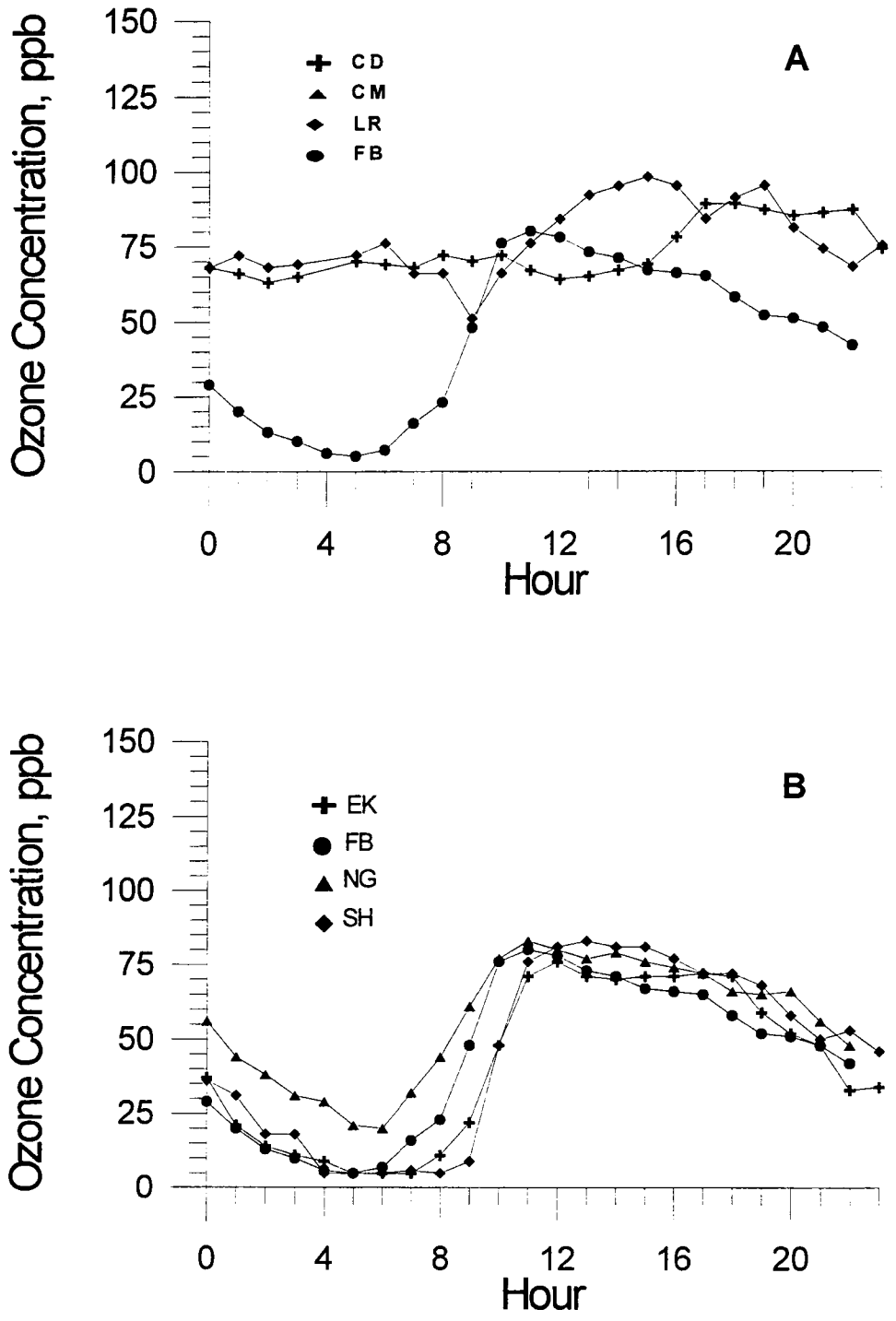

FIGURE 4.10. HOURLY MEAN OZONE CONCENTRATIONS OBTAINED FROM REGIONAL MONITORING STATIONS ON JULY 8, 1997 A. High elevation stations (located above 793m MSL) [Clingmans Dome (CD), Cove Mountain (CM), and Look Rock (LR)] and Freels Bend (elevation 247m MSL). B. Low elevation stations (below 343 m MSL)[East Knox (EK), Freels Bend (FB), Nances Grove (NG) and Spring Hill (SH)].

remained higher until 1000-1100. One final point to note, ozone concentrations at 0646 and 0803 were in excess of 90 ppb between heights of 400-500 m. Thus, surface concentrations recorded throughout the day did not significantly exceed concentrations aloft in the early morning.

JULY 14, 1995 Friday

On July 14, the minimum and maximum temperatures at ground-level were 21.6°C and 36.8°C, respectively. The minimum temperature occurred at 0524 and the maximum temperature at 1414. Wind speeds averaged 0.2 m/s in the early morning, increased to 2.2 m/s at 1800, and diminished to 0.7 m/s at 0000. The peak wind speed, 9.4 m/s, occurred at approximately 2200. The skies were clear throughout the day; there was no precipitation. Sunrise occurred at 0530 and sunset at 1953. Measurements were conducted during morning and afternoon-evening. However, at approximately 2015, thunder and lightening storms were observed NE of the site. Evening measurements were stopped at 2027 because of nearby lightening.

Morning profiles of potential temperature, ozone concentration, wind speed, and wind direction for morning measurements are presented in Figure 4.11. Measurements for the first set of profiles began at 0501 (29 minutes before sunrise), stopped at 0542 and the balloon reached 601 m. A strong, ground-based inversion extended 180 m. Ozone concentrations at the surface were less than 5 ppb, but approached 90 ppb above the stable boundary layer.

The second set of measurements were taken from 0556 (26 minutes after sunrise) to 0634 and the balloon reached 595 m. Stable boundary layer height remained 180 m.

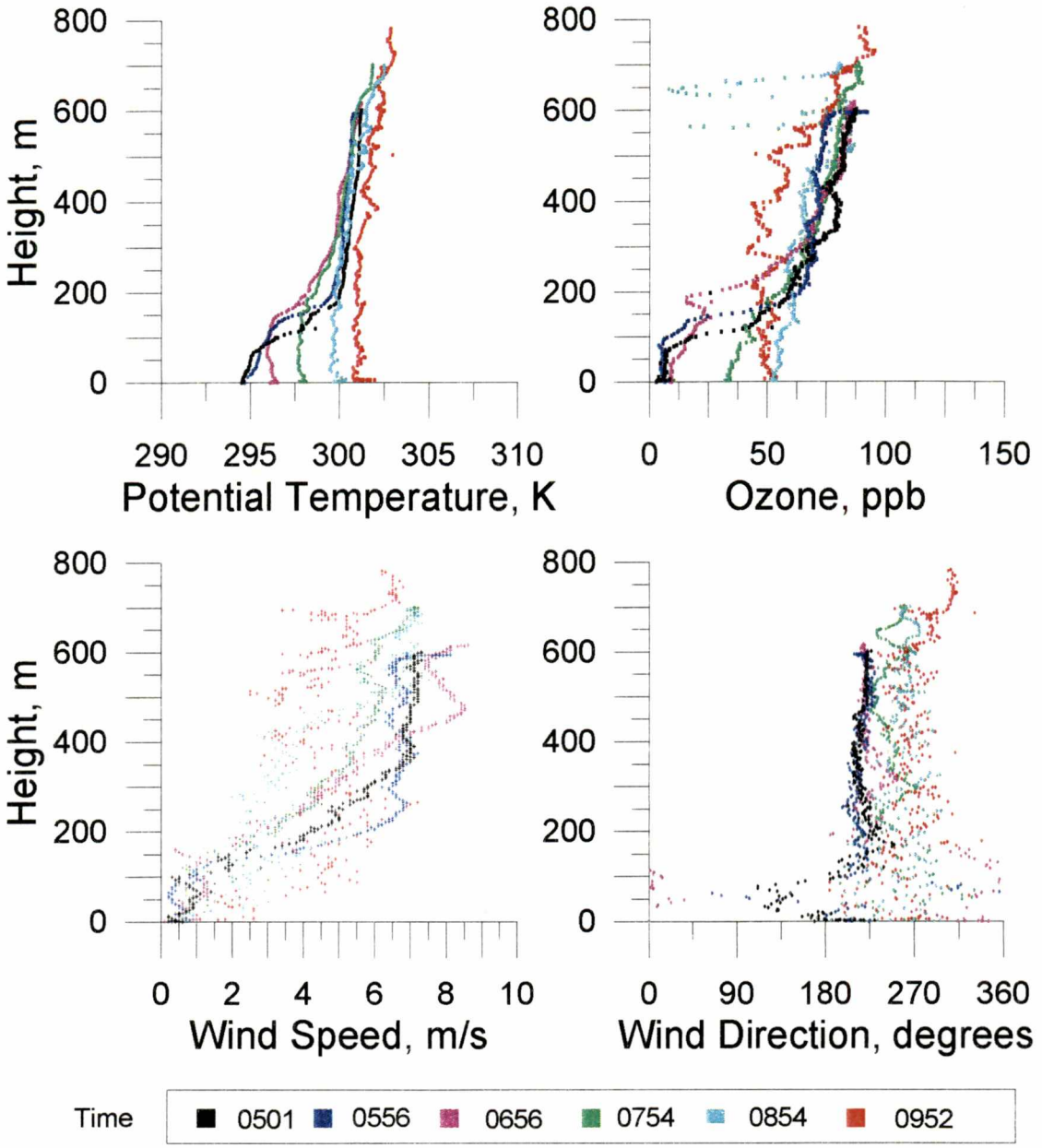

FIGURE 4.11. PROFILES OF POTENTIAL TEMPERATURE, OZONE CONCENTRATION, WIND SPEED AND WIND DIRECTION DEVELOPED FROM TETHERSONDE DATA OBTAINED DURING THE MORNING OF JULY 14, 1995. Tethersonde readings were initiated at 0501, and the final balloon ascent began at 0952.

The potential temperature inversion and increased ozone concentrations were far more pronounced between 120 and 180 m. Above the stable boundary layer (180 m), potential temperatures, ozone concentrations, wind speeds, and wind directions remained essentially unchanged.

Measurements for the third set of profiles were conducted from 0656 to 0731 and attained 617 m. Although a potential temperature inversion remained at the top of the stable boundary layer (150-180 m), increased erosion of the stable layer resulted in mixing between the surface and 150 m. In this region, the potential temperature was vertical and ozone concentrations increased from entrainment. Wind speeds increased and directional variability increased in height. The mixing height was estimated to be 150 m.

Measurements for the fourth set of profiles were obtained from 0754 to 0835 and were discontinued at 702 m. Potential temperatures were 298 °K at ground-level and increased to 302 °K at 700 m. Ozone concentrations at the surface increased from 10 ppb at 0656 to 32 ppb at 0754 as the result of entrainment. Concentrations at 600-700 m remained near 85 ppb at 0830. Below 200 m, wind speeds and wind direction variability increased. Erosion of the stable boundary layer was nearly complete based on the near vertical potential temperature profile. The stable boundary layer had broken up and was no longer of concern. The mixing height was estimated to be 200 m.

Measurements for the fifth set of profiles were conducted from 0854 to 0934 and were obtained up to 701 m. The potential temperature profile became more vertical as temperatures at ground-level increased to 300°K, and temperatures at 700 m remained

302 °K. Surface ozone concentrations increased from 32 ppb at 0754 to 52 ppb at 0854 while concentrations at 550 m remained near 85 ppb at 0923. Of special note was the depletion of ozone between 560 m and 690 m. The lower region of depletion occurred between 555 m and 615 m when concentrations of 85 ppb plummeted to 17 ppb at 564 m. The higher region of depletion occurred between 615 m and 685 m when concentrations plummeted to 8 ppb at 646 m. At 700 m, ozone concentrations remained comparatively high at 80 ppb. During this time, the wind direction was from the west. The Kingston Steam Plant, a Tennessee Valley Authority (TVA) power plant, is located on Watts Bar Lake, two miles north of Kingston, Tennessee. It is a nine-unit facility with maximum generating capacity of 1,723,250 kilowatts and an annual consumption of 4,300,000 tons of coal. Pollution control features include electrostatic precipitators and two 1,000-foot stacks (Martocci, 1995). The observed ozone depletion most probably resulted from encountering the power plant's plume. Below 600 m, wind speeds and wind direction variability increased, 330 m higher than observed in the preceding measurements. Based on the profiles, the mixing height was estimated to be 530 m.

Measurements for the sixth set of profiles were conducted from 0952 to 1041 and up to a height of 783 m. The potential temperature profile remained near vertical as temperatures at ground-level increased to 301 °K and temperatures at 700 m increased to 303 °K. Ozone concentrations at the surface remained 50-55 ppb, but concentrations exceeding 90 ppb were detected above 700 m. Depletion of ozone between 560 m and 690 m was no longer evident as the result of subtle changes in wind directions. Between the surface and 800 m, wind speed and wind direction variability increased. Wind speeds

below ridge-top height were typically below 3 m/s while speeds above averaged 5-6 m/s. Below 200 m, wind directions varied from S-SW to NW. Above 200 m, directions fluctuated between SW and NW. The mixing height exceeded 783 m AGL.

Afternoon-evening measurements began at 1759 and concluded at 2027. Profiles of potential temperature, ozone concentration, wind speed and wind direction are presented in Figure 4.12. Measurements for the first set of profiles were conducted from 1759 to 1831 to an altitude of 605 m. The potential temperature profile was almost vertical with surface temperature equal to 304 °K and temperature at 605 m equal to about 306 °K. Ozone concentrations at the surface were 50 ppb. Above 40 m, the profile was near vertical and concentrations were 65-70 ppb. Wind speeds below ridge-top height were below 2.5 m/s and winds above 100 m averaged 3.5-4.5 m/s. Winds were primarily from the NE.

Measurements for the second set of profiles were conducted from 1854 to 1921 to an altitude of 601 m. The potential temperature profile was almost vertical with surface temperatures equal to 304 °K and temperatures at 601 m equal to about 305 °K. Ozone concentrations at the surface averaged 55-60 ppb and higher concentrations averaged 75 ppb. Although wind speed variability decreased, magnitude remained essentially unchanged from the prior profile. Below ridge-top height, wind direction varied from NE to ESE. Above the ridges, wind direction gradually shifted between ridge-top height and 400 m. Above 400 m, wind direction remained constant from the NE. Although ozone concentrations at both the surface and aloft increased 5-10 ppb, differences between surface and aloft concentrations were more pronounced.

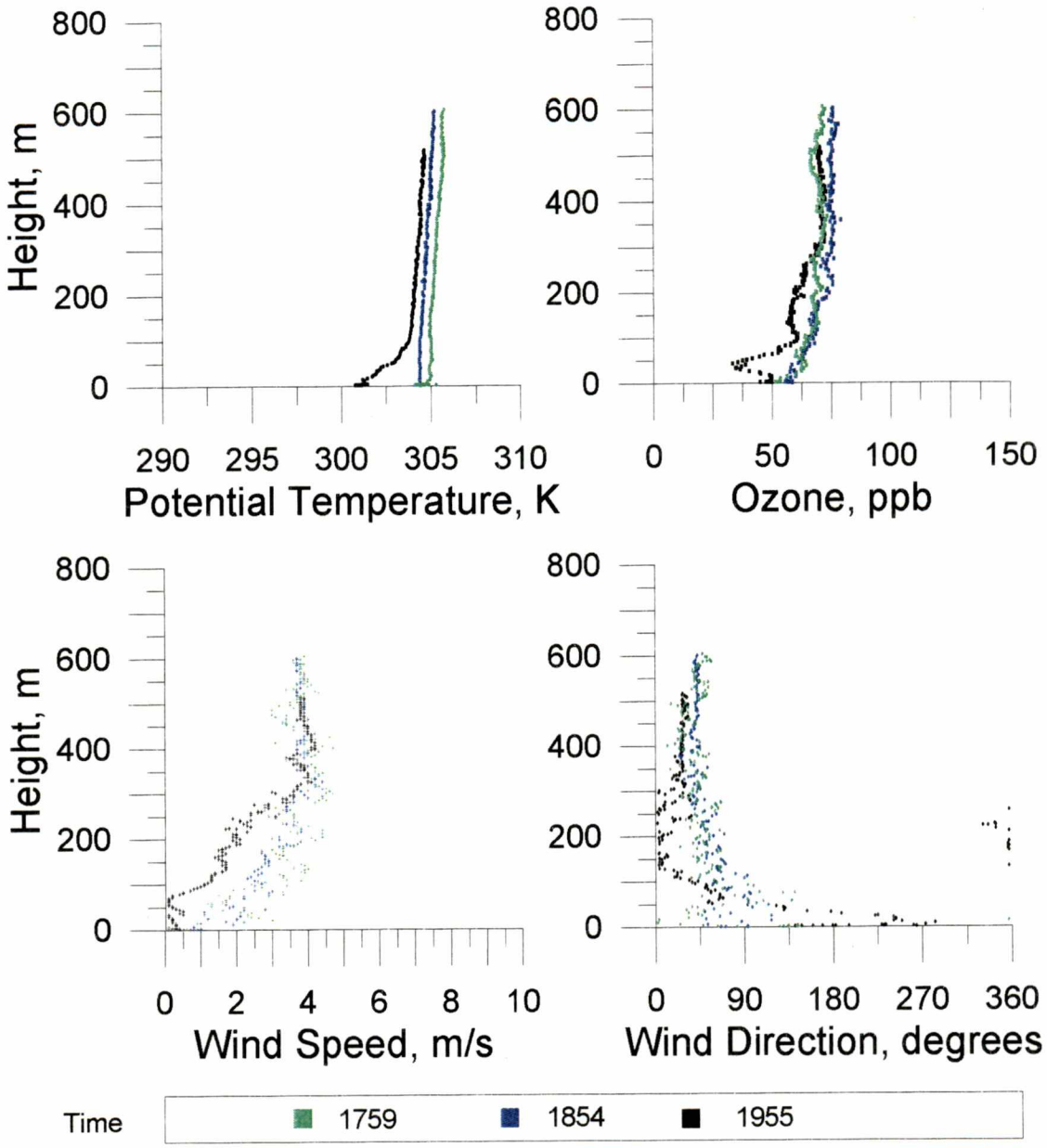

FIGURE 4.12. PROFILES OF POTENTIAL TEMPERATURE, OZONE CONCENTRATION, WIND SPEED AND WIND DIRECTION DEVELOPED FROM TETHERSONDE DATA OBTAINED DURING THE AFTERNOON-EVENING OF JULY 14, 1995. Tethersonde readings were initiated at 1759, and the final balloon ascent began at 1955.

Measurements for the third set of profiles were conducted from 1955 (two minutes after sunset) to 2027 to an altitude of 517 m. Potential temperatures at the surface dropped to 301 °K. Temperatures sharply increased with elevation between the surface and 50 m. From 50 m upwards, the potential temperatures gradually increased from almost 302 °K at 50 m to near 305 °K at 517 m. Ozone concentrations at the surface were approximately 50 ppb and were comparatively higher than the concentrations at 40 m which were near 35 ppb. Above 100 m, concentrations were depicted by a near vertical profile where concentrations at 100 m and 500 m equaled 60 and 70 ppb, respectively. Similar to the July 8 evening, the surface phenomenon was attributed to drainage winds transporting air parcels containing higher ozone concentrations from the ridge-tops to the valley floor. Wind speeds below ridge-top height dropped too less than 1 m/s. At higher altitudes, wind speed increased with elevation until peaking near 4 m/s at 325 m. Surface winds were variable from the SW-WSW-W. Above the ridges, wind direction gradually shifted toward the NNE. Above 300 m, winds were from the NNE. Based on the potential temperature profile, atmospheric mixing between the surface and aloft ceased and formation of the stable boundary layer began. The height of the stable boundary layer was estimated to be 95 m.

Tethersonde morning measurements exceeded concentrations at Look Rock while Tethersonde afternoon-evening measurements were lower than concentrations recorded at Look Rock (Figure 4.13). Tethersonde low-elevation measurements in Oak Ridge were similar to those at Freels Bend. Differences occurred at 0900-1000 and 1700 when concentrations at Freels Bend exceeded those observed in Oak Ridge by 15-25 ppb.

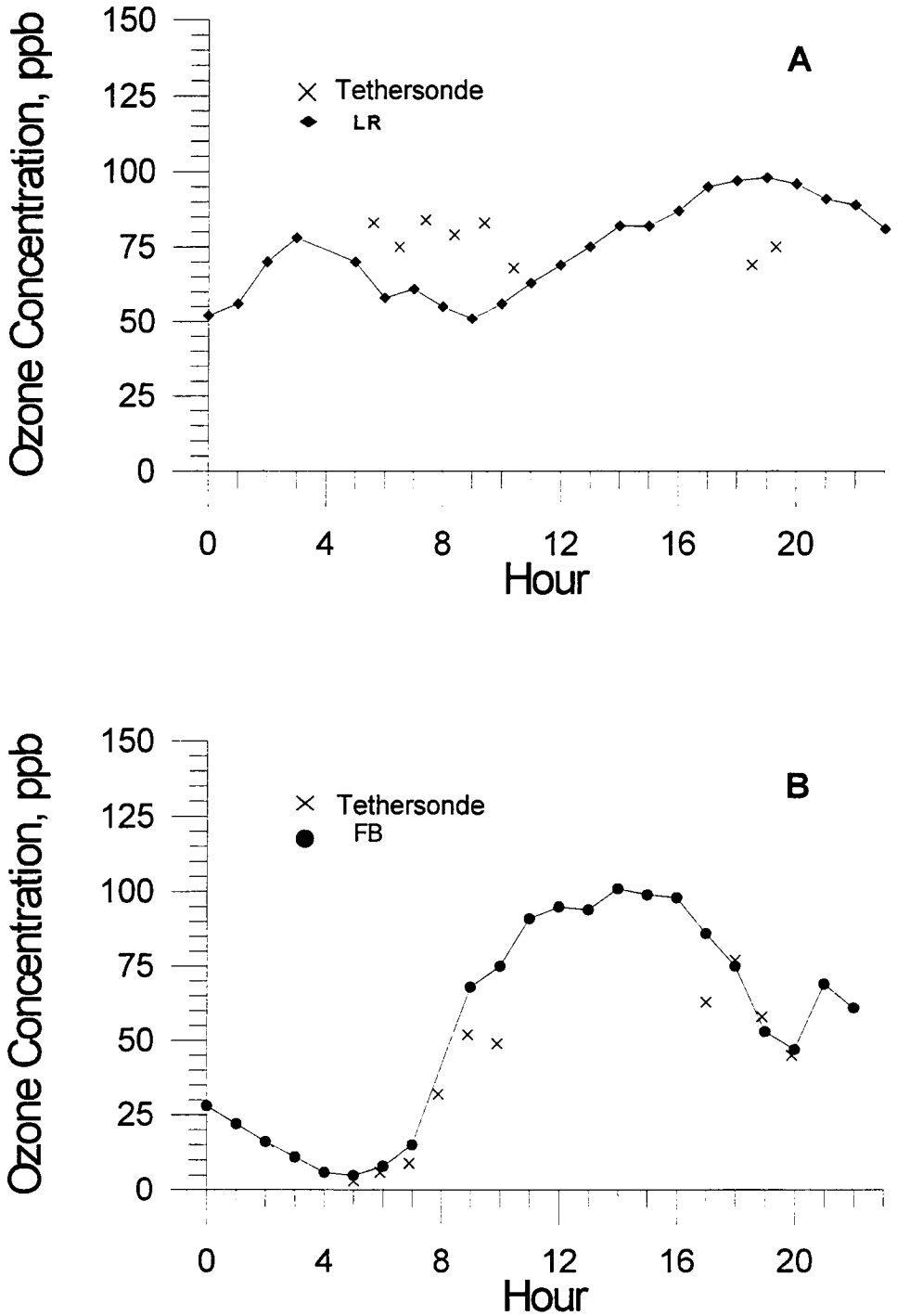

FIGURE 4.13. COMPARISON OF HOURLY MEAN OZONE CONCENTRATIONS ON JULY 14, 1995 OBTAINED FROM LOOK ROCK AND FREELS BEND REGIONAL MONITORING STATIONS WITH READING OBTAINED AT OAK RIDGE WITH TETHERSONDE INSTRUMENTATION. A) Look Rock and B) Freels Bend.

In comparing the regional ozone monitoring stations (Figure 4.14), ozone concentrations at the high-elevation stations showed little diurnal variation. The peak concentrations for Cove Mountain and Look Rock were 98 and 105 ppb, respectively. The peak concentration at Cove Mountain was recorded at both 1900 and 2100. The peak concentration at Look Rock occurred at 1400. Clingmans Dome was not operational on July 14. Ozone concentrations for the low-elevation stations were remarkably similar. The peak concentrations for East Knox, Freels Bend, Nances Grove and Spring Hill were 104, 101, 111, and 105 ppb, respectively. Those concentrations were recorded at 1300, 1400, 1300, and 1400. Concentrations at Nances Grove exceeded those of other low-elevation stations throughout the morning. One final point to note, Tethersonde measurements conducted at 0556 recorded ozone concentrations exceeding 90 ppb at approximately 600 m. Subsequent measurements at 0952 identified concentrations exceeding 90 ppb at 700-780 m. Thus, surface concentrations recorded throughout the day exceeded concentrations aloft by 10-20 ppb.

JULY 17, 1995 Monday

On July 17, the minimum and maximum temperatures at ground-level were 21.3°C and 36.4°C, respectively. The minimum temperature occurred at 0517 and the maximum temperature at 1352. Wind speeds averaged 0.2 m/s in the early morning, increased to 3.2 m/s at 1500, and diminished to 1.2 m/s at 0000. Peak wind speed, 11.7 m/s, occurred at approximately 1600. Sunrise occurred at 0532 and sunset at 1951. Although skies were clear throughout most of the day, storm clouds and rain occurred

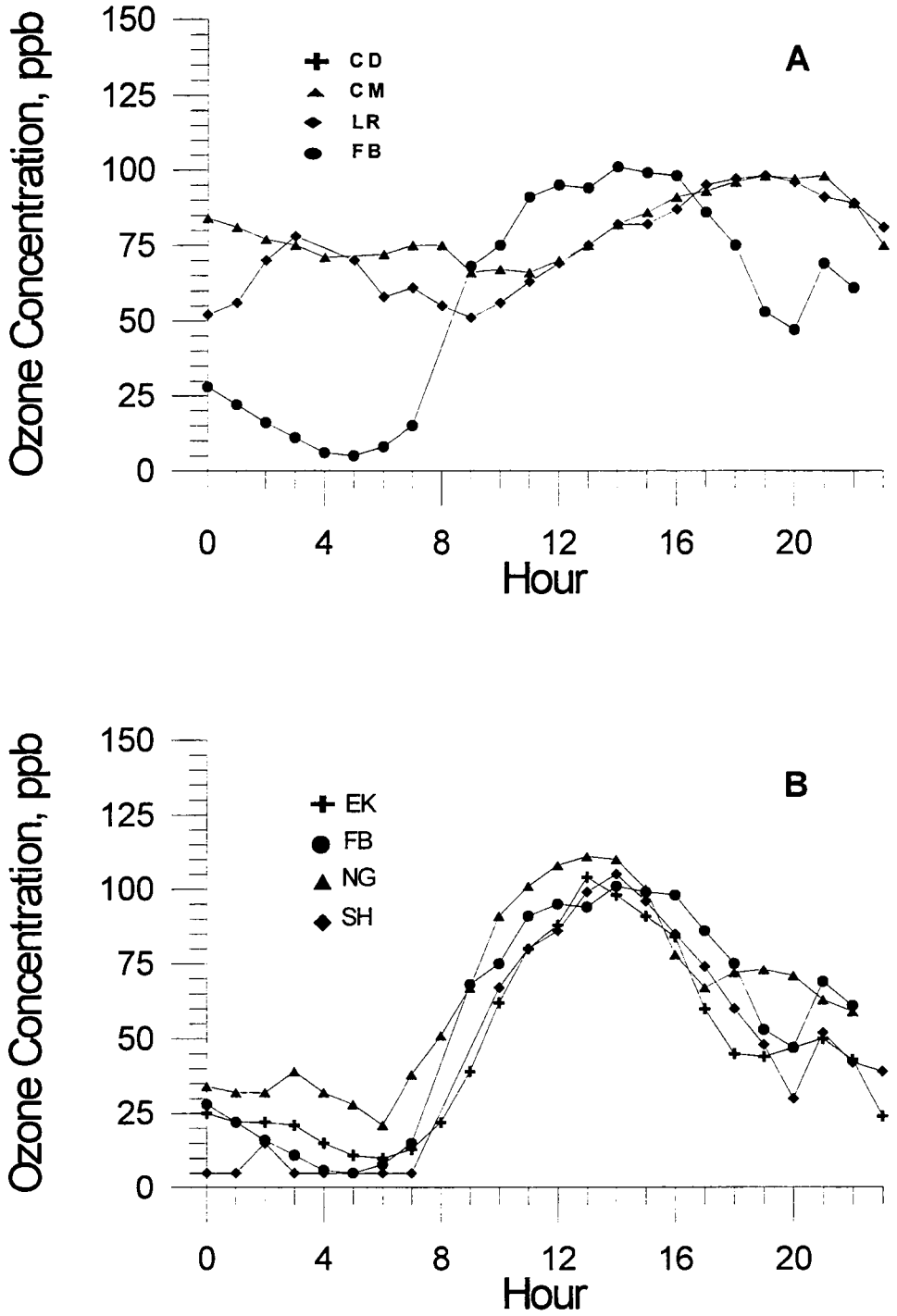

FIGURE 4.14. HOURLY MEAN OZONE CONCENTRATIONS OBTAINED FROM REGIONAL MONITORING STATIONS ON JULY 14, 1995. A. High elevation stations (located above 793m MSL) [Clingmans Dome (CD), Cove Mountain (CM), and Look Rock (LR)] and Freels Bend (elevation 247m MSL). B. Low elevation stations (below 343 m MSL)[East Knox (EK), Freels Bend (FB), Nances Grove (NG) and Spring Hill (SH)].

during two isolated periods. The first event occurred at approximately 1600 when a late afternoon thunderstorm deposited 0.3 mm precipitation. The second event happened near midnight when a storm produced 1.0 mm precipitation. Measurements were taken only during the morning. The measurements began at 0556 (24 minutes after sunrise) and concluded at 1126. Profiles of potential temperatures, ozone concentration, wind speed, and wind direction are presented in Figure 4.15.

Measurements for the first set of profiles were conducted from 0556 to 0651 and the balloon reached a height of 802 m. Potential temperatures at ground-level were 295°K and increased to 300.5°K at 300 m. Ozone concentrations between the surface and 100 m were less than 5 ppb. Between 100-300 m, concentrations increased from 5 ppb at 100 m to almost 90 ppb at 300 m. Above the stable boundary layer (300 m), concentrations were near 90 ppb. One noted exception occurred at 683 m where ozone concentrations peaked at 115 ppb. Surface wind speeds were less than 1 m/s below 115 m. Above ridge influences, speeds increased from less than 1 m/s at 115 m to almost 5 m/s at 300 m. Above 300 m, wind speeds were 5-6 m/s. Wind directions below 300 m were highly variable from 0-360°. Above 300 m, winds were primarily from NNW-NW. Based on the profiles, the height of the nocturnal inversion was estimated to be approximately 300 meters.

Measurements for subsequent profiles were performed 0701-0732, 0800-0842, 0855-0930, 0959-1040, and 1053-1126. Based on examinations of potential temperature, ozone concentration, wind speed, and wind direction profiles, estimation of the mixing height throughout the morning was determined. During the 0701-0732 measurements,

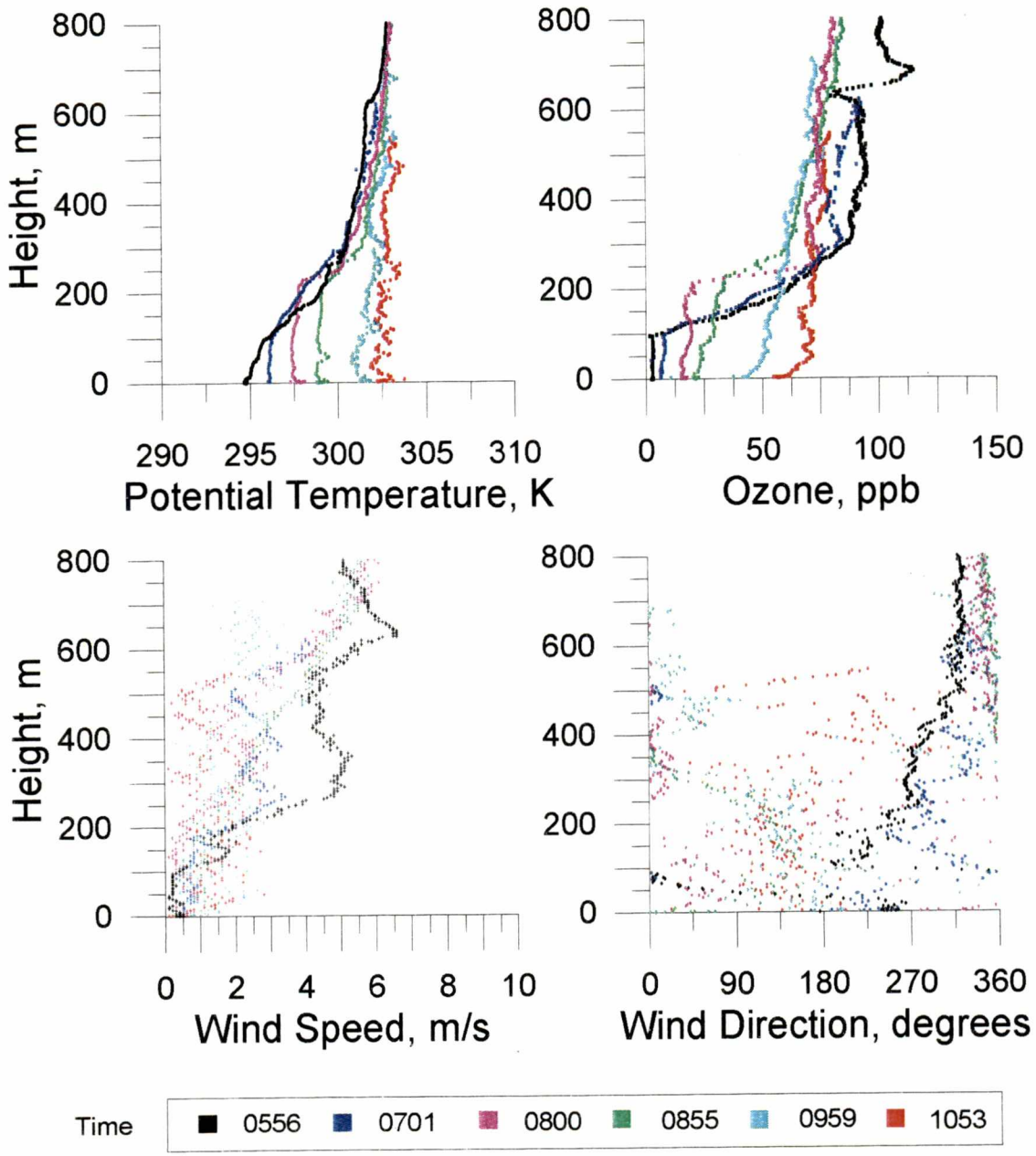

FIGURE 4.15. PROFILES OF POTENTIAL TEMPERATURE, OZONE CONCENTRATION, WIND SPEED AND WIND DIRECTION DEVELOPED FROM TETHERSONDE DATA OBTAINED DURING THE MORNING OF JULY 17, 1995. Tethersonde readings were initiated at 0556 and the final balloon ascent began at 1053.

the stable boundary layer height remained 300 m. The mixing height was estimated to be 110 m. Below 110 m, potential temperatures and ozone concentrations were essentially constant at 296 °K and 7 ppb, respectively. Based on measurements for the third set of profiles (0800-0842), the stable boundary layer height was estimated to be 250 m while the mixing height increased to 225 m. As the result of entrainment from higher ozone concentrations near the top of the stable boundary layer, ozone concentrations in the mixing regime increased to 15-20 ppb. When measurements for the fourth profiles (0855-0930) were analyzed, the stable boundary layer height increased to approximately 310 m; the mixing height remained 225 m. Within the mixing regime, potential temperatures increased to 299 °K and ozone concentrations increased to 20-30 ppb. Examination and subsequent interpretation of measurements for the fifth and sixth profiles (0959-1040 and 1053-1126) provided evidence for complete dissipation of the stable boundary layer and mixing throughout the measured height. Potential temperature and ozone concentration profiles were near vertical. Between 0959 and 1053, the potential temperature at the surface increased one degree from 301 to 302 °K. Breakup of the nocturnal boundary layer and subsequent entrainment of ozone from the residual layer reservoirs resulted in a dramatic increase of ozone concentrations at the surface. By 0959, concentrations at the surface increased to 40-45 ppb. Approximately one hour later (at 1053), concentrations had further increased to 60 ppb.

The morning Tethersonde measurements at 526 m exceeded concentrations recorded at Look Rock (Figure 4.16A). The largest difference occurred at 0630 when concentrations above Oak Ridge equalled 92 ppb and concentrations at Look Rock were

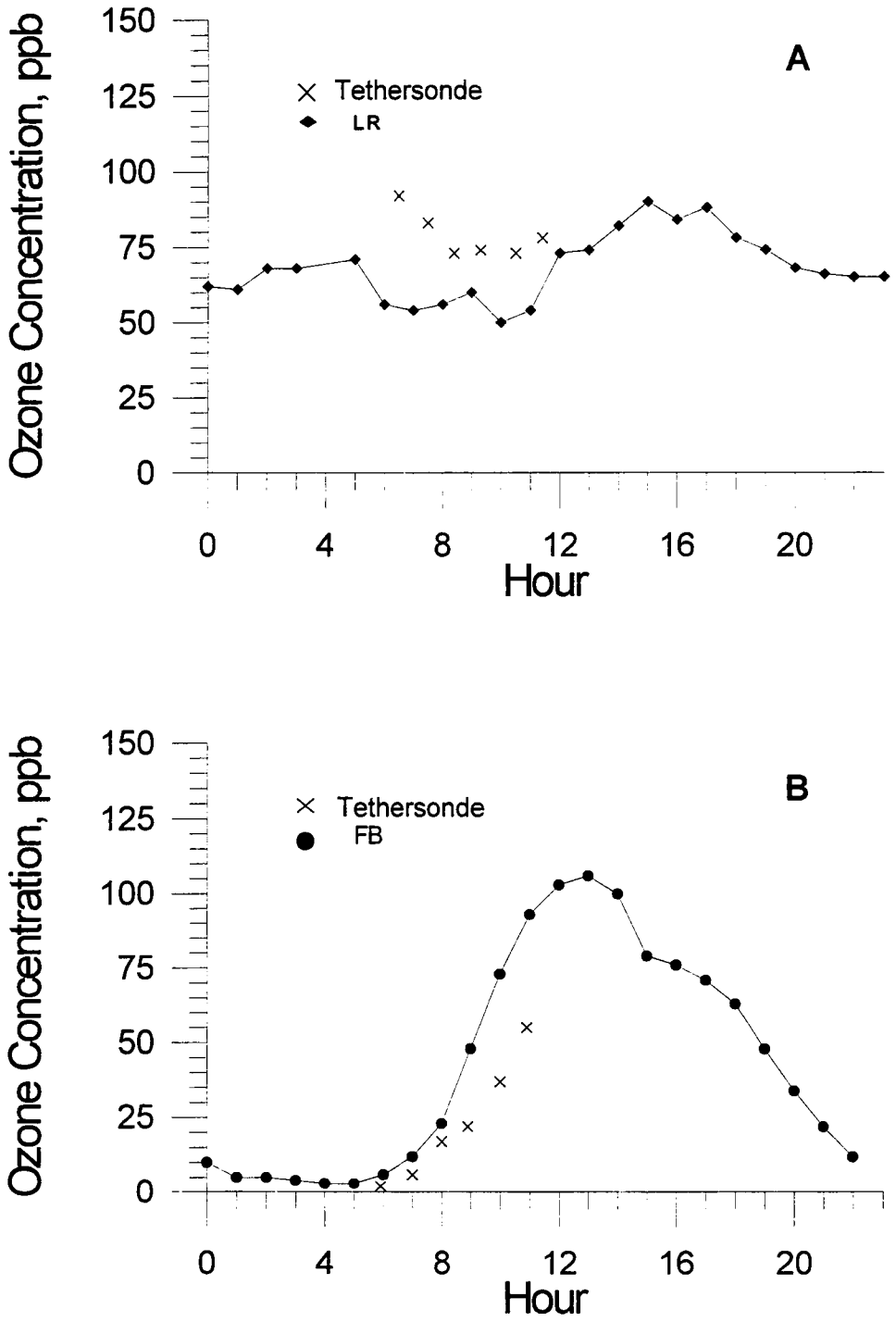

FIGURE 4.16. COMPARISON OF HOURLY MEAN OZONE CONCENTRATIONS ON JULY 17, 1995 OBTAINED FROM LOOK ROCK AND FREELS BEND REGIONAL MONITORING STATIONS WITH READING OBTAINED AT OAK RIDGE WITH TETHERSONDE INSTRUMENTATION. A) Look Rock and B) Freels Bend.

near 55 ppb. As the morning progressed, differences between the two locations became smaller. Low-elevation measurements in Oak Ridge compared favorably with concentrations at Freels Bend during the early morning (Figure 4.16B). However, differences occured beginning at 0900 and continuing through 1100 when concentrations at Oak Ridge fell below those obtained at Freels Bend. By 1100, concentrations at Oak Ridge were 55 ppb while concentrations at Freels Bend exceeded 90 ppb.

In comparing the regional ozone monitoring stations (Figure 4.17), ozone concentrations at the high-elevation stations showed little diurnal variation. The peak concentrations for Cove Mountain and Look Rock were 89 and 90 ppb, respectively. The peak concentrations at Cove Mountain and Look Rock occurred at 1700 and 1500, respectively. Clingmans Dome was not operational on July 17. Ozone concentrations for the low-elevation stations followed the same pattern. The peak concentrations for East Knox, Freels Bend, Nances Grove and Spring Hill were 78, 106, 89, and 108 ppb, respectively. Those concentrations were recorded at 1500, 1300, 1400, and 1500. Concentrations at Nances Grove exceeded those of other low-elevation stations thoughout the early morning. However, Freels Bend and Spring Hill concentrations were higher beginning at 1100 and 1400, respectively. During the 0556 Tethersonde measurements, ozone concentrations exceeding 90 ppb were found above 372 m. Above 653 m, concentrations exceeded 100 ppb. Between 670 m and 692 m, concentrations ranged 110-115 ppb. Thus, surface concentrations recorded throughout the day did not exceed concentrations aloft at 0556.

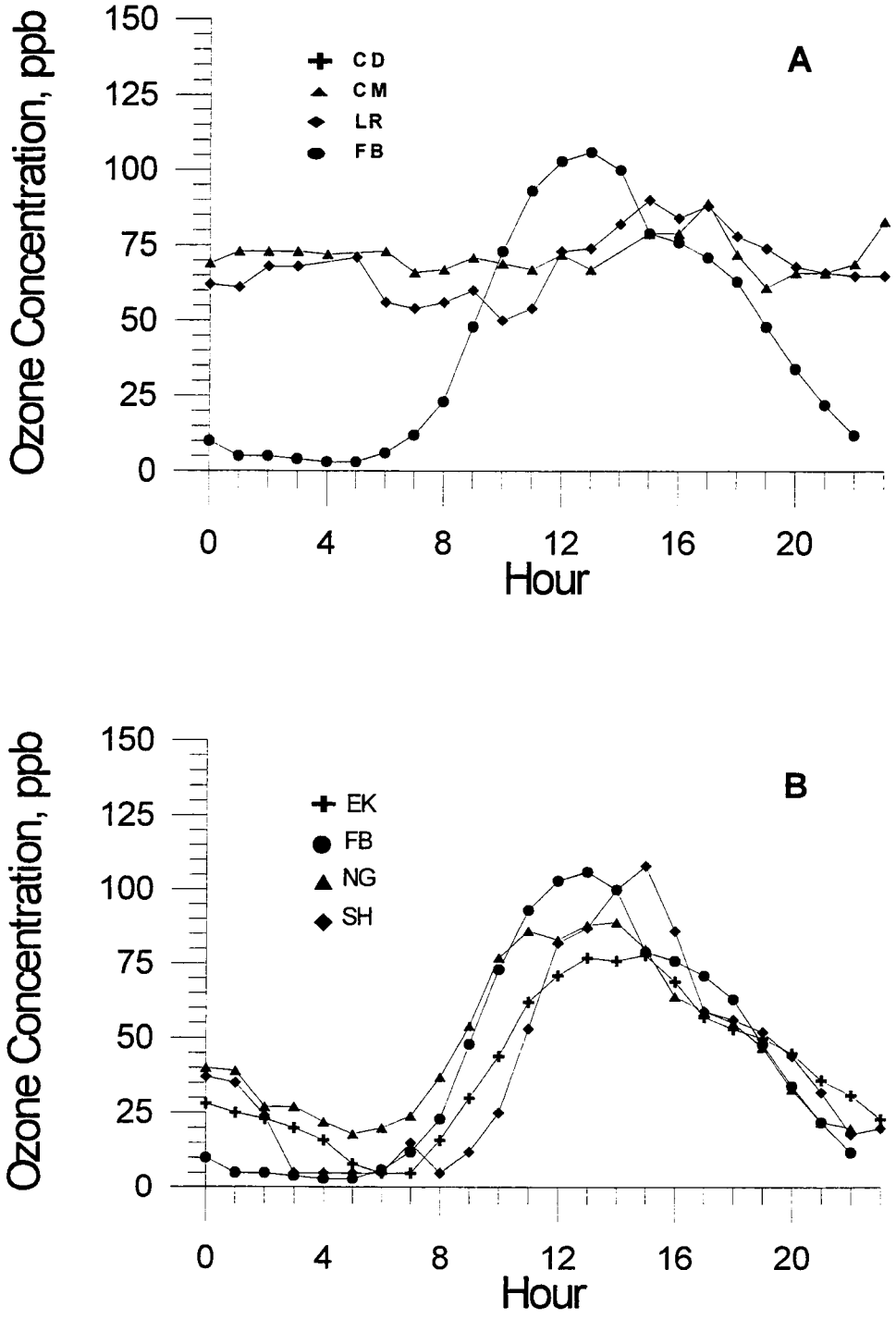

FIGURE 4.17. HOURLY MEAN OZONE CONCENTRATIONS OBTAINED FROM REGIONAL MONITORING STATIONS ON JULY 17, 1995. A. High elevation stations (located above 793m MSL) [Clingmans Dome (CD), Cove Mountain (CM), and Look Rock (LR)] and Freels Bend (elevation 247m MSL). B. Low elevation stations (below 343 m MSL)[East Knox (EK), Freels Bend (FB), Nances Grove (NG) and Spring Hill (SH)].

July 20, 1995 Thursday

On July 20, the minimum and maximum temperatures were 17.5°C and 36.4°C, respectively. Wind speeds averaged 0.2 m/s in the early morning, increased to a maximum 2.2 m/s by 1400, and dropped to 0.2 m/s by late evening. Sunrise occurred at 0534 and sunset at 1950. The skies were clear throughout the day. By late afternoon, the area was noticeably hazy. Although skies remained mostly clear, a few wispy clouds were noticed at 1900. Measurements were taken in the morning and afternoon-evening.

Measurements for the morning profiles began at 0554 and ended at 1143. Evaluation of potential temperature and ozone concentration profiles identified a surface-based inversion about 170 meters in height. Of special note was the depletion of ozone at approximately 450 m during early morning measurements (Figure 4.18). During this time, the wind direction was from the NE. The Bull Run Steam Plant, a Tennessee Valley Authority (TVA) power plant, is located on the east bank of Melton Hill Lake 8 km ENE northeast of Oak Ridge. It is a one-unit facility with a maximum generating capacity of 950,000 kilowatts and an annual gross output of 6,700,000 kilowatt-hours. Pollution control features include high-efficiency electrostatic precipitators for collection of fly ash, utilization of low-sulfur coal, and an 800-foot stack which ensures wide dispersal of emissions (Martocci, 1995). The observed ozone depletion was believed to result from encountering the power plant's plume. Based on measurements conducted at 0655, warming of the earth's surface initiated erosion of the stable boudary layer (nocturnal inversion). The mixing height was estimated to be 80 m. At 0757, the mixing height had increased to 170 m where a small temperature inversion remained. This

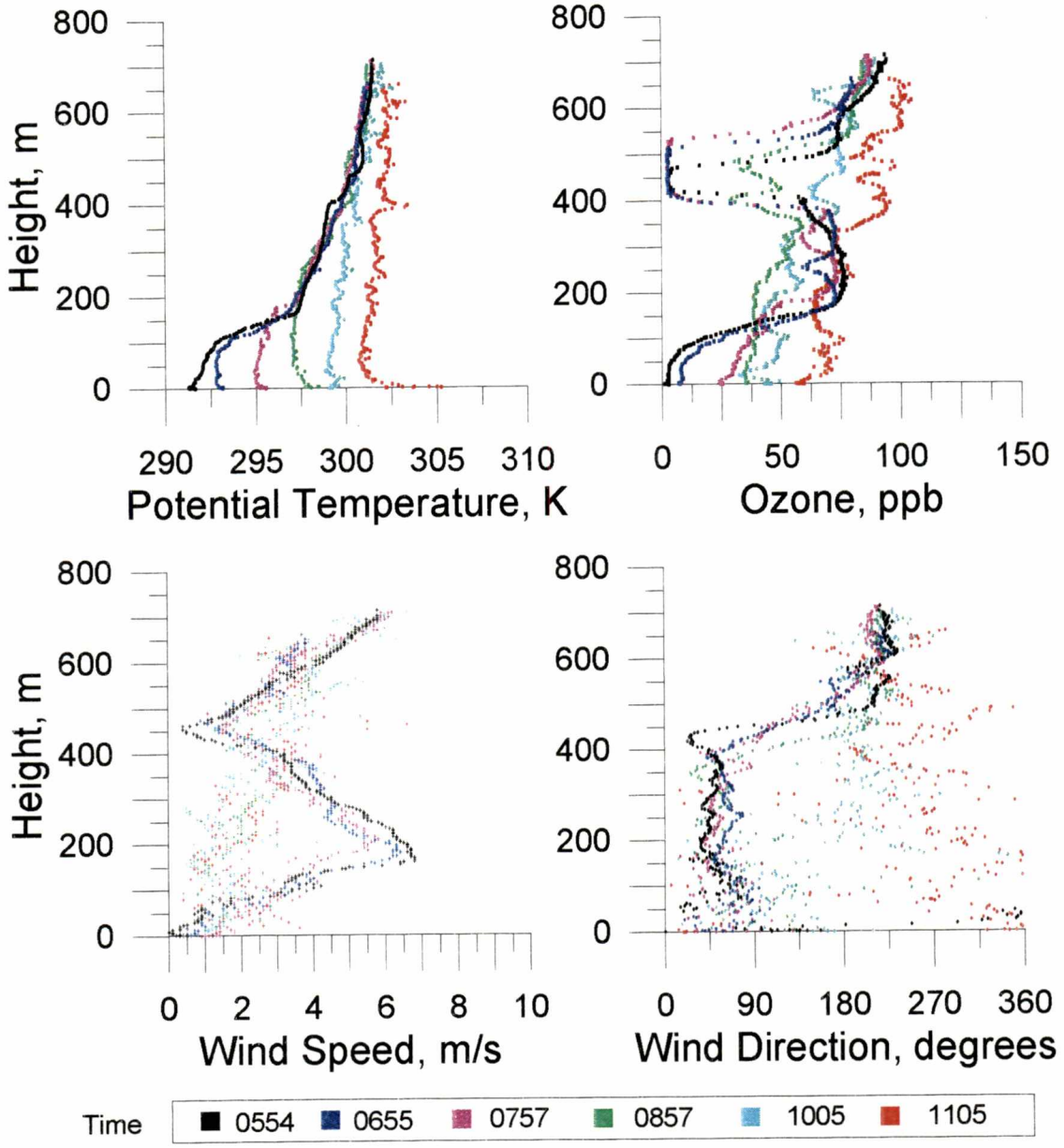

FIGURE 4.18. PROFILES OF POTENTIAL TEMPERATURE, OZONE CONCENTRATION, WIND SPEED AND WIND DIRECTION DEVELOPED FROM TETHERSONDE DATA OBTAINED DURING THE MORNING OF JULY 20, 1995. Tethersonde readings were initiated at 0554, and the final balloon ascent began at 1005.

inversion was a remnant of the morning's nocturnal inversion. By 0857, the surface layer inversion has dissipated and the mixing height had increased to 270 m. An elevated potential temperature inversion was present between 300-500 m, but it quickly became indistinguishable from the surface mixed layer. By 1005, the potential temperature profile was near vertical and atmospheric mixing exceeded measurement height. The height of the daytime mixed layer was well above the operating height of the Tethersonde system. As characterized by the morning profiles, ozone concentrations remained quite low (or near zero) until the early morning breakup of the nocturnal inversion. As the surface-based inversion disappeared, ozone levels climbed continuously and uniformly through the mixed layer. The concentrations eventually became uniform throughout the mixed layer. This uniform concentration was essentially that of the undisturbed elevated layer. The ozone concentrations at ground level began to rise as ozone aloft became entrained in the atmospheric mixing.

Measurements for the afternoon-evening profiles (Figure 4.19) began at 1405 and finished at 2308. Based on initial measurements, the vertical potential temperature profiles were indicative of thorough mixing. During the 1653 measurements, the presence of an ozone reservoir with a concentration of almost 170 ppb was detected at 606 m. The wind direction was from the west, west northwest, off the Cumberland Mountains. This was the highest ozone concentration detected during the study. Coincidentally, it was detected on the same day as the summer's highest concentration recorded by regional ground-level monitoring stations. On July 20, the Nances Grove recorded an hourly average ozone concentration of 132 ppb. Nances Grove is a low-

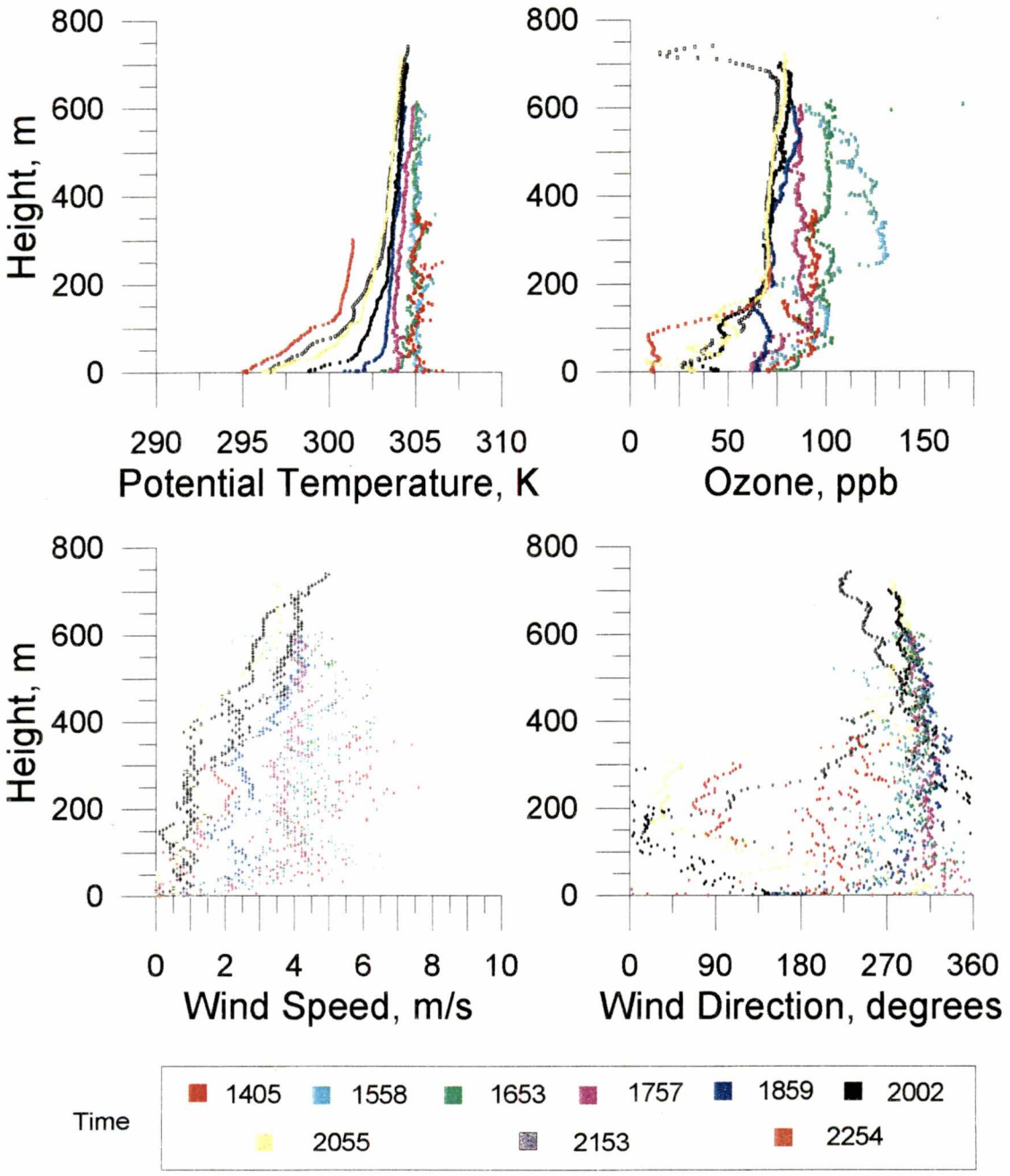

FIGURE 4.19. PROFILES OF POTENTIAL TEMPERATURE, OZONE CONCENTRATION, WIND SPEED AND WIND DIRECTION DEVELOPED FROM TETHERSONDE DATA OBTAINED DURING THE AFTERNOON-EVENING OF JULY 20, 1995. Tethersonde readings were initiated at 1405, and the final balloon ascent began at 2254.

elevation station located approximately 40 km northeast of Knoxville, Tennessee. By 1859, a potential temperature inversion began to form at the ground. Thus, atmospheric mixing between the surface and upper atmosphere stopped. At the ground, ozone concentrations quickly decreased to small values. The exception was a shallow layer at the surface which had elevated levels. This surface-based elevated concentration was attributed to drainage flow from the surrounding valley ridges. Surface ozone values tend to equal that at the ridge tops. Based on later evening measurements, ozone concentrations at ground level decreased whereas concentrations above the developing nocturnal inversion remained comparatively high.

Tethersonde measurements obtained at 526 m in the morning typically were similar to concentrations at Look Rock. Exceptions occurred when Tethersonde measurements encountered the Bull Run Steam Plant plume. Afternoon-evening measurements were slightly below values recorded at Look Rock (Figure 4.20A). Measurements obtained at the surface in Oak Ridge corresponded closely with concentrations recorded at Freels Bend during the early morning evening. Measurements between 1000 and 1800 were significantly below (30-40 ppb) Freels Bend concentrations (Figure 4.20B).

In comparing the regional ozone monitoring stations (Figure 4.21), ozone concentrations at the high-elevation stations showed less diurnal variation than low-elevatin stations. However, evening concentrations were higher than morning concentrations. The peak concentrations for Cove Mountain and Look Rock were 111 and 120 ppb, respectively. Those concentrations were recorded at 2100-2300 and 1900.

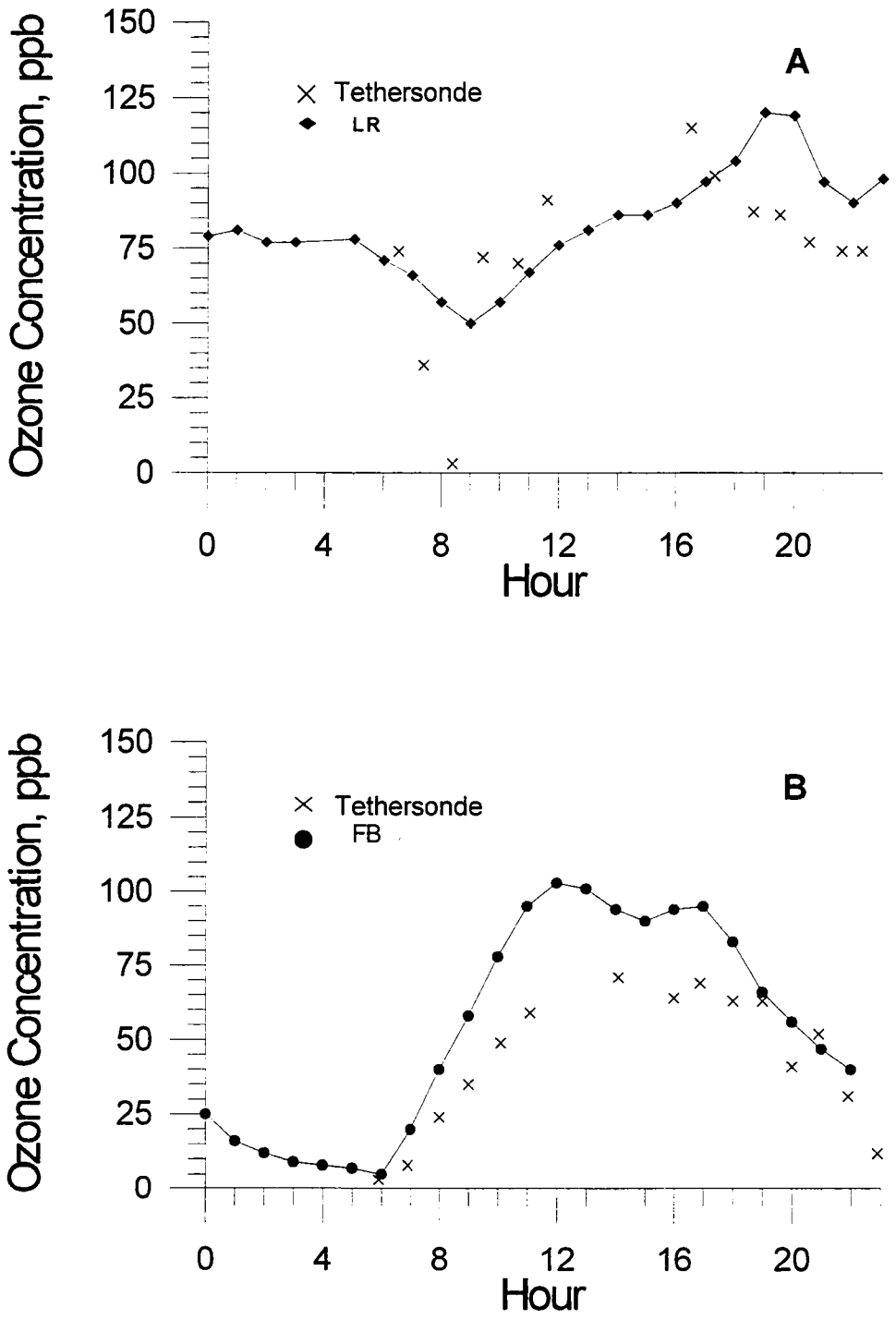

FIGURE 4.20. COMPARISON OF HOURLY MEAN OZONE CONCENTRATIONS ON JULY 20, 1995 OBTAINED FROM LOOK ROCK AND FREELS BEND REGIONAL MONITORING STATIONS WITH READING OBTAINED AT OAK RIDGE WITH TETHERSONDE INSTRUMENTATION. A) Look Rock and B) Freels Bend.

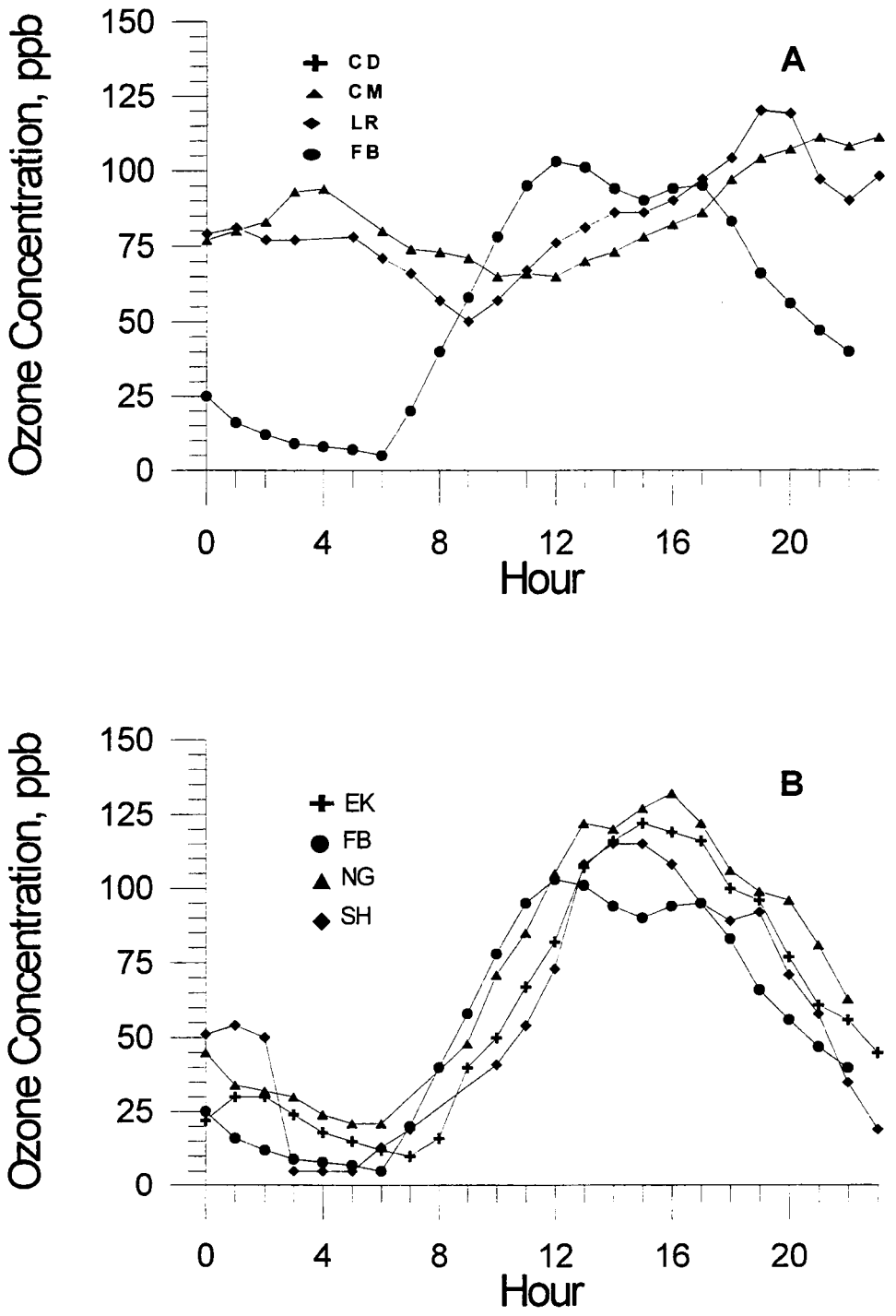

FIGURE 4.21. HOURLY MEAN OZONE CONCENTRATIONS OBTAINED FROM REGIONAL MONITORING STATIONS ON JULY 20, 1995. A. High elevation stations (located above 793m MSL) [Clingmans Dome (CD), Cove Mountain (CM), and Look Rock (LR)] and Freels Bend (elevation 247m MSL). B. Low elevation stations (below 343 m MSL)[East Knox (EK), Freels Bend (FB), Nances Grove (NG) and Spring Hill (SH)].

Clingmans Dome was not operational on July 8. Ozone concentrations for the low-elevation stations were similar. The peak concentrations for East Knox, Freels Bend, Nances Grove and Spring Hill were 122, 103, 132, and 115 ppb, respectively. Those concentrations were recorded at 1500, 1200, 1600, and 1400-1500, respectively. Of special note was the 132 ppb concentration at Nances Grove. As previously mentioned, this was the highest concentration recorded at the regional monitoring stations during 1995. One final point to note, Tethersonde measurements conducted at 0554 recorded ozone concentrations in excess of 90 ppb above 650 m. In addition, at 1653 concentrations of 169 ppb and 133 ppb were detected at approximately 600 m coming from the west.

July 30, 1995 Sunday

On July 30, the minimum and maximum temperatures at ground-level were 20.9°C and 37.6°C, respectively. The minimum temperature occurred at 0612 and the maximum temperature happened at 1401. Wind speeds averaged 0.2 m/s in the early morning, increased to 2.0 m/s at 1800, and diminished to 0.7 m/s at 2200. Maximum wind speed, 9.4 m/s, occurred at approximately 1800. The skies were clear throughout the morning and afternoon. Severe thunderstorms struck throughout Anderson County beginning near 1900. Sunrise occurred at 0542 and sunset at 1942. Although measurements were taken during both morning and afternoon-evening, evening measurements were stopped at 1917 because of nearby lightening.

The morning measurements began at 0559 (17 minutes after sunrise) and concluded at 1132. Profiles of potential temperature, ozone concentration, wind speed,

and wind direction are presented in Figure 4.22. A strong, ground-based inversion extended upward to approximately 400 m during the 0559-0647 measurements. Although the inversion remained during the 0656-0746 measurements, erosion at the bottom of the inversion began and the associated mixing height was estimated to be 100 m. By the 0758-0845 measurements, the mixing height had increased to 370 m. By the 0856-0936 measurements, the surface-based inversion had been destroyed and the mixing height was estimated to be 470 m at 0920. By 0953, the mixing height exceeded measurement heights for the 0953 and 1055 profiles. Based on profiles of ozone concentrations throughout the morning, vertical transport of ozone to the surface by entrainment from reservoirs aloft was important. Surface concentrations which were less than 5 ppb at 0559 increased with increasing mixing heights throughout the morning. By 0953, both potential temperatures and ozone concentrations were essentially vertical below 800 m AGL. Of special interest was the depletion of ozone during the early morning measurements. Winds were primarily from the southwest. Thus, depletion most probably resulted from encountering the Kingston steam plant plume. By 0953, there was adequate shift in wind directions to eliminate power plant influence.

The afternoon-evening measurements began at 1659 and concluded at 1917 (15 minutes prior to sunset). Profiles of potential temperature, ozone concentration, wind speed, and wind direction are presented in Figure 4.23. At 1659, the potential temperature profile was essentially vertical with temperatures near 305 °K. Although variable, winds were from the SSE. Of special note was the ozone concentration profile. Concentrations at the surface were significantly lower than concentrations above.

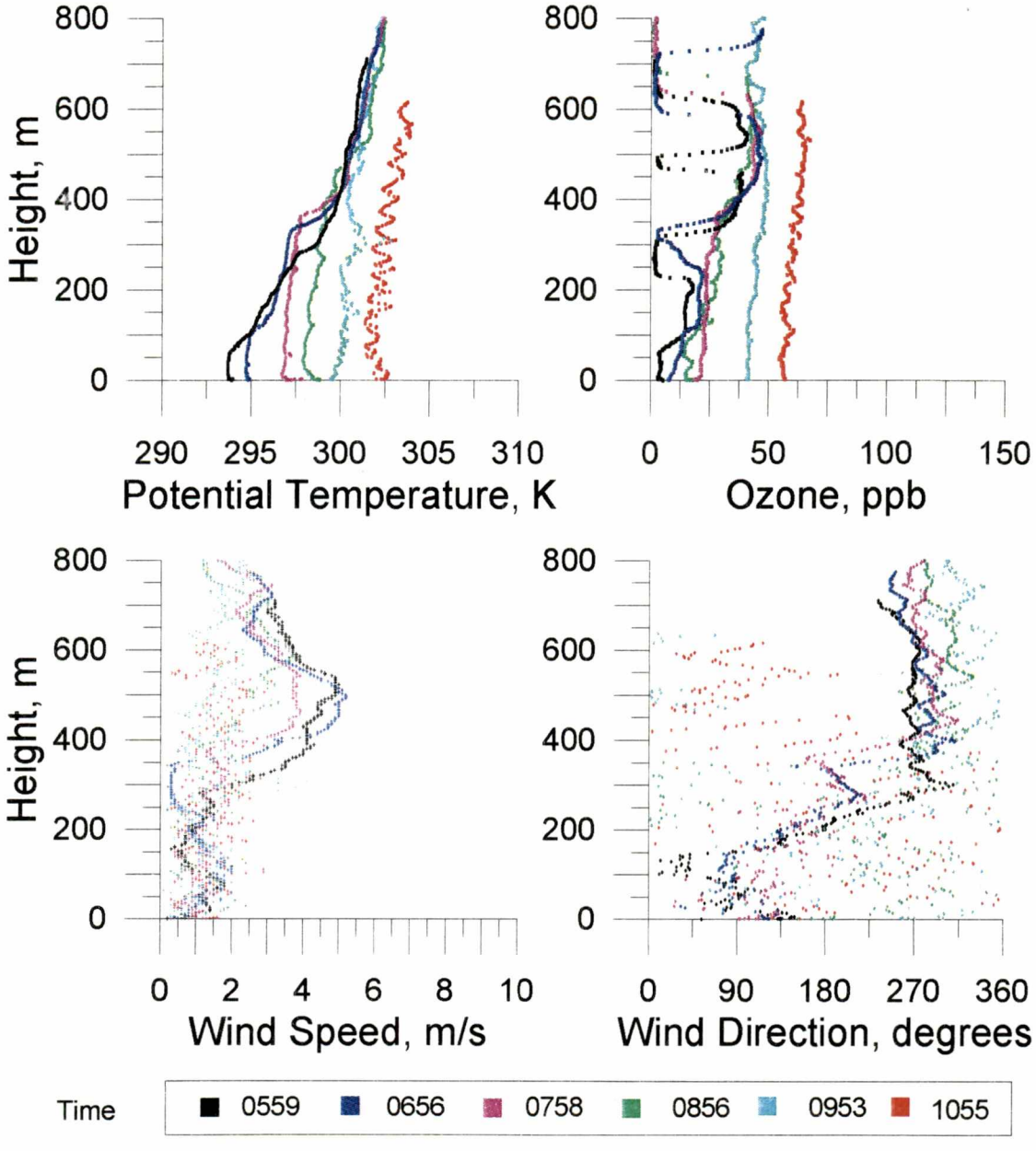

FIGURE 4.22. PROFILES OF POTENTIAL TEMPERATURE, OZONE CONCENTRATION, WIND SPEED AND WIND DIRECTION DEVELOPED FROM TETHERSONDE DATA OBTAINED DURING THE MORNING OF JULY 30, 1995. Tethersonde readings were initiated at 0559, and the final balloon ascent began at 1055.

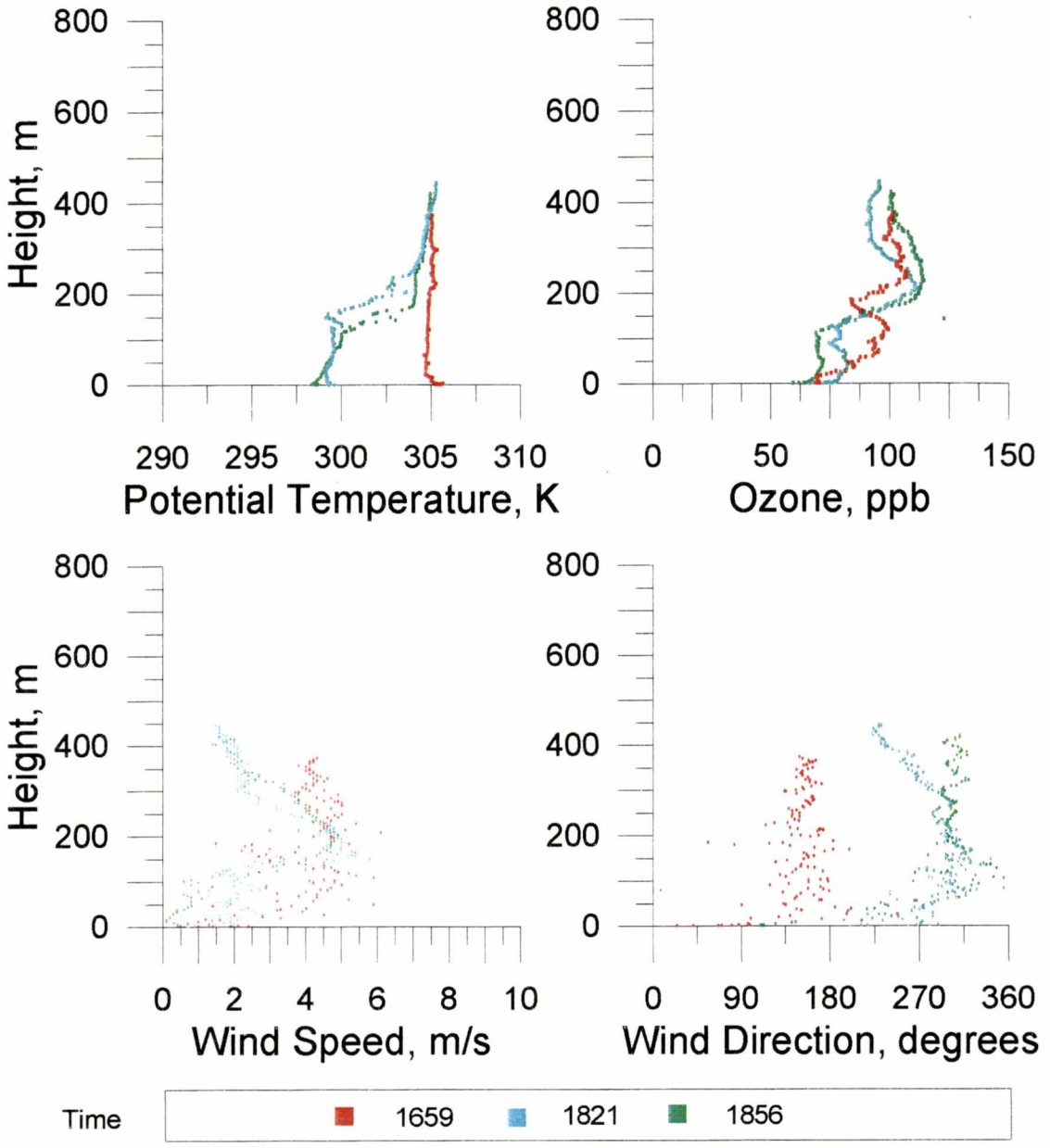

FIGURE 4.23. PROFILES OF POTENTIAL TEMPERATURE, OZONE CONCENTRATION, WIND SPEED AND WIND DIRECTION DEVELOPED FROM TETHERSONDE DATA OBTAINED DURING THE AFTERNOON-EVENING OF JULY 30, 1995. Tethersonde readings were initiated at 1659, and the final balloon ascent began at 1821.

Subsequent profiles at 1821-1849 and 1856-1917 were typical of those found during development of the stable boundary layer (nocturnal inversion). Therefore, atmospheric mixing between the surface and above had ceased by 1821, and the thermal mixing height was nonexistent. As the temperature inversion formed, wind speeds near the surface declined, wind directional variability decreased and winds shifted to the NW. Of special significance was the continued decrease of ozone concentrations at the surface and the continued presence of high concentrations in the residual layer. During the 1856 profile, surface concentrations were 65 ppb compared to concentrations in excess of 100 ppb above 140 m (the highest recorded concentration was 123 ppb at 143 m).

Tethersonde measurements were compared with concentrations at Look Rock and Freels Bend (Figure 4.24). Morning Tethersonde measurements at 526 m were similar to concentrations recorded at Look Rock (Figure 4.24A). Afternoon-evening measurements did not reach the height of Look Rock, and therefore, no comparison was made. Surface measurements in Oak Ridge were similar to concentrations at Freels Bend during both the morning and afternoon-evening (Figure 4.24B).

In comparing the regional ozone monitoring stations (Figure 4.25), ozone concentrations at the high-elevation stations showed little diurnal variation. The peak concentrations for Clingmans Dome, Cove Mountain, and Look Rock were 45, 62, and 56 ppb, respectively. Interestingly, the peak concentration for Clingmans Dome occurred at 0300. Peak concentrations at Cove Mountain and Look Rock occurred at 1800 and 1600-1700, respectively. The peak concentration for low-elevation stations occurred at Freels Bend when concentrations of 113 ppb were logged at 1500. Peak concentrations at

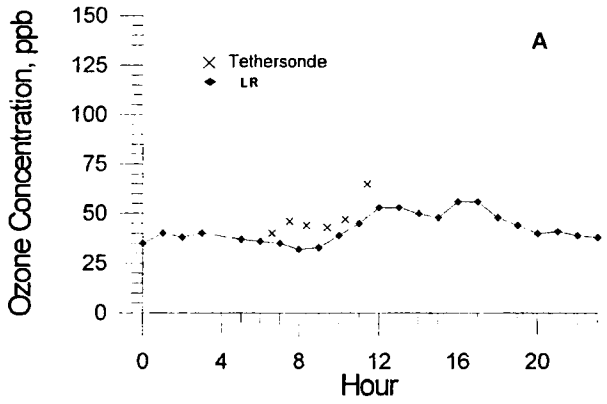

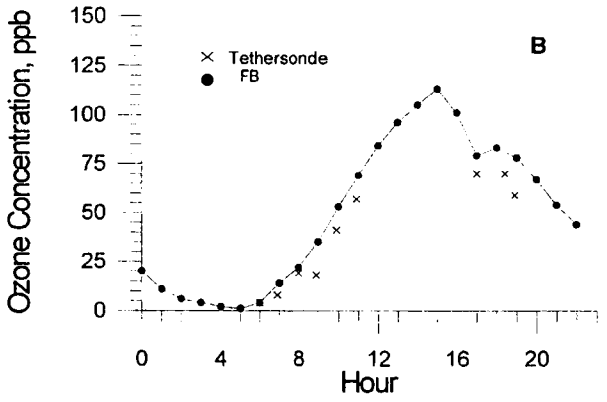

FIGURE 4.24. COMPARISON OF HOURLY MEAN OZONE CONCENTRATIONS ON JULY 30, 1995 OBTAINED FROM LOOK ROCK AND FREELS BEND REGIONAL MONITORING STATIONS WITH READING OBTAINED AT OAK RIDGE WITH TETHERSONDE INSTRUMENTATION. A) Look Rock and B) Freels Bend.

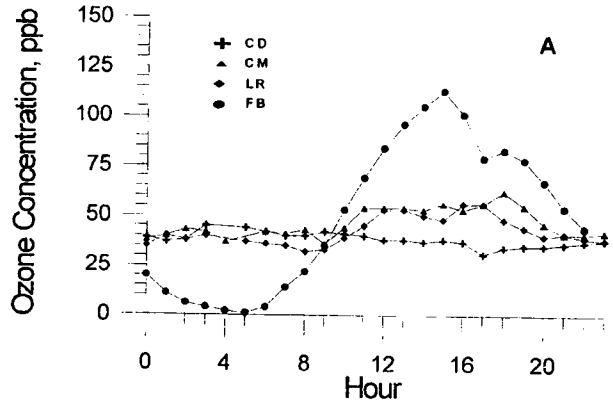

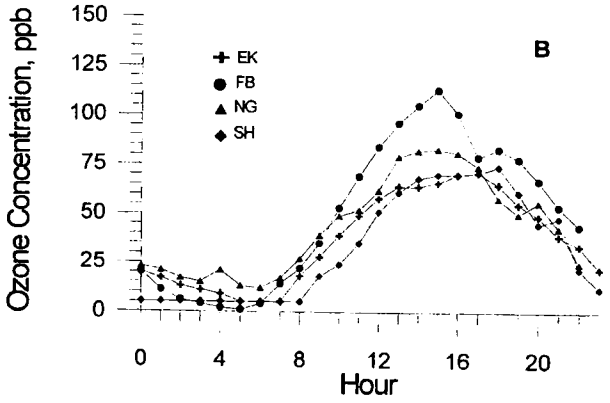

FIGURE 4.25. HOURLY MEAN OZONE CONCENTRATIONS OBTAINED FROM REGIONAL MONITORING STATIONS ON JULY 30, 1995. A. High elevation stations (located above 793m MSL) [Clingmans Dome (CD), Cove Mountain (CM), and Look Rock (LR)] and Freels Bend (elevation 247m MSL). B. Low elevation stations (below 343 m MSL)[East Knox (EK), Freels Bend (FB), Nances Grove (NG) and Spring Hill (SH)].

other low-elevation stations were significantly lower. East Knox, Nances Grove and Spring Hill peak concentrations were 71, 83, and 74 ppb, respectively. Those concentrations were recorded at 1700, 1500, and 1800. Although concentrations at Nances Grove exceeded those of other low-elevation stations thoughout the early morning, concentrations at Freels Bend were higher beginning at 1000 and remained higher throughout the day. Early morning Tethersonde measurements were typically less than 50 ppb ozone throughout the profiles. Surface concentrations recorded throughout the day greatly exceeded concentrations aloft in the early morning. It was difficult to determine plume impacts on the early morning concentrations aloft. Therefore, some uncertainty remained as to whether high afternoon concentrations at Freels Bend resulted from entrainment or photochemical production during this day.

JULY 31, 1995 Monday

On July 31, the minimum and maximum temperatures at ground-level were 20.4°C and 37.5°C, respectively. The minimum temperature occurred at 0607 and the maximum temperature at 1527. Wind speeds averaged 0.3 m/s in the early morning, increased to 2.9 m/s at 1800, and diminished to 0.9 m/s at 0000. Maximum wind speed, 14.7 m/s, occurred at approximately 1800. Although the skies were clear throughout the day; a powerful thunderstorm occurred in the evening. The storm began approximately 1815. Between 1815 and 2200, 17.3 mm rain fell. Sunrise occurred at 0542 and sunset at 1941. Because of storm activity, only morning measurements were taken.

Measurements began at 0604 (22 minutes after sunrise) and concluded at 1434. Profiles of potential temperature, ozone concentration, wind speed, and wind direction are

presented in Figure 4.26. A strong, ground-based inversion extended upward to approximately 135 m during the 0604-0657 measurements. By the 0707-0751 measurements, the inversion began to erode and the mixing height was estimated to be near 90 m. By the 0804-0846 measurements, the surface-based inversion had dissipated and the mixing height was estimated to be 325 m. Subsequent measurements at 0856-0934, 1002-1039, 1056-1128, and 1358-1434 were interpreted to imply the mixing height exceded measurement height by 0856. Surface concentrations which were less than 5 ppb at 0604 increased with increasing mixing heights throughout the morning. By 1002, both potential temperatures and ozone concentrations were essentially vertical below 700 m. By 1358, ozone concentrations at the surface had increased to 65 ppb. Above 700 m, concentrations of ozone were 75-80 ppb. Similar to earlier findings, vertical transport of ozone to the surface by entrainment from upper reservoirs appeared to be the primary reason for increased surface concentrations.

In comparing Tethersonde measurements with data recorded at Look Rock, morning and early afternoon measurements slightly exceeded concentrations at Look Rock except at 0600-0700 when concentrations were essentially equal (Figure 4.27A). Surface concentrations in Oak Ridge were slightly lower than concentrations at Freels Bend throughout the day (Figure 4.27B).

In comparing regional ozone monitoring stations (Figure 4.28), ozone concentrations at the high-elevation stations showed little diurnal variation. The peak concentrations for Clingmans Dome, Cove Mountain, and Look Rock were 60, 63, and 54 ppb, respectively. The peak concentration at Clingmans Dome was recorded at 1900.

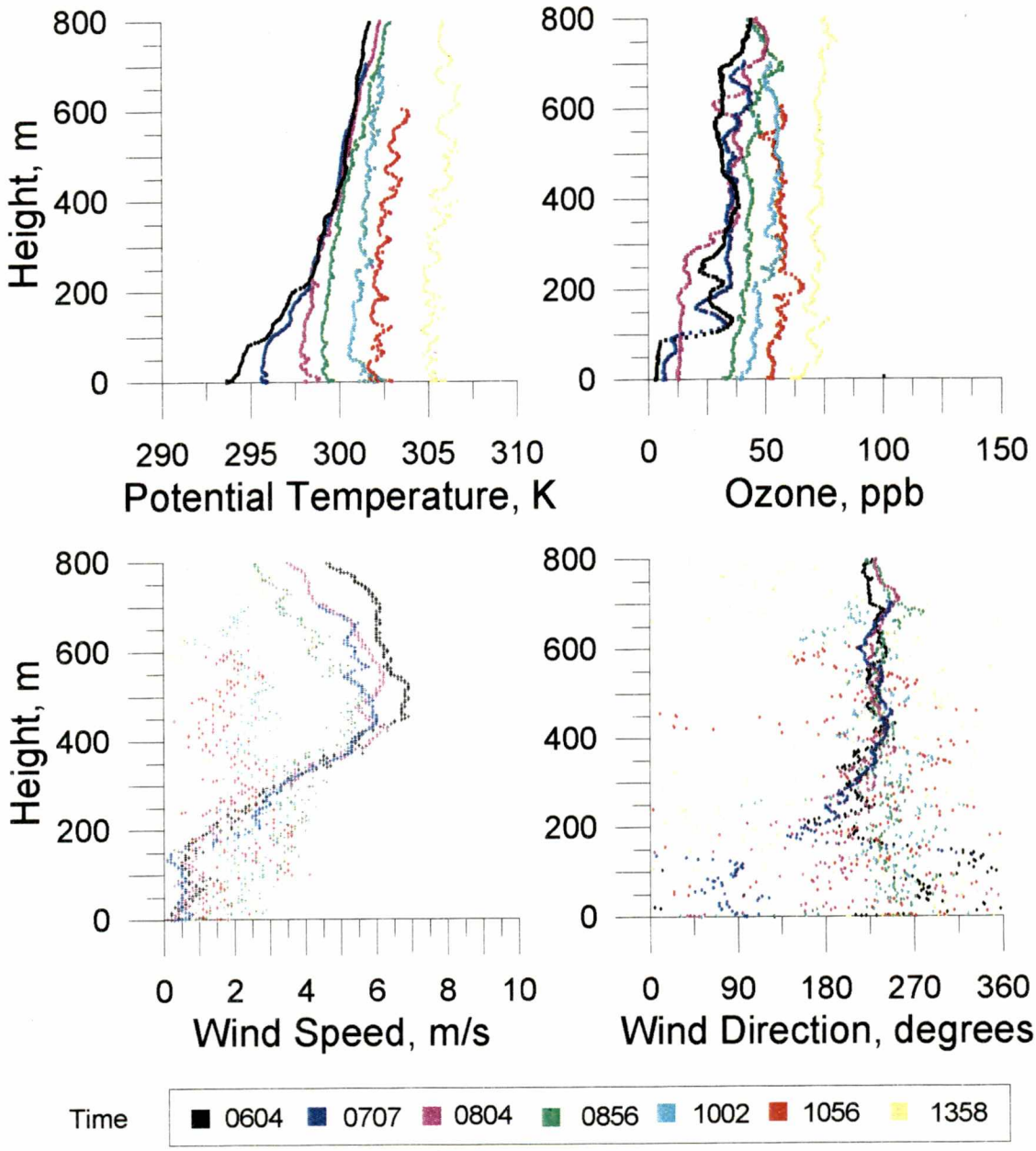

FIGURE 4.26. PROFILES OF POTENTIAL TEMPERATURE, OZONE CONCENTRATION, WIND SPEED AND WIND DIRECTION DEVELOPED FROM TETHERSONDE DATA OBTAINED DURING THE MORNING OF JULY 31, 1995. Tethersonde readings were initiated at 0604, and the final balloon ascent began at 1358.

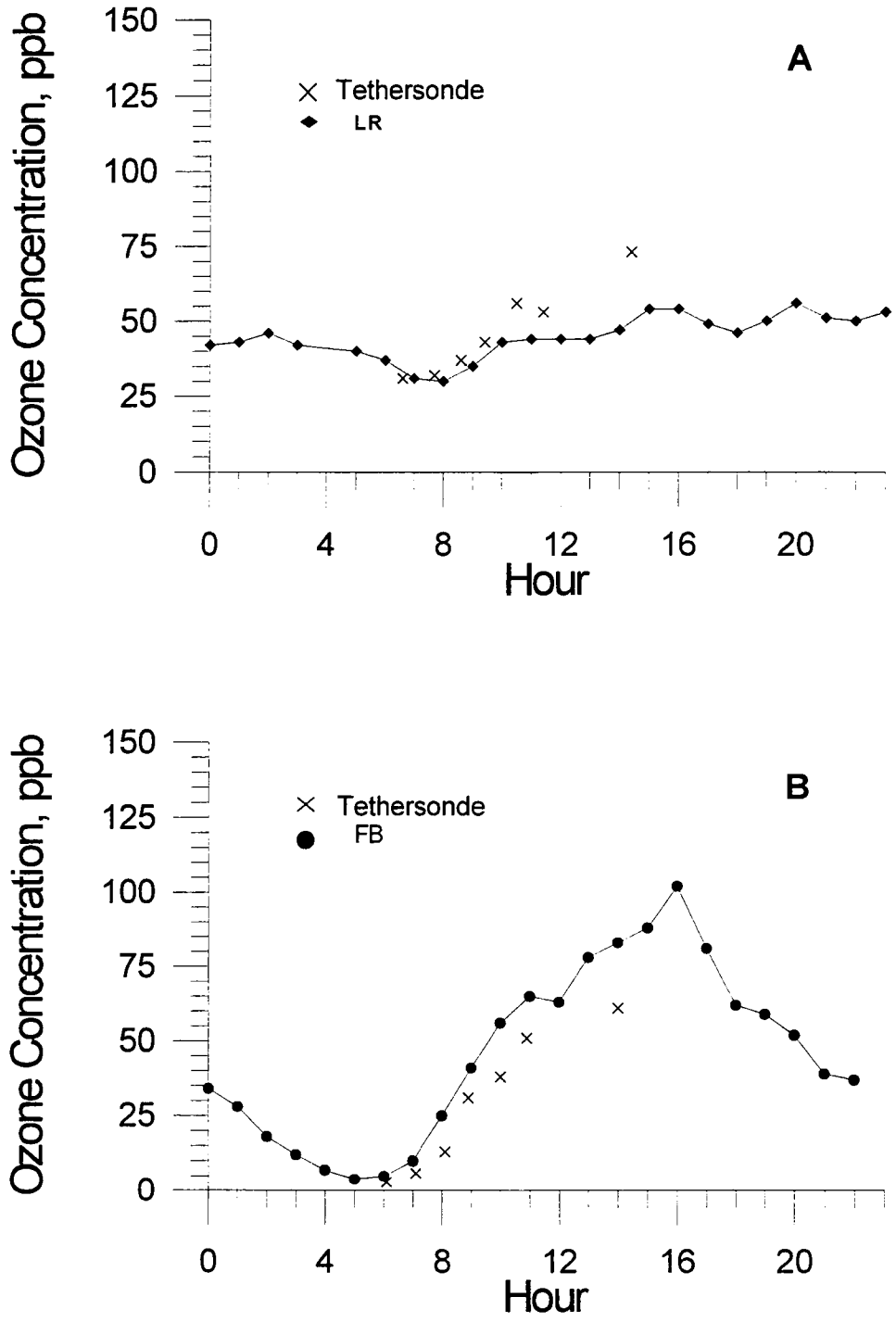

FIGURE 4.27. COMPARISON OF HOURLY MEAN OZONE CONCENTRATIONS ON JULY 31, 1995 OBTAINED FROM LOOK ROCK AND FREELS BEND REGIONAL MONITORING STATIONS WITH READING OBTAINED AT OAK RIDGE WITH TETHERSONDE INSTRUMENTATION. A) Look Rock and B) Freels Bend.

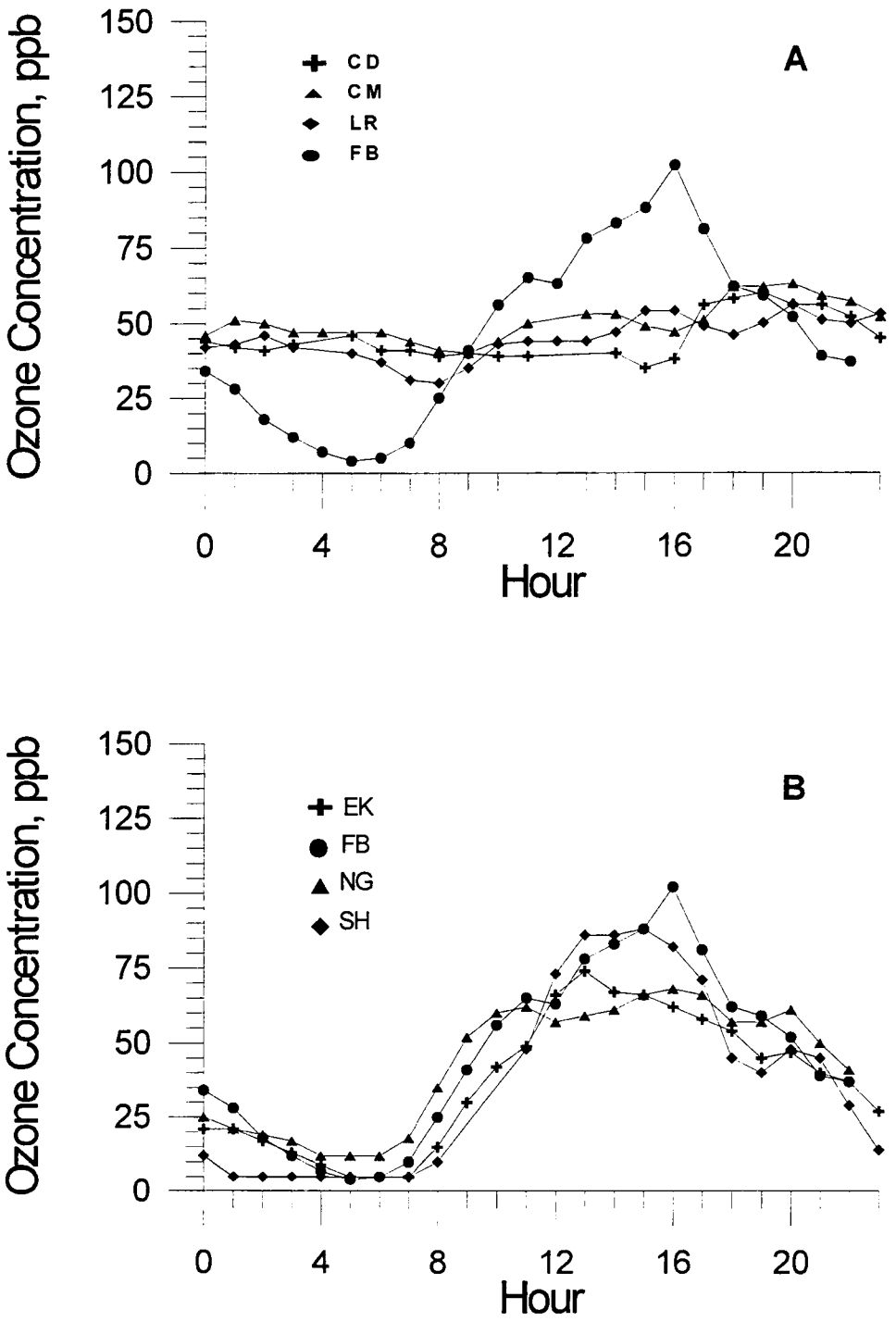

FIGURE 4.28. HOURLY MEAN OZONE CONCENTRATIONS OBTAINED FROM REGIONAL MONITORING STATIONS ON JULY 31, 1995. A. High elevation stations (located above 793m MSL) [Clingmans Dome (CD), Cove Mountain (CM), and Look Rock (LR)] and Freels Bend (elevation 247m MSL). B. Low elevation stations (below 343 m MSL)[East Knox (EK), Freels Bend (FB), Nances Grove (NG) and Spring Hill (SH)].

The highest concentration at Cove Mountain occurred at 2000. The peak concentration at Look Rock happened at 1500. Ozone concentrations for the low-elevation stations were similar. The peak concentrations for East Knox, Freels Bend, Nances Grove and Spring Hill were 74, 102, 68, and 88 ppb, respectively. Those concentrations were recorded at 1300, 1600, 1600, and 1500. Concentrations at Freels Bend exceeded those of other low-elevation stations most of the day. Tethersonde measurements conducted at 0604 recorded ozone concentrations exceeding 40 ppb above 725 m. The cause of high concentrations at Freels Bend (especially when compared to the other stations) was uncertain. The lateness of the day would favor photochemical production, but the location would suggest entrainment from a highly ozone-enriched reservoir aloft.

August 1, 1995 Tuesday

On August 1, the minimum and maximum temperatures at ground-level were 20.8°C and 35.3°C, respectively. The minimum temperature occurred at 0409 and the maximum temperature at 1359. Wind speeds averaged 0.3 m/s in the early morning, increased to 2.9 m/s at 1800, and diminished to 0.9 m/s at 0000. Maximum wind speed, 14.7 m/s, occurred at approximately 1800. The morning skies contained cloud remnants (scud) from thunderstorms the previous night. In addition, a ground-level fog was persistent at the NOAA laboratory. Sunrise occurred at 0543 and sunset at 1941. Measurements were conducted only during the morning. After measurements for the second profiles, sampling was cancelled because of mechanical problems with the winch.

Measurements began at 0557 (14 minutes after sunrise) and concluded at 0728. Profiles of potential temperature, ozone concentration, wind speed, and wind direction are

presented in Figure 4.29. A strong, ground-based inversion extended upward to approximately 210 m during the 0557-0641 measurements. There was no evidence of mixing. By the 0658-0728 measurements, the inversion began to erode and the mixing height was estimated to be near 135 m. During the first measurements, potential temperatures were constant below ridge-top height. Similarly, ozone concentrations were uniform in the same region. By the 0658-0728 measurements, potential temperatures below 130 m had increased. Ozone concentrations below 110 m increased and the profile between 100-135 m was vertical since air containing higher ozone concentrations became entrained.

Tethersonde measurements obtained at 526 m were similar to concentrations at Look Rock (Figure 4.30A). Surface concentrations in Oak Ridge were similar to concentrations at Freels Bend (Figure 4.30B).

Of the seven regional ozone monitoring stations (Figure 4.31), the highest concentrations were logged at Freels Bend. Concentrations at low-elevation stations exceeded concentrations at high-elevation stations. The peak concentration at Freels Bend was 88 ppb at 1300. Since Tethersonde measurements conducted at 0557 recorded ozone concentrations exceeding 60 ppb between 578 m and 729 m, entrainment from reservoirs aloft may have played a significant role in surface concentrations.

August 23, 1995 Wednesday

On August 23, the minimum and maximum temperatures at ground-level were 19.4°C and 34.9°C, respectively. The minimum temperature occurred at 0400 and the maximum temperature at 1430. Wind speeds averaged 1.5 m/s in the early morning,

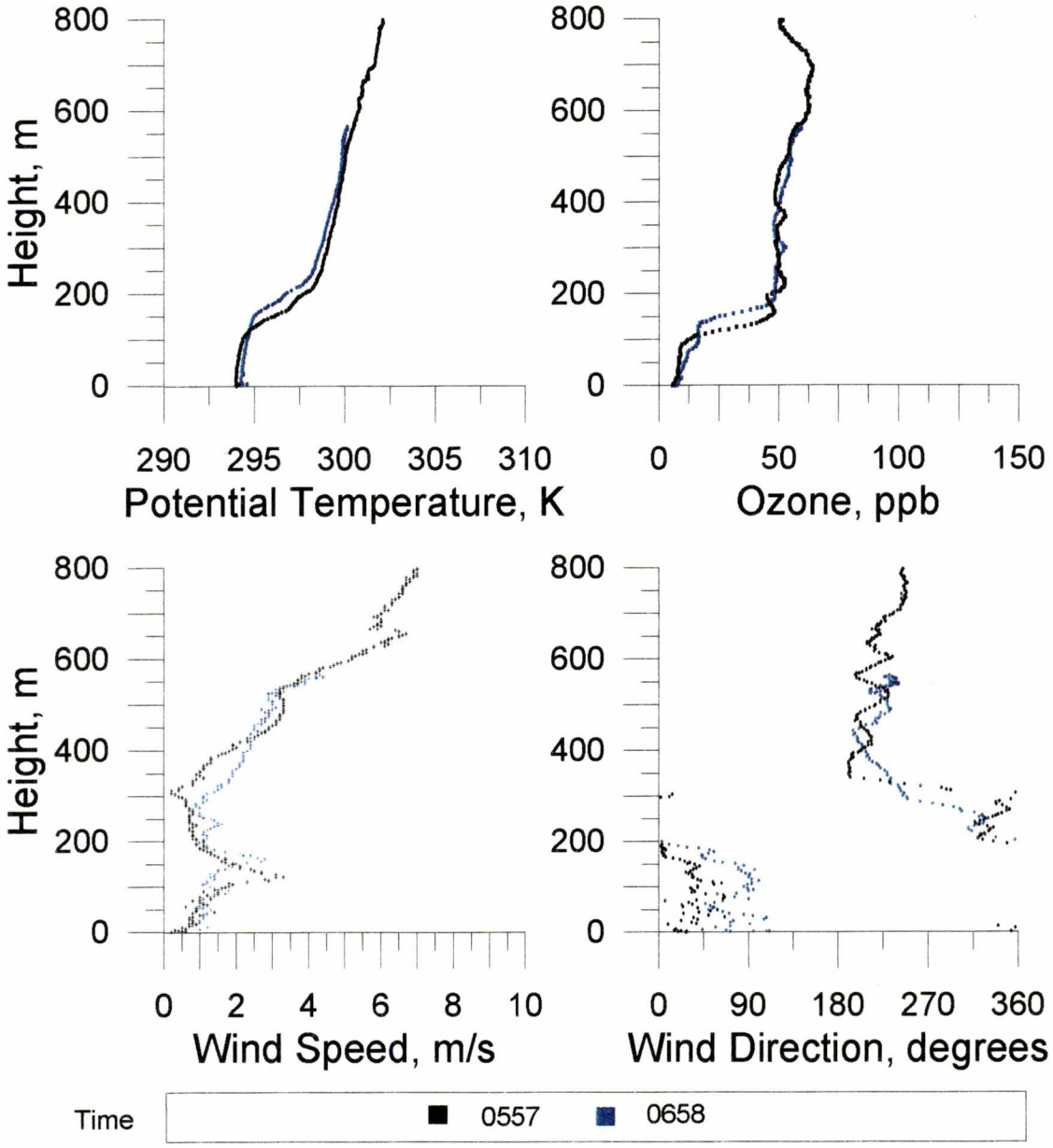

FIGURE 4.29. PROFILES OF POTENTIAL TEMPERATURE, OZONE CONCENTRATION, WIND SPEED AND WIND DIRECTION DEVELOPED FROM TETHERSONDE DATA OBTAINED DURING THE MORNING OF AUGUST 1, 1995. Tethersonde readings were initiated at 0557, and the final balloon ascent began at 0658.

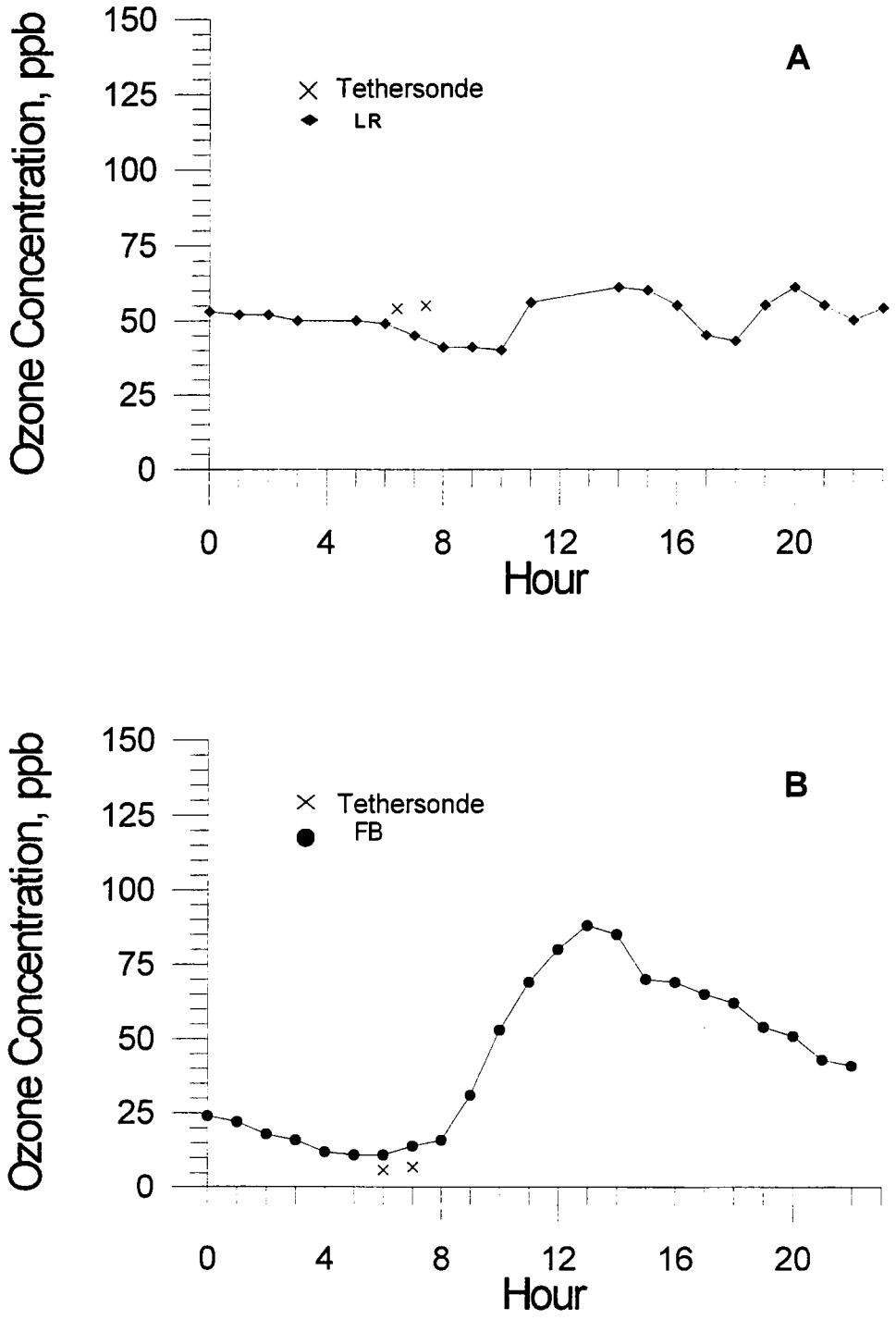

FIGURE 4.30. COMPARISON OF HOURLY MEAN OZONE CONCENTRATIONS ON AUGUST 1, 1995 OBTAINED FROM LOOK ROCK AND FREELS BEND REGIONAL MONITORING STATIONS WITH READING OBTAINED AT OAK RIDGE WITH TETHERSONDE INSTRUMENTATION. A) Look Rock and B) Freels Bend.

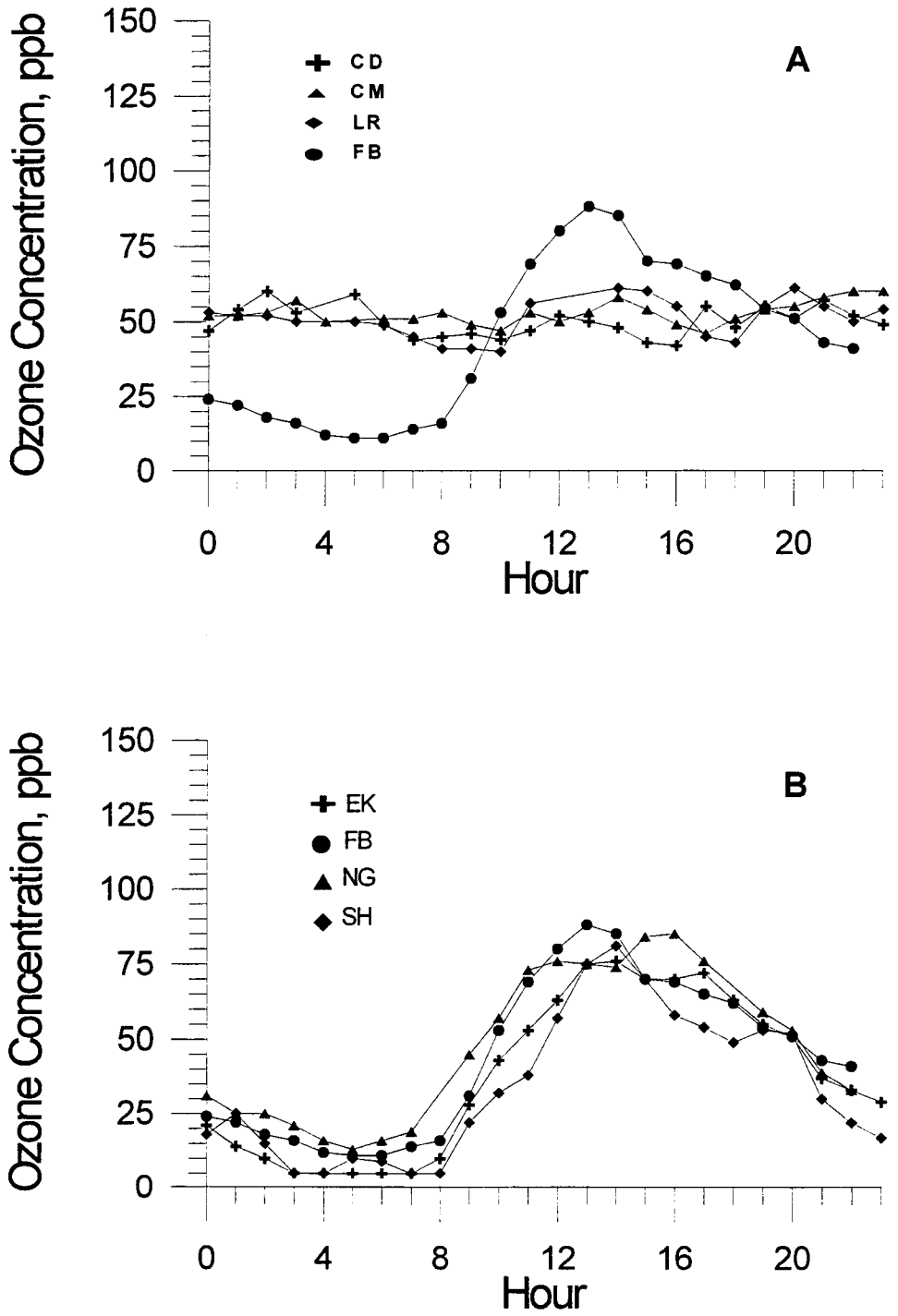

FIGURE 4.31. HOURLY MEAN OZONE CONCENTRATIONS OBTAINED FROM REGIONAL MONITORING STATIONS ON AUGUST 1, 1995. A. High elevation stations (located above 793m MSL) [Clingmans Dome (CD), Cove Mountain (CM), and Look Rock (LR)] and Freels Bend (elevation 247m MSL). B. Low elevation stations (below 343 m MSL)[East Knox (EK), Freels Bend (FB), Nances Grove (NG) and Spring Hill (SH)].

increased to 2.8 m/s at 1000, and diminished to 0.2 m/s by 2200. Maximum wind speed, 6.0 m/s, occurred at approximately 1000. The skies were clear throughout the night. There was no precipitation. Sunrise occurred at 0601 and sunset at 1915. Measurements were conducted only during the afternoon-evening.

The afternoon-evening measurements began at 1614 and concluded at 2315. Profiles of potential temperature, ozone concentration, wind speed, and wind direction are presented in Figure 4.32. At 1614, the potential temperature profile was essentially vertical with temperatures near 305°K. Although variable, winds were primarily from the N. The ozone concentration profile was also vertical with the exception of a region between the surface and 30 m. At the surface, concentrations were 60 ppb while 30 m concentrations were 70 ppb. This difference resulted from scavenging of ozone at the ground level. Subsequent profiles were typical of those found during development of the stable boundary layer (nocturnal inversion). As the temperature inversion began to form at 1853 (22 minutes prior to sunset), atmospheric mixing between the surface and aloft ceased. Thus, the mixing height reestablished near the surface, wind speeds near the surface declined, wind directional variability decreased, and winds were primarily from the northeast. Ozone concentrations at the surface decreased while concentrations in the residual layer remained high. By 1853, surface concentrations were below 60 ppb compared to concentrations above 90 ppb at 600 m. During the 1959 measurements, surface concentrations dropped to 30 ppb. However, concentrations between 550 m and 701 m ranged 100-110 ppb. By 2157, the temperature inversion was far more pronounced and ozone concentrations at the surface had dropped below 30 ppb.

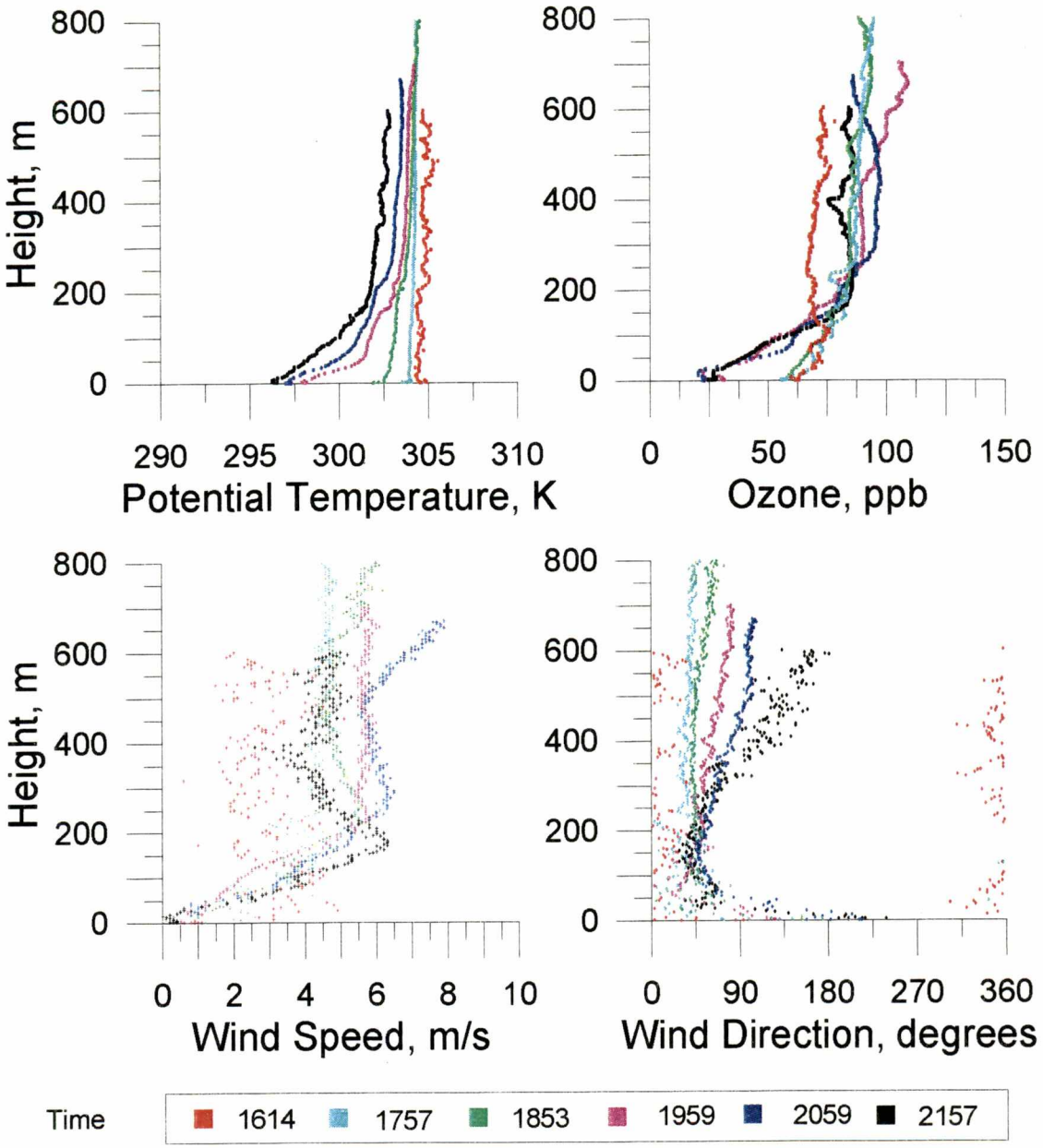

FIGURE. 4.32. PROFILES OF POTENTIAL TEMPERATURE, OZONE CONCENTRATION, WIND SPEED AND WIND DIRECTION DEVELOPED FROM TETHERSONDE DATA OBTAINED DURING THE AFTERNOON-EVENING OF AUGUST 23, 1995. Tethersonde readings were initiated at 1614, and the final balloon ascent began at 2157.

In general, Tethersonde measurements obtained at 526 m exceeded concentrations at Look Rock (Figure 4.33A). The 1638 measurement equaled concentrations at Look Rock. However, five subsequent Tethersonde measurements detected concentrations above Oak Ridge 15-30 ppb higher than concentrations at Look Rock. Ozone concentrations at the surface were similar to concentrations at Freels Bend (Figure 4.33B).

Of seven regional ozone monitoring stations (Figure 4.34), the highest concentrations were logged at East Knox. Peak concentrations at low-elevation stations exceeded concentrations at high-elevation stations. The day's peak concentration of 100 ppb occurred at East Knox at 1400. Freels Bend concentrations peaked at 93 ppb for a two hour period, 1300-1400. Thus, the difference between the urban-influenced East Knox station and the remote Freels Bend station was a mere 7 ppb. As previously mentioned, this difference occurred at midday when winds were primarily upvalley (from the southwest). Of special note was detection of an ozone-enriched reservoir aloft during the 1959 Tethersonde measurements. With winds from the east northeast and east, ozone concentrations exceeding 100 ppb were detected between 550 and 700 m.

August 24, 1995 Thursday

On August 24, the minimum and maximum temperatures at ground-level were 18.7°C and 35.1°C, respectively. The minimum temperature occurred at 0615 and the maximum temperature happened at 1430. Wind speeds averaged 0.2 m/s in the early morning, increased to 2.3 m/s at both 1000 and 1500, and diminished to 0.3 m/s by 0000. Maximum wind speed, 6.4 m/s, occurred at approximately 1500. The skies were clear

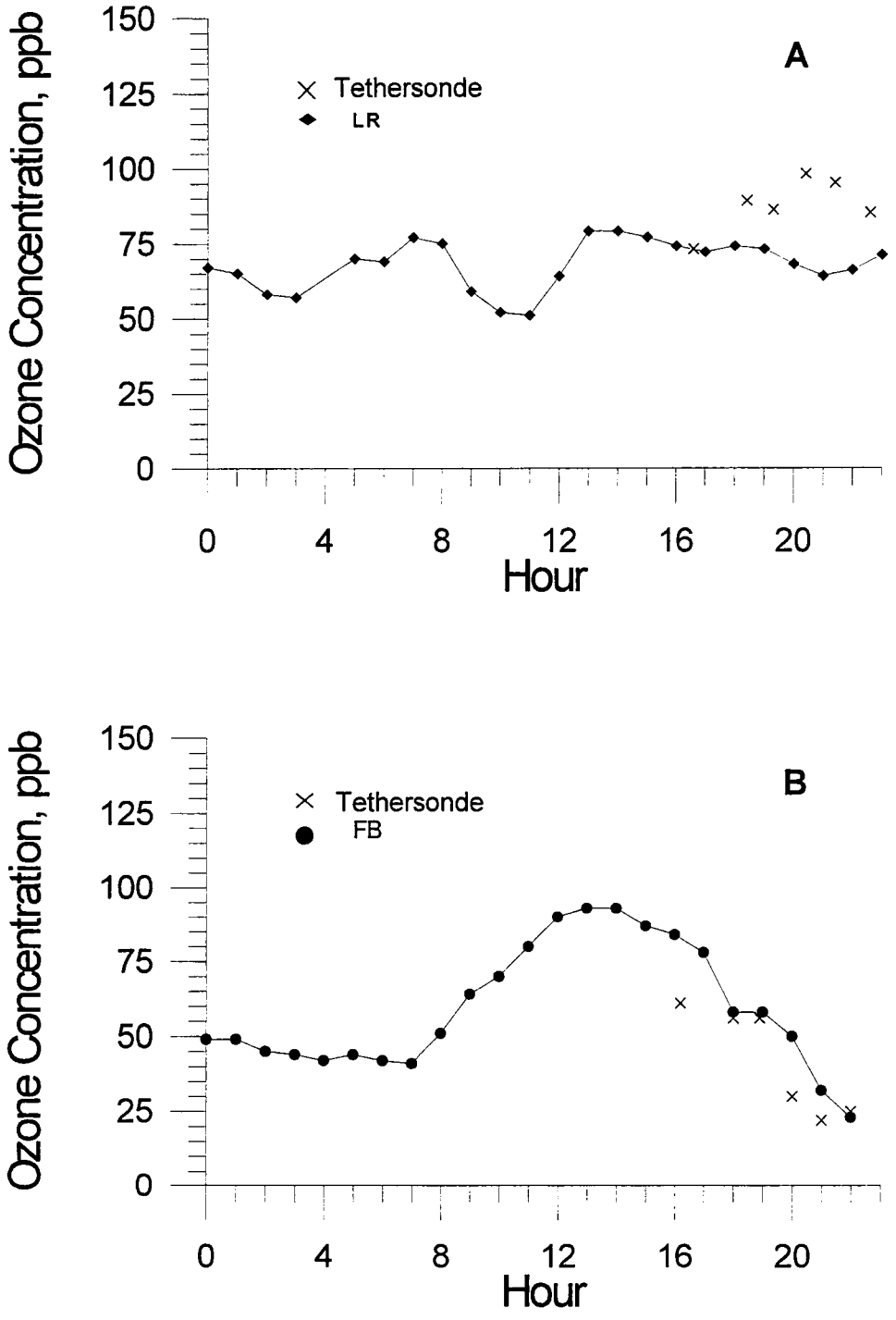

FIGURE 4.33. COMPARISON OF HOURLY MEAN OZONE CONCENTRATIONS ON AUGUST 23, 1995 OBTAINED FROM LOOK ROCK AND FREELS BEND REGIONAL MONITORING STATIONS WITH READING OBTAINED AT OAK RIDGE WITH TETHERSONDE INSTRUMENTATION. A) Look Rock and B) Freels Bend.

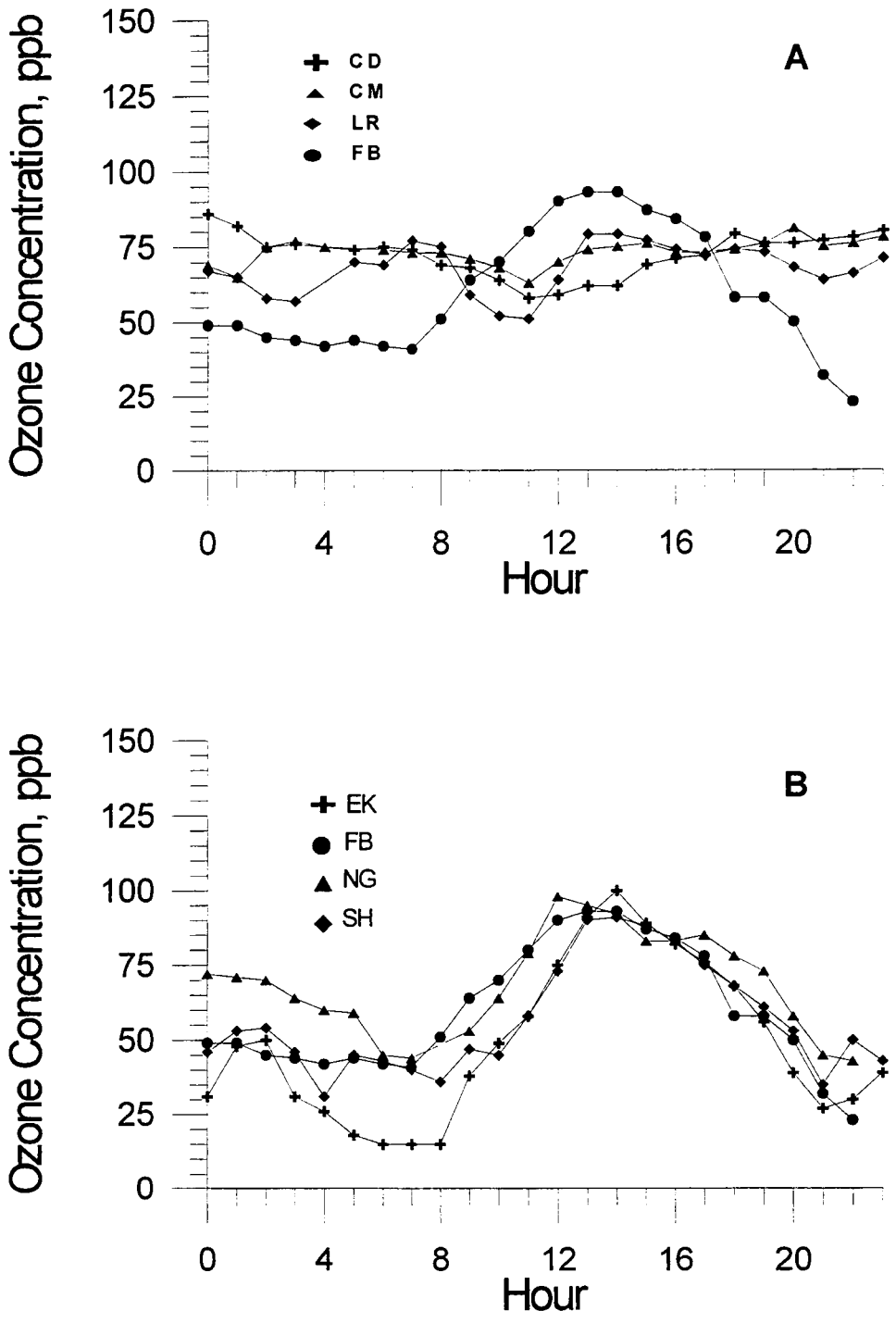

FIGURE 4.34. HOURLY MEAN OZONE CONCENTRATIONS OBTAINED FROM REGIONAL MONITORING STATIONS ON AUGUST 23, 1995. A. High elevation stations (located above 793m MSL) [Clingmans Dome (CD), Cove Mountain (CM), and Look Rock (LR)] and Freels Bend (elevation 247m MSL). B. Low elevation stations (below 343 m MSL)[East Knox (EK), Freels Bend (FB), Nances Grove (NG) and Spring Hill (SH)].

throughout the day. During the early evening, clouds covered the sky beginning at 1945. By 2100, skies cleared with the exception of two small clouds. One hour later, skies were completely clear and remained so the rest of the night. There was no precipitation. Sunrise occurred at 0601 and sunset at 1915. Measurements were conducted only during the afternoon-evening.

The afternoon-evening measurements began at 1831 and concluded at 2327. Profiles of potential temperature, ozone concentration, wind speed, and wind direction are presented in Figure 4.35. The measurements were very similar to those made the preceeding evening. By 1831 (44 minutes prior to sunset), formation of the potential temperature inversion began as a result of the earth's cooling. Thus, atmospheric mixing between the surface and upper atmosphere stopped. Ozone concentrations at the surface were lower than concentrations aloft as the result of scavenging. Wind speeds at the surface slowed and wind directional variability was minimal. Subsequent profiles were typical of those found during further development of the stable boundary layer (nocturnal inversion). Of special interest were ozone concentrations noted during the 1959-2024 measurements. Surface concentrations were about 40 ppb, but concentrations above 685 m exceeded 100 ppb. These high concentrations were transported by winds from the east northeast. By 2259, the temperature inversion had further developed, ozone concentrations at the surface had decreased to 20 ppb, and surface wind speeds were minimal. The changes in wind directions noted during the final measurements for the evening warrant attention. Below 200 m, winds were primarily from the northeast-east. Above 350 m, winds were from the south-west. Between 200-350 m, a directional

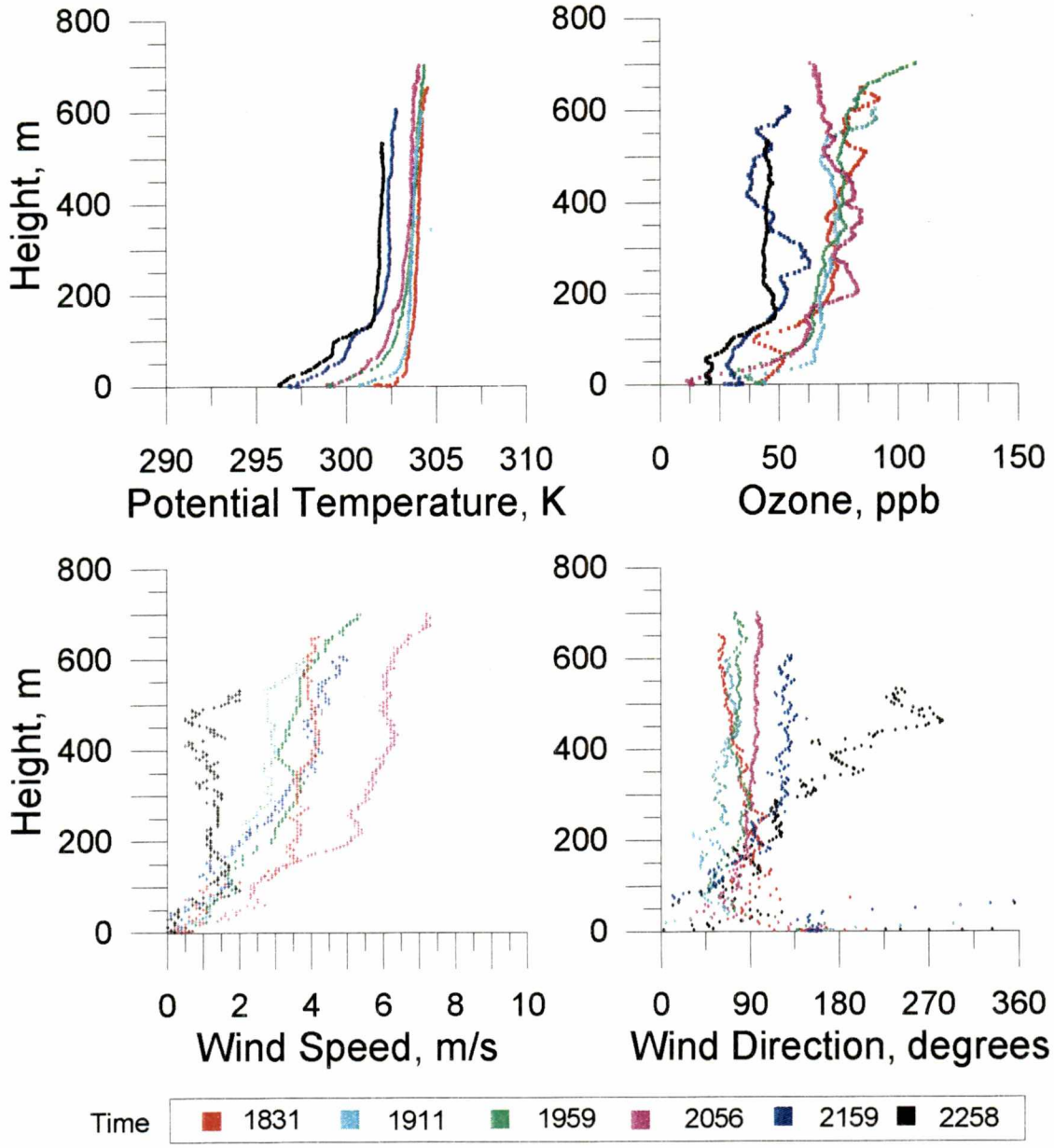

FIGURE 4.35. PROFILES OF POTENTIAL TEMPERATURE, OZONE CONCENTRATION, WIND SPEED AND WIND DIRECTION DEVELOPED FROM TETHERSONDE DATA OBTAINED DURING THE AFTERNOON-EVENING OF AUGUST 24, 1995. Tethersonde readings were initiated at 1831, and the final balloon ascent began at 2258.

transition occurred. This provided additional evidence for the presence of separate atmospheric layers.

Evening Tethersonde measurements at 526 m exceeded Look Rock concentrations by 15-25 ppb throughout the night. Ozone concentrations at the surface tended to equal concentrations at Freels Bend (Figure 4.36).

In comparing regional monitoring stations (Figure 4.37), Freels Bend was the site for the highest concentrations with a maximum 93 ppb occurring at 1300. East Knox, Nances Grove, and Spring Hill concentrations peaked at 81, 81, and 79 ppb, respectively. Thus, concentrations at Freels Bend exceeded all urban-influenced stations. Of special note for the high-elevation stations, concentrations at Clingmans Dome, Cove Mountain, and Look Rock peaked near midnight (0000-0100) with concentrations approximately 80 ppb. Ozone levels steadily decreased throughout the day and evening until reaching about 30 ppb at 2300.

August 29, 1995 Tuesday

On August 29, the minimum and maximum temperatures at ground-level were 18.9°C and 36.9°C, respectively. The minimum temperature occurred at 0630 and the maximum temperature at 1415. Wind speeds averaged 0.2 m/s in the early morning, increased to 2.1 m/s at 1600, and diminished to 0.2 m/s by 2200. Maximum wind speed, 6.0 m/s, occurred at approximately 1500. The skies were clear throughout the day and evening. There was no precipitation. Sunrise occurred at 0605 and sunset at 1908. Measurements were conducted only during the afternoon-evening.

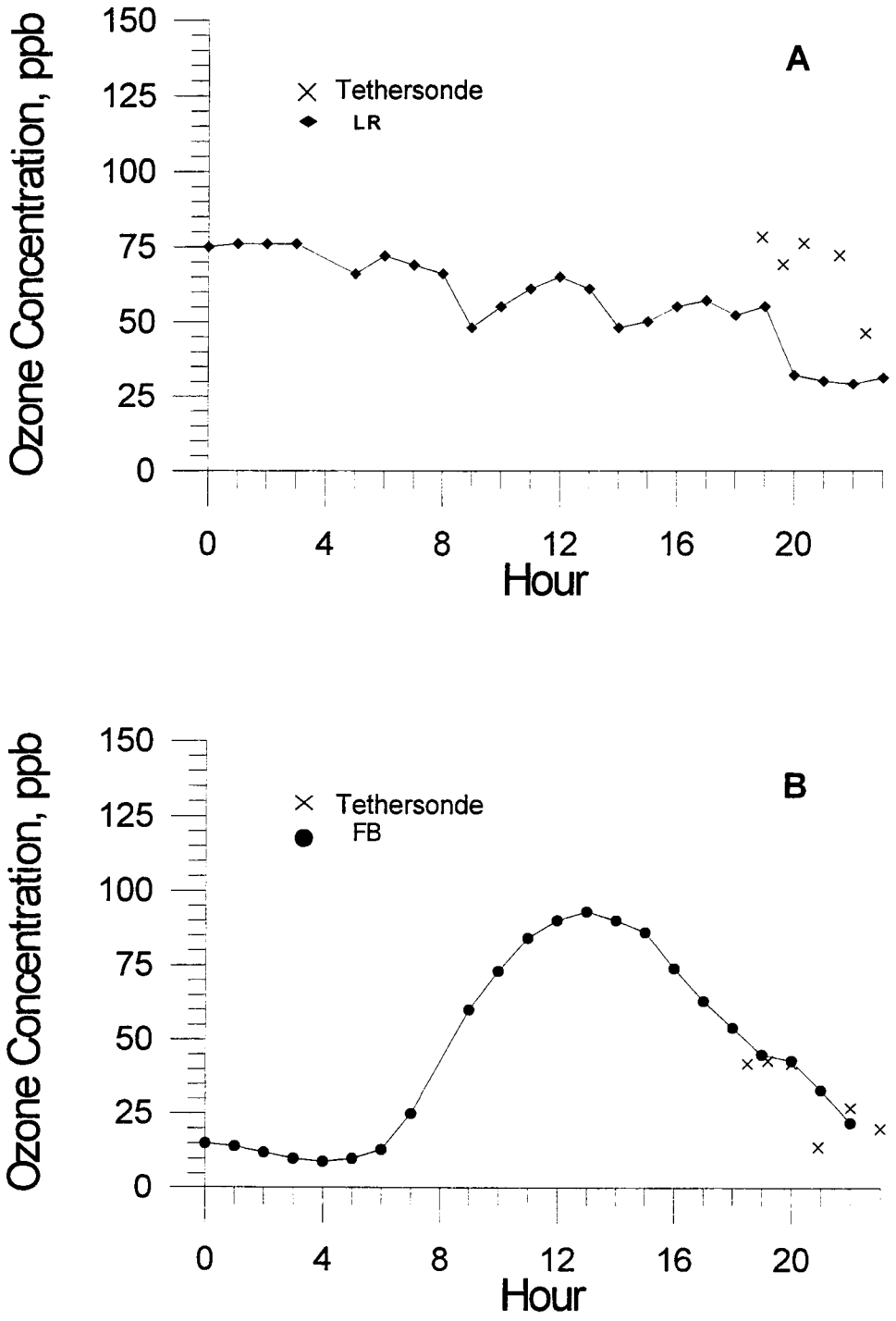

FIGURE 4.36. COMPARISON OF HOURLY MEAN OZONE CONCENTRATIONS ON AUGUST 24, 1995 OBTAINED FROM LOOK ROCK AND FREELS BEND REGIONAL MONITORING STATIONS WITH READING OBTAINED AT OAK RIDGE WITH TETHERSONDE INSTRUMENTATION. A) Look Rock and B) Freels Bend.

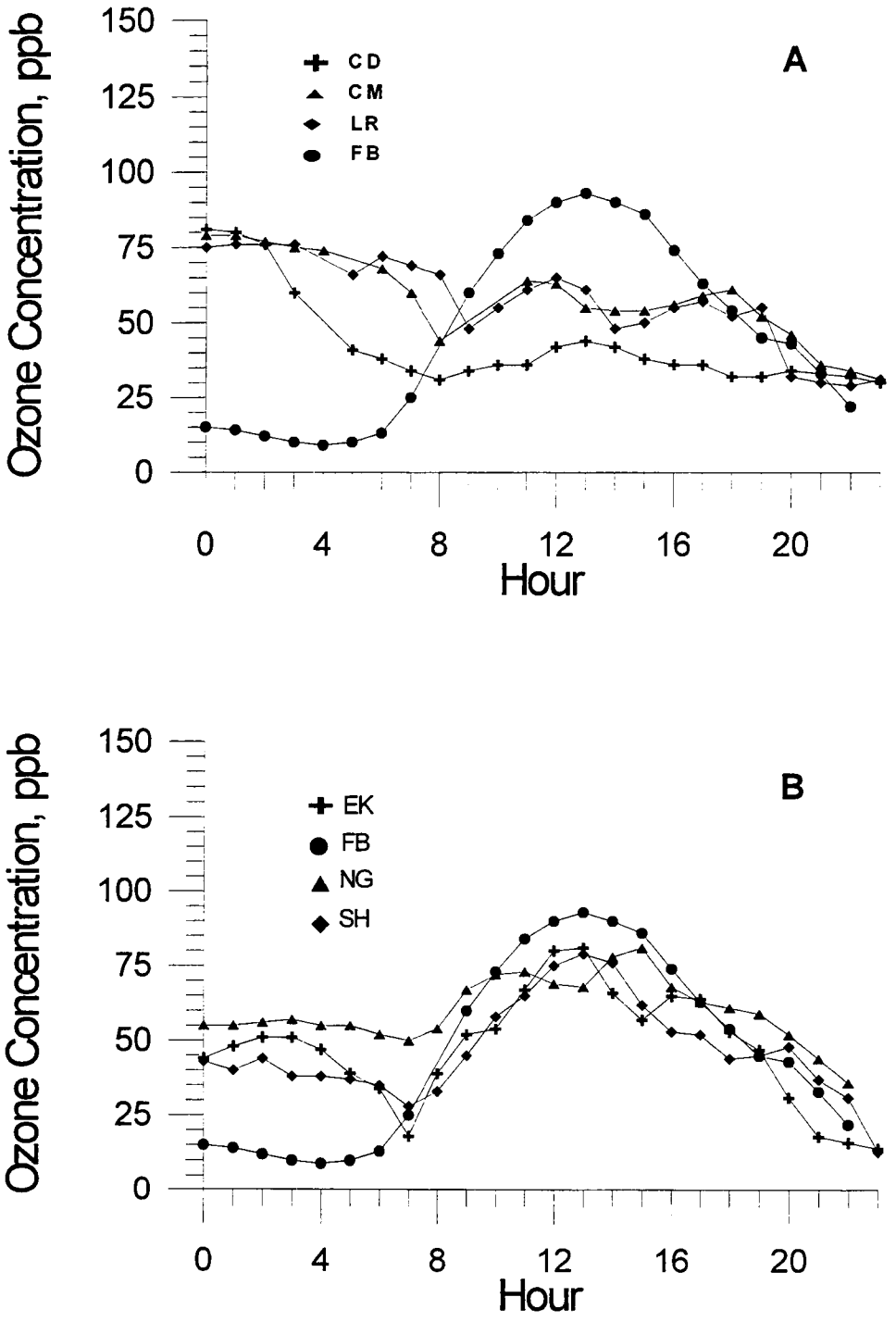

FIGURE 4.37. HOURLY MEAN OZONE CONCENTRATIONS OBTAINED FROM REGIONAL MONITORING STATIONS ON AUGUST 24, 1995. A. High elevation stations (located above 793m MSL) [Clingmans Dome (CD), Cove Mountain (CM), and Look Rock (LR)] and Freels Bend (elevation 247m MSL). B. Low elevation stations (below 343 m MSL)[East Knox (EK), Freels Bend (FB), Nances Grove (NG) and Spring Hill (SH)].

The afternoon-evening measurements began at 1601 and concluded at 2310. Profiles of potential temperature, ozone concentration, wind speed, and wind direction are presented in Figure 4.38. Measurements were very similar to those made during previous afternoon-evenings. At 1601, the potential temperature and ozone concentration profiles were near vertical. Potential temperatures were 304-305 °K, and ozone concentrations varied between 70-90 ppb. By 1656, potential temperatures at the surface decreased slightly and ozone concentrations dropped to 60 ppb. Wind speed and directional variability also decreased. By 1756 (72 minutes prior to sunset), a distinct potential temperature inversion began to form at the surface. Ozone concentrations at the surface were 50 ppb while concentrations above ridge-top height exceeded 80 ppb. Wind speeds near the surface decreased and wind directions were primarily from the north. Additional measurements throughout the night provided data for characterizing further development of the nocturnal boundary layer. Based on the potential temperature profiles, atmospheric mixing ceased at 1756 with the initial formation of the nocturnal boundary layer.

When compared with Look Rock ozone concentrations at the respective times, all Tethersonde measurements at 526 m were higher. Between 1622 and 1816, concentrations were less than 10 ppb higher. However, beginning with the 1900 measurements, Tethersonde concentrations exceeded Look Rock concentrations by as much as 25 ppb. During the 1959 measurements, ozone concentrations between 186 m and 704 m were 100-112 ppb. These extremely high concentrations were associated with winds from the north and north northeast. Ozone concentrations at the surface and Freels Bend were similar and decreased at the same time (Figure 4.39).

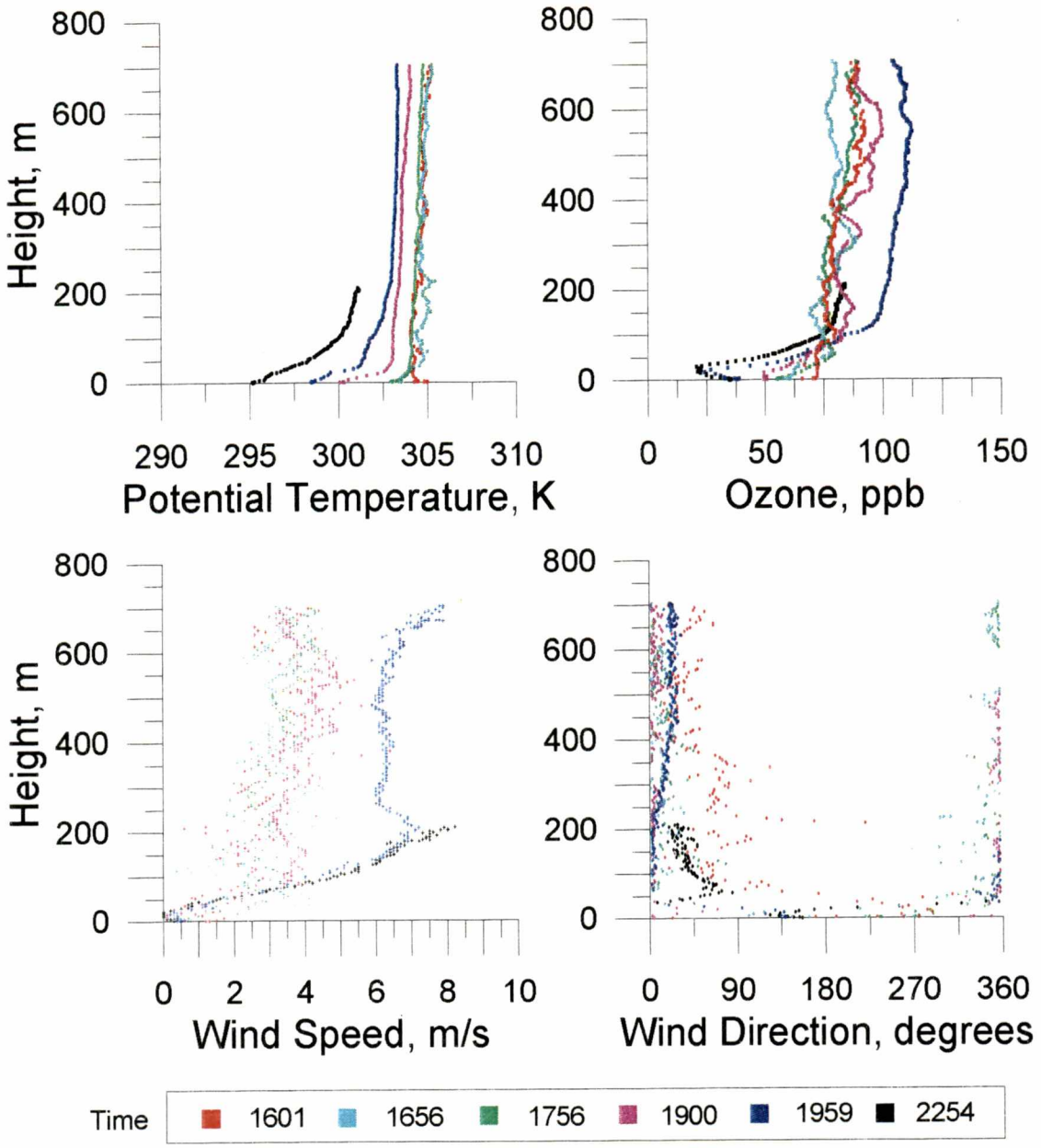

FIGURE 4.38. PROFILES OF POTENTIAL TEMPERATURE, OZONE CONCENTRATION, WIND SPEED AND WIND DIRECTION DEVELOPED FROM TETHERSONDE DATA OBTAINED DURING THE AFTERNOON-EVENING OF AUGUST 29, 1995. Tethersonde readings were initiated at 1601, and the final balloon ascent began at 2254.

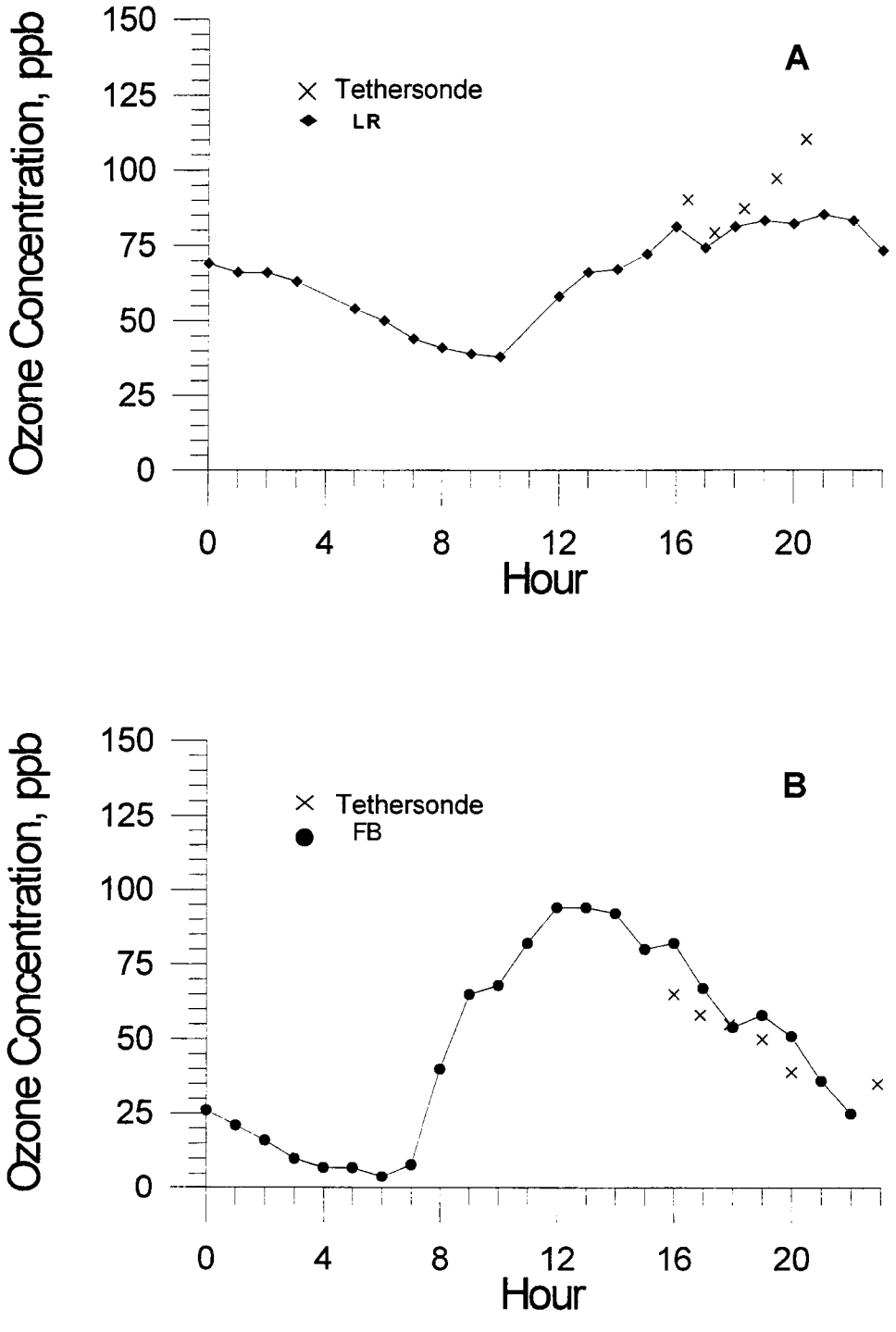

FIGURE 4.39. COMPARISON OF HOURLY MEAN OZONE CONCENTRATIONS ON AUGUST 29, 1995 OBTAINED FROM LOOK ROCK AND FREELS BEND REGIONAL MONITORING STATIONS WITH READING OBTAINED AT OAK RIDGE WITH TETHERSONDE INSTRUMENTATION. A) Look Rock and B) Freels Bend.

In comparing regional monitoring stations (Figure 4.40), Nances Grove was the site for the highest ozone concentrations with a maximum of 98 ppb occurring at 1300. At approximately the same time, Freels Bend concentrations peaked at 94 ppb. East Knox and Spring Hill concentrations peaked later in the afternoon at 81 and 85 ppb, respectively. Thus, concentrations at Freels Bend exceeded all urban-influenced stations. Clingmans Dome, Cove Mountain, and Look Rock concentrations in the mid-evening with concentrations approximately between 85-91 ppb.

August 30, 1995 Wednesday

On August 30, the minimum and maximum temperatures at ground-level were 19.9°C and 37.2°C, respectively. The minimum temperature occurred at 0615 and the maximum temperature at 1415. Wind speeds averaged 0.2 m/s in the early morning, increased to 1.9 m/s at 1000, and diminished to 0.3 m/s by 0000. Maximum wind speed, 5.4 m/s, occurred at approximately 1500. Skies were clear throughout the day except for a cloud bank to the west which blocked the sun from 1600 to 1800. However, during this period, skies overhead remained clear. There was no precipitation. Sunrise occurred at 0606 and sunset at 1907. Measurements were conducted during the morning and afternoon-evening.

The morning measurements began at 0511 and concluded at 1128. Profiles of potential temperature, ozone concentration, wind speed, and wind direction are presented in Figure 4.41 A surface-based inversion approximately 150 meters in depth was observed during the 0511 measurements. By 0702, the nocturnal inversion began to erode. Based on the near vertical potential temperature profile, the mixing height was

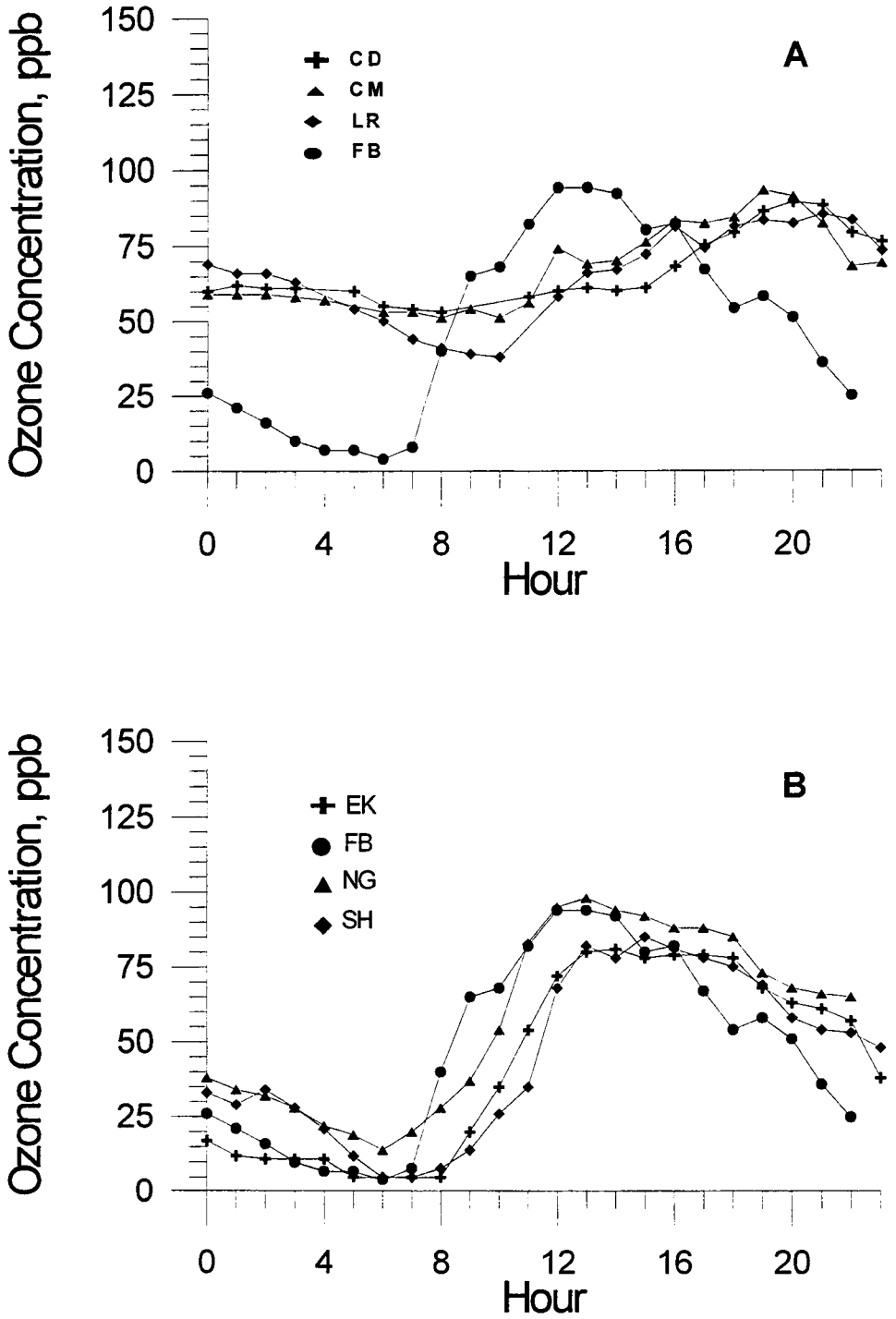

FIGURE 4.40. HOURLY MEAN OZONE CONCENTRATIONS OBTAINED FROM REGIONAL MONITORING STATIONS ON AUGUST 29, 1995. A. High elevation stations (located above 793m MSL) [Clingmans Dome (CD), Cove Mountain (CM), and Look Rock (LR)] and Freels Bend (elevation 247m MSL). B. Low elevation stations (below 343 m MSL)[East Knox (EK), Freels Bend (FB), Nances Grove (NG) and Spring Hill (SH)].

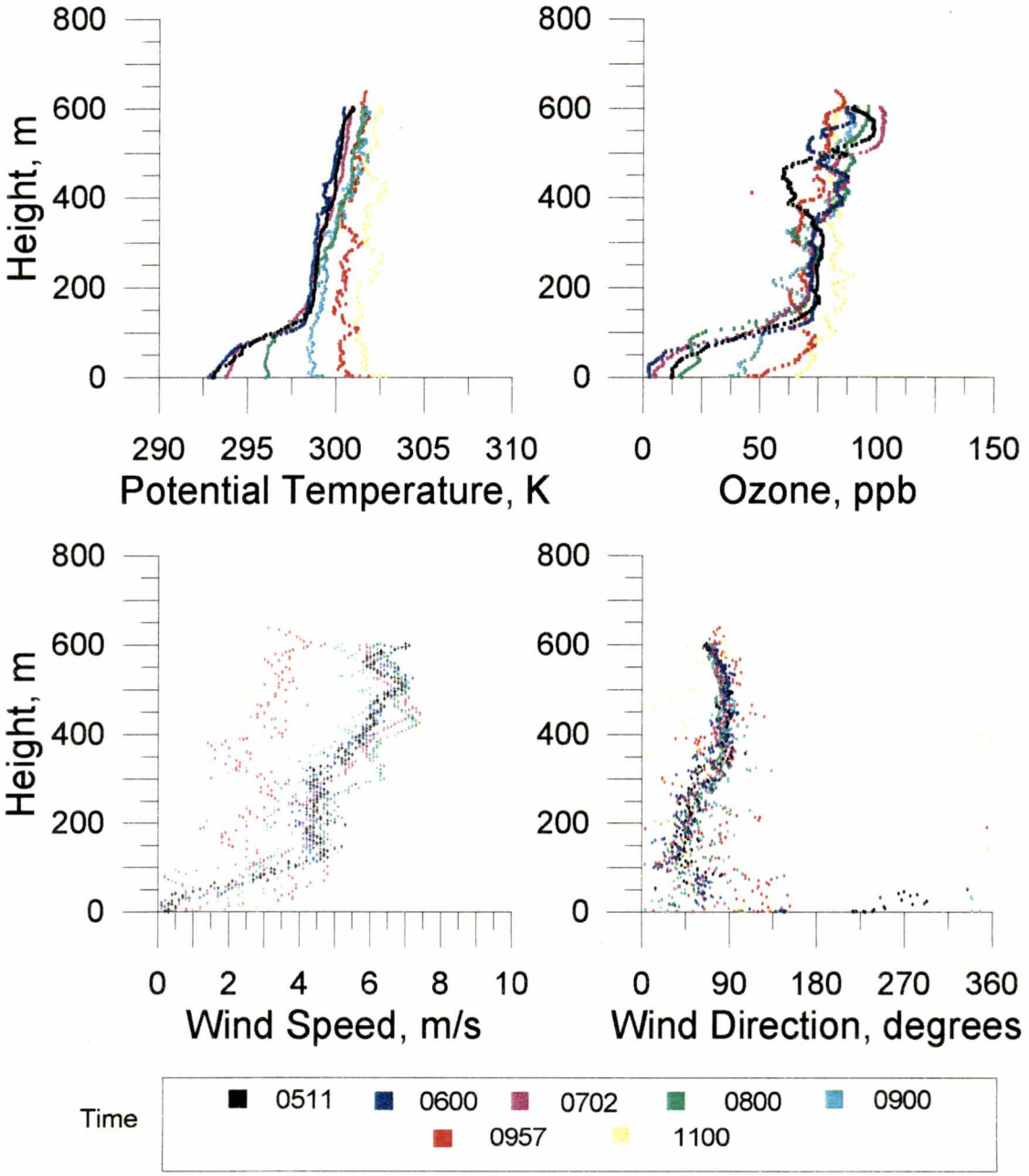

FIGURE 4.41. PROFILES OF POTENTIAL TEMPERATURE, OZONE CONCENTRATION, WIND SPEED AND WIND DIRECTION DEVELOPED FROM TETHERSONDE DATA OBTAINED DURING THE MORNING OF AUGUST 30, 1995. Tethersonde readings were initiated at 0511, and the final balloon ascent began at 1100.

estimated to be 70 m. Ozone concentrations at the surface slowly increased. At 0800, the mixing height increased to 100 m and ozone concentrations at the surface increased threefold. By 0900, breakup of the nocturnal inversion was essentially complete. The mixing height exceeded 601 m. The potential temperature profile approached near vertical and ozone concentrations continued to climb as the result of entrainment. Subsequent measurements at 0957 and 1100 were indicative of thorough mixing with mixing heights well above 639 m.

The afternoon-evening measurements began at 1605 and concluded at 2223. Profiles of potential temperature, ozone concentration, wind speed, and wind direction are presented in Figure 4.42. The first measurements were characterized by the vertical profiles for both potential temperature and ozone concentration. which suggested complete mixing from reservoirs aloft to the ground surface. By 1655, the ground began to cool and formation of a temperature inversion commenced. Atmospheric mixing between the surface and upper air ceased. Based on subsequent profile measurements at 1759, 1900, 2001, 2056, and 2157; the nocturnal inversion continued to grow until reaching upward approximately 400 m at 2214. Simultaneously, ozone concentrations at the surface quickly decreased in the stable layer. Once more, the exception was a shallow layer at the surface which had elevated concentrations attributed to drainage flow from the surrounding ridges. The surface ozone concentrations tended to equal those at ridge tops.

In general, Tethersonde measurements at 526 m were similar to Look Rock measurements throughout the entire day (Figure 4.43). Of fifteen Tethersonde

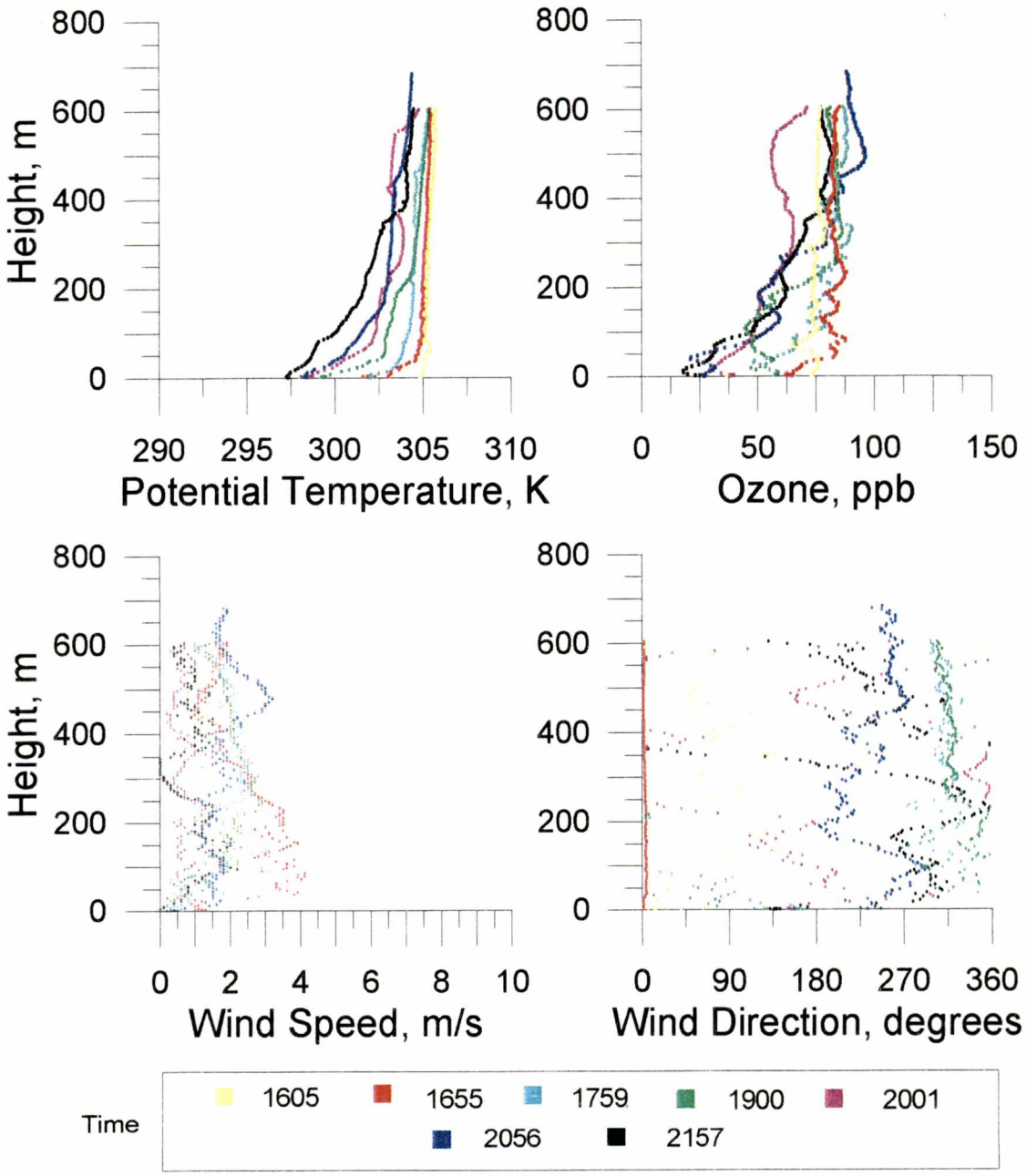

FIGURE 4.42. PROFILES OF POTENTIAL TEMPERATURE, OZONE CONCENTRATION, WIND SPEED AND WIND DIRECTION DEVELOPED FROM TETHERSONDE DATA OBTAINED DURING THE AFTERNOON-EVENING OF AUGUST 30, 1995. Tethersonde readings were initiated at 1605, and the final balloon ascent began at 2157.

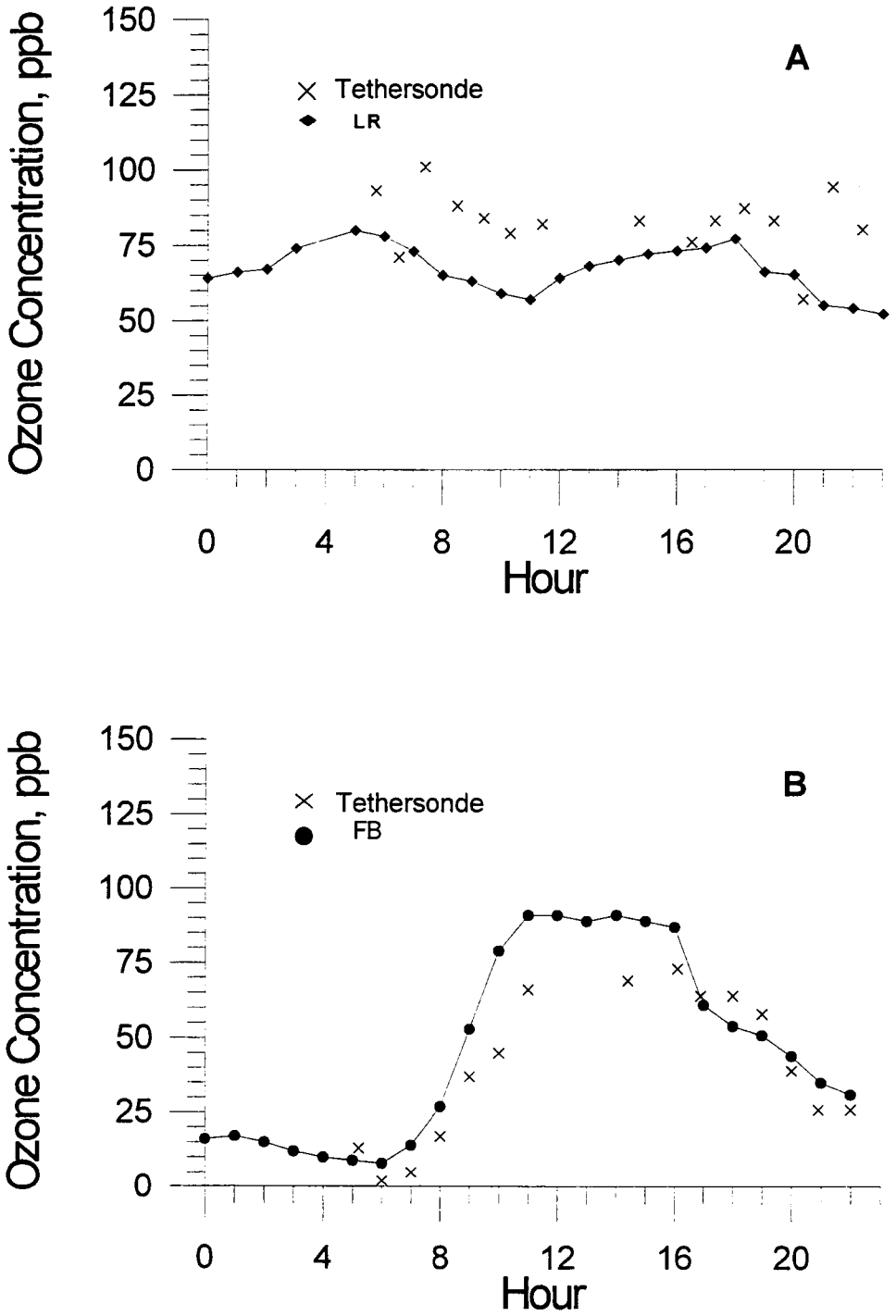

FIGURE 4.43. COMPARISON OF HOURLY MEAN OZONE CONCENTRATIONS ON AUGUST 30, 1995 OBTAINED FROM LOOK ROCK AND FREELS BEND REGIONAL MONITORING STATIONS WITH READING OBTAINED AT OAK RIDGE WITH TETHERSONDE INSTRUMENTATION. A) Look Rock and B) Freels Bend.

measurements, thirteen slightly exceeded respective measurements at Look Rock. Two remaining measurements, one morning and one evening, were less than 10 ppb lower than concentrations at Look Rock. When Freels Bend and Oak Ridge ozone concentrations were compared, early morning and late afternoon-evening concentrations were similar. However, mid-morning and early afternoon concentrations in Oak Ridge were as much as 30 ppb lower than concentrations at Freels Bend.

In comparing regional monitoring stations (Figure 4.44), Nances Grove reported the highest concentrations with a maximum 97 ppb occurring at 1200. At Freels Bend, concentrations peaked at 91 ppb at 1100-1200 and 1400. Also at 1400, concentrations at East Knox peaked at 90 ppb. At Spring Hill, concentrations peaked at 90 ppb three hours later (1700). The maximum concentrations for Cove Mountain and Look Rock occurred in the early morning. Cove Mountain had 90 ppb at 0200 and Look Rock had 80 ppb at 0500. Clingmans Dome concentrations peaked at 85 ppb in the evening (2100).

August 31, 1995 Thursday

On August 31, the minimum and maximum temperatures at ground-level were 20.4°C and 37.5°C, respectively. The minimum temperature occurred at 0630 and the maximum temperature at 1400. Wind speeds averaged 0.2 m/s in the early morning, increased to 2.0 m/s at 1400, and diminished to 0.4 m/s by 0000. Maximum wind speed, 7.9 m/s, occurred at approximately 1400. The skies were clear throughout the day and evening except for a brief storm shower at approximately 1500. There was 1.0 mm precipitation from the storm. Sunrise occurred at 0607 and sunset at 1904. Measurements were conducted only during the morning.

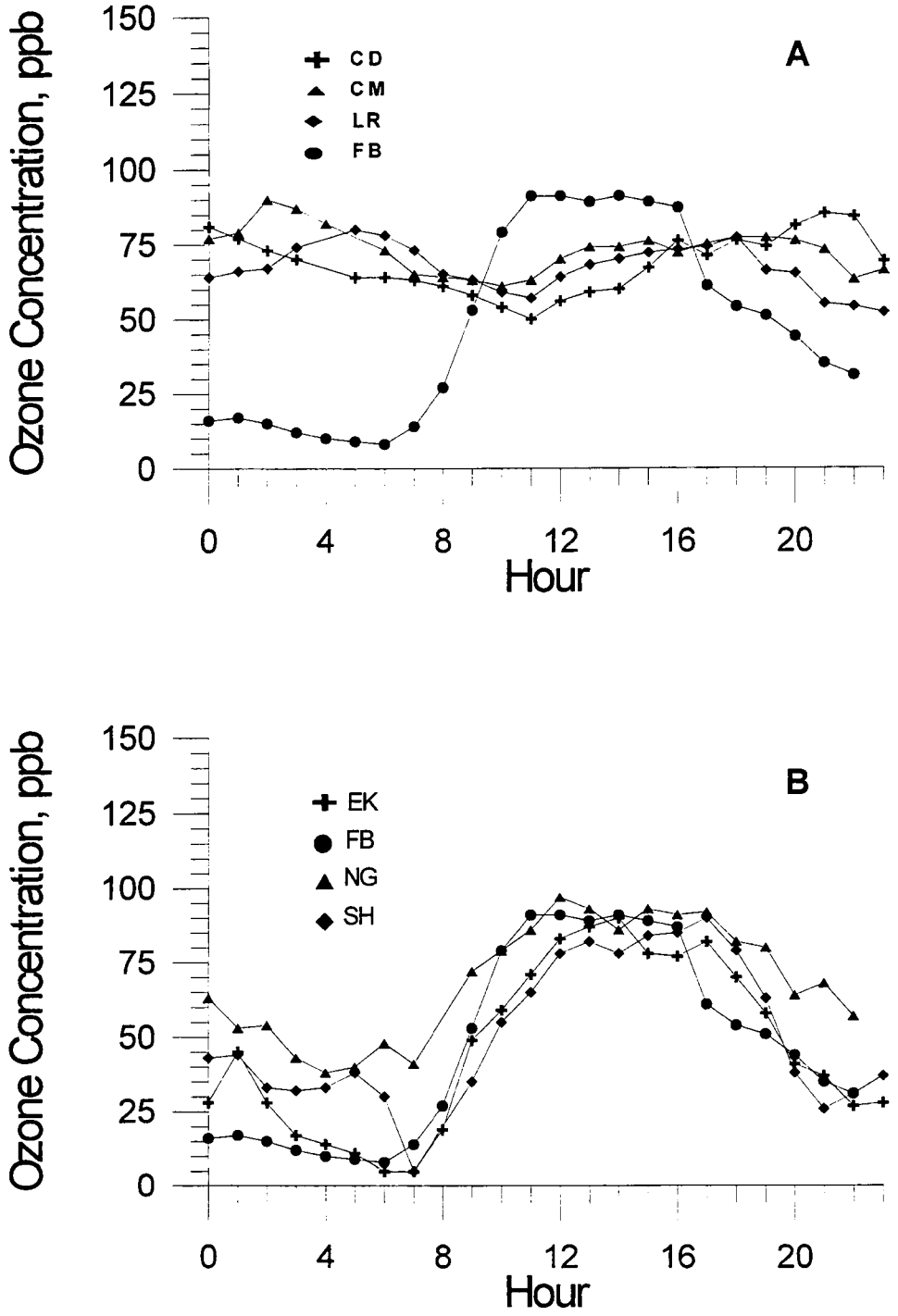

FIGURE 4.44. HOURLY MEAN OZONE CONCENTRATIONS OBTAINED FROM REGIONAL MONITORING STATIONS ON AUGUST 30, 1995 A. High elevation stations (located above 793m MSL) [Clingmans Dome (CD), Cove Mountain (CM), and Look Rock (LR)] and Freels Bend (elevation 247m MSL). B. Low elevation stations (below 343 m MSL)[East Knox (EK), Freels Bend (FB), Nances Grove (NG) and Spring Hill (SH)].

The morning measurements began at 0512 and concluded at 0812 when high wind speeds prevented Tethersonde operations. A strong, ground-based inversion extended upward to approximately 170 m during the 0512-0530 measurements. By the 0658-0712 measurements, the inversion began to erode as potential temperatures at the surface increased. The mixing height was estimated to be 25 m. Ozone concentrations at the surface were approximately 5 ppb. By 0759, the nocturnal inversion was gone. The potential temperature profile was near vertical between the surface and 250 m. As air containing higher ozone concentrations became entrained, concentrations at the surface climbed above 30 ppb. Southwest winds approached speeds of 10 m/s. Profiles of potential temperature, ozone concentration, wind speed and wind direction are presented in Figure 4.45. The mixing height was estimated to be 250 m.

Because of high wind speeds, Tethersonde measurements did not reach 526 m. Thus, comparisons with measurements at Look Rock were not possible. Ozone concentrations at Freels Bend and Oak Ridge were similar (Figure 4.46).

In comparing regional monitoring stations (Figure 4.47), Nances Grove was the site for highest concentrations with a maximum 112 ppb occurring at 1300. Also at 1300, concentrations at Freels Bend and Spring Hill peaked at 106 and 101 ppb, respectively. East Knox concentrations peaked one hour later (1400) at 107 ppb. Concentrations at the urban-influenced Nances Grove station exceeded concentrations at Freels Bend throughout the day. At Clingmans Dome, Cove Mountain, and Look Rock, concentrations were typically lower in the early morning than at late night. Specifically, at Clingmans Dome, concentrations were 60 ppb at 0000 and peaked at 88 ppb at 2000.

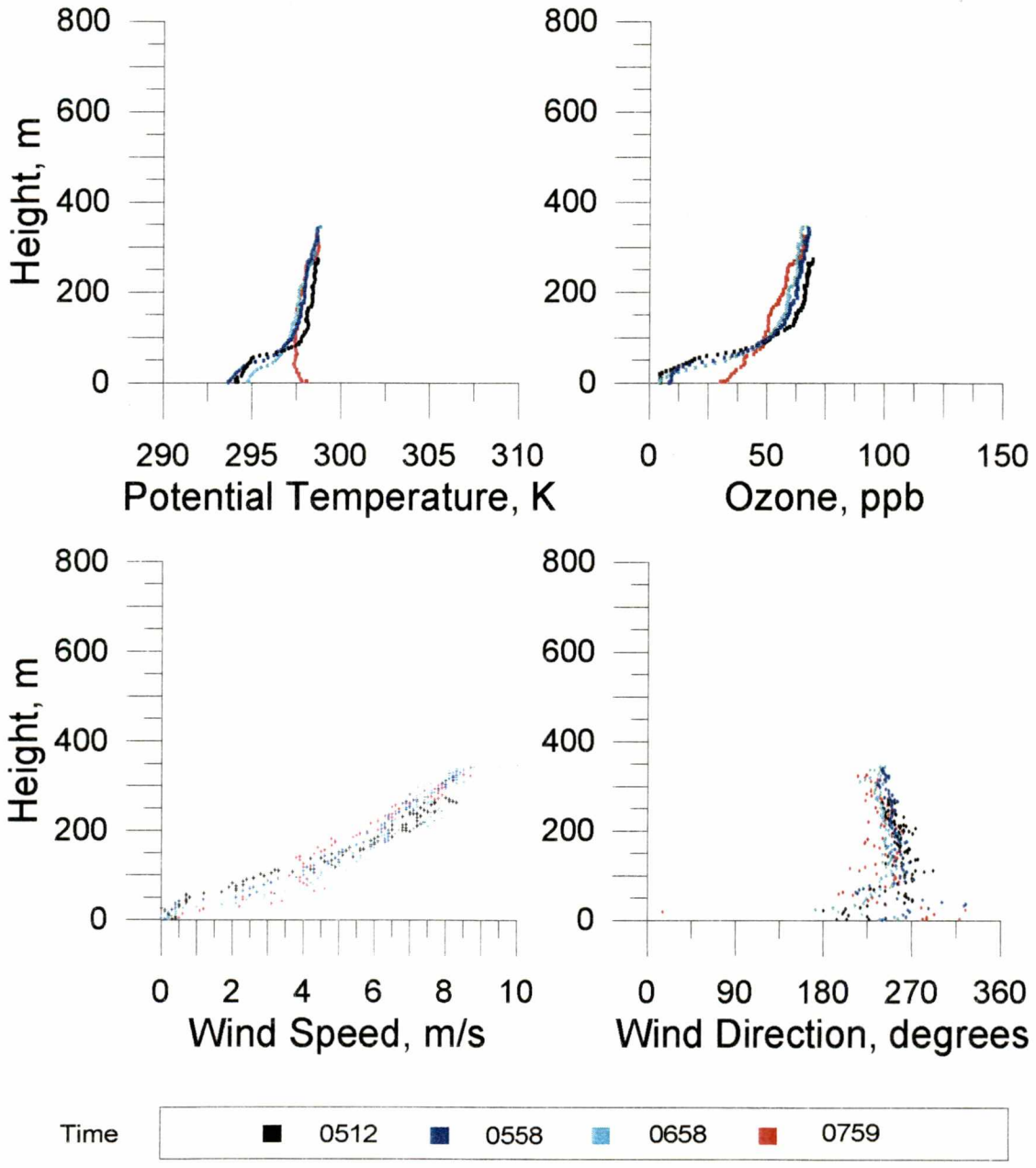

FIGURE 4.45. PROFILES OF POTENTIAL TEMPERATURE, OZONE CONCENTRATION, WIND SPEED AND WIND DIRECTION DEVELOPED FROM TETHERSONDE DATA OBTAINED DURING THE MORNING OF AUGUST 31, 1995. Tethersonde readings were initiated at 0512, and the final balloon ascent began at 0759.

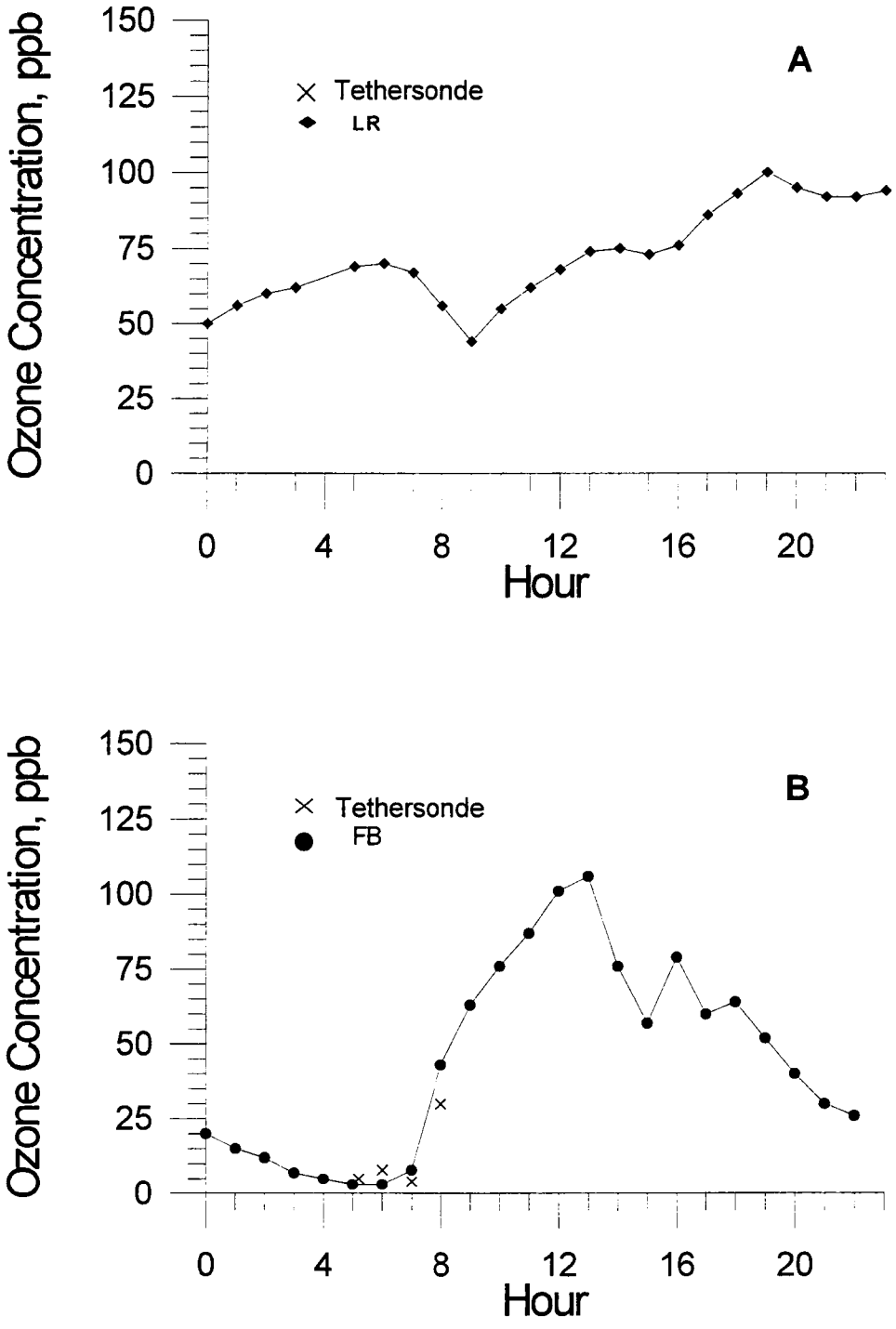

FIGURE 4.46. COMPARISON OF HOURLY MEAN OZONE CONCENTRATIONS ON AUGUST 31, 1995 OBTAINED FROM LOOK ROCK AND FREELS BEND REGIONAL MONITORING STATIONS WITH READING OBTAINED AT OAK RIDGE WITH TETHERSONDE INSTRUMENTATION. A) Look Rock and B) Freels Bend. Maximum Tethersonde height was below height of Look Rock (526 m).

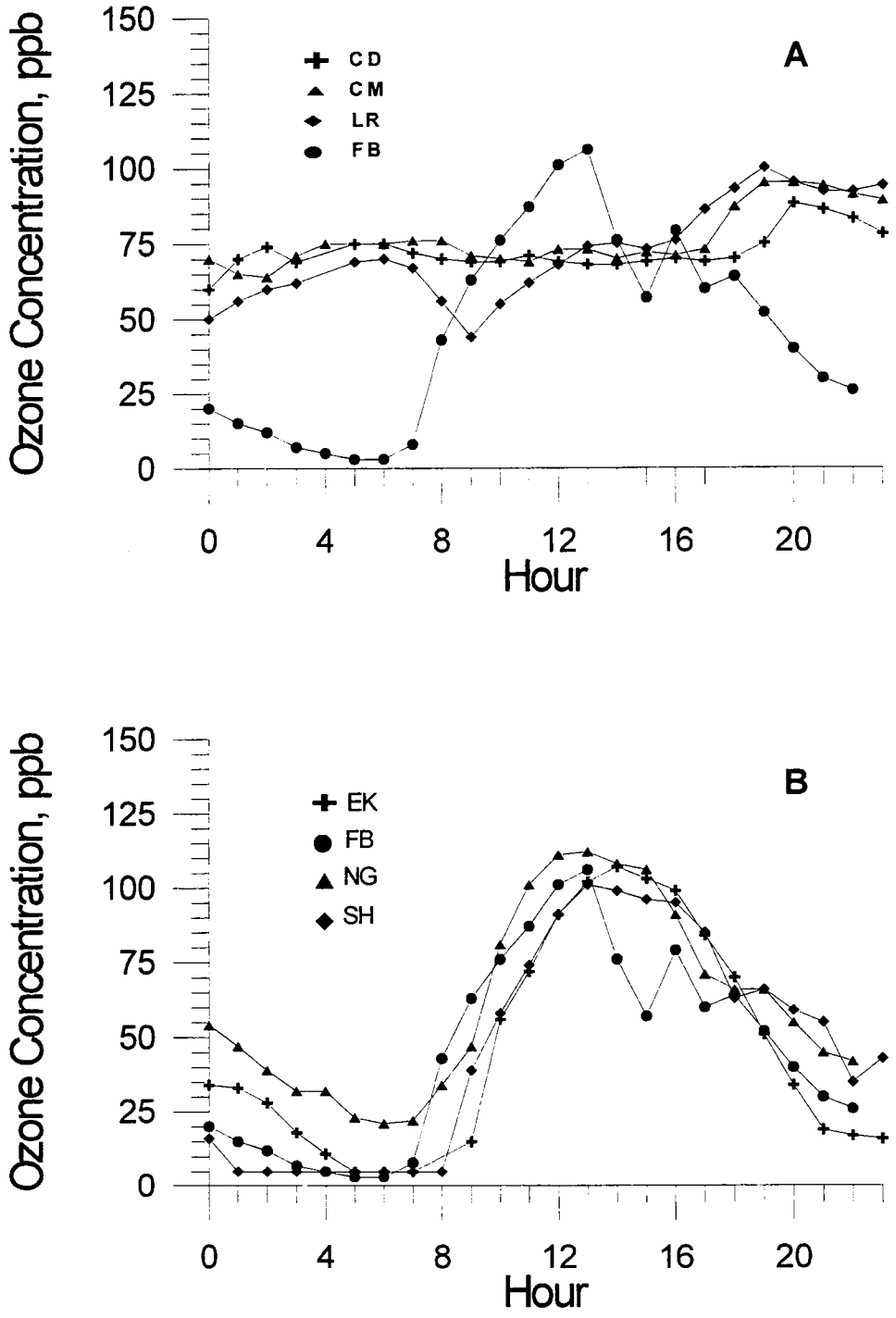

FIGURE 4.47. HOURLY MEAN OZONE CONCENTRATIONS OBTAINED FROM REGIONAL MONITORING STATIONS ON AUGUST 31, 1995 A. High elevation stations (located above 793m MSL) [Clingmans Dome (CD), Cove Mountain (CM), and Look Rock (LR)] and Freels Bend (elevation 247m MSL). B. Low elevation stations (below 343 m MSL)[East Knox (EK), Freels Bend (FB), Nances Grove (NG) and Spring Hill (SH)].

Similarly, at Cove Mountain, concentrations were 70 ppb at 0000 and peaked at 95 ppb at 1900-2000. At Look Rock, concentrations were 50 ppb at 0000 and peaked at 100 ppb at 1900.

4.2.2 Summary of Tethersonde Measurements

Tethersonde measurements were conducted during July and August, 1995. Measurements were taken in the morning, during development of the mixing height, and in the afternoon-evening, during reestablishment of the mixing height near the surface. Sampling was conducted on nine mornings and eight afternoon-evenings. On five days, measurements during both morning and afternoon-evening were obtained. Examination and interpretation of measurement data can be summarized as follows:

1. Prior to sunrise, the potential temperature profile was characteristic of a stable boundary layer (nocturnal inversion). Inversion heights ranged from a minimum 135 m on July 31 to a maximum 400 m on July 30. Beneath the nocturnal inversion, a mechanically- induced nocturnal surface layer mixing height was present. This MH was observed on the three mornings (July 14, August 30 and 31) when Tethersonde measurements were conducted prior to sunrise. Based on isothermal temperature profiles and homogeneous ozone concentrations, the nocturnal surface layer MH ranged from a minimum 25 m on August 30 and 31 to a maximum 70 m on July 14.

2. After sunrise, heating of the earth's surface led to an upward exchange of heat. The lowest layer of the inversion warmed as the result of heat flux convergence. This process progressively eroded the inversion layer until it dissipated around mid-morning. The potential temperature gradient ($d\theta/dz$) was negative or equal to zero in the region of

atmospheric mixing. Near sunset, as the result of radiative energy loss, an inversion formed at the surface. At that time, atmospheric mixing between the surface and upper atmosphere ceased; the mixing height reestablished near the surface. As night progressed, the bottom portion of the residual layer was transformed into a stable boundary layer (nocturnal inversion). As compared to daytime MHs which have clearly defined upper boundaries, the nocturnal inversions had poorly defined upper boundaries which blended with the residual layers above. The inversion height and strength increased throughout the evening.

Nocturnal inversion formation and growth were investigated by plotting inversion heights as determined from morning and afternoon evening Tethersonde potential temperature profiles as a function of time. (Hour zero was arbitrarily set to sunset.) (Figure 4.48). Inversions formed shortly before sunset and quickly grew to heights of 25 to 200 m. As night progressed to morning, inversion heights increased to 135 to 400 m as indicated by trend lines in Figure 4.48. By hour 14 (mid-morning of the next day), the nocturnal inversions were dissipated by the growing MHs.

3. During all morning measurements, ozone concentrations in the residual layer (above the nocturnal inversion) were significantly higher than ozone concentrations at the surface. This phenomenon was anticipated based on differences between regional high and low elevation ozone monitoring stations, and confirmed by these measurements.

4. As the mixing height developed, the entrainment of ozone from the residual layer played a significant, if not dominant, role in increased ozone concentrations at low elevation monitoring stations. This role was investigated using two methods. First,

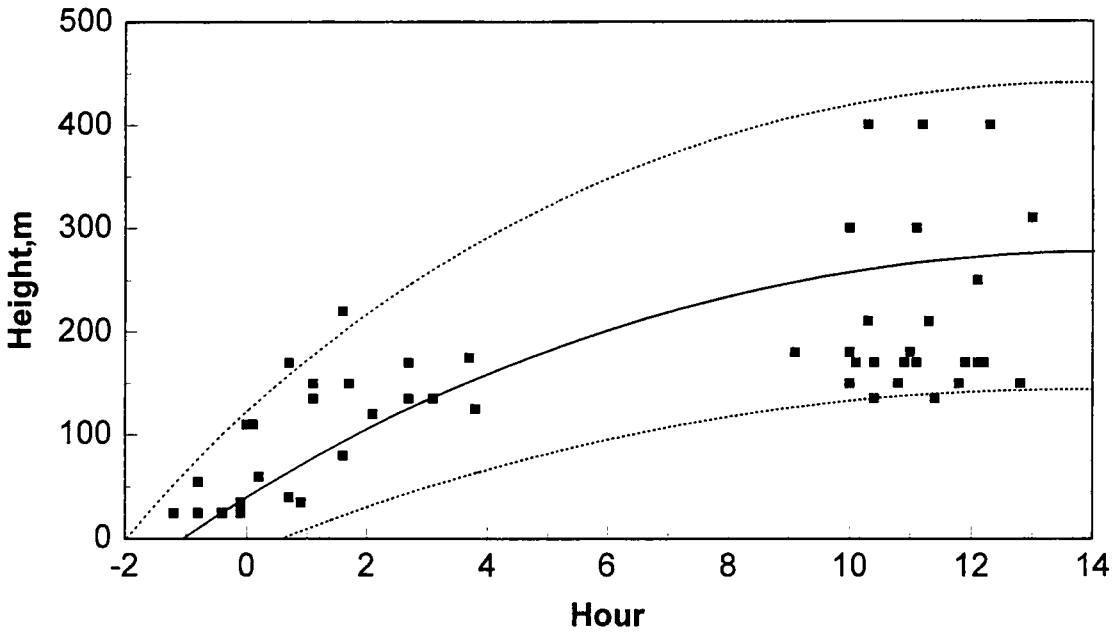

FIGURE 4.48. STABLE BOUNDARY LAYER (NOCTURNAL INVERSION) HEIGHT AS A FUNCTION OF TIME OF DAY. Sunset was arbitrarily set at hour zero.

mid-morning ozone concentration profiles were examined. Mid-morning profiles where the mixing height was determinable by inspection of the corresponding potential temperature profiles were selected. For example, two ozone concentration profiles from the morning of July 8, 1995 were selected (Figure 4.7). The initial profile, the 0646 profile, was from the second set of profiles for the day. Based on the 0646 potential temperature profile, the MH was estimated to be approximately 40 m, and concentrations above 40 m were higher than concentrations at the surface. For the subsequent profile (0803), the MH was estimated to be approximately 135 m. The initial (0646) ozone concentration profile intersects the subsequent (0803) ozone concentration profile at two points (at approximately 50 m and 150 m). The area between the two profiles from the surface to 50 m was defined as the near-surface area, and the area between the two profiles from 50 m to 150 m was defined as the aloft area (Figure 4.49). The near-surface area is representative of increased ozone at the surface. The aloft area is representative of the decreased ozone aloft. As the MH increased from 40 m at 0646 to 135 m at 0803, ozone concentrations near the surface increased while ozone concentrations between 40 m and 150 m decreased as the result of entrainment. By comparing the aloft area to the near-surface area, one is able to predict the percentage of near-surface ozone concentration attributable to entrainment from the ozone-enriched reservoir aloft. For July 8, the aloft area was calculated to be 1351 m x ppb, and the near-surface area was calculated to be 929 m x ppb. When the aloft area was compared to the near-surface area, the ratio equaled 1.45. Based on these data, the entrainment of ozone from aloft would account for 1.45 times the amount of ozone observed near the surface. Differences

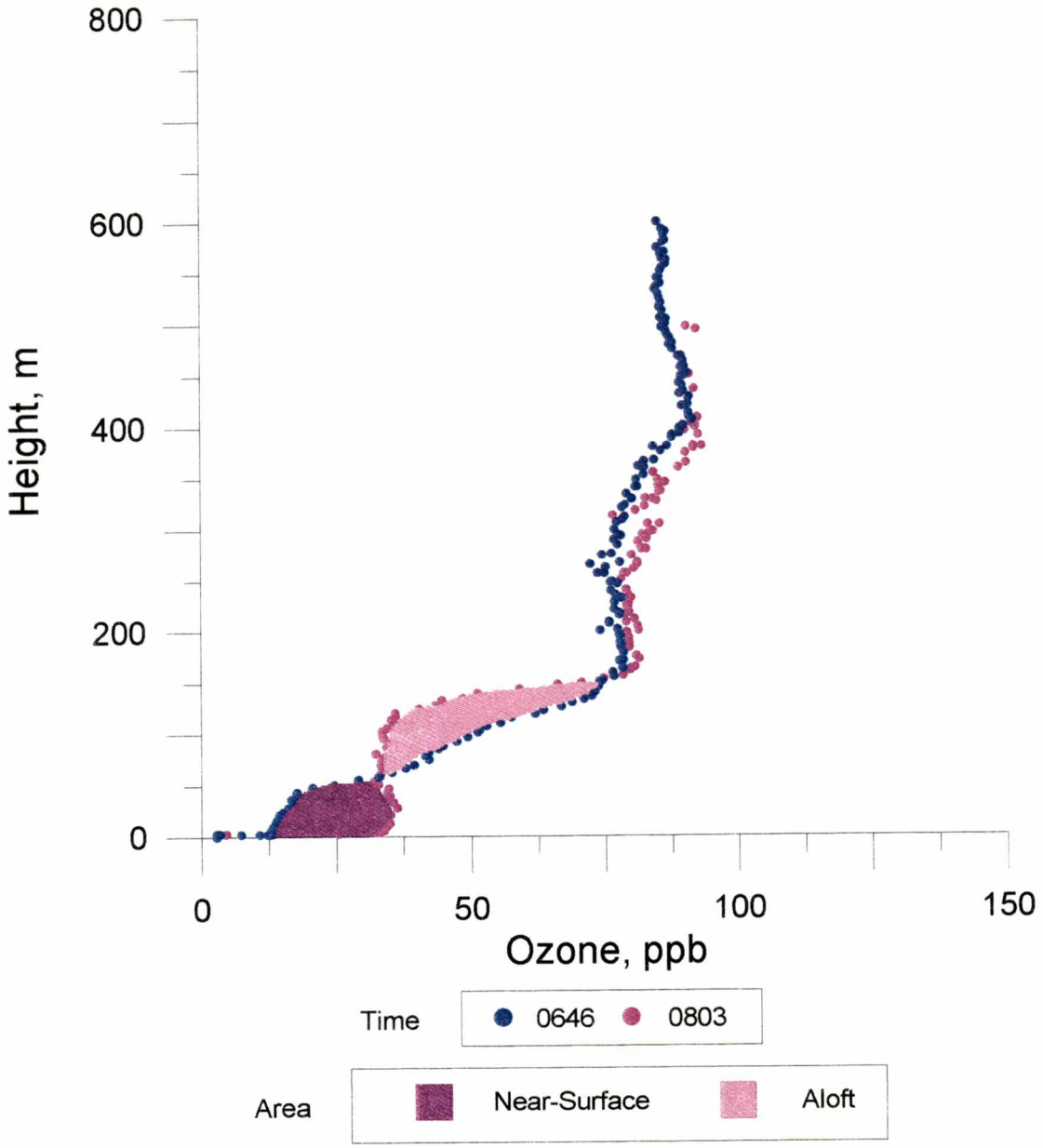

FIGURE 4.49. PROFILES OF OZONE CONCENTRATIONS DEVELOPED FROM TETHERSONDE DATA OBTAINED ON JULY 8, 1995 AND USED TO DEFINE NEAR-SURFACE AND ALOFT OZONE CONCENTRATIONS.

between predicted ozone concentrations at the surface and observed ozone concentrations at the surface may result from scavenging associated with nearby automobile emissions, minor changes in ozone concentrations over the 1.25 hour time difference between the two profiles, deposition of ozone on the nearby forest canopy, or combination thereof. Table 4.7 presents similar information for all mornings with the exception of July 20, July 30, and August 1. July 20 and 30 were excluded because of interferences from power plant plumes, and August 1 was excluded because of the limited data available. In all cases, except one, entrainment of ozone from aloft predicted greater ozone concentrations than those observed near the surface. The one exception occurred on August 30 when entrainment only accounted for 75 percent of ozone observed at the surface. Although it is difficult to explain this anomaly, one possible explanation is the presence of higher ozone concentrations near the surface than typically observed near 0800. Typically, ozone concentrations at the surface increased throughout the mornings. However, on August 30, the 0600 and 0702 Tethersonde measurements recorded ozone concentrations at the surface below concentrations recorded during the 0511 measurements (refer to Figure 4.41). If one compared the respective areas between the 0511 and 0800 profiles, entrainment would account for ozone concentrations observed at the surface.

Second, daily peak concentrations recorded at Freels Bend were compared with peak concentrations recorded by Tethersonde measurements in the early morning (i.e. prior to daily photochemical production of ozone) (Table 4.8). Figure 4.50 provides information on observed ozone concentrations in the stable boundary layer and residual layer; and predicted ozone concentrations in the mixed layer for all days except July 20,

TABLE 4.7. CHANGES IN NEAR-SURFACE AND ALOFT OZONE CONCENTRATIONS. Areas are calculated from the origin to the first point of intersection of the two profile curves (near-surface) and from the point of first intersection to the point of second intersection (aloft).

DATE	**PROFILE** (initial)	**PROFILE** (second)	**AREA** (near-surface) (m x ppb)	**AREA** (aloft) (m x ppb)	$\frac{\text{Area (aloft)}}{\text{Area (near-surface)}}$
07-08-95	0646	0803	929	1351	1.45
07-14-95	0556	0656	852	3391	3.98
07-17-95	0701	0800	1178	2490	2.11
07-31-95	0707	0804	431	3285	7.6
08-30-95	0702	0800	699	527	0.75
08-31-95	0658	0759	699	1303	1.86

TABLE 4.8. COMPARISON OF OZONE CONCENTRATIONS MONITORED AT FREELS BEND, TN AND AT THE NOAA RESEARCH LABORATORY (OAK RIDGE, TN). Ozone concentrations were determined by a stationary monitoring station (Freels Bend) or a Tethersonde ozone monitoring system (NOAA).

Sampling Date	Sunrise	Maximum Ozone at Freels Bend (Hourly Average/ Time of Occurrence)	Selected Morning Tethersonde Readings [Ozone Concentration (Height)/ Time of Occurrence]
JULY 8	0527	80 ppb/1100	75.4 ppb (172 m)/0619 90 ppb (410 m)/0707
JULY 14	0530	101 ppb/1400	88 ppb (601m)/0543 92 ppb (600)/0634
JULY 17	0532	106 ppb/1300	115 ppb (683 m)/0642 93 ppb (610 m)/0732
JULY 20	0534	103 ppb /1200	94 ppb (703 m)/0640 81 ppb (643 m)/0732
JULY 30	0542	113 ppb/1500	41 ppb (538 m)/0636 47 ppb (774 m)/0746
JULY 31	0542	102 ppb/1600	44 ppb (797 m)/0656
AUGUST 1	0543	88 ppb/1300	64 ppb (695 m)/0635
AUGUST 30	0606	91 ppb/1100	98 ppb (552 m)/0541 90 ppb (577 m)/0634
AUGUST 31	0607	106 ppb/1300	70 ppb (270 m)0530

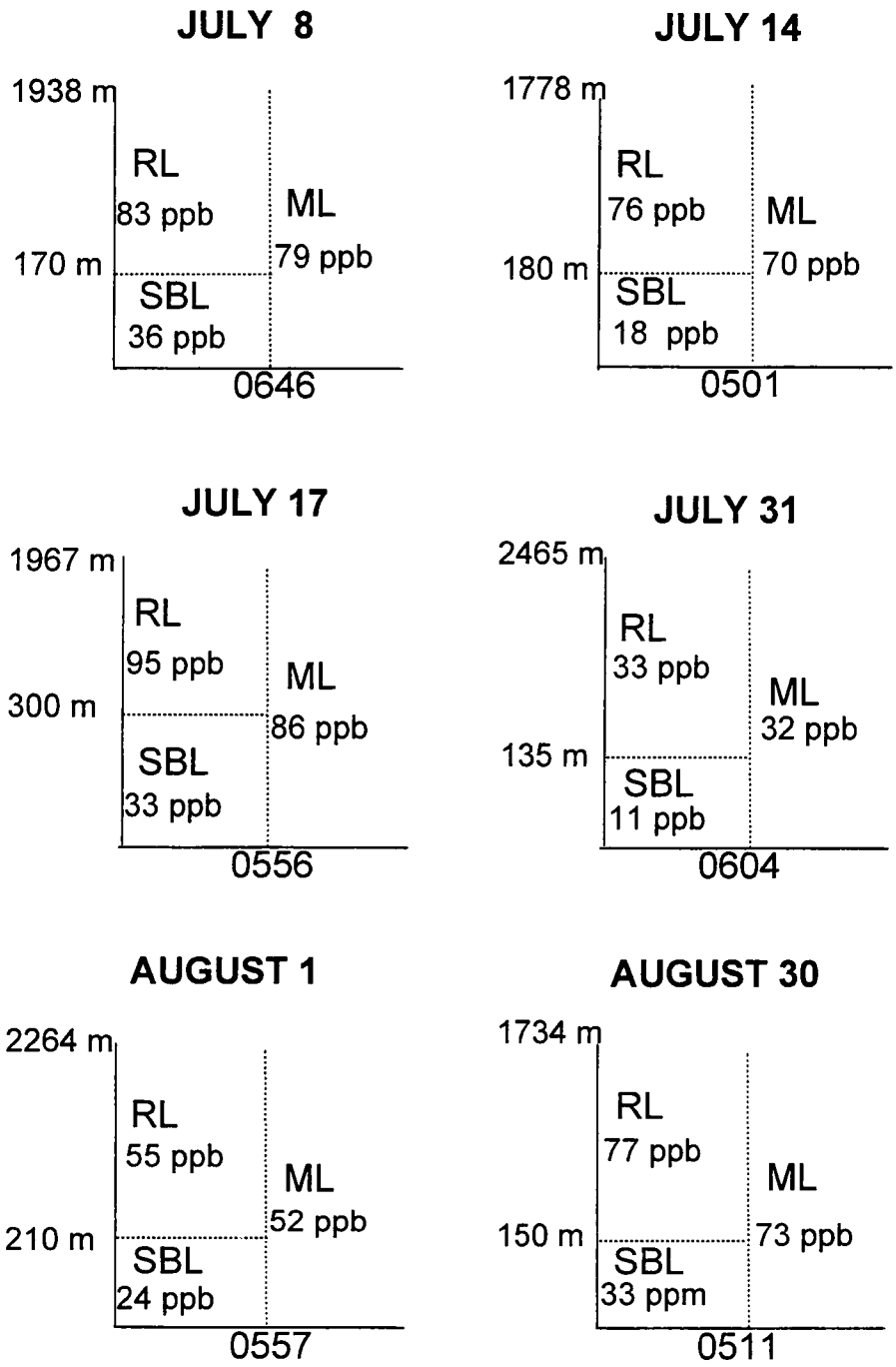

FIGURE 4.50. MEAN OZONE CONCENTRATIONS MEASURED IN THE RESIDUAL AND STABLE BOUNDARY LAYERS AND PREDICTED IN THE MIXED LAYER. The date and start time of the Tethersonde measurements appear at the top and bottom of each figure, respectively. Relative heights refer to the height above ground of the stable boundary layer (bottom height), and the height of the Tethersonde measurement (top height).

July 30, and August 31. July 20 and July 30 were excluded because ozone concentrations in the RL were scavenged by plumes from nearby power plants. August 31 was excluded because high wind speeds prevented measurements above 375 m. In the early morning, ozone concentrations in the RL were typically two to four times higher than concentrations in the SBL. Predicted ozone concentrations in the ML were then calculated based on an assumption that complete mixing occurred throughout the respective measurement height. The predicted concentrations were compared with the observed maximum hourly-averaged ozone concentrations for the respective day at FB (Figure 4.51). Ozone concentrations resulting from entrainment of RL ozone accounted for more than 50 percent of observed concentrations on all days except July 31. Ozone concentrations at Freels Bend typically peaked between 1100-1400. Noted exceptions occurred on July 30-31 when ozone concentrations peaked at 1500 and 1600, respectively.

5. In the afternoon-evening, even when potential temperature profiles remained vertical, ozone concentrations at the surface in Oak Ridge decreased. This resulted from scavenging and dry deposition (although wet deposition was a consideration during rainstorms). Ozone concentrations decreased throughout the night and early morning. In addition, periods of increased ozone concentrations at the surface most likely occurred when drainage winds from nearby ridges flowed to the valley floor. During these times, ozone concentrations at the surface roughly equaled concentrations at ridge-top heights.

6. When Tethersonde measurements at the surface in Oak Ridge were compared with surface measurements at Freels Bend, there was agreement during the early morning and

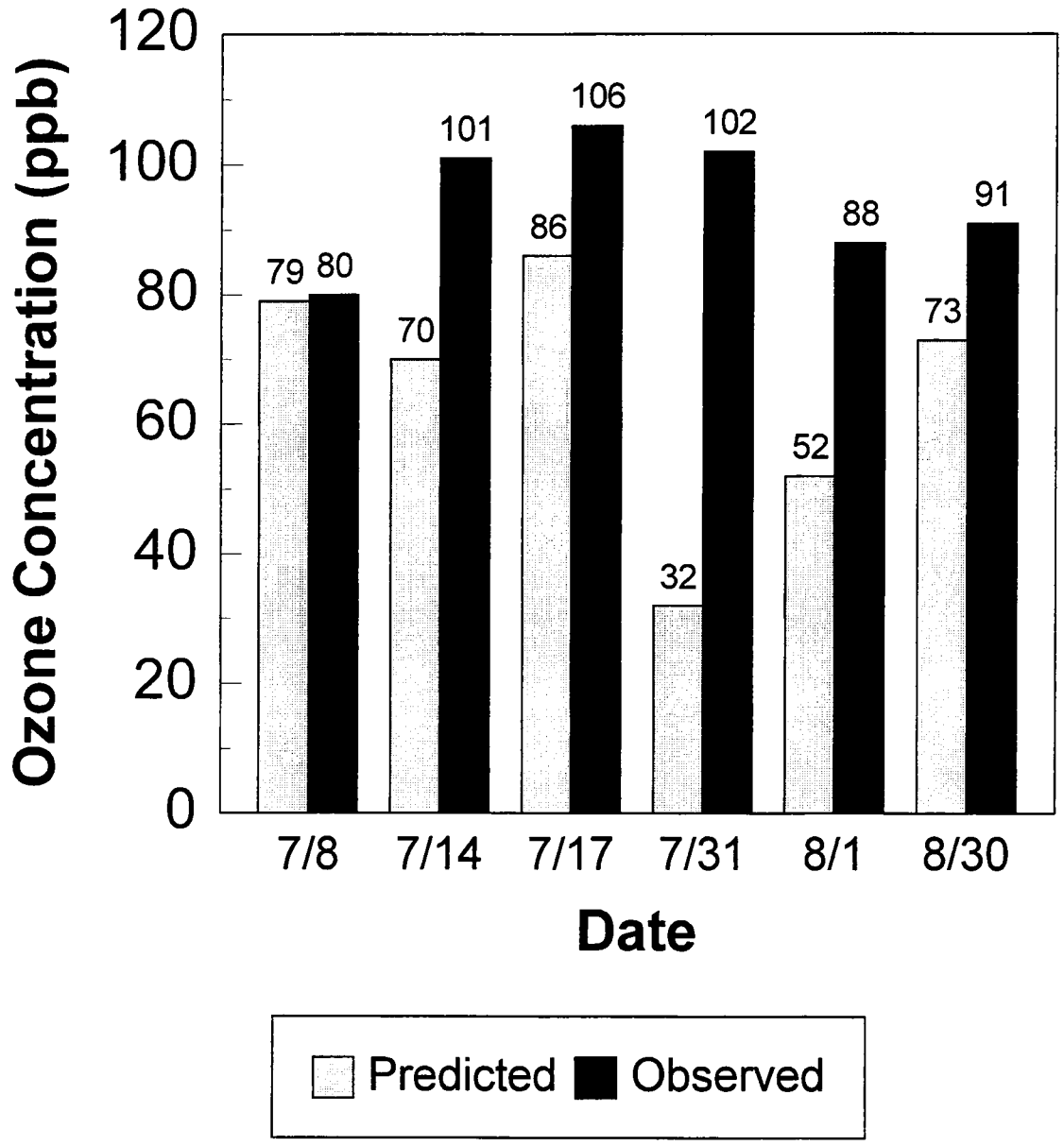

FIGURE 4.51. A COMPARISON OF PREDICTED OZONE CONCENTRATIONS VERSUS OBSERVED OZONE CONCENTRATIONS AT FREELS BEND.

evening. Midday concentrations in Oak Ridge were typically lower than concentrations at Freels Bend. Proximity of automobile traffic and the associated scavenging from exhaust may have accounted for this difference. When Tethersonde measurements at 526 m above Oak Ridge were compared with surface measurements at Look Rock (same relative height), ozone concentrations above Oak Ridge generally agreed with ozone concentrations at Look Rock.

7. In all cases, near surface wind speeds increased markedly after sunrise, attained maximum speeds in the afternoon, and decreased rapidly near sunset.

8. Regional wind directions were typically up-valley (from the southwest) during the daytime and down-valley (from the northeast) during the nighttime.

4.3 Objective 3: Mixing Height Profiles and Thermophysical Relationships

4.3.1 Mixing Height Profiles

Atmospheric mixing occurs under conditions of neutral to unstable and ceases once a stable layer begins to form at the surface. For the Tethersonde data, potential temperature profiles were used to estimate MH for each profile. During early mornings, potential temperatures increased with height denoting stable atmospheres. As the morning progressed, potential temperature gradients changed from positive to zero or negative, connoting atmosphere changes from stable to neutral or unstable, respectively. The MH is so named because vertical mixing in the atmosphere tends to leave conserved variables such as potential temperature constant with height. Therefore, under neutral conditions, potential temperature profiles are vertical. When unstable conditions exist,

potential temperature profiles decrease with height (Arya, 1988; Stull, 1988; Wark and Warner, 1981).

Mixing height profiles for July 8, 14, and 20 are presented in Figures 4.52, 4.53, and 4.54, respectively. The profiles were constructed by plotting MH versus time (hours 1-24). In all three cases, MHs did not begin to increase until after sunrise. Early morning MH growth was slower than late morning growth because of nocturnal inversions. The presence and strength of nocturnal inversions are two factors which inhibit growth rates of the MHs. By midmorning, continued heating of the earth's surface resulted in dissipation of the inversions, and MHs quickly rose to peak MHs (assumed to be the afternoon MHs from NCDC data). The development of the MHs in the morning as determined by Tethersonde measurements was consistent with observations made by Kelly et al. (1984) in Louisiana and Virginia. The afternoon MHs were held constant until reestablishment of the MHs near the surface as determined by Tethersonde measurements (formation of a potential temperature inversion at the surface). The duration of MH reduction was assumed to be instantaneous. MH reestablishment at the surface occurred near sunset on all three days.

4.3.2 Thermophysical Relationships

Since MH development is generally a convective process, the thermophysical relationship between heat absorbed by the atmosphere and MH development is of concern. In atmospheric science, heat flux is rarely measured directly. Instead, parameters such as temperature and wind speed are measured. Therefore, heat flux (Q_H), which is expressed in SI units of [$J/m^2 \cdot s$], may be redefined in kinematic form by

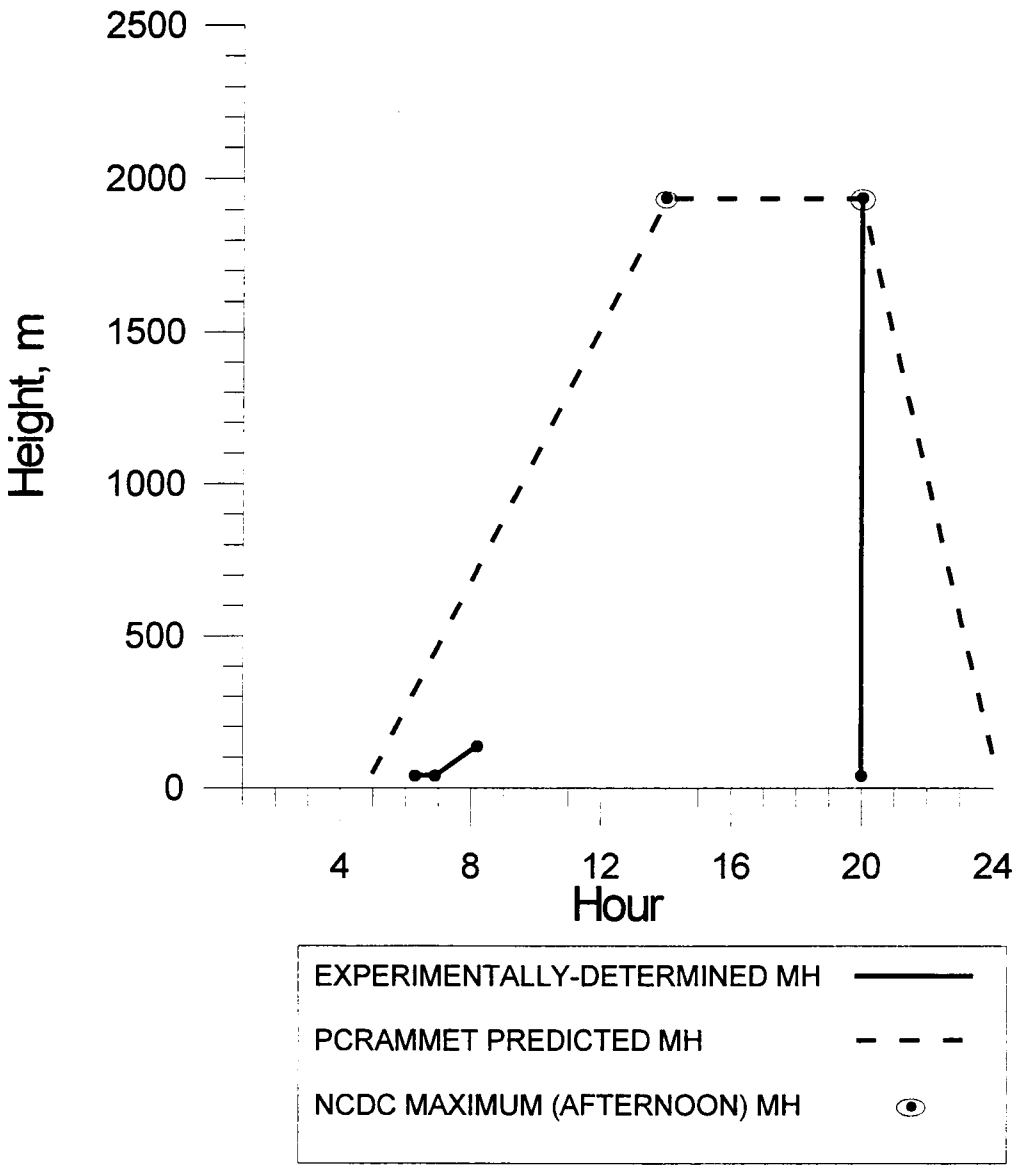

FIGURE 4.52. MIXING HEIGHT PROFILE FOR JULY 8, 1995. Profiles were generated from data collected at Oak Ridge, TN using Tethersonde instrumentation and data collected from the National Climatic Data Center.

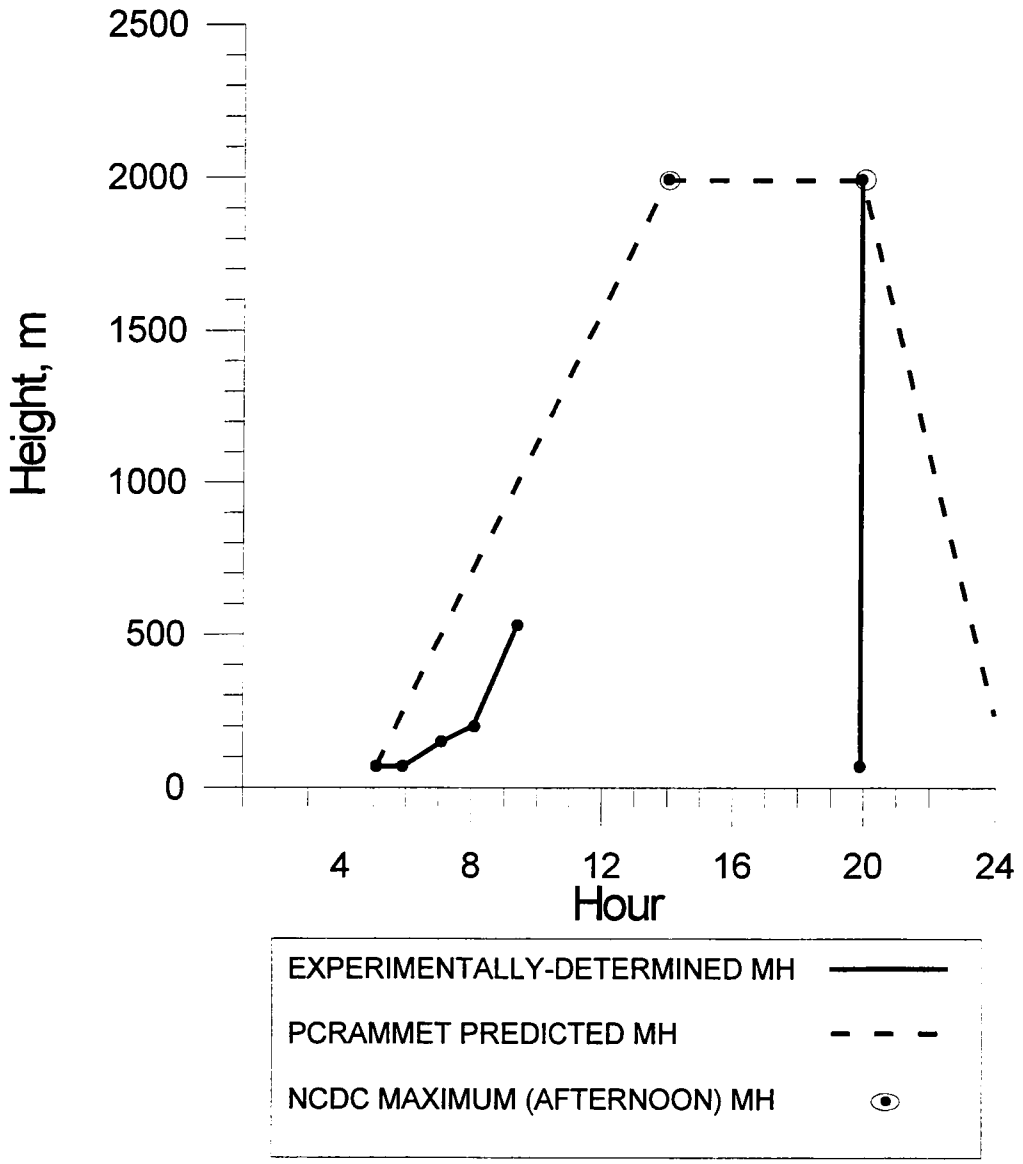

FIGURE 4.53. MIXING HEIGHT PROFILE FOR JULY 14, 1995. Profiles were generated from data collected at Oak Ridge, TN using Tethersonde instrumentation and data collected from the National Climatic Data Center.

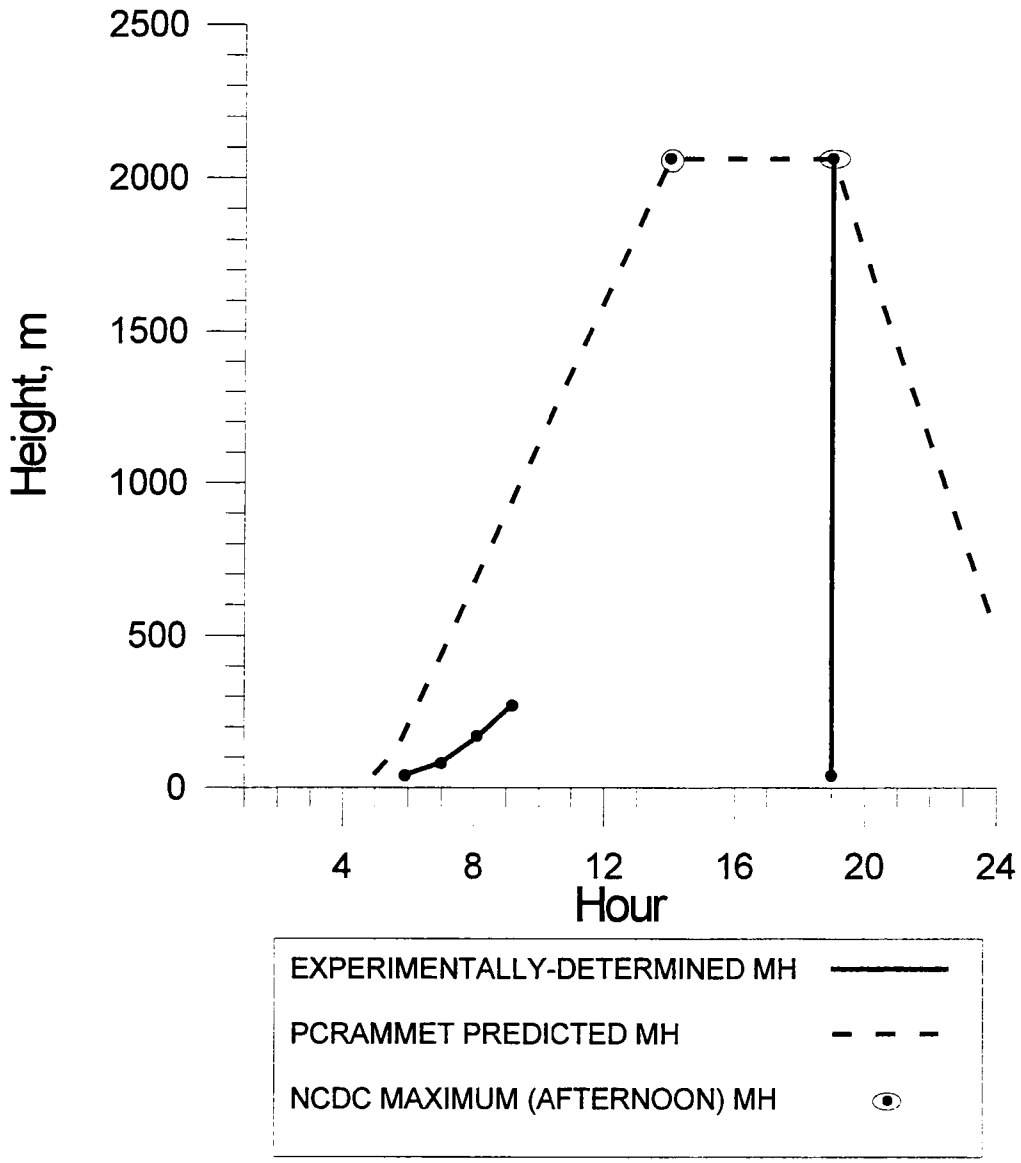

FIGURE 4.54. MIXING HEIGHT PROFILE FOR JULY 20, 1995. Profiles were generated from data collected at Oak Ridge, TN using Tethersonde instrumentation and data collected from the National Climatic Data Center.

dividing by the density of moist air (ϱ_{air}) and the specific heat of air. The term, ϱC_p = 1.216 x 10^3 (W/m^2)/(K•m/s), permits one to easily convert between normal heat fluxes and kinematic heat fluxes.

One of the simplest methods to investigate the relationship between MH development and temperature is to focus only on the thermodynamics which explain 80 to 90 percent of observed variations in MHs(Stull, 1976; Boers, et al., 1984; Stull, 1988; Stull, 1998). This investigation into the thermophysical relationship between heat absorbed by the atmosphere and MH development focused on measured changes in potential temperatures. Horizontal advection of warm air into the region was assumed to be negligible. Thus, the areas (K•m) between Tethersonde soundings were directly related to heat input both from the surface and from warm air entrained from aloft.

The heat input to the atmosphere (both from the surface and from warm air entrained from aloft) was calculated for all nine mornings. After investigating linear and curvilinear models, the relationship between heat input and MH was found to be linear (F Value = 198.621, d.f. = 22, R^2 = 0.9044). Figure 4.55 shows both the data and linear regression model:

$$MH = 0.446\ X + 49.6$$

where X is the heat input expressed in kinematic units (K•m) and MH is the mixing height in meters. It should be noted that the linear relationship may be limited to MH below 600 m.

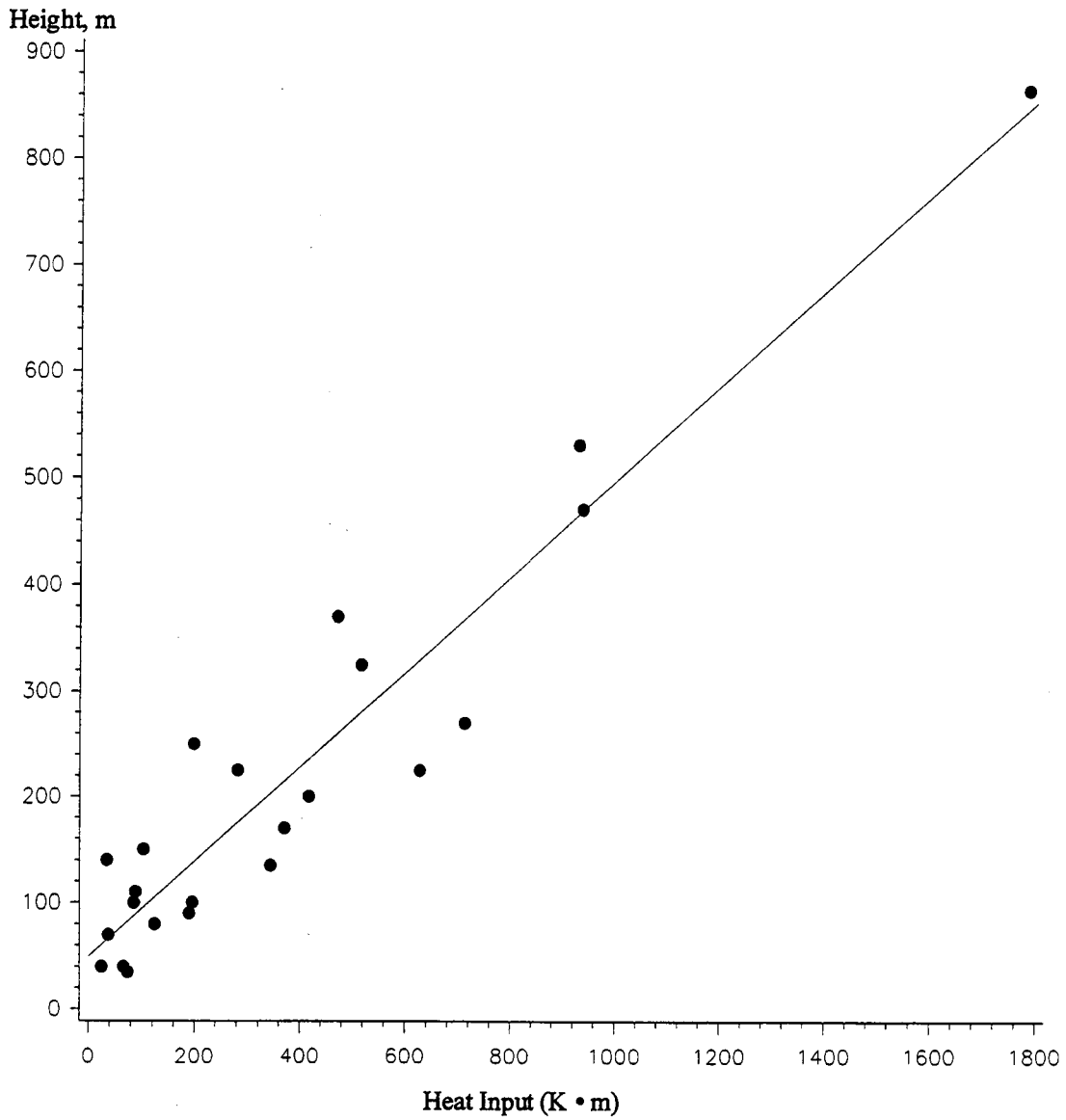

FIGURE 4.55. THERMOPHYSICAL RELATIONSHIP BETWEEN HEAT INPUT AND MIXING HEIGHT. Heat input (K • m) to the atmosphere was calculated for nine mornings; each morning had more than one mixing height (m). F value = 198.621; d.f. = 22; $R^2 = 0.9044$.

4.4 Objective 4: Comparison of Observed Mixing Height Profiles to PCRAMMET Modeled Mixing Height Profiles

The PCRAMMET computer code is the primary EPA model used to obtain hourly MHs. The PCRAMMET processes hourly surface meteorological observation data (an input for each hour of interest) to determine a stability class for each hour and subsequently interpolates between twice daily MH data (an input for each day of interest) to produce MH values for each hour. A schematic illustration of the PCRAMMET interpolation procedures is found in Figure 3.2.

The morning MH was calculated as the height above ground at which the dry adiabatic extension of the morning minimum surface temperature plus 5 °C intersected the vertical temperature profile observed at 1200 Greenwich Median Time (GMT) [also frequently referred to as Zulu (Z) time]. The minimum temperature was determined from the regular hourly reports from 0200 through 0600 LST. The additional 5 °C was intended to allow for the usual effects of the nocturnal and early morning urban heat island since NWS upper-air-measuring stations are located in rural or suburban surroundings. Thus, more properly, the urban morning MH was calculated. The value 5 °C was determined arbitrarily after inspection of urban-rural differences in minimum temperature for many locations (Turner, 1964). For general application, 5 °C was considered a slight overestimation of an overall average minimum temperature difference. Thus, the plus 5 °C was interpreted to include the effects of some surface heating shortly after sunrise. Therefore, the time of urban morning MH coincides approximately with that of the typical diurnal maximum concentration of slow-reacting pollutants in many

cities, occurring around the morning commuter rush hours. This treatment of the urban morning MH is a gross simplification of actual conditions, but is considered reasonable for use. The afternoon MH is less complicated than the morning, but is calculated in the same manner with one exception. Instead of the minimum temperature plus 5 °C, the maximum surface temperature observed from 1200 through 1600 LST is used. Urban-rural differences of maximum surface temperature are considered negligible. The typical time of the afternoon mixing height may be considered to coincide approximately with the usual mid-afternoon minimum concentration of slow-reacting urban pollutants (Holzworth, 1972).

PCRAMMET uses two interpolation schemes to estimate hourly MH, one for rural sites and the other for urban sites. Both estimates are included in the program's output file. Times for sunrise and sunset are calculated within PCRAMMET based on the date, latitude, longitude and time zone. The date is included in the two input files. The remaining information is not included in the CD-144 format, but is submitted in response to queries in the program's interactive mode.

PCRAMMET recognizes seven stability classes. The first six classes correspond to Pasquill's (1974) classifications, A-F. The seventh stability class corresponds to the "dashes" in the original classification by Pasquill and indicates a strong, surface-based nocturnal temperature inversion with non-definable wind flows. The final stability classification criteria is selected from a table based on wind speed, daytime insolation, and nighttime conditions. Turner's (1964) method whereby insolation classes are

determined as a function of solar altitude is encompassed in the final classification criteria.

In order to calculate hourly mixing heights, PCRAMMET uses the maximum mixing height (MAX) from the previous day (i-1), the computation day (i) and the following day (i+1). For urban sites, between midnight and sunrise, under neutral stability, the interpolation is between MAX_{i-1} at sunset on the previous day, and MAX_i at 1400 LST on the current day. If conditions are stable, the minimum mixing height value (MIN) is used. Between sunrise and 1400 LST, if conditions were neutral during the hour prior to sunrise, the earlier interpolation between MAX_{i-1} and MAX_i is continued. If the hour prior to sunrise was stable, interpolation is between MIN_i and MAX_i . For the period 1400 LST to sunset, the MAX_i value is used. During the hours between sunset and midnight under neutral conditions, interpolation is between MAX_i at sunset and MAX_{i+1} at 1400 LST the next day. If the stability is stable, interpolation is between MAX_i at sunset and MIN_{i+1} at midnight. For rural sites, between midnight and sunrise, interpolation is between MAX_{i-1} at sunset on the previous day and MAX_i at 1400 LST on the current day. During the hours between sunrise and 1400 LST, if stability is neutral during the hour prior to sunrise, the earlier interpolation between MAX_{i-1} and MAX_i is continued. If stability is stable during the hour prior to sunrise, interpolation is between 0 and MAX_i. Between 1400 LST to sunset, the MAX_i value is used. During sunset to midnight, interpolation is between MAX_i at sunset and MAX_{i+1} at 1400 LST the next day.

Per the methodology, the NCDC twice daily mixing height file was modified to include "dummy" mixing height data for December 31, 1994 and January 1, 1996.

Without this data, PCRAMMET will not process the respective input file. The "dummy" mixing heights were created by simply copying the January 1, 1995 data and changing the date to December 31; and copying the December 31, 1995 data and changing the date to January 1, 1996.

After preparing the two input files (hourly surface data and twice daily mixing heights), information regarding the latitude, longitude, and time zone for both the Knoxville and Nashville NWS stations was obtained from the EPA SCRAM bulletin board http:/(www.epa.gov/scram001). Using the interactive mode, the mixing height data filename, hourly surface data filename; and latitude, longitude, and time zone information were submitted. The PCRAMMET code produced an output file which contained year, month, day, hour, random flow vector, wind speed (m/s), ambient temperature (K), stability category, rural mixing height (m), and urban mixing height (m). Year, month, day, hour, and mixing height data were used to construct mixing height profiles for July 8, 14, and 20, 1995.

PCRAMMET modeled (rural and urban) and experimentally-determined MH profiles for July 8, 14, and 20 are presented in Figures 4.56, 4.57, and 4.58, respectively. The PCRAMMET rural MH algorithm predicted MHs exceeding 1800 m throughout the nights and most of the days. In the early mornings, the MHs exceeded 1800 m prior to decay between 0400 and 0500. Near 0500, daily minimum MHs of approximately 100 m occurred. Beginning at 0500, the rural algorithm predicted a rapid rise in MHs until peaking between 1200 and 1300. The PCRAMMET urban MH algorithm predicted MHs of approximately 2000 m throughout the afternoons. Minimum MHs less than 100 m

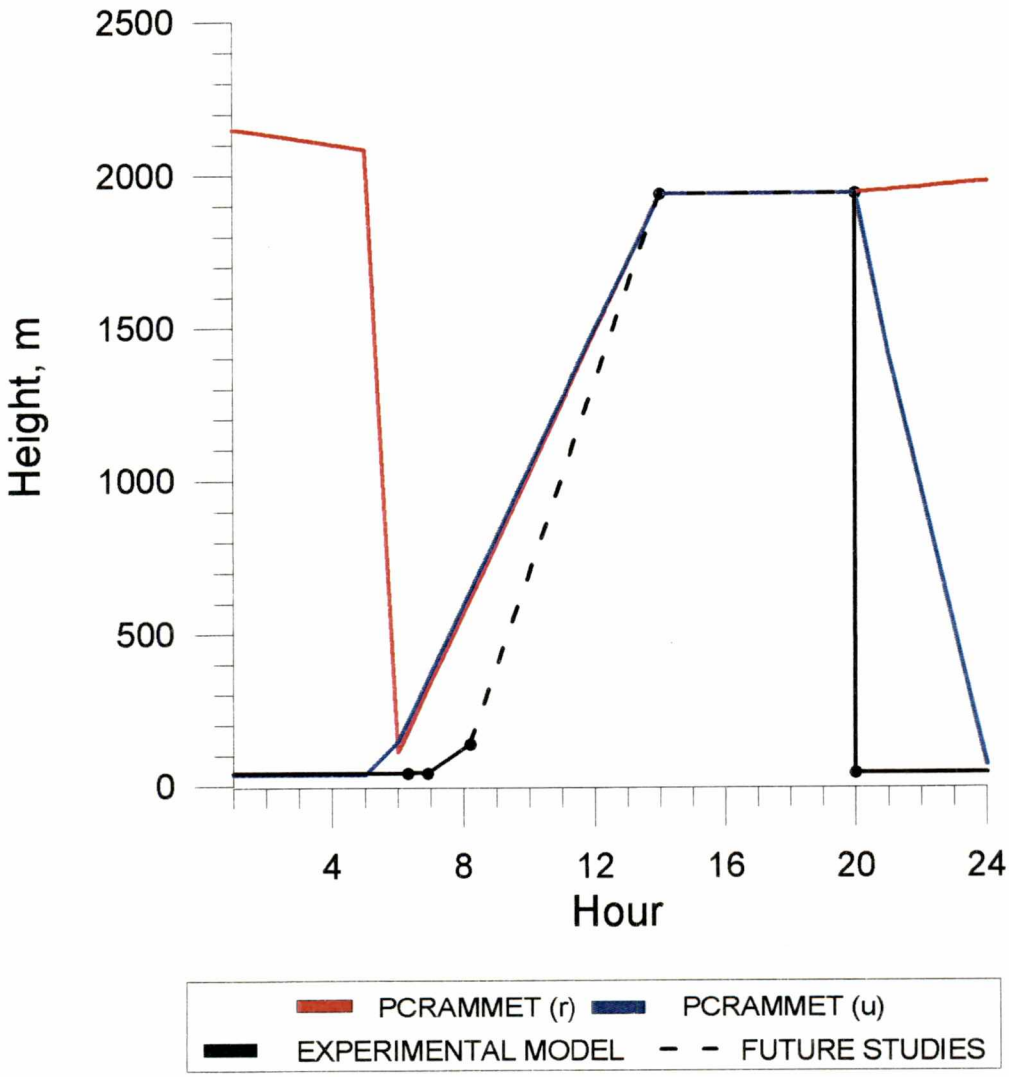

FIGURE 4.56. EXPERIMENTALLY- DETERMINED AND PCRAMMET-MODELED MIXING HEIGHT PROFILES FOR JULY 8, 1995.

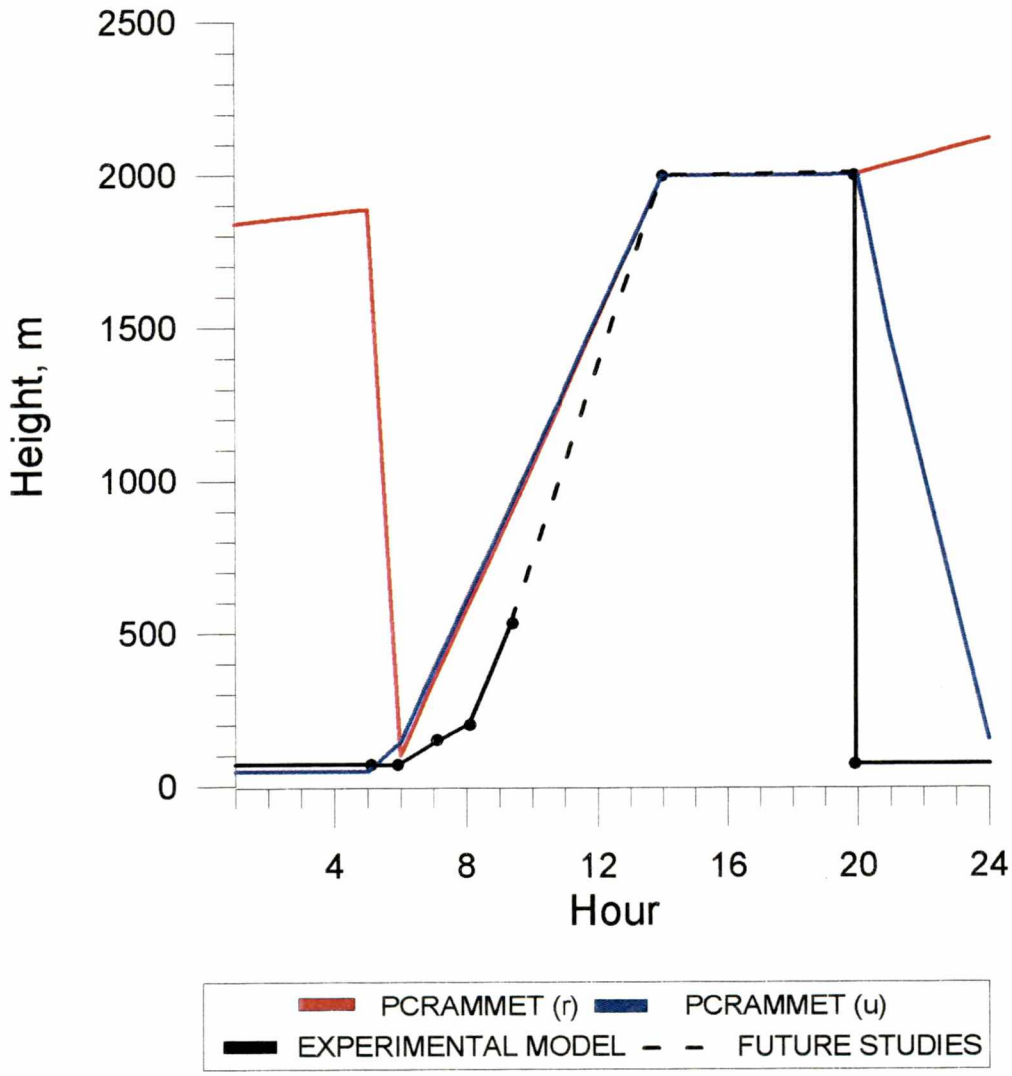

FIGURE 4.57. EXPERIMENTALLY- DETERMINED AND PCRAMMET-MODELED MIXING HEIGHT PROFILES FOR JULY 14, 1995.

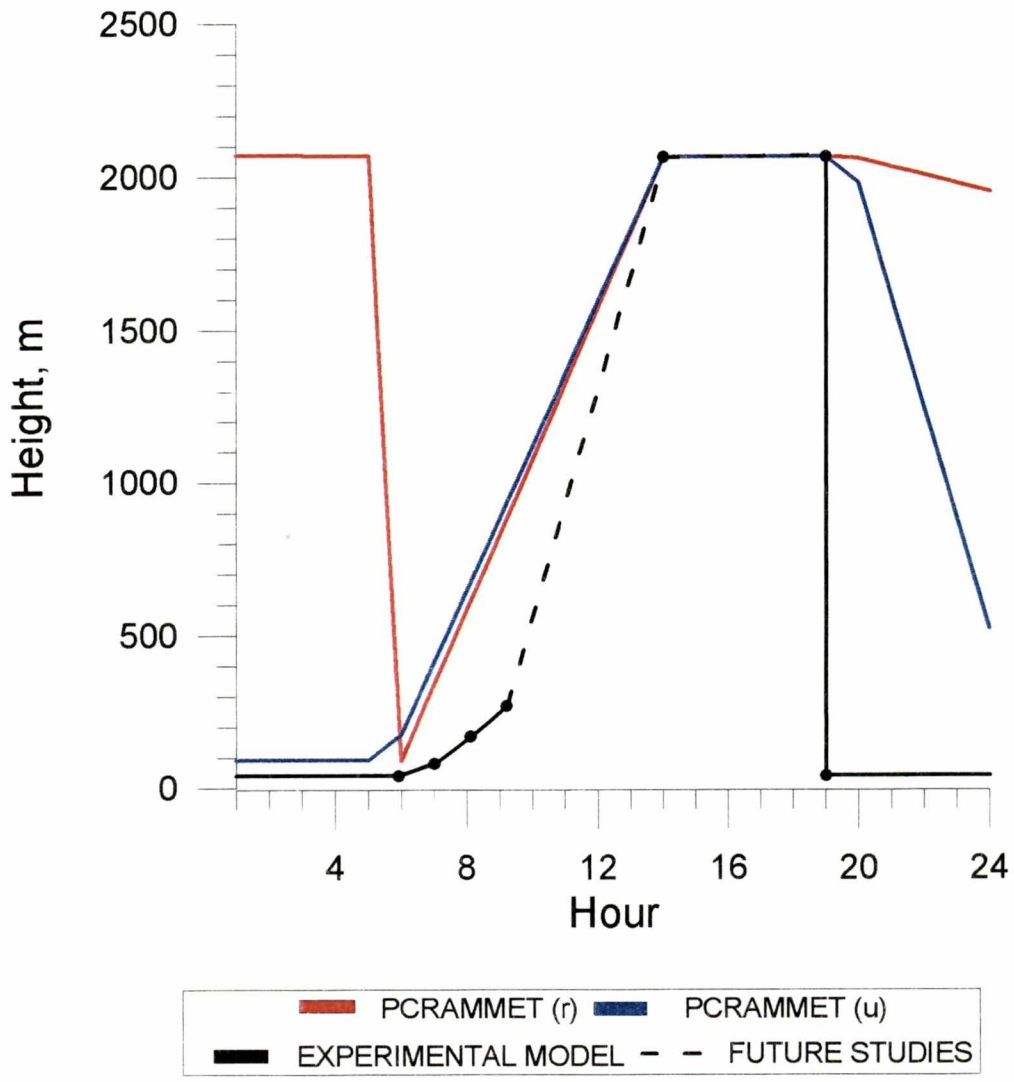

FIGURE 4.58. EXPERIMENTALLY- DETERMINED AND PCRAMMET-MODELED MIXING HEIGHT PROFILES FOR JULY 20, 1995.

occurred in the early mornings. Beginning at 0400, MHs growth began and continued throughout the morning until reaching maximum MHs of approximately 2000 m near 1200. The maximum MHs remained constant until one hour prior to sunset when decay of the MHs begins. MH decay began one hour prior to sunset until near midnight. Minimum MHs throughout the night were less than 100 m. In experimentally-determined MH, MHs did not begin to increase higher than the nocturnal, mechanically-mixed surface layer until after sunrise. In addition, MH growth appeared curvilinear rather than linear. Above Tethersonde measurements, it was assumed that the NCDC afternoon mixing height was the maximum mixing height and the author deferred to the PCRAMMET model. In the afternoon-evening, reduction and reestablishment of the MH near the surface occurred near sunset. The height of the nocturnal, mixed layer at the surface was assumed to equal the morning height.

In summation, the PCRAMMET-modeled and experimentally-determined MH profiles differ substantially. First, experimentally-determined MH increase did not begin until after sunrise and development of the MH was curvilinear. These two observations differ from the PCRAMMET-modeled predictions. Second, experimentally-determined reduction and reestablishment of the MH near the surface occurred near sunset. The PCRAMMET urban model shows reduction and reestablishment of the MH at the surface to occur over a much longer time period than experimentally observed. The PCRAMMET rural model MHs did not begin decay until 0400. Therefore, with respect to MH development in the morning and reduction and reestablishment near the surface in

the evening, both rural and urban models were poor predictors of field-measured observations.

4.5 Objective 5: Alternative Predictive Model for Mixing Heights

The predictive model for mixing heights is composed of four components: 1) a nocturnal surface-layer mixing height, 2) the developing mixing height during the morning, 3) a relatively constant MH in afternoon-early evening, and 4) MH reduction and reestablishment near the surface at approximately sunset (Figure 4.59).

The first component, the nocturnal surface-layer mixing height, is primarily mechanically induced. Although mechanical mixing is present during the daytime also, the mechanical mixing is typically indistinguishable from convective mixing and is a minor component of daytime mixing heights. Based on isothermal temperatures and homogenous ozone concentrations, mechanical mixing was estimated to occur between the surface and 25 m (canopy height) on August 30 and 31; and up to 50-70 m on July 14 (slightly below ridge-top height). The mean height of isothermal temperatures for the three days was approximately 40 m. The mean height of homogenous ozone concentrations for the three days was also approximately 40 m. Thus, the nocturnal surface-layer mixing height component of the predictive model was set equal to 40 m. This value was used for the MH during the nighttime interval between the time of MH reduction and reestablishment near the surface (near sunset) and the respective time for sunrise on days of interest.

The second component, mixing height development during the morning, was observed to consist of an initial shallow MH which slowly increased in height as the

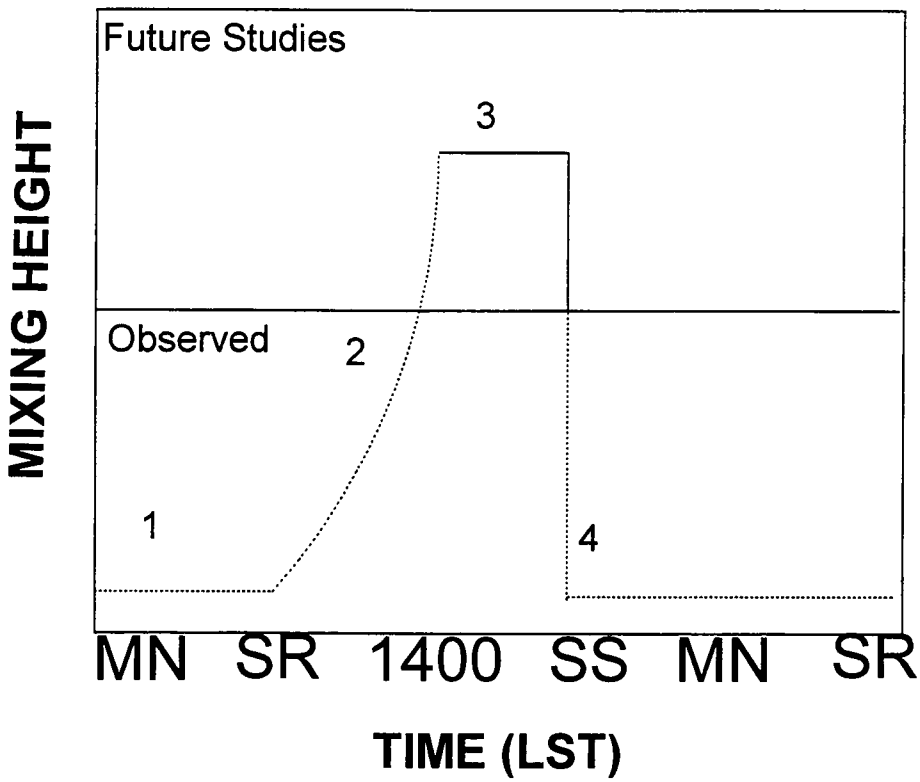

FIGURE 4.59. SCHEMATIC ILLUSTRATION OF THE PREDICTIVE MODEL FOR MIXING HEIGHTS. The model is composed of four components: 1) a nocturnal, surface layer mixing height, 2) morning, developing mixing height, 3) afternoon-evening, constant maximum mixing height, and 4) evening reduction and reestablishment of the mixing height near the surface (MN = midnight, SR = Sunrise, SS = Sunset).

result of thermal (convective) turbulence. As MH growth progressed, the nocturnal inversion (stable boundary layer) was eroded from beneath. As the nocturnal inversion neared complete dissipation (burn-off), MH growth underwent a rapid-rise phase (RRP) where growth accelerated. During this stage, there was strong entrainment from the RL into the ML. Preliminary inspection of the data and consideration of the theoretical growth suggested an exponential model. An exponential regression was modeled (SAS PROC REG):

$$Y = \alpha\beta^{X}\epsilon$$

Numerical estimates of α and β and a regression equation of the form $\hat{Y}_i = ab^X$ were obtained by transformation of the exponential model into a linear model:

$$\hat{Y} = \alpha\beta^{X}$$

$$\log \hat{Y}_i = \log \alpha + X \log \beta$$

$$\hat{Y'}_i = \alpha' + \beta' X$$

where $\hat{Y} = \log \hat{Y}$, $\alpha' = \log \alpha$, and $\beta' = \log \beta$. Y values were then transformed in $\hat{Y'}_i = \log \hat{Y}_i$ and a straight line, $\hat{Y'}_i = a' + b'X$, to the logarithms was fitted. The regression coefficients of the exponential regression equation were determined by taking the antilogarithms of a′ and b′. a′ and b′ equalled 3.567050 and 0.658555, respectively (F Value = 113.663, d.f. = 28, $R^2 = 0.8081$). Mixing height development may therefore be predicted by the following equation:

$$M.H. = (35.41)(1.93)^{X}$$

where X is the time (hours) after sunrise and M.H. is the mixing height (m). This equation was based on experimentally determined data from nine mornings (Figure 4.60).

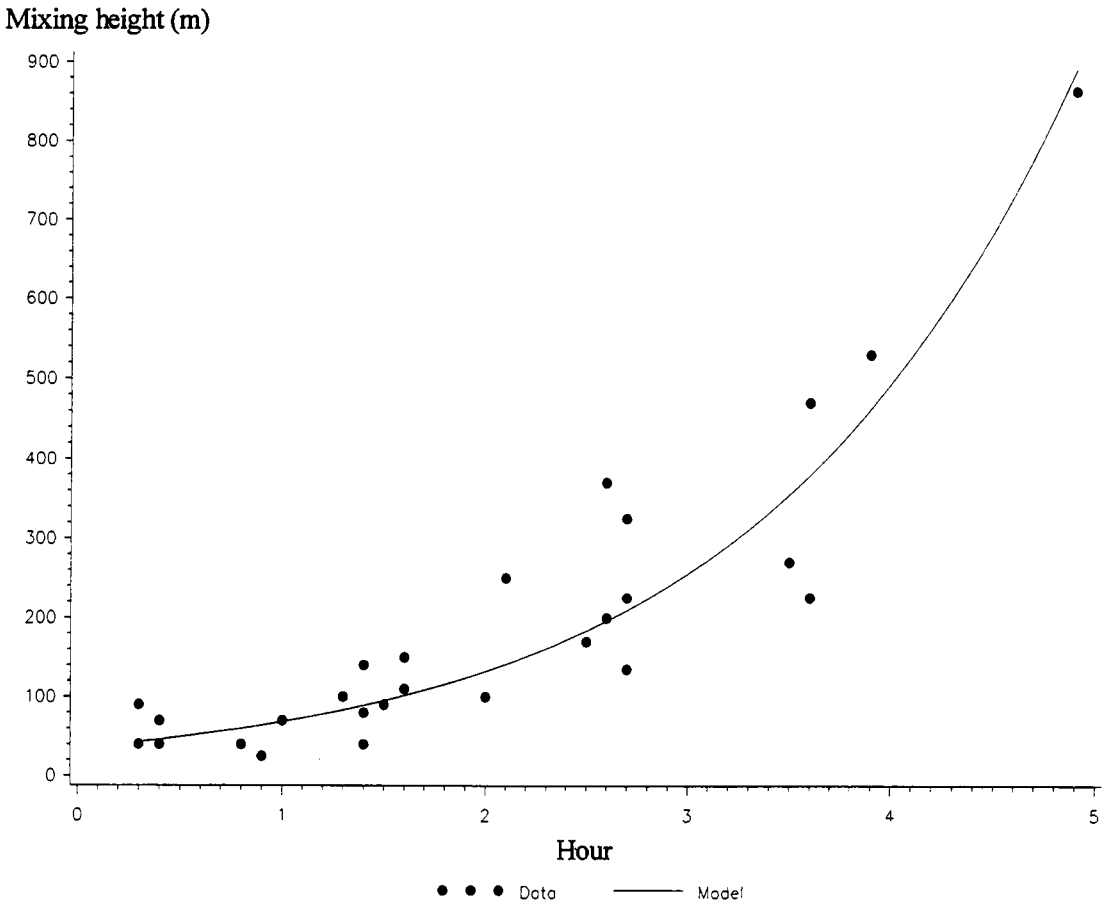

FIGURE 4.60. EXPONENTIAL MODEL FOR MIXING HEIGHT (m) AS A FUNCTION OF TIME OF DAY. Sunrise was arbitrarily set at hour zero.

At present, it is recommended that the equation be used to calculate MHs until reaching the height of the NCDC afternoon MH.

The third component, a relatively constant MH in afternoon-early evening, is simply the afternoon MH as determined by NCDC. It was assumed this afternoon MH was the respective day's maximum mixing height.

The final component, reduction and reestablishment of MH near the surface at approximately sunset was assumed to occur instantaneously near sunset. Specifically, "near sunset" was determined to be an average 27-33 minutes prior to sunset based on potential temperature profiles for six afternoon-evenings. Therefore, in the predictive model, MH reduction and reestablishment near the surface (straight-line interpolation) occurs instantaneously at 0.5 hours (30 minutes) prior to sunset (Figure 4.61).

In summary, the predictive model for MHs was based on data discussed in previous sections of this chapter. The following conclusions were used as assumptions in the construction of the predictive model: 1) A nocturnal surface-layer mixing height exists throughout the night. 2) Mixing height development begins after sunrise. 3) Mixing height reduction and reestablishment near the surface occurs thirty minutes prior to sunset. 4) The maximum MH (as determined by NCDC) was held constant until MH reduction and reestablishment near the surface near sunset. 5) Mixing height reduction and reestablishment near the surface occurred instantaneously thirty minutes prior to sunset.

When compared with PCRAMMET MHs, the alternative predictive model offers an improved model which more accurately represents environmental conditions observed

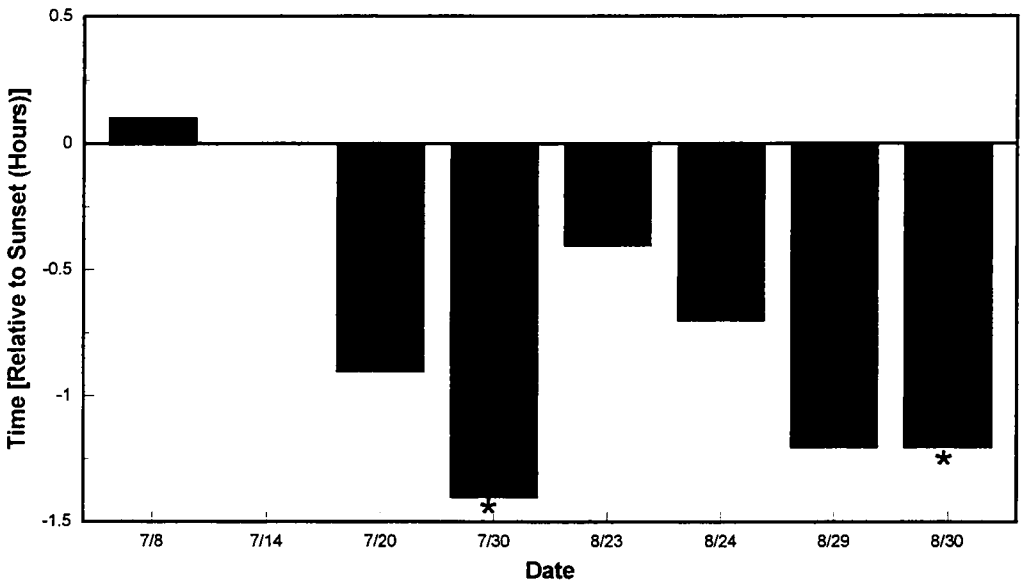

FIGURE 4.61. REDUCTION AND REESTABLISHMENT OF MIXING HEIGHTS NEAR THE SURFACE WITH RESPECT TO SUNSET. Sunset was arbitrarily set at hour zero. * denotes day during which the mixing height was prematurely reduced due to meteorological conditions.

below 1000 m. The PCRAMMET model (rural) typically produced a MH profile whereby development of the mixing height began prior to sunrise and continued in a linear manner until reaching the NCDC-determined afternoon mixing height shortly after 1200 (similar to the urban mode). After reaching the afternoon MH, the MH remained relatively constant throughout the afternoon and night until it began to reduce at approximately 0400-0500 the following morning. Reduction occurred rapidly over a 1-2 hour period until the MH reestablished near the surface at approximately 0600. The PCRAMMET model (urban) typically produced a MH profile whereby development of the mixing height began prior to sunrise and continued in a linear manner until reaching the NCDC-determined afternoon mixing height shortly after 1200. After reaching the afternoon MH, the MH remained relatively constant until reduction began at 1900-2100. Reduction typically continued over a four-hour period until the MH reestablished near the surface.

In comparing the PCRAMMET model (urban and rural) and the predictive model, surface layer mixing heights absent thermal turbulence for the three models are similar. The experimentally-determined height of 40 m used in the predictive model was similar to heights predicted by both PCRAMMET models. However, the PCRAMMET rural model predicted a surface layer mixing height at only one time (approximately 0600) during the 24-hour cycle. The PCRAMMET urban model predicted a surface layer mixing height from near midnight to approximately 0500. The experimentally-determined predictive model defers to the nocturnal surface layer MH absent thermal turbulence from thirty minutes prior to sunset to sunrise. Thus, the surface layer MH

dominated a much longer time period than that predicted by either the PCRAMMET rural or urban models. In addition to differences in surface layer mixing heights, noted differences exist between times whereby development of the MH occurs. Both PCRAMMET rural and urban options predicted MH growth to begin in the early morning, prior to sunrise. Experimental data suggested growth actually occurs several hours later, 0700-0800, and at a slower rate than predicted by linear interpolation. Thus, the predictive model uses a exponential model to characterize the initial, slower growth and increasingly rapid later growth of the MH. The relatively constant afternoon MH was identical for all three models since each was based on the NCDC-determined MH for the respective day. However, substantive differences occur when examining the reduction and reestablishment of the MH at the surface. The PCRAMMET rural model predicted a relatively constant afternoon-night mixing height until approximately 0500 the next morning. The PCRAMMET urban model predicted a constant afternoon MH until initial reduction at 1900-2100 and subsequent reestablishment at the surface layer MH near midnight. The experimental data suggested a markedly different model. The predictive model assumed that decay of the MH began thirty minutes prior to sunset and was instantly followed by reestablishment of the MH near the surface.

CHAPTER 5

CONCLUSIONS

The purpose of this study was to characterize both development and reduction of MHs; and investigate relationships between MHs and ozone concentrations aloft. To accomplish this purpose five objectives were met. 1) Ozone concentration data from selected high and low elevation monitoring stations in eastern Tennessee were compared and assessed for compliance with new EPA standards. The new standard (had it been in place in 1995) would have been exceeded on many occasions. 2) The MH and ozone concentration were characterized. The MH was demonstrated to initiate development after sunrise, and to reduce and reestablish near the surface at approximately sunset. 3) Regional MH profiles were constructed. In the early morning (after sunrise), the thermophysical relationship between MH development and added atomospheric heat was linear. 4) The MH profiles constructed were compared to MH profiles generated by PCRAMMET. Predictions by PCRAMMET did not fit experimental observations of development and reduction of the MH. 5) A model which is better predictive of MHs during periods when regions are under the influence of both high-pressure systems and high temperatures was developed.

This study makes two major contributions. First, Tethersonde measurements for all mornings confirmed the presence of significantly higher ozone concentrations in the residual layer (aloft) than were present at the surface. Although this phenomenon was anticipated based on ozone concentration differences between regional high and low

elevation monitoring stations, it was confirmed by this study. As the MH developed, the entrainment of ozone from the residual layer played a significant, if not dominant, role in increased ozone concentrations at low elevation monitoring stations. Second, Tethersonde measurements enabled characterization of MH development and reduction. This information was used to construct a predictive model which was more representative of experimental observations than the current EPA MH model, PCRAMMET, under typical meteorological conditions associated with high-ozone episodes (hot, clear days and nights under the influence of a high-pressure system).

In closing, the ability of photochemical models to accurately predict surface pollutant concentrations is dependent upon the accurate representation of boundary layer meteorology. Furthermore, the development of air pollutant control strategies is dependent on models. Models must be representative of chemical and meteorological processes that determine the composition of the atmosphere. The predictive model developed in this study is a more accurate representation of MH development and reduction than the current EPA model, PCRAMMET. The model should be further validated and expanded to include experimentally-determined MHs exceeding 1000 m and other meteorological conditions.

REFERENCES

REFERENCES

Adams, M.B., Edwards, N.T., Taylor, G.E. and Skaggs, B.L. 1990. Whole plant ^{14}C-photosynthate allocation in *Pinus taeda*: seasonal patterns at ambient and elevated ozone levels. Can. J. For. Res. 20:152-158.

Adams, W.C., Savin, W.M. and Christo, A.E. 1981. Detection of ozone toxicity during continuous exercise via the effective dose concept. J. Appl. Physio: Respir. Environ. Exercise Physiol. 51:415-422

Ahrens, C.D. 1985. Meteorology Today. An Introduction to Weather, Climate, and the Environment. 2nd ed. West Publishing Co. New York. 523p.

Altshuller, A.P. 1987. Estimation of the natural background of ozone present at surface rural locations. JAPCA 37:1409-1417.

Anderson, R.L., Brown, H.D., Chevone, B.I. and McCartney, T.C. 1988. Occurence of air pollution symptoms (needle tip necrosis and chlorotic mottling on easternern white pine in the southern Appalachian Mountains. Plant Dis. 72:130-132.

Anonymous. 1955. Meteorology and Atomic Energy. Office of Technical Information Service, Department of Commerce. Washington, D.C. 177p.

Anonymous. 1980. Atmospheric mixing. Environ. Sci. Technol. 14:15-17.

Anonymous. 1995. "Synoptic discussion," Southern Regional Climate Newsletter 4(8):1-2 (1995).

Arya, S.P. 1988. Introduction to Micrometeorology. Academic Press, Inc. San Diego. 307 pp.

Beckett, W.S., McDonnell, W.F., Horstman, D.H. and House, D.E. 1985. Role of the parasympathetic nervous system in acute lung response to ozone. J.Appl. Physiol. 59:1879-1885.

Benoit, L.F., Skelly, J.M., Moore, L.D. and Dochinger, L.S. 1983. The influence of ozone on Pinus strobus L. pollen germination. Can J. For. Res. 13:184-187.

Birdwell, K.R. 1995a. Climatological Data for Tennessee: July 1995: Atmospheric Turbulence and Diffusion Division Site, National Oceanic and Atmospheric Administration, Oak Ridge, TN, 1995.

Birdwell, K.R. 1995b. Climatological Data for Tennessee: August 1995: Atmospheric Turbulence and Diffusion Division Site, National Oceanic and Atmospheric Administration, Oak Ridge, TN, 1995.

Boers, R., Eloranta, E.W. and Coulter, R.L. 1984. Lidar observations of mixed layer dynamics: tests of parameterized entrainment models of mixed layer growth. J. Clim. Appl. Meteor., 23, 247-266.

Brawner, E.R., 1997. Personal communication. State of Tennessee: Department of Environment and Conservation: Division of Air Pollution Control, Nashville, TN.

Byers, H.R. 1974. General Meteorology. 4th ed. McGraw-Hill, Inc. New York. 461p.

Calvert, J.G. 1976. Hydrocarbon involvement in photochemical smog formation in Los Angeles atmosphere. Environ. Sci. Technol. 10:256-262.

Calvert, J.G., Demerjian, K. and McQuigg, R.D. 1972. Photolysis of formaldehyde as a hydrogen atom source in the lower atmosphere. Science 175:751-752.

Cardelino, C.A. and Chameides, W.L. 1990. Natural hydrocarbons, urbanization, and urban ozone. J. Geophys. Res. 95:13,971-13,979.

Carter, W.P.L., Lloyd, A.C., Sprung, J.L. and Pitts, J.N.,Jr. 1979. Computer modeling of smog chamber data: progress in validation of a detailed mechanism for the photooxidation of propene and n-butane in photochemical smog. Int. J. Chem. Kinet. 11:45-103.

Chameides, W.L., Linsay, R.W., Richardson, J.L. and Kiang, C.S. 1988. The role of biogenic hydrocarbons in urban photochemical smog: Atlanta as a case study. Science 241:1473-1475.

Chang, T.Y., Chock, D.P., Hammerle, R.H., Japar, S.M., Salmeen, I.T. 1992. Urban and regional ozone air quality: issues relevant to the automobile industry. Crit. Rev. Environ. Control 22:27-66.

Chappelka, A.H., Heldebrand, E., Skelly, J.M., Mangis, D. and Renfro, J.R. 1992. Effects of ambient ozone concentrations on mature easternern hardwood trees growing in Great Smoky Mountains National Park and Shenandoah National Park. Proceedings of Air and Waste Management Association. Pittsburg, PA. paper no. 92-150.04.

Darrall, N.M. 1989. The effect of air pollutants on physiological processes in plants. Plant Cell Environ. 12:1-30.

Eagleman, J.R. 1991. Air Pollution Meteorology. Trimedia Publishing Co. Lenexa, KS. 255p.

EPA. 1990. User's Guide for the Urban Airshed Model. Vol. II: Users's Manual for the UAM (CB-IV) Modeling System (EPA-450/4-90-007A). U.S. Environmental Protection Agency, Office of Research and Development. Research Triangle Park, NC.

EPA 1995. PCRAMMET User's guide. U.S. Environmental Protection Agency, Office of Research and Development. Research Triangle Park, NC.

EPA. 1996. Air quality criteria for ozone and related photochemical oxidants. EPA/600/P-93/004a-cF. U.S. Environmental Protection Agency, Office of Research and Development. U.S. Government Printing Office. Washington, D.C.

Federal Register. 1997. National primary and secondary ambinet air quality standards. F.R. (July 18).

Fehsenfeld, F., Meagher, J. and Cowling, E. (ed.) 1993. Southern Oxidants Study. North Carolina State University. Raleigh. 92p.

Folinsbee, L.B., Drinkwater, B.L., Bedi, J.F. and Horvath, S.M. 1978. The influence of exercise on the pulmonary function changes due to low concentrations of ozone. In: Environmental Stress: Individual Human Adaptations. Folinsbee, L.B., Wagner, J.A., Borgia, J.F., Drinkwater, B.L., Gliner, J.A. and Bedi, J.F. (ed). Academic Press. New York. pp.125-145.

Folinsbee, L.B., McDonnell, W.F. and Horstman, D.H. 1988. Pulmonary function and symptom responses after 6.6-hour exposure to 0.12 ppm ozone with moderate exercise. JAPCA 38:28-35.

Gery, M.W., Whitten, G.Z. and Killus, J.P. 1988. Development and testing of the CMB-IV for urban and regional modeling. EPA/600/3-88/012.

Gilliam, F.S. and Turrill, N.L. 1995. Temporal patterns of ozone pollution in West Virginia: implications for high-elevation hardwood forests. J. Air Waste Manage. Assoc. 45:621-626.

Grosjean, D., Grosjean, E. and Williams, E.L.,III. 1993. Atmospheric chemistry of unsaturated alcohols. Environ. Sci. Technol. 27:2478-2485.

Hanna, S.R., Briggs, G.A. and Hosker, R.P. 1982. Handbook on Atmospheric Diffusion [DE82002045 (DOE/TIC-11223). U.S. Department of Energy. Springfield, VA.

Hazucha, M.J., Silverman, F., Parent, C., Field, S. and Bates, D.V. 1973. Pulmonary function in am after short-term exposure to ozone. Arch. Environ. Health 27: 183-188.

Hazucha, M.J., Bates, D.V. and Bromberg, P.A. 1989. Mechanism of action of ozone on the human lung. J. Appl. Physiol. 67: 1535-1541.

Hazucha, M.J., Folinsbee, L.J. and Seal, E., Jr. 1992. Effects of steady-state and variable ozone concentration profiles on pulmonary function. Am. Rev. Respir. Dis. 146: 1487-1493.

Hess, S.L. 1979. Introduction to Theoretical Meteorology. Robert E. Krieger Publishing Co. Huntington, NY. 362p.

Heath, R.L. 1984. Air pollutant effects on biochemicals derived from metabolism: organic, fatty and amino acids. pp. 275-290 In; Gaseous Air Pollutants and Plant Metabolism. Koziol, M.J. and Whatley, F.R.(ed). Butterworths, London.

Holland, J.Z. 1953. A Meteorological Survey of the Oak Ridge Area. Final Report Covering the Period 1948-1952. ORO-99. Office of Technical Information Service, Department of Commerce, Washington,DC. 584p.

Holzworth, G.C. 1972. Mixing heights, wind speeds, and potential for urban air pollution throughout the contiguous United States. Research Triangle Park, NC: U.S. Environmental Protection Agency, Office of Air Programs; publication no. AP-101. Springfield, VA.

Hortsman, D.H., Folinsbee, L.J., Ives, P.J., Abdul-Salaam, S. and McDonnell, W.F. 1990. Ozone concentration and pulmonary response relationships for 6.6-hour exposures with five hours of moderate exercise to 0.08, 0.10 and 0.12 ppm. Am. Rev. Respir. Dis. 142:1158-1163.

Horvath, S.M., Bedi, J.F., Drechsler-Parks, D.M. and Williams, R.E. 1991. Alterations in pulmonary function parameters during exposure to 80 ppb ozone for 6.6 hours in healthy middle aged individuals. pp. 59-70 In: Tropospheric ozone and the environment: papers from an international conference. R.L. Berglund, D.R. Lawson, and D.J. McKee (ed.). Air and Waste Management Association, Pittsburgh, PA.

Hutton, E.K. 1993. The Importance of the Residual Layer in Characterizing Ozone Emissions in East Tennessee. M.S. Thesis. University of Tennessee. Knoxville, TN. 201p.

Jefferies, H.E., Kamens, R., Sexton, K.G. and Gerhardt, A.A. 1976. Outdoor smog chamber studies: light effects relative to indoor chambers. Environ. Sci. Technol. 10:1006-1011.

Kelly, N.A., Wolff, G.T. and Ferman, M.A. 1984. Sources and sinks of ozone in rural areas. Atmospheric Environment 18:7, 1251-1266.

Kehrl, H.R., Folinsbee, L.J., Horstman, D.H. Gerrity, T.R. Abdul-Salaam, S., Seal, E., Kowalsky, R.J. and McCartney, W.H. 1991. Pulmonary function and ^{99m}Tc-DTPA clearance after repeated prolonged exposure to 0.12 ppm ozone. Am. Rev. Respir. Dis. 143:A93.

Kinney, P.L. and Ozkaynak, H. 1991. Associations of daily mortality and air pollution in Los Angeles County. Environ. Res. 54:99-120.

Kress, L.W. and Miller, J.E. 1983. Impact of ozone on soybean yield. J. Environ. Qual. 12:276-281.

Kulle, T.J., Sauder, L.R., Hebel, J.R. and Chatham, M.D. 1985. Ozone response relationships in healthy nonsmokers. Am. Rev. Respir. Dis. 132:36-41.

Lamb, B., Guenther, A., Gay, D. and Westberg, H. 1987. A national inventory of biogenic hydrocarbon emissions. Atmos. Environ. 21:1695-1705.

Lamb, B., Gay, D., Westberg, H. and Pierce, T. 1993. A biogenic hydrocarbon emission inventory for the U.S.A. using a simple forest canopy model. Atmos. Environ. Part A 27:1673-1690.

Lange, N.A. and Forker, G.M. 1961. Handbook of Chemistry (10th ed.) McGraw-Hill, New York. 2001p.

Larsen, R.I., McDonnell, W.F., Horstman, D.H. and Folinsbee, L.J. 1991. An air quality data analysis system for interrelating effects, standards and needed source reductions: part 11. a lognormal model relating human lung function to decrease to O_3 exposure. J. Air Waste Manage. Assoc. 41:455-459.

Lefohn, A.S. 1992. Surface Level Ozone Exposures and Their Effects on Vegetation. Lewis Publishers, Chelsea MI. 366p.

Lefohn, A.S., Foley, J.K. Shadwick, D.S. and Tilton, B.E. 1993. Changes in the diurnal patterns related to changes in ozone levels. J. Air Waste Manage. Assoc. 43:1472-4178.

Lefohn, A.S., Edwards, P.J., and Adams, M.B. 1994. The characterization of ozone exposures in rural West Virginia and Virginia. J. Air Waste Manage. Assoc. 44:1276-1283.

Leone, J.A., Flagan, R.C., Grojean, D. and Seinfeld, J.H. 1985. An outdoor smog chamber and modeling study of toluene-NO_x photooxidation. Int. J. Chem. Kinet. 17:177-216.

Levy, H.,II. 1971. Normal atmosphere: large radical and formaldehyde concentrations predicted. Science 173:141-143.
Lyons, T. and Scott, B. 1990. Principles of Air Pollution Meteorology. Belhaven Press. 224p.

Mann, L.K., McLaughlin, S.B. and Shriner, D.S. 1980. Seasonal physiological responses of white pine under chronic air pollution stress. Environ. Exp. Bot. 20:99-105.

Marsik, F.J., Fischer, J.W., McDonald, T.D. and Samson, T.J. 1995. Comparison of methods for estimating mixing height used during the 1992 Atlanta Field Intensive. J. Appl. Meterol. 34:1802-1814.

Martocci, B.V.E. 1995. Personal communication. Tennessee Valley Authority. Knoxville, TN.

McDonnell, W.F., Horstman, D.H., Hazucha, M.J., Seal, E., Jr., Haak, E.D., Salaam, S.A. and House, D.E. 1983. J. Appl. Physiol.: Respir. Environ. Excercise Physiol. 54:1345-1352.

McDonnell, W.F., Kehrl, H.R., Abdul-Salaam, S., Ives, P.J., Folinsbee, L.J., Devlin, R.B., O'Neil, J.J. and Horstman, D.H. 1991. Respiratory response of humans exposed to low levels of ozone for 6.6 hours. Arch. Environ. Health 46:145-150.

McLaughlin, S.B., McConathy, R.K., Duvick, D. and Mann, L.K. 1982. Effects of chronic air pollution stress on photosynthesis, carbon allocation and growth of white pine trees. For. Sci. 28:60-70.

McKeen, S.A., Hsie, E.-Y., and Liu, S.C. 1991. A study of the dependence of rural ozone on ozone precursors in the eastern United States. J. Geophys. Res. 96:15,377-15,394.

Meagher, J.J., Lee, N.T., Valente, R.J. and Parkhurst, W.J. 1987. Rural ozone in the southeastern United States. Atmos. Environ. 21:605-615.

Miller, J.E. 1987. Effects of ozone and sulfur dioxide stress on growth and carbon allocation in plants. Rec. Adv. Phytochem. 21:55-100.

Miller, J.E. 1988. Effects on photosynthesis, carbon allocation and plant growth associated with air pollutant stress. pp. 287-314. In: Assessment of Crop Loss from Air Pollutants. W.W. Heck, O.C. Taylor and D.T. Tingley (ed.). Elsevier, London.

Miyake, H., Furukawa, A., Totsuka, T. and Maeda, E. 1984. Differential effects of ozone and sulphur dioxide on the fine structure of spinach leaf cells. New Phytol. 96:215-228.

Mudd, J.B. 1982. Effects of oxidants on metabolic function. pp. 189-201. In: Effects of Gaseous Air Pollution on Agriculture and Horticulture. M.H. Unsworth and D.P. Ormond (ed.). Butterworth Scientific, London.

Mueller, S.F. 1994. Characterization of ambient ozone levels in the Great Smoky Mountains National Park. J. Appl. Meteorol. 33:465-472.

Muller, R.A. 1995. "Synoptic discussion," Southern Regional Climate Newsletter 4(7):1 (1995).

Nappo, C.J., Herwehe, J.T., and Thompson, A.M. 1989. Observations of Ozone Profiles in the Developing Convective Boundary Layer. In: Ozone in the Atmosphere, R.D. Bajkov and P. Fabian, eds., A. Deepak Publishing, ISBN 0-937194-15-8.

Pasquill, F. 1974. Atmospheric Diffusion, 2nd edition. D. Van Nostrand Company, Ltd., London.

Peterson, D.L., Silsbee, D.G., Poth, M., Arbaugh, M.J. and Biles, F.E. 1995. Growth response of bigcone Douglas fir (Pseudotsuga macrocarpa) to long-term ozone exposure in Southern California. J. Air Waste Mange. Assoc. 45: 36-45.

Pielke, R.A. 1984. Mesoscale Meteorological Modeling. Academic Press, New York. 612p.

Pinkerton, J.E. and Lefohn, A.S. 1987. The characterization of ozone data for sites located in forested areas of the eastern United States. JAPCA 37:1005-1010.

Plate, E.J. 1971. Aerodynamic Characteristics of Atmospheric Boundary Layers. National Technical Information Center, Springfield, VA. 190p.

Pryor, W.A., Giamalva, D.H. and Church, D.F. 1984. Kinetics of ozonation. II. Amino acids and model compounds in water and comparison to rates in nonpolar solvents. J. Am. Chem. Soc. 106:7094-7100.

Rasmussen, R.A. 1972. What do the hydrocarbons from trees contribute to air pollution? J. Air Pollut. Control Assoc. 22:537-543.

Randerson, D. (ed.) 1984. Atmospheric Science and Power Production. Technical Information Center. U.S. Dept. Energy, Washington, DC. 850p.

Renfro, J.R. 1995-1996. Personal Communication. U.S. Department of Interior, National Park Service. Gatlinburg, TN.

Rogers, M.O. and Davis, D.D. 1989. A UV photofragmentation/laser-induced fluorescence sensor for the atmospheric detection of HONO. Environ. Sci. Technol. 23:1106-1115.

Seal, E., Jr., McDonnell, W.F., House, D.E., Salaam, S.A., Dewitt, P.J., Butler, S.O., Green, J. and Raggio, L. 1993. The pulmonary response of white and black adults to six concentrations of ozone. Am. Rev. Respir. Dis. 147:804-810.

Seinfeld, J. 1989. Urban air pollution: state of the science. 243:745-752.

Sisterson, D.L., Shannon, J.D., Hales, J.M. 1979. An examination of regional pollutant structure in the lower troposphere - some results of the diagnostic atmospheric cross-section experiment (DACSE-I). J. Appl. Meteor. 18:1421-1428.

Slade, D.H. (ed). 1968. Meteorology and Atomic Energy 1968. Technical Information Center, U.S. Dept. Energy, Washington, DC. 445p.

Spence, R.D., Rykiel, E.J. and Sharpe, P.J.H. 1990. Ozone alters carbon allocation in loblolly pine: assessment with carbon-11 labeling. Environ. Pollut. 64:93-106.

Sperling, D. 1990. An incentive-based transition to alternative transportation fuels. In: Energy and the Environment in the 21st Century. J.W. Tester, D.O. Woods and N.A. Ferrari (ed.) MIT Press, Cambridge, MA. pp. 251-264.

Stockwell, W.R. 1986. A homogeneous gas phase mechanism for use in a regional acid deposition model. Atmos. Environ. 20:1615-1632.

Stull, R.B. 1976. Mixed layer depth model based on turbulent energetics. J. Atmos. Sci., 33, 1268-1278.

Stull, R.B. 1988. An Introduction to Boundary Layer Meteorology. Kluwer Academic Publishers, London.

Stull, R.B. 1998. Personal communication. University of British Columbia. Vancouver, British Columbia, Canada.

Thomson, W.W., Nagahashi, J. and Platt, K. 1974. Further observations on the effects of ozone on the ultrastructure of leaf tissue. pp. 83-93 In: Air Pollution Effects on Plant Growth. M. Dugger (ed.). ACS Symposium Series 3. American Chemical Society, Washington, DC.

Trainer, M., Williams, E.J., Parrish, D.D., Buhr, M.P., Allwine, E.J., Westberg, H.H., Fehsenfeld, F.C. and Liu,L.C. 1987. Models and observations of the impact of natural hydrocarbons on rural ozone. Nature 329:705-707.

Trainer, M., Buhr, M.P., Curran, C.M. Fehsenfeld, F.C., Hsie, E.Y., Liu, S.C., Norton, R.B., Parrish, D.D., Williams, E.J., Gandrud, B.W., Ridley, B.A., Shetter, J.D., Allwine, E.J., Westberg, H.H. 1991. Observations and modeling of the reactive nitrogen photochemistry at a rural site. J. Geophys.Res. 96:3045-3063.

Turner, D.B. 1964. A diffusion model for an urban area. J. Appl. Meterol. 3:83-91.

Wark, K. and Warner, C.F. 1981. Air Pollution: Its Origin and Control. 2nd ed. Harper & Row, New York. 526p.

Wesely, M.L. and Hicks, B.B. 1977. Some factors that affect the deposition rates of sulfur dioxide and similar gases on vegetation. J. Air Pollut. Control Assoc. 27:1110-1116.

Westberg, H. and Lamb, B. 1985. Ozone production and transport in the Atlanta, Georgia region. EPA/600/S3-85/013, U.S. Environmental Agency, Research Triangle Park, NC.

White, M.C., Etzel, R.A., Wilcox, W.D. and Lloyd, C. 1994. Exacerbations of childhood asthma and ozone pollution in Atlanta. Environ. Res. 65:56-68.

Wilkinson, T.G. and Barnes, R.L. 1973. Effects of ozone $^{14}CO_2$ fixation patterns in pines. Can. J. Bot. 51:1573-1578.

VITA

Steven Mack Trotter was born in Knoxville, Tennessee on May 30, 1955. He graduated from Farragut High School in August, 1972. He received a Bachelor of Arts in Liberal Arts with an emphasis in History from The University of Tennessee in May 1976. After a brief stint at The University of Tennessee Law School, he was employed at the DOE facilities in Oak Ridge. He first worked as a health physics and environmental monitoring technician. While working full-time, he continued his academic pursuits and was promoted to Environmental Engineer at the Y-12 manufacturing facility. Mr. Trotter received a M.S. in Environmental Engineering in August, 1988. Since that initial promotion, he has continued to progress in his career both at the Y-12 and K-25 facilities. He has served both as a project engineering manager and a program manager.

Immediately after receiving his M.S. degree, Mr. Trotter began his doctoral program at The University of Tennessee. Along the way he was briefly sidetracked by his marriage to Kimberly Gwinn (1992) and the birth of his son, Jackson Lucas Trotter (1997). He graduated as a Doctor of Philosophy in Civil Engineering in August 1998.

Mr. Trotter is a plenary member of the Health Physics Society and a member of the Air and Waste Management Association. He is a member of St. George Greek Orthodox Church where he is an active member of the homeless ministry.